2012

NOVEL AROMATIC ION–PAIRS: SYNERGY BETWEEN ELECTROSTATICS AND Π-FACE AROMATIC INTERACTIONS

Pramod Prasad Poudel
University of Kentucky, chemistpoudel@gmail.com

STUDENT AGREEMENT:

I represent that my thesis or dissertation and abstract are my original work. Proper attribution has been given to all outside sources. I understand that I am solely responsible for obtaining any needed copyright permissions. I have obtained and attached hereto needed written permission statements(s) from the owner(s) of each third-party copyrighted matter to be included in my work, allowing electronic distribution (if such use is not permitted by the fair use doctrine).

I hereby grant to The University of Kentucky and its agents the non-exclusive license to archive and make accessible my work in whole or in part in all forms of media, now or hereafter known. I agree that the document mentioned above may be made available immediately for worldwide access unless a preapproved embargo applies.

I retain all other ownership rights to the copyright of my work. I also retain the right to use in future works (such as articles or books) all or part of my work. I understand that I am free to register the copyright to my work.

REVIEW, APPROVAL AND ACCEPTANCE

The document mentioned above has been reviewed and accepted by the student's advisor, on behalf of the advisory committee, and by the Director of Graduate Studies (DGS), on behalf of the program; we verify that this is the final, approved version of the student's dissertation including all changes required by the advisory committee. The undersigned agree to abide by the statements above.

Pramod Prasad Poudel, Student

Dr. Arthur Cammers, Major Professor

Dr. John E. Anthony, Director of Graduate Studies

NOVEL AROMATIC ION–PAIRS: SYNERGY BETWEEN ELECTROSTATICS AND Π-FACE AROMATIC INTERACTIONS

DISSERTATION

A dissertation submitted in partial fulfillment of the
requirements for the degree of Doctor of Philosophy
in the College of Arts and Sciences
at the University of Kentucky

By

Pramod Prasad Poudel

Lexington, Kentucky

Director: Dr. Arthur Cammers, Associate Professor of Chemistry

Lexington, Kentucky

2012

ABSTRACT OF DISSERTATION

NOVEL AROMATIC ION–PAIRS: SYNERGY BETWEEN ELECTROSTATICS AND ΠΙ-FACE AROMATIC INTERACTIONS

This dissertation focuses on the design and study of charged aromatic molecules where weak π-π interactions synergize with electrostatic interactions to enhance the overall interaction between aromatic moieties. Each chapter investigates some aspect of this hypothetical synergy between electrostatics and π-face aromatic cohesion.

The first chapter unveiled the importance of electrostatics in the intramolecular stacking of flexible aromatic molecular templates **1-2Br** and **2a**. While our previous studies found dicationic molecular template **1-2Br** to have intramolecular π-stacking between electron poor pyridinium and electron rich xylylene moieties, no such stacking interaction was observed in the neutral analog **2a**.

Chapter two systematically explored the stacking pattern of electron poor aromatics in the form of oxygen- and / or nitrogen- substituted triangulenium cations, $[\mathbf{1}(NR)_3]^+$ and $[\mathbf{1}(O)_3(OH)_3]^+$. As indicated in the chemical literature, triazatriangulenium cations $[\mathbf{1}(NR)_3]^+$ with *N*- ethyl (and longer alkyl chains) chains were found to pack as face-to-face dimers. This study found the formation of columnar, face-to-face, n-meric association between aromatic cations in the structures with decreased steric interactions of the side chains in the stacking planes ($[\mathbf{1}(NMe)_3]^+$ and $[\mathbf{1}(O)_3(OH)_3]^+$). Similar iso-structural triangulene based aromatic anions, $(\mathbf{2})^-$ and $(\mathbf{3})^{2-}$ didn't indicate any facial interactions in the solid states.

The possible synergy between unit charge electrostatics and π-face aromatic interactions was explored in aromatic ion pairs **1•2** of triangulene based aromatic cations and aromatic anions. This charge-assisted π-π stacking seems to be the novel way of getting strong π-system interactions where the strongest non-covalent force and the weakest non-covalent force: ionic bonding and π-stacking respectively synergize together. The π-π interaction between ionic aromatics in the solid state was investigated by means of single crystal x-ray diffraction and powder x-ray diffraction (PXRD). The interaction in the solution state was examined by UV-Vis spectroscopy, electrospray ionization mass spectroscopy (ESI-MS) and electrochemical studies. Studies found that

optimal synergy was possible only in the ion pairs with no steric interactions of alkyl (or aryl) side chains in the stacking planes (**1**$(O)_3$•**2** & **1**$(NMe)_3$•**2**) and the interaction was found to be comparable with the strongest radical-assisted π-stacking described in the chemical literature.

KEYWORDS: Aromatic ion-pairs, MO (Molecular Orbital) calculation, radical assisted π-stacking, charge-assisted π-stacking, ion-pairing energy.

Pramod Prasad Poudel

02/21/2012

NOVEL AROMATIC ION–PAIRS: SYNERGY BETWEEN ELECTROSTATICS AND Π-FACE AROMATIC INTERACTIONS

By

Pramod Prasad Poudel

Dr. Arthur Cammers

_____

Director of Dissertation

Dr. John E. Anthony

_____

Director of Graduate Studies

02/21/2012

_____

Date

Dedicated to

My parents

Mr. Ram Prasad Sharma Poudel

and

Mrs. Dol Kumari Poudel

Acknowledgements

Although the following dissertation is the result of my individual work, there are so many people who are directly / indirectly involved during the course of my PhD research to ease my graduate life at the University of Kentucky. It is my great pleasure to thank all of them who made this dissertation possible.

First of all, I would like to express my sincere gratitude to my PhD advisor, Dr. Arthur Cammers, who tiredlessly encouraged, supported and guided me throughout my entire PhD studies. His great strengths on critical thinking and logically analyzing / interpreting results have great impact on me and I am sure it will reflect on my future career. This dissertation would not have been possible without his outstanding contribution.

I would like to thank Dr. Bruce hinds, Dr. David Atwood, Dr. Leonidas G. Bachas and Dr. Mark D. Watson for their excellent service on my graduate advisory committee. I am especially grateful to Dr. Mark D. Watson for providing me with continuous suggestions relevant to my research and giving me open access to his research lab and the various analytical instruments therein. I would also like to thank Dr. Mark S. Meier, Dr. Robert B. Grossman, and John E. Anthony, the directors of Graduate Studies of the Chemistry Department, for their advice and support. Also, I am thankful to all professors, staffs and entire body of the Chemistry department for their help on different aspects of my graduate life at the University of Kentucky.

Thanks also go to all present and past members of Dr. Cammers' research group, especially to Dr. Jing Chen, Dr. Sihui Long, and Mr. Shubrahmanyam Modekrutti for their helps, supports and discussions throughout my PhD work.

I would like to show my gratitude to Dr. Manjiri A. Patwardhan, supervisor of the organic labs, with whom I worked as a teaching assistant (TA) / super TA for many semesters and she was always supportive and flexible to work wih my research schedule as long as my teaching duties were done. Dr. Jack Goodman, Mr. John Layton, and Dr. Sean Parkin, are another set of key persons to thank for their help with mass spectrometry, NMR and single crystal X-ray diffraction respectively.

Finally, I would like to express my deep sense of gratitude to my parents, Ram Prasad Sharma Poudel and Dol Kumari Poudel for their endless love, support and encouragement. I am very proud to be their son. A very special ‘thank you’ goes to my brother, Dr. Prakash Raj Poudel who was the key person to encourage me to come to the USA (not to any other countries) for my PhD degree. Thanks also go to my parents-in-law, Tanka Prasad Subedi and Harimaya Subedi for their enormous encouragements and supports. I am also thankful to all of my sisters, brother-in-laws and the complete poudel family including Pramila Poudel (my sister-in-law), Pallavi Poudel and Pramit Poudel for their constant support and love.

It’s an honour for me to thank my wife Banita Subedi Poudel who spent five years almost in a room without much doing outdoor. I couldn’t even imagine finishing my PhD degree without her continuous encouragement, support and love. She is undoughtfully a very big contributor to my PhD degree. Very sweet thanks goes to my lovely son, Prashid Poudel for coming into my life bringing a special joy during my PhD period.

TABLE OF CONTENTS

LIST OF TABLES

LIST OF FIGURES

Chapter 1

Effect of Charge in Intramolecular Π-stacking of Isoelectronic Conformational Probes: A ^{1}HNMR Based Analysis

We have been studying electronic effects in π-stacking with conformational probes.[1-4] These molecular templates associate and dissociate phenyl rings and we have been characterizing the conformations to study these aromatic interactions. Studies to date show that we are certainly measuring an interaction between aromatic moieties and that this interaction is very dependent on the electrostatic nature of the aromatic moieties.

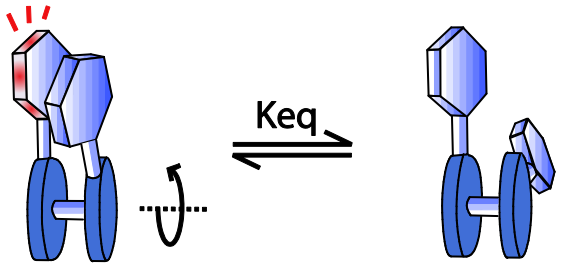

Figure1.1. Association/dissociation of phenyl groups due to conformational flexibility of the molecule.

Although our previous studies found the importance of charge for the intramolecular interaction of aromatic moieties, there was no neutral model in the studies to support the results drawn from the conformational analysis of charged compounds. In chapter one, we reinvestigated the conformational analysis of our previously studied dicationic molecular template, **1a-2Br** (Figure 1.2) and applied the same technique to study conformational behavior of neutral molecule, **2a** (Figure 1.2) to probe the effect of charge in the intramolecular association of aromatic moieties in the conformationally flexible molecular templates. **1b-2Br** and **2b** were synthesized as reference molecules for **1a-2Br** and **2a** respectively where there were no possibilities of intramolecular association of aromatic moieties. **1a-2PF$_6$** and **2a-2PF$_6$** were synthesized to study the

effects of counter anions in the conformational distribution of charged compounds, **1a** and **1b**.

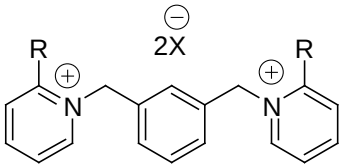

1a; R = Ph, X = Br, PF_6
1b; R = CH_3, X = Br, PF_6

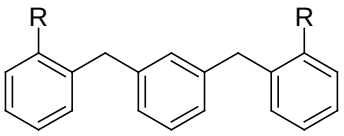

2a; R = Ph
2b; R = CH_3

Figure 1.2. Structure of charged and neutral molecular templates under study.

Once a compelling procedure to determine the conditional conformational distribution of **1a-2Br** in solution phase was developed, this work focused on neutral molecule **2a** to determine the electrostatic contribution to the attraction between aromatic rings. **2a** also allowed us to investigate aromatic interaction in less polar solvents due to the increased solubility of neutral structure. To our surprise, the neutral model **2a** didn't tend to associate aromatic moieties. This observation reconciled the results of the work with dication **1a** with previous literature in the study of π-stacking, because the literature points to the importance of electron withdrawal in π-stacking. The work presented in this chapter has been published.[5]

1.1 Introduction

π - Stacking which is also referred to as π-π interaction is the non-covalent interaction between faces of two or more π moieties. The interaction is also termed as aromatic interaction when the interaction is between aromatic groups. Π-stacking is always a face-to-face (**FF**) interaction. When the π face of one π moiety interacts with an X-H (X = O, N or C) σ bond, the interaction is called σ-π interaction. Due to the shape of the interaction, the σ-π interaction is also called T-stacking where there is an edge-to-face (**EF**) interaction. Π-stacking is important in base pair interaction in DNA,[6-8] protein folding,[9] molecular self assembly,[10-14] molecular recognition,[15,16] supramolecular design and crystal engineering.[17-19] Although π-stacking exists widely in nature, its origin has

been the subject of controversy. This is likely due to the fact that the interaction is very weak. There are several models proposed to study the cause of π-stacking which will be discussed in next chapter. Π-stacking is a weak non-covalent interaction and hence experimental quantification of π-stacking is still a challenge to chemists.

Literature shows that several spectroscopic techniques have been used to study conformational analysis of organic or biological molecules in solution state. UV,[20,21] IR,[22-24] and CD[25,26] are some examples of spectroscopic methods used to study conformational analysis. These studies are mostly qualitative. NMR techniques have been used extensively to study conformational analysis qualitatively[27-29] and quantitatively.[30-35]

1.2 NMR Chemical Shift in Quantitative Conformational Analysis

In 1970, Karabatsos[36] mentioned that the chemical shift of a specific proton (δ**Ha**) in different conformations was neither known nor understood very clearly; at the time this was true. For this reason he said the change in chemical shift values of **Ha** in different conformations couldn't be used as a measure of quantitative conformational analysis. This is not the case today. NMR Chemical shift can be predicted and modeled by *ab initio* calculations.[37,38] The details about the NMR chemical shift calculations used in this study applying density functional theory (DFT) is discussed in the review by Jaszunski et.al.[39]

1.3 ^{1}H NMR Chemical shift as a Function of Change in Conformation

^{1}H NMR chemical shift changes with changes in electronic environment. Solvents,[40] temperature[41-45] and conformation[46-49] are some key factors that perturb the ^{1}H NMR chemical shift of hydrogen nuclei in molecules by changing electron density around them. Since π bonding in molecules gives rise to asymmetric electron clouds, groups like aromatic rings produce distance dependent field effects on the chemical shifts of proximal hydrogen atoms. This is called magnetic anisotropy. These changes have been used to probe conformation qualitatively. The series of studies from our research group, of which this one is the last, push these methods toward quantitative.

1.4 Magnetic Anisotropy in Conformational Study

Π electrons are more easily polarized than σ electrons. Aromatic moieties and other π molecules when placed under external magnetic field produce secondary magnetic fields around them. As discussed above, any change in conformation of the molecule should change electron density around the hydrogen atoms in the molecule which causes changes in chemical shift. If an aromatic ring interacts with a specific proton in a conformationally flexible molecule, changes in chemical shift due to anisotropy of the aromatic ring on that proton can be analyzed as a change in conformation of the molecule under study.[50] As used in the previous studies by our group,[2-4] calculations of the effect of magnetic anisotropy of an aromatic ring on hydrogen atoms of interest in the model compound and the reference molecule is the key in the NMR based conformational analysis used in this research.[5]

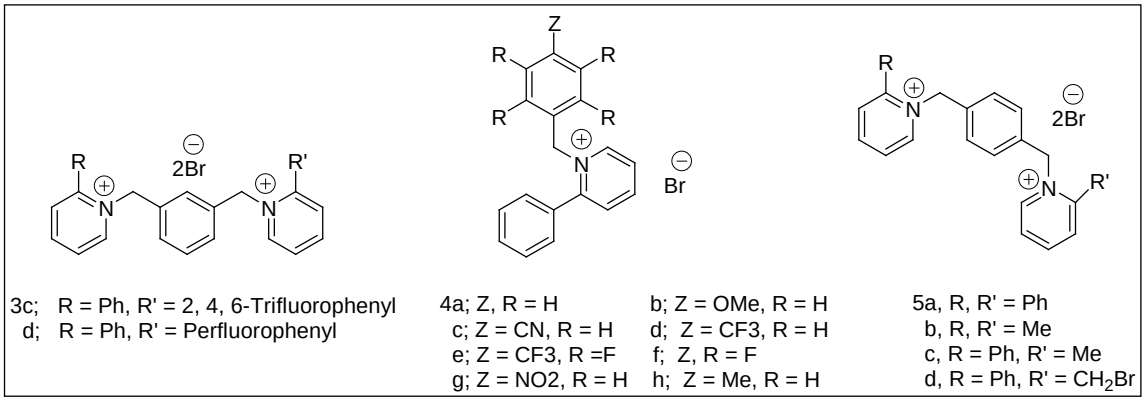

Figure 1.3. Structures of some FF π-stacking models previously studied by our group.

1.5 Previous Conformational Studies of 1

Cammers *et. al.* has explored the conformational dynamics of derivatives of N-Benzyl-2-phenyl pyridinium cation, **1a-2Br** (Figure 1.2)**, 3c-d, 4a-h, 5a and 5c-d** (Figure 1.3) as face-to-face (**FF**) π-stacking models.[1-4] Solid state studies were done by examining conformations in crystal structures and solution state studies were done by DFT calculation-based / ^{1}H NMR based conformational analysis. Conformational flexibility of these model compounds allow aryl groups either to interact with solvent or to interact with each other—see next section for conformational details. Reference molecules (**1b-2Br, 5b**) were studied to correct solvent effects on NMR chemical shifts

in the model compounds. Since the terminal phenyl groups are substituted with methyl groups in these reference molecules, there is no interaction between the aryl rings. Conformational distribution of these model compounds were studied in various polar solvents like water, alcohols, dimethyl sulfoxide (DMSO) and fluorinated solvents like hexafluoro-2-propanol (HFIP) and hexafluoroacetone (HFA).

Solution state studies on the model compounds **4a-h, 1a-2Br, 3c-d, 5a,** and **5c-d** by experimental ^{1}H NMR chemical shift technique coupled with molecular modeling and magnetic anisotropy calculations show that the preferred conformations of these compounds in the solution state are stacked.[1-4] The fact that compounds **4a-e** (Figure 1.3) crystallized in a intramolecular **FF** stacking of the phenyl groups show that preferred conformations of these model compounds are 'stacked' in solid states also.[51] Compound **1a-2Br** (Figure 1.2) also crystallized in a **FF** stacking between the phenyl groups and central xylylene ring. The favored crystal-state conformations were the same as the solution state conformations.[2]

1.6 1, 3-bis-[(biphenyl-2-yl) methyl] Benzene (2a) as a Neutral Model

The studies thus far do not address the whether the charges in the pyridinium moieties may have played an important role in the intramolecular π-stacking in solid and solution states of these cationic model compounds. Previous studies lacked conformational analysis of any neutral model that would potentially answer the question whether charge affected intramolecular π-stacking in these models. To answer this question, we studied the solution and solid states of the neutral analogue **2a** (Figure 1.2) that is isoelectronic to 1**a-2Br** (Figure1.2). **2a** differs from **1a** by two protons and two neutrons on a nuclear level, but has an identical electronic configuration. In addition, results with the neutral molecules add solid state evidence for three competing solution states conformations that were previously predicted by calculations and used in the conformational analysis of the charged molecules.[4] Conformational analysis of **1a-2Br** (Figure 1.2) was reinvestigated in different solvents and with different counter anions, PF_6^- (**1a-2PF$_6^-$**), to validate the previous results and see the effects of counter anions in the conformational distributions.

The approach used previously[4] to study solution state conformational analysis of charged model, **1a-2Br** (Figure 1.2) is reinvestigated to apply the technique to the study of conformational analysis of the neutral model, **2a** (Figure 1.2). The steps involved in the NMR based conformational analysis presented here are given below.

1. Molecular modeling and crystal structure studies of a molecule under study to identify local minimum-energy conformations.
2. Grouping of these conformations in different classes.
3. Design of reference molecules where there is no effect of magnetic anisotropy on the chemical shift of analogous protons. The reference molecule is necessary to correct any changes in chemical shift of a particular proton due to solvent effect. Compounds **1b** and 2**b** (Figure 1.2) serve as reference molecule for **1a** and **2a** respectively.
4. Calculation of the effect of magnetic anisotropy on chemical shift of key protons in these conformations of the model compound and the reference one. Figure 1.4 shows the shielding (at faces) and deshielding (at edges) regions of the benzene ring due to magnetic field anisotropy of the ring calculated at rb3lyp/6-311++g(2d,2p) level.
5. Experimentally measuring the difference in chemical shifts of key protons in the molecule under study and the reference molecule.
6. Determine the equilibrium constants between low-energy conformers of the molecule of interest in a particular solvent at a particular temperature by solving simultaneous equations designed to output the conformational distribution given the calculated chemical shift and experimental chemical shift as inputs.

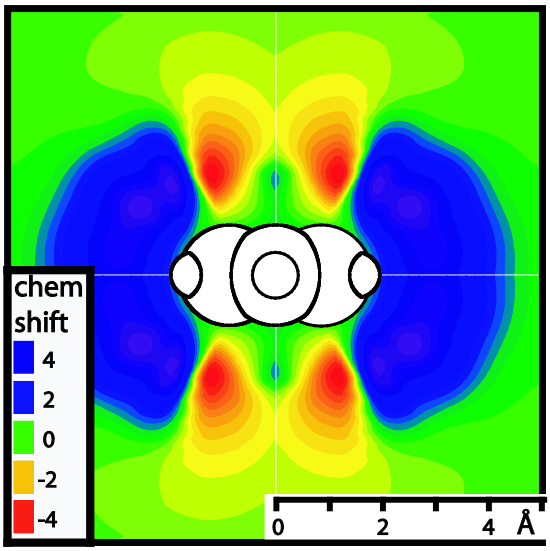

Figure 1.4. Shielding tensor of the benzene ring around its faces and edges due to magnetic anisotropy of the ring calculated at rb3lyp/6-311++g(2d,2p). The numbers are chemical shifts and plotted as a contour slice through C_6H_6, shown in CPK. The calculation starts at 2 Å on the x axis and 1.5 Å on the z axis from the centre of the benzene ring.

1.7 Methods

1.7.1 Molecular Modeling and Anisotropic Shielding of 1a

Different conformations of dicationic model compound **1a** based on molecular modeling and crystal structure studies are shown in Figure 1.5. Two unfolded, splayed (**S**) and one folded, cluster (**C**) and two folded face-to-face (**F**) conformations could compete at room temperature because the energy barriers and the difference in energy among these conformational classes are low. **Ha**, **Hb** and **Hc** are the key protons in the conformational study and chemical shift of these protons are different in different conformations due to magnetic anisotropy of terminal phenyl groups attached to the pyridinium moieties.[2,3] Two terminal phenyl groups interact with the central 1,3-xylylene moiety to form a 3-ring cluster in the conformational class **C.** Due to this cluster, proton signal of **Ha** shifts upfield relative to proton signals of **Hb** and **Hc**. As indicated by the molecular modeling,[2] conformational class **C** has only one microstate and is the lowest

energy conformation (global minimum). There is a face-to-face interaction between the terminal phenyl groups and the central xylylene moiety in the **F** conformational class**.** Conformation **F** has three microstates: one has phenyl ring above **Ha**, another has phenyl ring above **Hb**. The third microstate puts the phenyl ring in a space with respect to **Hb** in a identical manner as **C** state with respect to **Ha**. The structural average of these three microstates is represented by **F** state. **F** state causes upfield shift of **Ha** and **Hb** almost equally. The third conformation class, **S** has sub classes associated with it: one subclass **Sef** has edge-to-face relationship between phenyl ring and xylyl ring whereas another subclass **See** has edge-to-edge relationship between phenyl and xylyl rings. Modeling indicated the existence of two microstates associated with each subclass of **S** state.

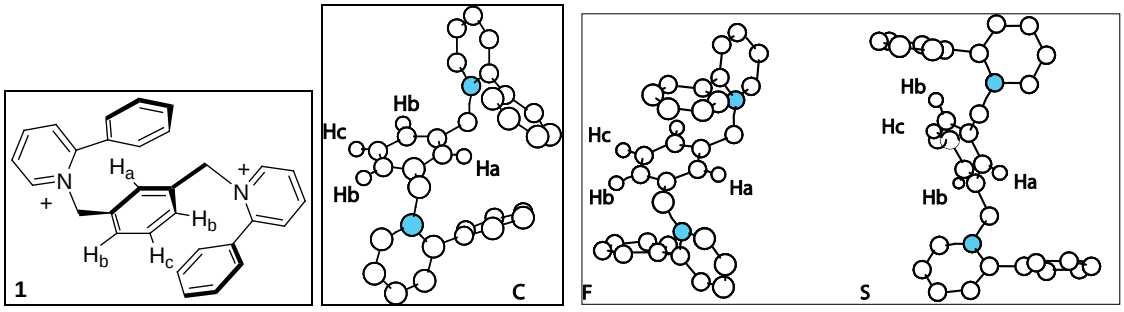

Figure1.5. Different conformations of **1** obtained by molecular modeling**. C** and **F** associate phenyl rings**, S** doesn't**.**

Once different conformations were obtained by modeling, the next step was to calculate the effects of magnetic anisotropic shielding of terminal phenyl groups on the chemical shifts of key protons (**Ha**, **Hb** and **Hc**) in these conformations. Because of the difficulty in calculating shielding tensor of two terminal phenyl rings simultaneously on xylylene **Ha**-**Hc**, the model compound was simplified to two C_{2v} symmetric parts. So the shielding effect of only one phenyl ring on the chemical shift of key protons was calculated at a time. The central xylylene ring and only one terminal phenyl group were considered while doing the calculation. As represented in Figure 1.6, the calculation was further simplified[4] by deleting the bond that connects the xylylene ring with pyridinium

moiety, replacing the pyridinium group with a fluorine atom, deleting quaternary carbons on the xylylene ring and replacing remaining four carbons on the xylyl ring with hydrogen atoms. During these operations, the relative positions of atoms left on the structure remained unchanged.

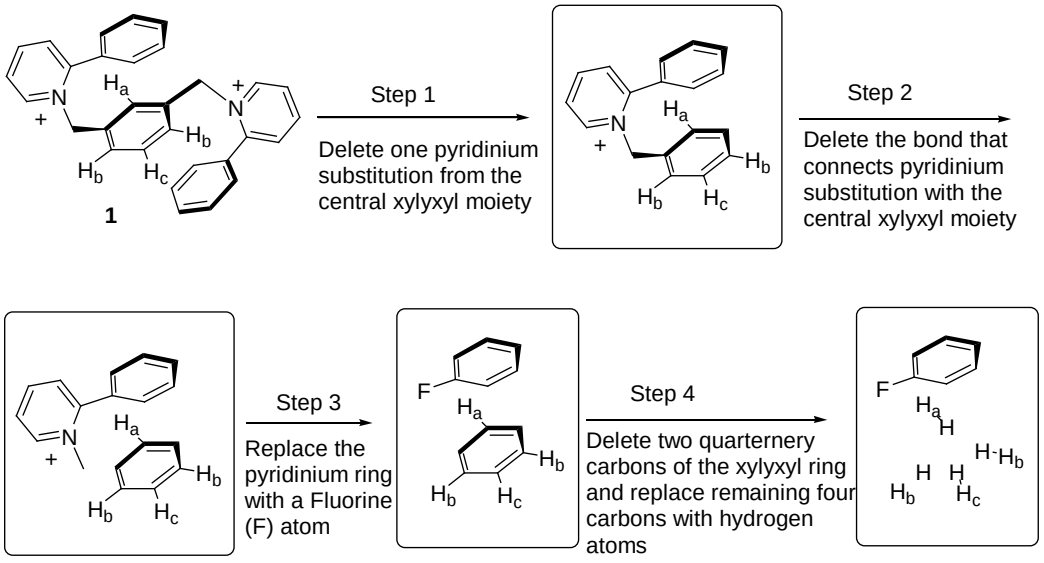

Figure 1.6. Steps taken while calculating the anisotropic field effect of a phenyl ring on **Ha-Hc** of central xylyxyl ring.

The shielding tensor of the phenyl ring on chemical shift of Ha-Hc was then calculated. Because the reference molecule (**1b**) lacks terminal phenyl groups, there are no such effects of anisotropy on chemical shift of **Ha-Hc** of the xylylene ring. So, calculated shielding tensor of phenyl group on chemical shift of **Ha-Hc** of the model compound (**1a**) can also be considered as the difference in chemical shift of **Ha-Hc** between the model and reference molecule. These differences in calculated chemical shifts due to anisotropy are used as coefficients in the mathematical equations designed to give conformational distributions as outputs. The calculated differences in chemical shift of **Ha-Hc** between the model compound (**1a**) and the reference molecule (**1b**) are given in table 1.1. The calculation was done at the rb3lyp/6-311++g (2d, 2p) level of theory. Because gas phase calculations of the anisotropy overestimated the shielding on chemical shift of **Hc** in **Sef** when there was space available for the solvent to come between phenyl

ring and **Hc**, the small shielding tensors of phenyl ring on **Hc** (in **Sef**) were replaced with 0.00 to correct shielding by solvents (last entry, lower right table 1.1).[4]

Conformation	Ha (**1b-1a**)	Hb (**1b-1a**)	Hc (**1b-1a**)
C	1.70 (C_a)	0.19 (C_b)	0.07 (C_c)
F	0.52 (F_a)	1.26 (F_b)	0.40 (F_c)
See	-0.80 (See_a)	-0.67 (See_b)	0.13 (See_c)
Sef	0.14 (Sef_a)	0.22 (Sef_b)	0.00 (Sef_c)

Table1.1. Calculated chemical shift differences of model compound 1a and reference compound 1b at Ha, Hb and Hc in different conformations.

1.7.2 Application of the mathematical model on 2a

The mathematical model used to study conformational distribution of **1a** was also applied in the study of **2a.** The reference molecule that corrects the effects of the solvents is **2b** in this case. As described already, the model compound **1a** was simplified to make the calculations more tractable**.** One simplification was to replace pyridinium moiety with a fluorine atom. So in the actual calculations, the magnetic anisotropy of mono-substituted fluorobenzene on **Ha**-**Hc** was studied. To apply the mathematical model used in the study of **1a** to 2**a**, it is required to have similar anisotropic effects of various mono-substituted phenyl rings on the chemical shifts of proximal protons.

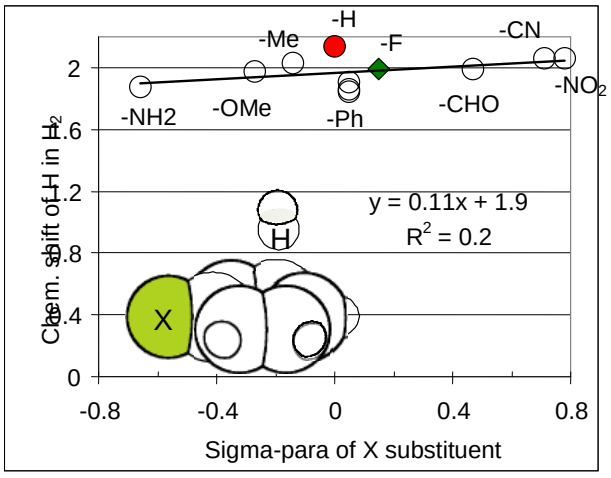

Figure 1.7. The effect of anisotropy of mono substituted benzene ring on the chemical shift of H (in H_2) as a function of σ-para constant of substituents (X).

To check the applicability of this mathematical model to the study of **2a,** chemical shifts of an H-atom in H_2 molecule put proximal to several mono-substituted benzene rings was calculated. The substituents chosen were to follow the linear free energy relationship and the results as shown in Figure 1.7 were plotted against Hammett σ-para constant of the substituents. Calculations were made by putting phenyl ring in the horizontal position with respect to C1 and C4; all carbon atoms in the ring were in the *xy* plane with phenyl centroid at 0,0,0.

As shown in Figure 1.7, various substitutions ranging from those having electron pushing effects (-NH_2, -MeO, -Me have negative σ_{para} effect) as well as electron withdrawing effects (-F, -CHO, -CN, -NO_2 have positive σ_{para} effect) were used in the calculations. Unsubstituted benzene (X=H) also used to see the effects of mono-substituted vs. unsubstituted benzene and as shown in the graph benzene ring (X=H) deviated most from the trend. There were three points for phenylbenzene (X=Ph) because most popular biphenyl dihedral angles were tried for the calculation. Plotting chemical shift value against σ_{para} of the substituents gave an almost a horizontal line (slope =0.11) which indicated that anisotropy is more dependent on mono substitution than the nature of the substitutions.

Thus the same mathematical model which simplified the structure by substituting the aryl ring with fluorine (F) was used. After replacing pyridinium moiety (in **1a**) and analogous aromatic ring (in **2a**) with a fluorine atom, any differences in shielding tensor of the terminal phenyl rings in **1a** and **2a** should be corrected by the reference molecules **1b** and **2b** respectively. Had we not obtained the flat line as in Figure 1.7, we would have needed different mathematical model for **2a**.

1.7.3 Experimental Chemical Shift Measurements

^{1}H NMR chemical shifts of model compounds **1a-2Br**, 1**a-2PF$_6^-$** and **2a** along with reference molecules **1b-2Br**, **1b-2PF$_6^-$** and **2b** respectively were collected in different solvents of varying polarity. Solvents tried for NMR were C_6D_6, toluene-d_8, $CDCl_3$, acetone-d_6, CD_3OD, CD_3CN, DMF-d_7, DMSO-d_6 and D_2O. Any missing NMR data of the model compounds in one or more of these solvents was due to insolubilities. Data were collected by putting the model compound in one NMR tube and the reference molecule in another NMR tube in the same solvents. As described above, **Ha**, **Hb** and **Hc** at the central xylylene moiety are the key protons in the analysis and differences in the chemical shift of model compound and the reference molecule at **Ha**, **Hb** and **Hc** are the only experimental inputs used in the set of mathematical equations designed to give conformational distributions of the model compound as outputs. The experimental chemical shifts of these key protons in the charged and neutral model along with their reference molecules are given in table 1.2 (**1a-2Br, 1b-2Br**), 1.3 (**1a-2PF$_6$, 1b-2PF$_6$**) and 1.4 (**2a, 2b**). All chemical shifts were measured in PPM at 30 °C.

Solvents	Ha (1a-2Br)	Ha (1b-2Br)	Difference Ha{(1b-2Br)-(1a-2Br)}	Hb (1a-2Br)	Hb (1b-2Br)	Difference Hb{(1b-2Br)-(1a-2Br)}	Hc (1a-2Br)	Hc (1b-2Br)	Difference Hc{(1b-2Br)-(1a-2Br)}
CD_3OD	6.58	7.36	0.78	6.92	7.32	0.40	7.25	7.55	0.30
D_2O	6.13	7.08	0.95	6.88	7.27	0.39	7.21	7.53	0.32
DMSO-d_6	6.34	7.22	0.88	6.83	7.26	0.43	7.18	7.50	0.32
$CDCl_3$	7.53	7.72	0.19	6.74	7.49	0.75	7.03	7.53	0.50
DMF-d_7	6.89	7.64	0.75	7.07	7.51	0.44	7.26	7.58	0.32

Table 1.2. Experimental chemical shift differences between 1a-2Br and 1b-2Br.

Solvents	Ha (1a-2PF_6)	Ha (1b-2 PF_6)	Difference Ha{(1b- PF_6)-(1a-2 PF_6)}	Hb (1a-2 PF_6)	Hb (1b-2 PF_6)	Difference Hb{(1b-2 PF_6)-(1a-2 PF_6)}	Hc (1a-2 PF_6)	Hc (1b-2 PF_6)	Difference Hc{(1b-2 PF_6)-(1a-2 PF_6)}
DMSO-d_6	6.31	7.19	0.88	6.83	7.24	0.41	7.18	7.50	0.32
D_2O	6.11	7.04	0.93	6.87	7.25	0.38	7.20	7.51	0.31
CD_3OD	6.50	7.22	0.72	6.91	7.33	0.42	7.24	7.56	0.32
$(CD_3)_2CO$	6.81	7.52	0.71	7.09	7.46	0.37	7.32	7.60	0.28
CD_3CN	6.36	7.01	0.65	6.91	7.25	0.34	7.24	7.52	0.28
DMF-d_7	6.74	7.52	0.78	7.09	7.47	0.38	7.31	7.60	0.29

Table 1.3. Experimental chemical shift differences between 1a-2PF_6 and 1b-2PF_6.

Solvents	Ha (2a)	Ha (2b)	Difference Ha{(2b)-(2a)}	Hb (2a)	Hb (2b)	Difference Hb{(2b)-(2a)}	Hc (2a)	Hc (2b)	Difference Hc{(2b)-(2a)}
C_6D_6	6.65	6.93	0.28	6.77	6.87	0.10	6.96	7.03	0.07
$CDCl_3$	6.54	6.95	0.41	6.75	6.94	0.19	7.02	7.17	0.15
DMSO-d_6	6.39	6.95	0.56	6.71	6.92	0.21	7.01	7.17	0.16
$(CD_3)_2CO$	6.51	7.00	0.49	6.76	6.95	0.19	7.03	7.17	0.14
CD_3CN	6.37	6.97	0.60	6.72	6.95	0.23	7.00	7.17	0.17
CD_3OD	6.38	6.87	0.49	6.69	6.90	0.21	6.97	7.13	0.16
$C_6D_5CD_3$	6.59	6.88	0.29	6.72	6.82	0.10	6.93	7.00	0.07
DMF-d_7	6.56	7.07	0.51	6.80	6.99	0.19	7.08	7.22	0.14

Table 1.4. Experimental chemical shift differences between 2a and 2b.

1.7.4 Mathematical equations

Following set of equations[4] were used to determine mole fraction of different conformations (**C**, **F**, **See** and **Sef**) in different solvents for charged compounds **1a-2Br** and 1**a-2PF$_6$** and the neutral analogue 2**a**.

$$X_C + X_F + X_{See} + X_{Sef} = 1 \quad (1)$$

$$\text{Expt. } [\delta(Ha)r - \delta(Ha)m] = 2\mathbf{C}_a\mathbf{X_C} + 2\mathbf{F}_a\mathbf{X_F} + 2\mathbf{See}_a\mathbf{X_{See}} + 2\mathbf{Sef}_aX_{\mathbf{Sef}} \quad (2)$$

$$\text{Expt. } [\delta(Hb)r - \delta(Hb)m] = \mathbf{C}_b\mathbf{X_C} + \mathbf{F}_b\mathbf{X_F} + \mathbf{See}_b\mathbf{X_{See}} + \mathbf{Sef}_b\mathbf{X_{Sef}} \quad (3)$$

$$\text{Expt.}[\delta(Hc)r - \delta(Hc)m] = 2\mathbf{C}_c\mathbf{X_C} + 2\mathbf{F}_c\mathbf{X_F} + 2\mathbf{See}_c\mathbf{X_{See}} + 2\mathbf{Sef}_c\mathbf{X_{Sef}} \quad (4)$$

Equation (1) expresses mass balance. Equations 2-4 represent the difference in chemical shift between model compound and the reference molecule at **Ha**, **Hb** and **Hc**. C_a, F_a, See_a and Sef_a in equation 2 and analogous parameters in equations 3 and 4 are calculated difference in chemical shift between reference and model compound at **Ha** and similar parameter in equations 3 and 4 are the calculated chemical shift differences at **Hb**

and **Hc** respectively and these values are given in table 1.2. The term "Expt. [δ (Ha)r – δ(Ha)m]" in equation (2) is the difference in experimental chemical shift of reference (r) and model (m) compound at **Ha**. Similar parameters in equations 3 and 4 are for protons **Hb** and **Hc** respectively. Since two phenyl rings can simultaneously affect "**Ha**" and "**Hc**", their corresponding coefficients are multiplied by 2 in equation (2) and (4). X_C, X_F, X_{See} and X_{Sef} are mole fraction of different conformations (**C**, **F**, **See** and **Sef**) in a particular solvent.

1.8 Results and Discussions

1.8.1 Solid State Study

Among all low-energy conformations identified from molecular modeling, solid state evidence for only one of the microstates of the **F**-state (phenyl rings above **Ha**) was presented in the previous study.[2] This conformation can be seen in the crystal structure of **1a-2Br** (Figure 1.8, top, left). All other microstates of conformation **C, F a**nd S were calculated based on molecular modeling. Subsequently, the solid state of **2a** (Figure 1.8, bottom, left) was found to crystallize in the **S** state.[5,52] This study found solid state evidence for one more microstate of **F** with phenyl rings above **Hb** as seen in crystal structure of **1a-2PF$_6$** (Figure 1.8, top, right).

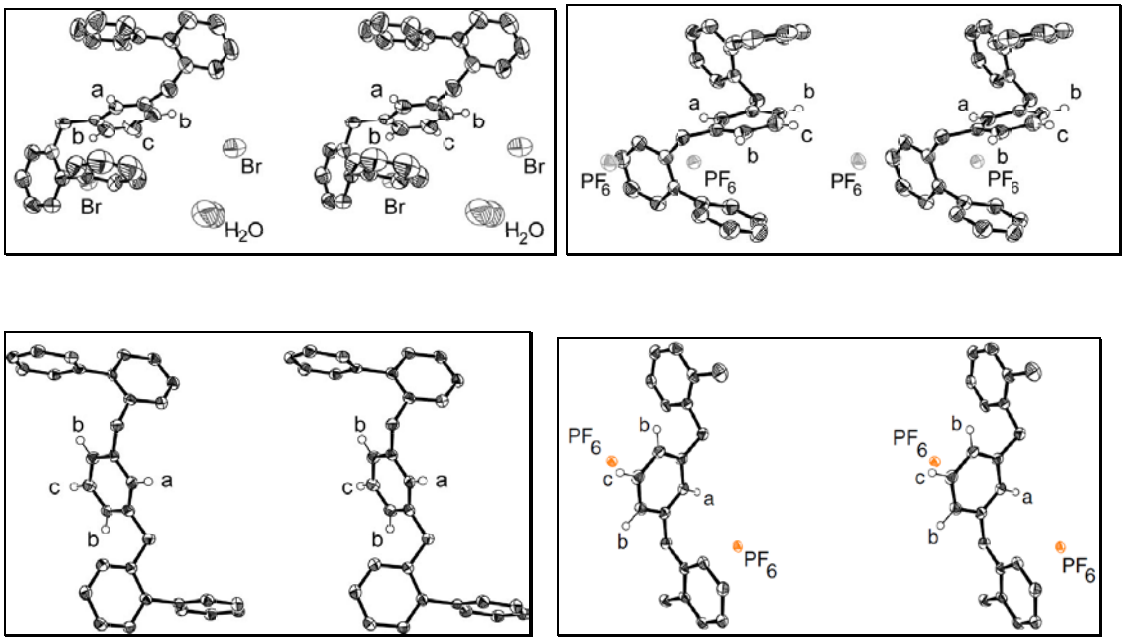

Figure 1.8. Ortep stereoviews of crystal structures of 1a-2Br+H_2O (top left), 1a-2PF_6 (top right), 2a (bottom left) and 1b-2PF_6 (bottom right). F-atoms not shown, Xylylene Ha-c are labeled.

To lend support to the fact that the atomic coordinates of crystalline **1a-2PF_6** belong to **F**-state with phenyl rings above Hb, atomic positions for half structure of crystalline **1a-2PF_6** and those of the calculated microstate of **F**-state in which phenyl rings were proximal to Hb were compared.[5] The atomic coordinates of the calculated and crystal structures were read into gOpen Mol. All hydrogen atoms, anions and solvent molecules were removed from the crystal structure and analogous atoms in the calculated and crystal structures were given the same numeric labels. The analogous atoms in the half structures were then compared by calculating RMS (root mean square) difference between the analogous atomic pairs. As shown in Figure 1.9, exporting and importing the results file to return atomic RMS difference showed that the two structures overlapped with RMS difference of 0.2 Å.

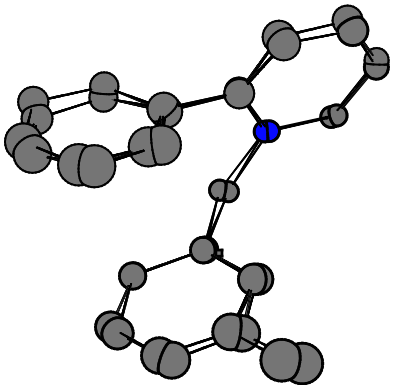

Figure 1.9. RMS overlay of the half structure of the crystal coordinates of 1**a-2PF$_6$** with the **F** state conformer in which the phenyl ring is proximal to **Hb**.

When nitrogen atoms in **1a** were replaced with carbon atoms to get neutral all-carbon analogue **2a**, unstacked (splayed) conformation was preferred in the solid state as seen in the crystal structure of **2a** (Figure 1.8, bottom left). Analyzing the crystal structure of **2a** showed that it had two symmetry-unrelated **S** conformations at either end of the molecule. To determine which one of the four microstates of **S** the crystal structure of **2a** belonged to, RMS differences between the two ends of the crystal of **2a** and the different microstates of **S** were calculated and the results were compared with the RMS differences between the crystal structure of **2a** and calculated **C** and **F** conformations (Figure 1.10, right). The atomic coordinates of crystal structure of **2a** overlapped with two microstates of **S.** Root mean square (RMS) overlay of the atomic coordinates of **2a** crystal with a matching **S** conformation is presented in Figure 1.10 (left). The RMS difference between coordinates of one end of the 2**a** crystal and one end of calculated **S** state was found to be 0.4 Å (black bar in Figure 1.10, right). The difference between other end of 2a crystal and other end of calculated **S** state was found to be around 0.5 Å. These differences between the crystal coordinates of **2a** and calculated **C** and **F** states were close to 1.6 Å and 1.8 Å respectively. So, solid state of **2a** crystal was assigned to be the **S** conformation.

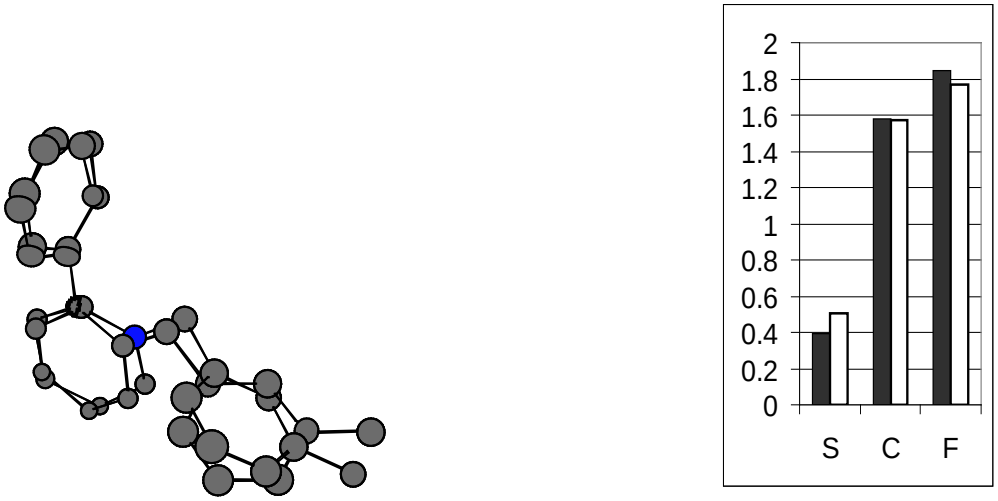

Figure 1.10. RMS overlay of half structure of **2a** with a matching **S** conformation (left). RMS differences in atomic positions of the best matches between the two ends (black and white) of the crystal structure of **2a** and conformations of **S**, **C** and **F** respectively (right).

1.8.2 Solution State Study

Conformational distributions of different model compounds **1a-2Br**, **1a-2PF$_6$** and **2a** in different solvents were calculated by substituting numbers for experimental and calculated chemical shift differences between the model and reference molecule in the set of mathematical equations as described above under the heading "*Mathematical equations*". Mole fractions of different conformations for **1a-2Br, 1a-2PF$_6$** and **2a** are shown in table **1.5**, **1.6** and **1.7** respectively.

Solvents	D_2O	DMSO (d_6)	CD_3CN	DMF (d_7)	CD_3OD	Acetone (d_6)
Dielectric	78.5	46.7	37.5	36.7	32.7	20.7
C	0.248	0.209	0.173	0.166	0.188	0.176
F	0.304	0.320	0.264	0.328	0.296	0.271
See	0.158	0.132	0.169	0.132	0.139	0.144
Sef	0.290	0.339	0.394	0.374	0.377	0.408
S-sum (See + Sef)	0.448	0.472	0.563	0.506	0.516	0.552
F-sum (C + F)	0.552	0.528	0.437	0.494	0.484	0.448

Table 1.5. Mole fractions of conformations C, F, See and Sef of 1a-2Br in different solvents.

Solvents	D_2O	DMSO (d_6)	CD_3CN	DMF (d_7)	CD_3OD	Acetone (d_6)
Dielectric	78.5	46.7	37.5	36.7	32.7	20.7
C	0.244	0.218	0.173	0.195	0.167	0.176
F	0.293	0.313	0.264	0.281	0.322	0.271
See	0.156	0.147	0.169	0.143	0.148	0.144
Sef	0.307	0.322	0.394	0.381	0.363	0.408
S-sum (See + Sef)	0.463	0.469	0.563	0.524	0.511	0.552
F-sum (C + F)	0.537	0.531	0.437	0.476	0.489	0.448

Table 1.6. Mole fractions of conformations C, F, See and Sef of 1a-2PF_6 in different solvents.

Solvents	DMSO (d_6)	CD_3CN	DMF (d_7)	Acetone (d_6)	$CDCl_3$	Toluene (d_8)	C_6D_6
Dielectric	46.7	37.5	36.7	20.7	4.8	2.4	2.3
C	0.174	0.179	0.163	0.157	0.137	0.122	0.119
F	0.120	0.134	0.098	0.099	0.110	0.015	0.016
See	0.147	0.140	0.144	0.145	0.159	0.150	0.150
Sef	0.559	0.547	0.595	0.599	0.594	0.713	0.715
S-sum (See + Sef)	0.706	0.687	0.739	0.744	0.753	0.863	0.865
F-sum (C + F)	0.294	0.313	0.261	0.256	0.247	0.137	0.135

Table 1.7. Mole fractions of conformations C, F, See and Sef of 2a in different solvents.

The results in tables 1.5 – 1.7 are graphically represented in Figure 1.11 to clearly show the trends. As seen in the graph in Figure 1.11 (or tables 1.5-1.6), the conformational distributions of **1a-2Br** and 1**a-2PF$_6$** in the same solvent are very similar to each other. This shows that conformational distribution of these dications did not depend on the nature of counter anions lending support to the previous study[2] of conformations of **1a-2Br** and 1**a-2Cl**. Analyzing the graph (or results in tables 1.5-1.7), it is clear that conformational behavior of dications (**1a**) as well as neutral model (**2a**) depend on solvent. Both dication and neutral compounds prefer folded conformations in the solvents with high dielectric and this preference decreases with decreases in dielectric of the solvents. This trend is probably because of increased solvophobicity[53] of the terminal phenyl rings in high dielectric solvents and is applicable to all the solvents tried except acetonitrile.

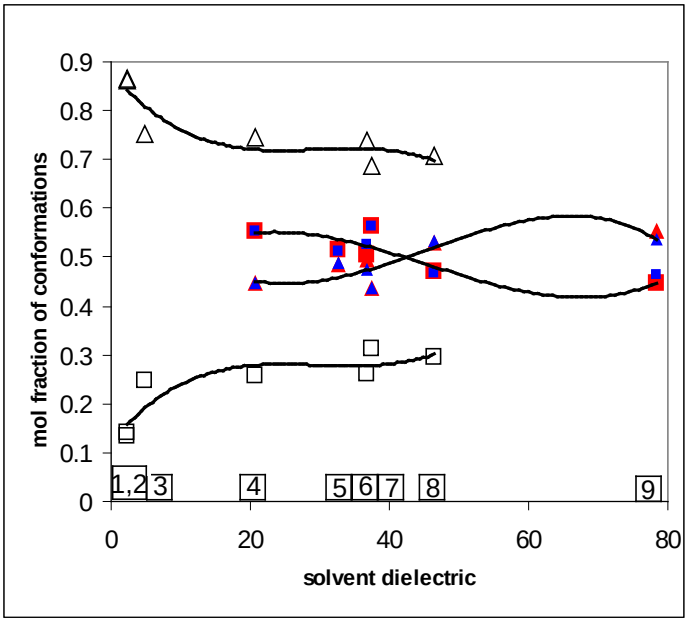

Figure 1.11. The mole fraction of folded (F+C) [rectangle] and unfolded S [triangle] conformers of 1a-2PF_6 [red], 1a-2Br [blue] and 2a [white] as a function of solvent dielectric. Solvents: (1) C_6D_6 (2) Tol-d_8 (3) $CDCl_3$ (4) Acetone-d_6 (5) CD_3OD (6) DMF-d_7 (7) CD_3CN (8) DMSO-d_6 (9) D_2O.

Acetonitrile is an outlier solvent in this study but the interesting thing is that it behaves similarly in the dications as well as the neutral model. There might be some microscopic solvent properties dominating the bulk solvent effects in this solvent but these effects are not the part of current study. Although both charged compounds and neutral model tend to prefer folded conformations in the solvents with increased dielectric, the extent of folding in the neutral compound (**2a**) is much less than that in charged compounds (**1a-2Br** and 1**a-2PF$_6$**). As stated already, the solvophobic effect should increase the folded conformations in high dielectric solvent but the mole fraction of folded conformation of the neutral compound was only 0.3 in DMSO, the highest dielectric solvent used for **2a**. The average mole fraction of folded conformations of **1a-2Br** and **1a-2PF$_6$** in DMSO was 0.53. So, presence of charge in the model compounds increased the folded conformations by 0.23 in DMSO. This increase in folded conformations due to the presence of charge (in **1a-2Br** and **1a-2PF$_6$**) was 0.224 in DMF and 0.192 in acetone. These numbers representing the differences in folded

conformations between the charged and neutral compounds are not same in the different solvents showing that the extent of folding of charged and neutral compounds in different solvent is not same.

Solvent plays an important role in the conformations of many biological polymers like proteins and DNA due to combined effects of many interactions towards the native state. However, the conformational dependence of small organic molecules on the solvents is generally small although there are some examples of strong solvent dependence of conformations on solvents.[54] The current study shows that the conformations of model compounds depend on the solvents.

Literature shows that intramolecular π interactions between aromatic moieties in varieties of molecular templates depend on the electronic/electrostatic nature of the aromatic rings; favorable interactions were observed when at least one of the interacting aromatic moieties was electron-deficient.[55] Intramolecular stacking of electron poor pyridinium cation with aryl group has been well demonstrated by Yamada[56] and Fossey *et al.*[57] As shown in Figure 1.12, conformationally flexible phenyl alkyl pyridine when converted into its N-alkylpyridinium salt prefers stacked conformation as suggested by NMR and fluorescence spectroscopy.[57] There is also a solid state evidence[56] for the intramolecular stacking of electron deficient pyridinium cation with aryl group. There are some other examples of intramolecular cation-π interactions between two aryl groups in small organic molecules.[58-60] Literature also reveals the intramolecular cation-π interactions between a non-aromatic cation (aliphatic cation or metal cation) with aryl groups.[61-63]

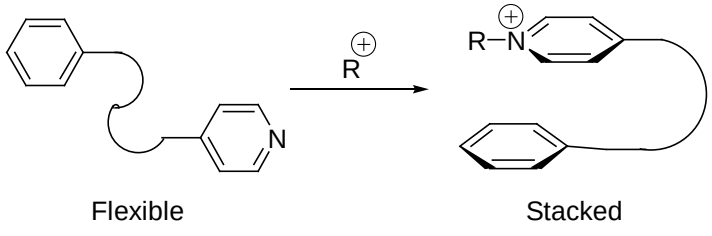

Figure1.12. Conformationally flexible phenylalkyl pyridine and its stacked cationic form.

Such interactions between aromatic moieties were not observed when both of the interacting aromatic rings were electron poor or electron-rich or simply hydrocarbons.[64-66] In the molecular template shown in Figure 1.13, while there were no sign of intramolecular interaction between two anthracenyl groups (**A2**) or two 3,5-dinitrophenyl groups (**N2**) in the symmetric diesters, the assymetric diester (**AN**) was found to have interaction between terminal aromatic groups.[67] The authors described this interaction to have resulted from the quadrupolar moments of two aromatic rings with opposite quadrupole signs.[67] There is at least one example in the chemical literature[68] where alkyl/aromatic interactions were more cohesive than aromatic/aromatic interactions. The interaction between aromatic moieties changes with change in the electronic nature of the interacting rings.[69,70]

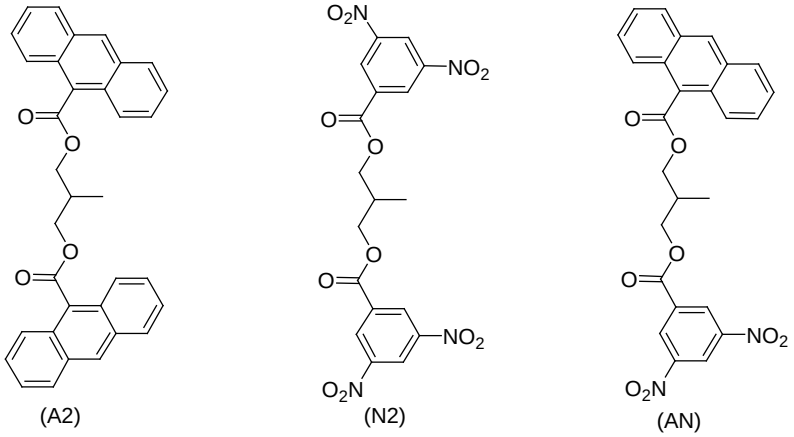

Figure 1.13. Molecular templates for intramolecular aromatic interactions.

1.9 Conclusion and Further Studies

Although the conformations in solid state and solution state did not have to coincide, this study showed that the preferred conformations of the molecular templates in solid and solution states are very likely similar. The dicationic model compound **1a-2Br** and 1**a-2PF$_6$** crystallized in folded conformations and preferred folded solution states whereas the neutral model compound **2a** crystallized in an open, splayed conformation and preferred this conformation in the solution states. Increased preference of folded conformations in the charged models (**1a-2Br**, 1**a-2PF$_6$**) and unfolded

conformations in the neutral analogue (**2a**) showed the importance of the positive charge in the interaction of aromatic moieties in isoelectronic molecular templates.

Literature shows that at least one electron-deficient group is probably needed to observe favorable intramolecular[55] or intermolecular[71-73] aromatic interactions. This study corroborated the literature finding the need of electron deficient aromatic moieties (as in **1a-2Br**, 1**a-2PF$_6$)** to detect folded stacked conformations. Similar to the literature finding of no favorable interactions between electron rich aromatics (or aromatic hydrocarbons), this study also found muted interactions between phenyl groups of aromatic hydrocarbons (as in **2a**).

This work brought questions to mind that inspired the work presented in the next chapter. What if both the interacting aromatic rings were electron deficient? Would there be any interaction between two electron deficient aromatic groups? What if we introduced a positive and a negative charge between two interacting partners? How would these two ionic aromatics interact? Could we hope to get some synergy between π-system interaction and the electrostatic interaction between fully developed charges? To extend our query into the effects of charge on π-stacking and to see whether two or more electron-deficient aromatics stack and to see if these interactions differ from the interactions between aromatic anions, we studied the stacking behavior of polycyclic charged aromatic molecules. These studies are presented in the next chapter. Chapter 3 will focus on the stacking between ionic aromatics bearing opposite charges in the search for synergy between π-stacking and hard electrostatics.

1.10 Experimental

Compounds **1a-2Br**[2] and **1b-2Br**[2] were synthesized following the literature methods. Compounds **2a**[5,52] and **2b**[5,52] were synthesized in our lab by Jing Chen and are described in his thesis.[52] Counter ion exchange to synthesize **1a-2PF$_6$** and **1b-2PF$_6$** was carried out as below.

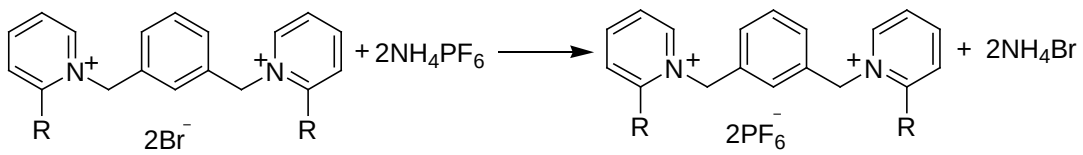

1a-2Br, R = Ph
1b-2Br, R = Me

1a-2PF_6, R = Ph
1b-2PF_6, R = Me

_m_-xylylene-N,N′-bis-2-phenylpyridinium dihexafluorophosphate (1a-2PF_6)

To a solution of α,α′-*m*-xylylene-*N*,*N*′-*bis*-2-phenylpyridinium dibromide, **1a**-2Br[2] (66 mg, 0.115 mmol) in water (20 mL) was added ammonium hexafluorophosphate (50 mg, 0.307 mmol). White precipitate formed immediately which dissolved upon heating under N_2. Slow cooling of the solution to room temperature gave white needle-like crystals of **1a**-2PF_6 (73.4 mg, 91% yield). MP 219-221°C (decomp.). ^{1}H NMR data in D_2O were indistinguishable from the published spectrum of **1a**-2Br.[2] X-ray diffraction analysis of the crystal thus obtained confirmed atomic connectivity and hexafluorophosphate ions.

α,α′-*m*–xylylene-N,N′-bis-2-methylpyridinium dihexafluorophosphate (1b-2PF_6)

To a solution of α, α'-*m*-xylylene-N, N'-bis-2-methylpyridinium dibromide, **1b-2Br**[2] (100 mg, 0.222 mmol) in water (10 mL) was added ammonium hexafluorophosphate (85 mg, 0.521 mmol). White precipitate formed immediately which dissolved upon heating under N_2. The reaction flask was capped properly. Slow cooling of the solution to room temperature gave colorless crystalline solid which was washed with cold water (1mL X 5) to get pure **1b-2PF_6** (110 mg, 85.3 % yield). MP 188-190 ^{0}C (decomp.). ^{1}H NMR data in D_2O were very similar to the published data of **1b-2Br**.[2] A small amount of this compound (5 mg) was dissolved in deuterated water (1 mL) and the solution was transferred into small vial. Slow evaporation of water from the open vial gave colorless crystal which was analyzed by X-ray diffraction to confirm atomic connectivity and presence of hexafluorophosphate ions.

Chapter 2

Effects of Charge in the Intermolecular Stacking of Triangulene Ions

Chapter one discussed the effects of two positive charges on the intramolecular face-to-face π-stacking of three aromatic moieties in a template molecule. Pertinent to this result, careful reading of the literature regarding π-stacking indicated the necessity of at least one electron deficient group as the stacking partner when the stacking partners are neutral. The literature on neutral π-system interactions with cations and anions indicate that the cation-π interaction is the most observable interaction with lingering questions about the veracity of the anion-π interaction. There is strong evidence that the cation-π interaction is stronger than any neutral π-π interaction and favorable anion-pi interactions are likely mythical

These facts hint at a native preference for the association of π-systems with electron deficient species, be they aromatic or otherwise. The obvious question is whether two large positively charged aromatic groups would be cohesive and whether there was a basic difference in energy between such an interaction and the interaction between two structurally analogous negatively charged molecules.

The literature on triangulene cations and anions partially satisfied some questions,[74-76] but raised other important questions. This chapter documents the pursuit of the basic question regarding differences in face-to-face cohesion between polycyclic aromatic cations ($[\mathbf{1}(NR)_3]^+$: R = Me, Et, Ph, *n*-Dec, *n*-Dodec, *n*-Hexadec and $[\mathbf{1}(O)_3(OH)_3]^+$) and analogous anions ($(\mathbf{2})^-$ and $(\mathbf{3})^{2-}$) in the solid state.

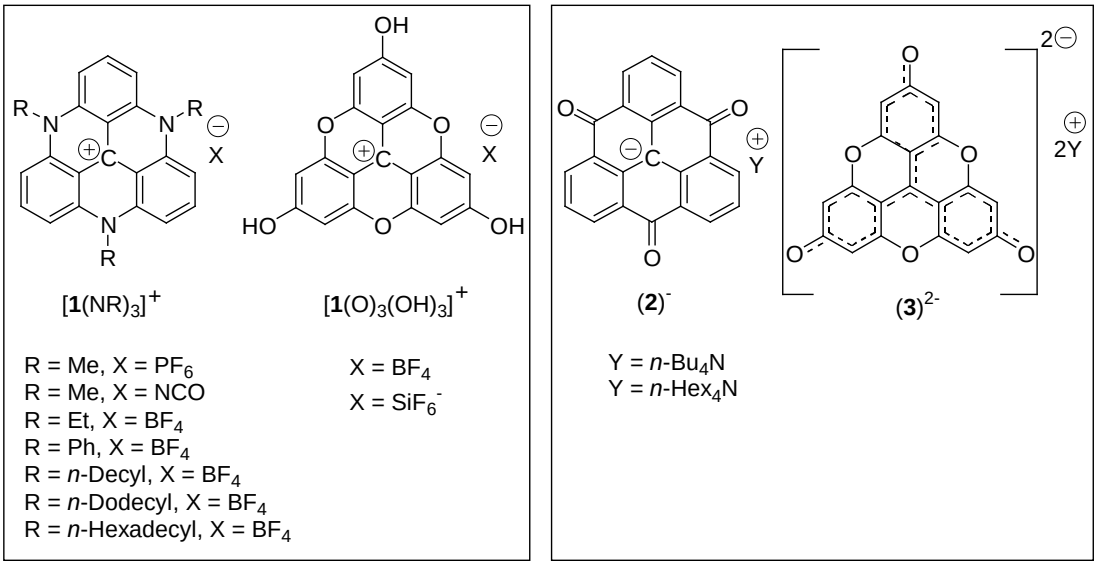

Figure 2.1. Aromatic cations and aromatic anions under study.

2.1 Major Findings of this Project

Solid states of two triazatriangulenium cations[74] ($[\mathbf{1}(NPr)_3]^+BF_4^-$ and $[\mathbf{1}(NOct)_3]^+BF_4^-$**),** trioxatriangulenium cations,[75] $[\mathbf{1}(O)_3]^+$ with various counter ions and a triangulene anion,[76] $(\mathbf{2})^-Bu_4N^+$ are published in the chemical literature before this project started. We obtained solid state structures of nine more triangulenium cations ($[\mathbf{1}(NR)_3]^+$ and $[\mathbf{1}(O)_3(OH)_3]^+$) and two more triangulene anions, $(\mathbf{2})^-$ $Hex_4N^+$and $(\mathbf{3})^{2-}$ with various counter ions as specified in Figure 2.1. We studied their solid state interactions to investigate the fundamental differences in facial cohesiveness of triangulene based aromatic cations and anions. As per literature indication, triazatriangulenium cations with *N*-ethyl chains and longer alkyl side chains ($[\mathbf{1}(NR)_3]^+$: R ≥ Et) packed as face-to-face dimers with the side chains of one stacking partner pointing above the plane and that of other stacking partner directed below the plane and these interdigitate with the alkyl chains of a vicinal dimer.

In our work we found that decreasing the steric interactions of the side chains ($[\mathbf{1}(NMe)_3]^+$ and $[\mathbf{1}(O)_3(OH)_3]^+$), resulted in the formation of columnar, face-to-face, polymeric association between cations in the crystal state. Comparing the crystalline state structural characteristics of the cations with those of the analogous anions in this work

and the literature shows that the cations tend to associate face-to-face to much greater extent than the anions. Among many examples of crystalline states cationic π-faces always adhere face-to-face as either dimers or n-mers whereas no example of anionic face-to-face association was observed. This work also found that **FF**-interaction in triangulene based aromatic cations depends on stability / electrophilicity of the cations and sterics of the side chains such that more stable and weakly elecrophilic cations with less steric bulkiness of the side chains have better **FF**-stacking than the ones with low stability, high electrophilicity and more steric bulkiness of the side chains. Among the cations with non-aromatic counter ions, the more electrophilic cations had less π-face association because these conserved proximity to the anions more than the cationic discotics with decreased lewis acidity and decreased reduction potential.

The fact that aromatic cations are more cohesive than their analogous anions was also supported by MO calculations.

2.2 Interactions Involving π-Systems Based on Electrostatics, an Introduction

The following review is presented for completeness in the spirit of a chemistry dissertation. The informed reader might want to skip to section 2.5 Radical Assisted p-Stacking / Pancake Bonding. Intermolecular forces can be broadly classified into six types: (1) Van der Waals interaction,[77] (2) dipolar interaction, (3) interactions between polar moments of higher symmetry, (4) hydrogen bonding,[78,79] (5) ionic interaction and (6) covalent bonding. Some of these aforementioned forces are composites of others but are cited due to their particular place in the history of chemistry. For example the hydrogen bond is a composite between, an electrostatic and a covalent interaction, the weight ascribed to each is a question of context.

In general these forces that attract and repel molecules toward or away from each other are not equal in magnitude. Van der Waals forces are much weaker than ionic interactions with hydrogen bonding somewhere in the middle. Furthermore increasing symmetry in the polar moments decreases the magnitude of the repulsions and attractions. For example with all other things equal the interaction between two dipoles will be greater than the interaction between two quadrupoles.

Van der Waals interaction is due to induced dipole in the molecules. The interaction is also termed as London dispersion force[80] and is caused by instantaneous dipole developed in the molecule due to unsymmetrical distribution of electrons present within the molecule.

Hydrogen bonding is a dipole-dipole interaction. It is the attraction between an electron donor atom and a hydrogen atom bonded to an electronegative atom. The strength of a hydrogen bond is about 2-10 kcal/ mole for neutral molecules[81,82] and about 20-30 kcal/ mole for the charged species.[82] Hydrogen bonding can be tuned by chemical syntheses.[82]

Ionic interaction is the attraction between two oppositely charged species (ions). Ions are formed by complete transfer of one or more electrons from one species to another: the species which accepts the extra electron develops a negative charge and the one which donates the electron develops a positive charge. Ionic interactions are stronger than hydrogen bonding interactions and their strength are in the range of 150-1400 kcal/ mole as observed in halides of alkali and other metals.[83] What we find in common in all of these aforementioned interactions is that attraction is really due to electrostatic forces of some kind or other. Among these interactions, an ionic interaction is purely electrostatic (Columbic) in nature and is the strongest one. The force (F) between two charges q and q' is expressed by Coulomb's equation:

$$F = (q\ q') / (\varepsilon\ r^2)$$

where ε is the dielectric constant of the medium. So, electrostatic attraction between charges is directly proportional to the magnitude of product of two charges and inversely proportional to the square of distance between them. Increase in size of ions increases the distance between them and hence decreases the force (F) holding them together.

In addition to these non covalent interactions, investigators often define another force of attraction found in organic compounds that involve π electrons as weak electron donors and acceptors. The interactions where there is only one π-system may involve an ion or covalently bonded hydrogen as another interacting partner. When interaction is between two π-systems, it is commonly called the π-π interaction or π-stacking.

2.3 π–– non π-Interaction

It is a well known fact that π bonded electrons are less stable than σ bonded electrons and hence π bonded electrons more easily serve as Lewis bases and to a lesser degree their corresponding antibonds serve more effectively as Lewis acids than σ antibonds. Sigma bonded electrons tend to be more localized than π bonded electrons which typically populate large conjugated orbitals often involving many concatenated atoms. Thus, aromatic and other pi-conjugated systems are relatively electron-rich with higher-energy populated orbitals, so it is possible for the π systems to polarize and interact more strongly with Lewis acids and electropositive regions in molecules leading to weak intermolecular attraction.

2.3.1 OH–π Interaction

Unlike ordinary hydrogen bonding where interaction is between a hydrogen atom bound to an electronegative group or atom (–OH, –NH or –HF) and a lone pair of electron on an electronegative atom (O, N or F), the OH–π interaction is between a hydrogen bond donor and a π system of bound electrons. In an OH–π interaction, electron deficient hydrogen atom accepts π-electrons from the π–system leading to a weak interaction. The interaction between OH and π–systems has been extensively studied [84-87] by Oki and Iwamura. The OH–π interaction is observed in simple aliphatic unsaturated compounds,[88,89] aromatic compounds,[90] and bio-molecules.[91] There is much spectroscopic[92] and crystallographic[92,93] evidence for the OH–π interactions.

2.3.2 NH-π Interaction

Very similar to OH–π interaction, NH–π interaction is also between a hydrogen atom of (–NH) and a π–system of bound electrons. The NH–π interaction was first observed[87] by Oki and Iwamura in 1959 while they were studying IR absorptions of benzylaniline derivatives to support the presence of OH-π interactions. X-ray crystallographic study of the binding of drug with human hemoglobin indicated a close distance between the amino group of an asparagine residue and the centre of benzene ring of the drug.[94] Calculations showed the interaction between an amino group and the centre

of a benzene ring to be about 3 kcal/mol[95] which is about half the strength of normal hydrogen bond between water molecules.

2.3.3 CH-π Interaction

Unlike O-H and N-H bonds, the C-H bond is non-polar. The difference between the electronegativities of C (2.6) and H (2.2) are relatively small compared to those involving N (3.0) and O (3.4) atoms. This slight difference in the electronegativity polarized bonded electrons slightly towards the carbon atom. This electronic displacement develops slight positive charge on hydrogen atoms and negative charge on the carbon atoms. Now it is possible for the hydrogen atom to interact with an electron-rich π-system. Adenine with four ring nitrogen atoms, an electron donating amino group and without electron withdrawing group is a highly electron rich hetero-aromatic compound. X-ray crystallographic study of binding of adenine ring with protein residues clearly indicates the presence of CH–π interactions in complex biological molecules.[96] There are many other reports in the literature that describe the importance of CH–π interactions in the associations of biomolecules,[97-100] conformational selectivity[101-108] and molecular recognition.[68,109-113] A recent study found the involvement of CH–π interaction as a key component in stereo selectivity in chemical synthesis.[102,114]

2.3.4 Origin of the OH-π, NH-π and CH-π Interactions

Tsuzuki *et al*. studied the interaction energies of methane, water and ammonia with the π–face of benzene by means of *ab initio* calculations.[115] The interaction energies of the gas-phase benzene complexes with water, with ammonia and with methane corroborated the notion that π–systems are native electron donors. Atomistic electronegativities and the strength of the hydrogen bond donor thus should determine the magnitude of the interactions. This hypothesis rationalizes the relative energies of the benzene complexes above 3.17, 2.22 and 1.45 kcal/mol respectively in the OH–π, NH–π, and CH–π interactions. These calculations considered the dispersion force (very difficult to accurately calculate), electrostatic force and repulsive force and found the electrostatic force of attraction as the major contributor to stabilization. Ammonia, water or methane was positioned above the centre of the benzene ring as well as above one of the carbon

atoms in the ring. In all cases, the overall interaction energy was found to be stronger when the interacting group was epicentric.

2.3.5 Ion-π Interaction

The interaction of non π-ions with π-system is discussed in this section. The ion-π interaction in which both the interacting partners are π-systems will be discussed under π-π interaction.

2.3.5.1 Cation-π Interaction

Formation of a π-complex between a metal ion and an aromatic system has been known for the long time.[116,117] Due to many loosely bound π-electrons, benzene and its derivatives are considered electron rich species. When positively charged ionic species come closer to the aromatic system, they induce a dipole in the aromatic system and they develop an electrostatic attraction between ionic species and the induced dipole of the aromatic moiety. Gas phase calculations predict that the binding energy of sodium ion with benzene molecule is 25.6 kcal/ mole when sodium is optimally placed above the centre of benzene ring.[118] The decrease in stabilization energy when sodium is displaced from above the centre of the ring toward one of the benzene C atoms is evidence for a π-complex that is dependent on the other p-orbitals.

Similar to this, the most stable structure of protonated benzene ($C_6H_7^+$) has been found to be the one where the added proton is epicentric to the benzene ring.[119] The calculated binding energy for K^+-benzene complex is 19 kcal/ mol as compared to 18 kcal/ mol for K^+-water complex.[118] The study of the binding energy of K^+ with a series including 1, 2, 3 or 4 molecules of water or benzene shows that K^+-benzene interactions are stronger than K^+-water interactions.[118] There is also experimental as well as computational evidence for the binding of more complex cations with benzene.[120,121]

The fact that electrostatic attraction is the major contributor to the cation-π can be clearly seen from the study of the binding of alkali metals with a benzene ring. The experimental binding energies of alkali metal ions with benzene ring are found to be Li^+ (38.3 kcal/ mol)[122] > Na^+ (28 kcal/ mol)[123] > K^+ (19.2 kcal/ mol).[118] This is the electrostatic trend one would expect if benzene were replaced by a halide anion. The

same electrostatic trend is found from the computational studies of binding of these cations with a benzene ring.[124] In another study, calculated binding energies of these alkali metal ions with benzene ring were found to be Li^+ (39.5 kcal/ mol) > Na^+ (24.4 kcal/ mol) > K^+ (19.2 kcal/ mol) > Rb^+ (15.8) which supports the importance of electrostatic attractions in the cation-π binding. If dispersion and polarizability were dominant, one would expect to see the binding energy of benzene with metal ions increase with increasing in size of the ions. In that case benzene-Rb^+ binding would be the strongest one.

2.3.5.2 Anion-π Interaction

Although cation-π interactions have been well-studied in the literature, the anion-π interaction has been less attended. This is probably because of unfavorable interaction expected to occur (and observed) between two electron-rich species. The first experimental observation of the anion-π interaction was found in 1993 by Schneider *et al* in their study of interactions between organic hosts containing negatively charged groups and organic guests containing electro-neutral π-moieties.[125] NMR studies of such host-guest complexes in aqueous solution found the binding energy to be around 0.48 kcal/ mol.

Analogous to the cation-π interaction where the interaction is stronger with electron rich π-moieties, the anion-π interaction increases with increasing electron deficiency in the interacting π-moieties. The favorable interaction between an anion and electron-deficient, aromatic moiety has been predicted by theoretical calculations.[126-128] The chemical literature presents evidence that the anion-π interaction is dominated by electrostatic attraction with some contribution from anion-induced polarization of the aromatic moiety. Theoretical studies of binding energies of halide ions with hexafluorobenzene predicted the general electrostatic trend as the binding energies were found to be C_6F_6•F^- (17.44 kcal/ mol) > C_6F_6•Cl^- (10.97 kcal/ mol) > C_6F_6•Br^- (9.42 kcal/ mol).[126]

Careful examination of the interactions of anions with different aromatic systems shows that the quadrupole moment of the aromatics is an important parameter to be considered. Due to slight electronegativity difference between hydrogen and carbon

(hydrogen being more electropositive), carbon atoms in the benzene ring develops slight negative charge which causes the benzene ring to have a negative quadrupole moment (Q_{zz} = −8.48 B) where as hexafluororobenzene has a positive quadrupole moment (Q_{zz} = +9.5 B) because fluorine atoms are more electronegative than carbon atoms.[129] Theoretical binding energy of Cl^- with C_6F_6 (10.97 kcal/ mol,[126]) is much higher than that with 1, 3, 5-trinitrobenzene (4.8 kcal/ mol,[129] Q_{zz} $C_6H_3F_3$ = + 0.57 B). This indicates the importance of quadrupole moment in the anion-π interaction.

2.4 π-π Interaction

The π-π interaction, the attractive non-covalent interaction between two neutral π-moieties has been widely cited in the biological and chemical literature. To mention a few examples, it is observed in base pair interaction in DNA,[6-8] protein folding,[9] molecular self assembly,[10,11] molecular recognition,[15,16] supramolecular design and crystal engineering.[17-19] Despite being known of many years and so diverse in nature, the exact nature of π-π interaction is still not fully known to chemists and hence its root cause is still a matter of debates. The π-π interaction between two aromatic moieties is also termed as aromatic interaction. π-π interaction acts very weakly between flat polycyclic aromatic hydrocarbons because of many delocalized π-electrons. The magnitude of neutral π-π interactions is in the order of van der Waals attraction and these forces depend on the Lennard–Jones potential;

$$V(r) = 4\varepsilon [(\sigma / r)^{12} - (\sigma / r)^{6}]$$

Where,

$(1/ r)^{12}$ terms describes repulsion

$(1/ r)^{6}$ terms describes attraction

ε is the depth of potential well and

σ is the finite distance where potential is zero.

2.4.1 π-π Interactions between Benzenoid Hydrocarbons

Delocalized π-electrons on the carbon atoms of benzene and slight residual positive charges on the hydrogen atoms, result in the T-shaped (Edge to Face or EF) packing arrangement of crystalline benzene. The hydrogen atoms of the one benzene ring

are attracted to the more electron rich π-face of the another benzene ring to give a herringbone arrangement of molecules.[130] The fact that C_6H_6 preferentially arranges in the crystalline state in an EF manner indicates that face-to-face (FF) interactions are nearly equal or weaker. In larger polycyclic aromatic hydrocarbons where the C-atom to H-atom ratios are higher, interactions between aromatic rings become more important. The result is that large polycyclic aromatic hydrocarbon molecules associate in an FF manner in the crystalline state.[131]

Many researchers have studied dimeric benzene theoretically as the model for π-π interactions.[132-137] Their studies show that EF and face-to-face edge-to-centre (FFEC) dimeric benzene is the most stable configuration and that face-to-face centre-to-centre (FFCC) is the most unstable one with the difference in gas-phase energies of ~ 0.98 Kcal/mol[136] between them.

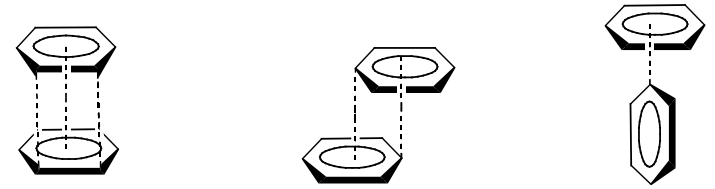

Figure 2.2. Different form of benzene dimmer. FFCC and EFCC are pi-stacked (π-π interaction) form whereas EF is T-stacked (CH-π interaction).

The two aromatic rings are said to be in a 'stacked' arrangement when they lie one above another co-facially and inter-planar distance between them should be within or less than the sum of Van der Walls radii of two carbon atoms (3.4 Å) for the effective interactions between π-orbitals. Only the **FFCC** and **FFEC** can have stacked arrangement of molecules. The reader should not confuse π-π interactions (π-stacking) with CH-π interactions (T-stacking). These are defined atomistically as different interactions (*vide supra* sections 2.2 and 2.3) in this document although in the literature T-staking and FF interactions have been considered in many reports as π-stacking.

2.4.2 What drives π-stacking?

Although the root cause of π-π interactions is not fully known to chemists, there are different approaches in the literature that describe the origin of the interactions. Some approaches adopted by chemists to describe "what drives π-stacking?" are presented here.

2.4.2.1 Quadrupole model for π-π interaction

A good example for understanding of π-stacking comes from the study of crystal packing of benzene and hexafluorobenzene. The equimolar co-crystal formed from C_6H_6 and C_6F_6 shows that these two units are packed alternately along the C_6 axis of the benzene ring in a **FFCC** packing arrangement.[138] Weak interactions between these two units can be demonstrated by the lower melting points of C_6H_6 (5 ºC) and C_6F_6 (4 ºC) their pure form compare to that of the co-crystal (24 ºC).[139] The interactions between C_6F_6 and C_6H_6 are marginally stronger than the interactions between the pure C_6F_6 or pure C_6H_6. It is believed that the **FFCC** packing pattern is probably due to the difference in quadrupole moments between hexafluorobenzene and benzene.[138,140] The dispersive van der Waals attractions are the main energy sources for the typical π-π interaction, while the electrostatic interactions related to quadrupole interactions determine the orientation of the stacking[141]

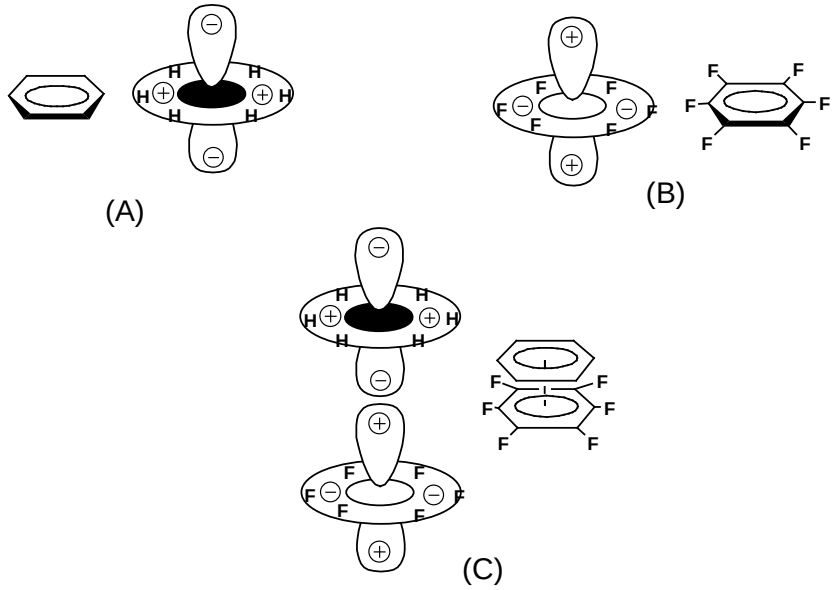

Figure 2.3. Quadrupole models of C_6H_6 (A), C_6F_6 (B) and the FFCC (C) interaction between the two.

2.4.2.2 Dipole interaction model for π-π interaction

Chen, Jing, a former group member, has recently reviewed this model in his Ph. D. dissertation.[142] In this model, each atom in an aromatic ring is assigned a partial charge based on calculated electronic distributions. The orientations of interactions between aromatic rings are determined based on whether or not bond dipoles in one ring can be aligned with those in another ring. If there is an alignment between partial opposite charges on two rings, preferential **FFCC** interactions exist in the crystalline state. If no such alignment, **EF** interactions are observed to predominate in the crystalline state.

Hamilton *et. al*.[143] found that diester macrocycle (**N)** and diether macrocycle (**O)** form a complex with 1-butylthymine (**M)** to produce different packing patterns. Diester and thymine arrange **FFCC** while diether and thymine preferr **EF** arrangement. Structurally (**N)** and **(O)** are similar; except that the carboxylate groups of (**N)** are replaced by butoxyl groups in (**O)**. Hamilton used the bond dipole model based on calculated atomic charges to explain the packing difference between (**M: N)** and (**M: O**). The strong **FFCC** stacking interaction in the co-crystal of **M** and **N** is due to alignment of five pairs of oppositely charged atoms on different rings as shown in Figure 2.4. Changing the carboxylate groups of **N** to butoxyl groups will change the charge distribution pattern of the naphthalene ring which in turn will change the packing pattern of the complex formed between **M** and **O**[143].

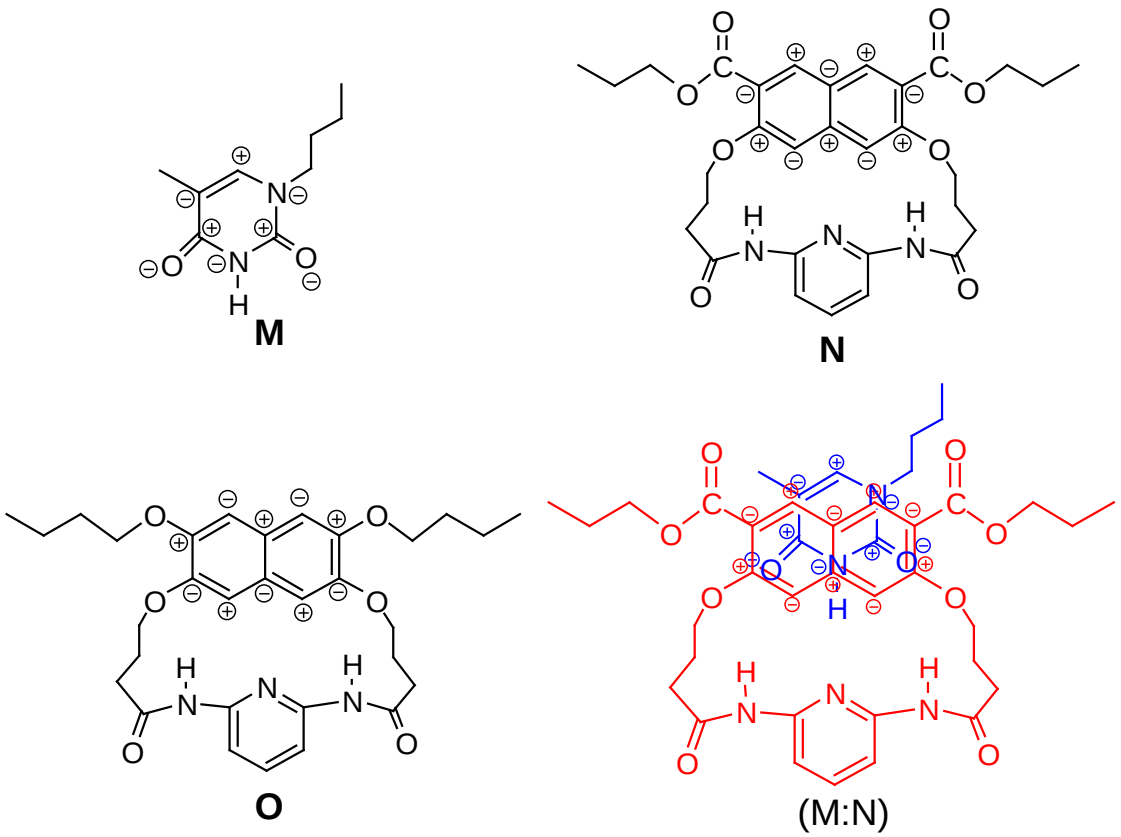

Figure 2.4. Atomic charge model. Partial charge distribution on atoms of molecules (M, N, O) and face to face, centre to centre (FFCC) stacking in M: N due to charge alignments.

2.4.2.3 Solvophobic effects on π-stacking

The solvophobic contribution to the cohesive force between two π-systems in a competitive solvent is due to repulsion between solvent and π-moieties. Interaction between two π-moieties in different solvents driven by solvophobicity has been well-studied in the literature.[144-146]

Studies of complexes formed between cyclophane hosts and pyrene guests in water and various organic solvents showed a continuous decrease in binding with decreasing solvent polarity.[147] For example, the binding energy of the complexes in water (9.4 kcal/ mol) was found to be much higher than that in carbon disulfide (1.3 kcal/mol).[147] The authors concluded that the most stable π-π complexes were of apolar substrates formed in solvents with low molecular polarizabilities and high dielectric. It is

worth mentioning that water fits this description well and in this special case *solvophobic* becomes well-known hydrophobic effect.

Similar trends were found in another study of self assembly in N-alkyl hexaaryltriindoles.[148] As suggested by NMR, while these triindoles had all monomers in chloroform, addition of polar co-solvent like methanol or acetone induced aggregation.[148] The study also showed that electronic effects of side chains on the central triindole rings were important for the self assembly of these indoles; while electron donating groups favored aggregation, electron withdrawing side chain inhibited aggregation in the solution phase. [148]

2.4.2.4 Electron donor-acceptor (charge-transfer) model

This model describes the attractive interaction in π-stacking to be arisen from the electrostatic attraction developed when electron rich (donor) and electron poor (acceptor) π-moieties come close within interactive distance and form an excited electronic state. The excited state is a result of transfer of a fraction of electronic charge from the donor π-system to the acceptor π-moiety. The formation of charge transfer complex can be easily detected by the presence of new absorption peaks in UV-vis spectroscopy. The electrostatic attraction thus developed stabilizes the π-π interaction. Π-stacking arguments driven by donor-acceptor complex are well studied in the literature. [17,149-152]

2.5 Radical Assisted π-Stacking / Pancake Bonding

The literature referred to above provide examples of π-stacking and species-π interactions assisted by electrostatics. Π-stacking can also be assisted by the presence of unpaired electrons in the π-moieties. Pairing radical cations or pairing radical anions brings two π-moiety monomers in proximitry but strong repulsion between the two like charges does not allow the two monomers to form a typical covalent bond.

However, radical salts condense into crystalline phases resulting in the formation of long-range, multi-center, 2-electron bonds between **FF** stacked π-moieties. These so called 'pancake' bonds between π-faces are well-discussed in the literature.[153-162] The **FF** interaction in the homo-dimer of tetracyanoethylene radical anion [TCNE(•)]^{153,161} is the typical example of pancake bonding and radical assisted π-stacking. Gas phase

calculations indicate that $[TCNE_2]^{-2}$ species are repulsive, but sufficient charge dispersion occurs between cations and [TCNE(•)] in crystalline and solid phases so as to allow for an electronic singlet π-face dimer. In terms of frontier MOs, bonding is a 4-center, 2-electron π*-π* interaction and these are characterized by C-C distances ~3.29 Å--just within the van der Waals radii of 3.4 Å (Figure 2.5).

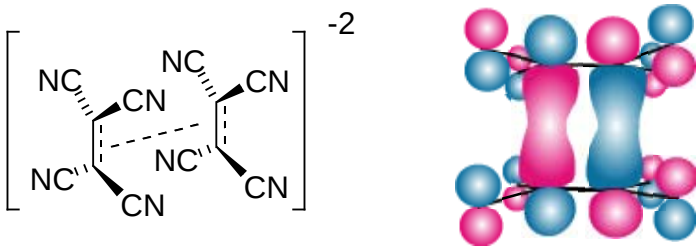

Figure 2.5. Bonding MO of $[(TCNE)_2]^{2-}$. Reproduced from Novoa, 2001. [153]

2.6 Basic Approaches in Designing Aromatics with Stronger π-π Interactions

No matter how different models describe π-stacking, there are three basic approaches in designing aromatic interactions: (1) High Molecular π-surface to Perimeter Ratio, (2) Introducing Bulky Aliphatic Side Chain, and 3) Introducing Electron-Rich and Electron Deficient Groups. (1) **High Molecular π-surface to Perimeter Ratio**: As stated already, benzene and other small aromatic hydrocarbons do not tend to stack[130] but flat, fused, polycyclic hydrocarbons with increased π-surface area (relative to its circumference) [163] tend to stack.[131] When π-surface area increases, the polarizability of the π-system increases. This unequal distribution of electrons installs temporary dipole moments in molecules and enhances crystalline-state FF stacking. This has not been observed for long aromatic hydrocarbons like acenes presumably due to small π-surface area to circumference. (2) **Introducing Bulky Aliphatic Side Chain**: As found in the crystalline states of benzene and other small aromatics, the default interaction between two aromatic hydrocarbons is **EF**. Putting one or more bulky groups on such compounds promote face-to-face disposition,[164,165] probably by destroying their **EF** interaction. (3) **Introducing Electron-Rich and Electron Deficient Groups:** Electron donating and electron withdrawing groups at opposite ends of the aromatic hydrocarbon tends to induce **FF** stacking. This disposition of EWGs and EDGs at head and tail of the molecule

establishes a molecular dipole and the stacking interactions that result are due to preferential opposite alignment of these dipole moments (Fig 2.4). This ultimately leads to one dimensional **FF** stacking.

Watson and co-workers[163] exploited this approach to get 1 dimensional stacks of molecules with ~3.37 Å interplanar distances. While there was **EF** interaction in the hydrocarbon analog, they found that introduction of perfluoro groups at one end of the molecule brings **FF** stacking to the crystalline state. Similar results were found by introducing perfluoro groups at one end and the thiophene group at the other end.

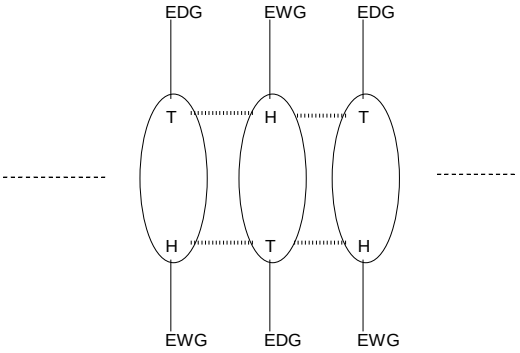

Figure 2.6. 1-D FF stacked column with EWG and EDG at opposite ends of the same molecule.

2.7 Importance of π-π Interaction in Organic Solids

There are many papers in the literature which explore the importance of π-π interaction in organic solids. *Supramolecular Chemistry* and *Crystal Engineering* are two fast-growing fields which utilize the concept of π-π interactions to rationalize structure-property relationships in materials.[166-168] Π-π stacking interactions have been utilized in varieties of research fields such as molecular conductors,[169-171] molecular machines,[172,173] and electronics.[174,175]

The π-π interaction has its application in relatively new type of liquid crystal material that is discotic liquid crystal. Discovered in 1977 by Chandrashekar and co-worker,[176] discotic liquid crystal composed of array of one dimensional column formed through co-facial pi-stacking of centre rigid aromatic core which is surrounded externally by an insulating hydrocarbon wrapper.[177] Discotic liquid crystals are known to have interesting opto-electronic properties.[166,178,179] The extent of π-π interaction and

intermolecular distance between the neighboring molecules are two key parameters for investigating the electric properties of organic materials.[180] However, the herringbone-like stacking in a crystal structure is not the optimum packing for achieving materials with properties that depend on the interaction between π-systems because edge-face (**EF**) packing decreases π-overlap between adjacent molecules compared to face-to-face packing.[181,182] Recently, many researchers have focused their research in synthesizing novel organic materials with co-facial (face to face, centre to centre) π-stacking arrangement.[183-185]

2.8 Aromatic Cations and Anions Studied in this Work

Aromatic cations and anions studied in this chapter are derivatives of triangulene hydrocarbon, **4** (Figure 2.7). Triangulene hydrocarbons, also called Clar's hydrocarbons, are difficult to synthesize because of their instability.[186] Since the Kekule structure can not be drawn for the triangulene hydrocarbons, these are classified as non-Kekule aromatic hydrocarbons. The parent molecule, **4**, can be represented as an aromatic biradical.

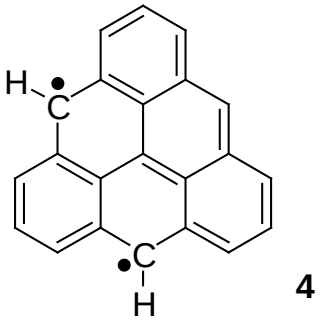

4

Figure 2.7. Triangulene hydrocarbon, 4.

After a few unsuccessful attempts to synthesize non-Kekule aromatic hydrocarbons by Clar and co-workers,[186,187] trioxy derivative of triangulene (**5**) was synthesized in 1995 as the first non-Kekule aromatic compound (Figure 2.8) by two-electron reduction of trioxytriangulene anion, $(\mathbf{2})^-$.[76]

All aromatic cations and aromatic anions in this study are flat, and very stable due to strong delocalization of charge. There are 13 degenerate resonance structures each for the triangulene anion $(\mathbf{2})^-$ and triangulene cation $[\mathbf{1}(NR)_3)]^+$.

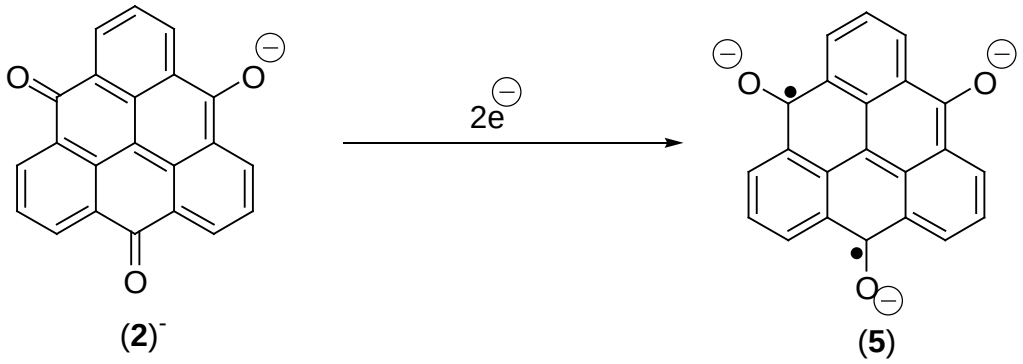

Figure 2.8. Synthesis of the first non-Kekule aromatic compound (5).

2.8.1 Synthesis of Aromatic Cations and Anions

Martin and Smith[188] first prepared tris-(2,6-dimethoxyphenyl) carbonium ion (**6**) by treating *o*-lithiated resorcinol dimethyl ether with diethyl carbonate and subsequent acidification of the hindered alcohol. Compound **6** is the key in the synthesis of aromatic cations in this study. They also synthesized trioxatriangulenium cation (**7**) by ring closing reaction of (**6**) in presence of pyridine hydrochloride. While *o*-lithiation of resorcinol dimethyl ether was carried out in ether, the following step of the reaction *i.e.* addition to diethyl carbonate did not occur in ether or THF. Decreasing the solvent polarity with the addition of benzene was required. Ring closing reaction of highly hindered alcohol to give trioxatriangulenium cation (**7**) was found to be inferior when carried out in presence of other acid catalysts ($AlBr_3$, $AlCl_3$, HBr).

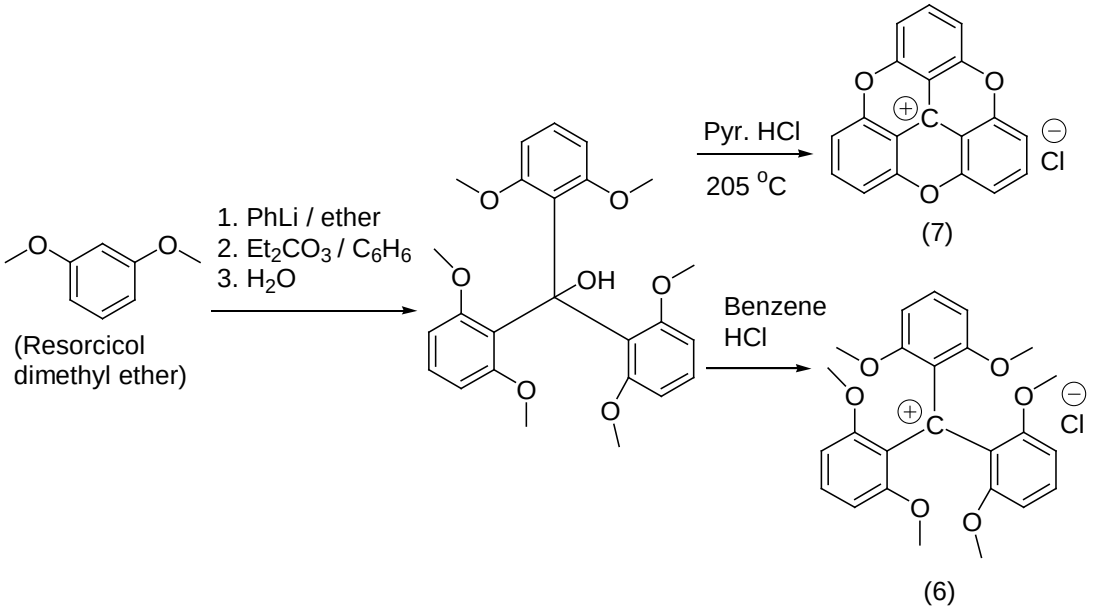

Figure 2.9. Synthesis of key compound (6) for the synthesis of aromatic cations under study and trioxatriangulenium cation (7).

Laursen and Krebs developed the method of formation of nitrogen bridged triangulenium (azatriangulenium) cations by nucleophilic aromatic substitution (S_NAr) reactions of tris(2,6-dimethoxyphenyl)carbenium ion (**6**) with primary amines.[74,189] They also showed that one, two or three N-bridged triangulenes could be prepared by controlling the reaction parameters. As shown in Figure 2.10, *tris*-(2, 6-dimethoxyphenyl) cation (**6**-BF_4) and partially N-bridged cations (**8a**-BF_4, **8b**-BF_4) can be cyclized with an O-bridge by heating them in NMP (N-methylpyrollidinone) in presence of excess pyridine hydrochloride.[74,188]

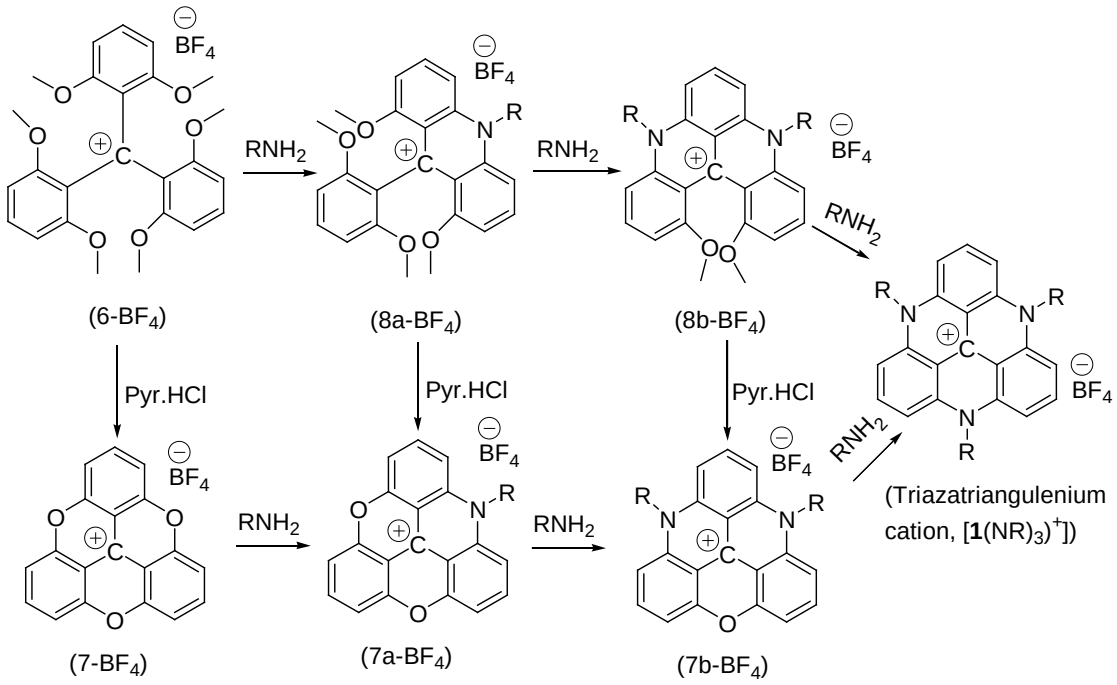

Figure 2.10. Synthetic schemes for making aromatic cations, $[\mathbf{1}(NR)_3]^+$.

A few partially or fully N-bridged triangulenium cations along with $[\mathbf{1}(NMe)_3]^+PF_6^-$ are reported in the literature.[74,189] All other N-bridged aromatic cations $[\mathbf{1}(NR)_3]^+$ studied in the current research were synthesized following the similar procedure mentioned in the literature.[74,189]

Before we prepared aromatic cation $[\mathbf{1}(O)_3(OH)_3]^+$, it was reported in a patent[190] as a potential *in vivo* glucose biosensor but synthetic details were not available. We synthesized cations $[\mathbf{1}(O)_3(OH)_3]^+$ with BF_4^- and SiF_6^{2-} counter ions conveniently from tris-(2,4,6-trimethoxyphenyl)carbenium ion (**9**).[191] The carbenium ion (**9**) was refluxed with excess of pyridinium hydrochloride in NMP to give yellow dihydroxy ketone derivative of trioxatriangulene (**10**) which had poor solubility in common organic solvents. The dihydroxy ketone derivative of trioxatriangulene, **10** was protonated with aqueous HBF_4 and H_2SiF_6 to give $[\mathbf{1}(O)_3(OH)_3]^+$ with respective counter anions (Figure 2.11). Although the procedure for making trihydroxytrioxa cations, $[\mathbf{1}(O)_3(OH)_3]^+$) has been recently reported in a literature.[192] Compounds $[\mathbf{1}(O)_3(OH)_3]^+BF_4^-$ and $[\mathbf{1}(O)_3(OH)_3]^+SiF_6^{2-}$ were found to be stable only in the acidic medium. Diffraction-quality crystals of these compounds were grown in organic solvent containing these with

slight excess of aqueous HBF_4 or H_2SiF_6. Both compounds $[\mathbf{1}(O)_3(OH)_3]^+BF_4^-$, and $[\mathbf{1}(O)_3(OH)_3]^+SiF_6^{2-}$ had good solubility in organic solvents.

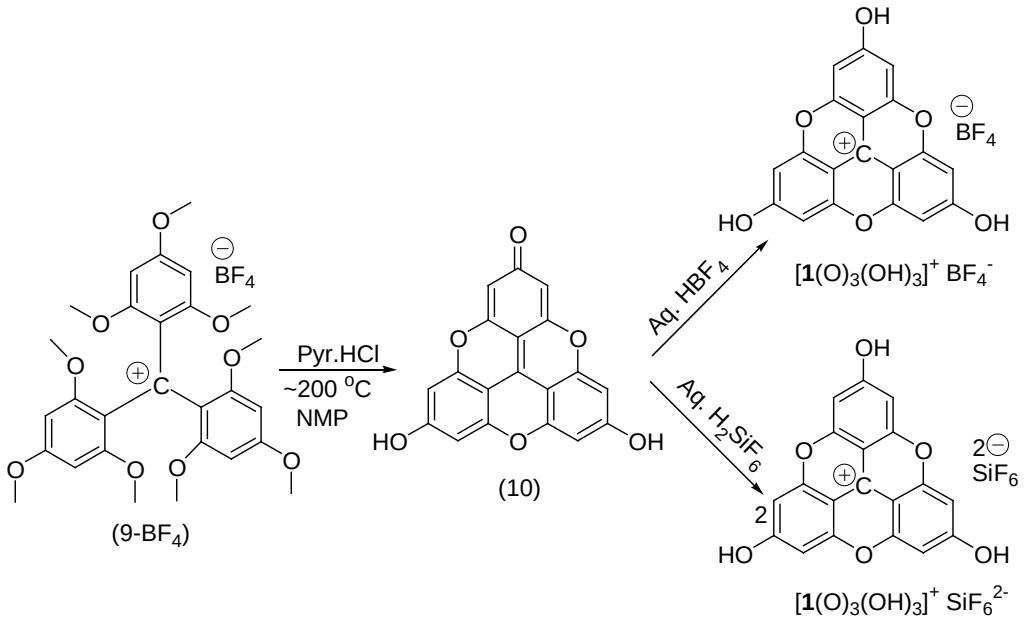

Figure 2.11. Synthesis of aromatic cations, $[\mathbf{1}(O)_3(OH)_3]^+$.

Aromatic anion, $[(\mathbf{2})^-Bu_4N^+]$ is a known compound and was prepared following a literature procedure.[76] The only difference is that the sodium amalgam used in the reduction steps was replaced by zinc powder activated with copper to avoid the use of mercury.[81] Another aromatic anion, $[(\mathbf{2})^-Hex_4N^+]$ was obtained simply by cationic exchange of $[(\mathbf{2})^-Bu_4N^+]$ with excess of tetra-*n*-hexyl ammonium bromide (Figure 2.12) in the mixture of CH_3CN and $CHCl_3$ (1:3). Diffractable quality dark blue crystals of $[(\mathbf{2})^-Hex_4N^+]$ were obtained by slow evaporation of solvent mixture (CH_3CN: $CHCl_3$ = 1:3) at room temperature.

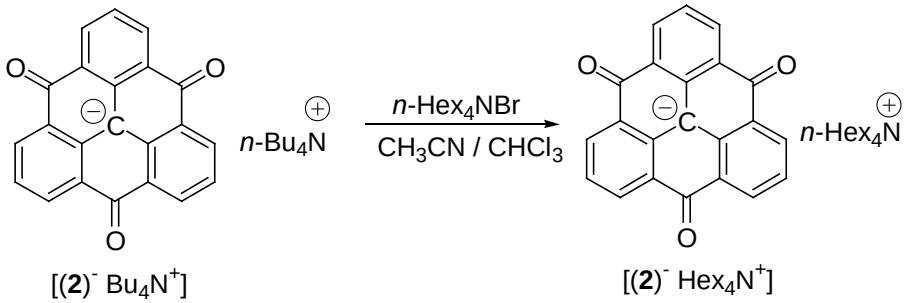

Figure 2.12. Cationic exchange of $[(\mathbf{2})^-Bu_4N^+]$ with Hex_4NBr to prepare $[(\mathbf{2})^-Hex_4N^+]$.

Aromatic dianion [(**3**)$^{2-}$ 2Bu_4N^+] was prepared in our lab by deprotonation of both phenolic hydrogens of dihydroxy ketone derivative of trioxatriangulene (**10**) with 48% aq. *n*-tetrabutylammonium hydroxide. Although the procedure for making dianion, **10** has been recently published in a literature.[192]

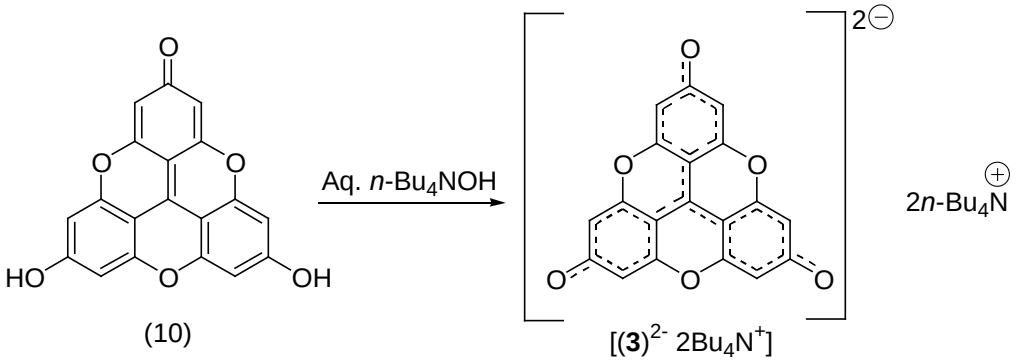

Figure 2.13. Synthesis of aromatic dianion, [(**3**)$^{2-}$ 2Bu_4N^+].

2.9 Methods

2.9.1 Crystal Structure Analysis

Crystals of all aromatic cations ([**1**$(NR)_3]^+$ and [**1**$(O)_3(OH)_3]^+$) and aromatic anions ((**2**)$^-$ and (**3**)$^{2-}$) under study were grown by various procedure and in various solvents. A detailed procedure for crystallization of each aromatic ion is presented in the experimental section at the end of this chapter. Quick view of crystals of aromatic cations and aromatic anions showed the central aromatic core of these ions to be almost completely planar. Different aspects of interaction between aromatic cores in the solid state were studied by calculating dihedral angle (Θ_d), horizontal displacement of the centres of two aromatic cores (D_h) and vertical displacement of the centres of two aromatic cores (D_v). Finally area of overlap (A_o) between two adjacent aromatic cores was calculated from average radii (R_1 and R_2) of two adjacent aromatic cores and D_h. Horizontal displacement (D_h) can also be correlated with the angle between two aromatic centres (Θ_c).

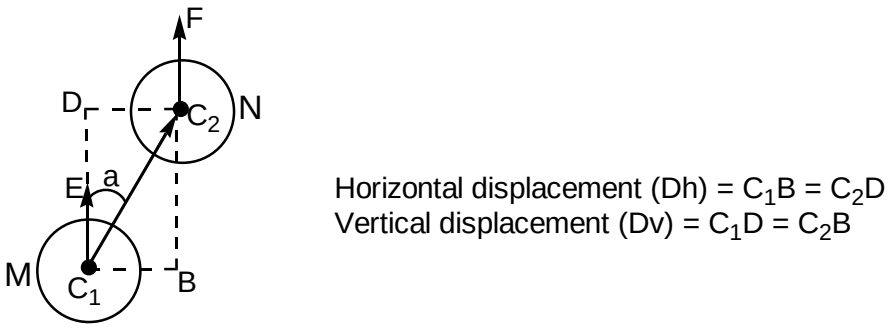

Figure 2.14. Diagram representing 2 interacting aromatic cores as circles (M and N) with centres C1 and C2 respectively. C1E and C2F represent the average unit normal vectors of the circles M and N respectively viewed from above the π face.

For the mathematical calculation of above mentioned parameters of crystals of aromatic ions, crystal coordinates of central aromatic core were imported into excel sheet, vectors between the central carbon atom and each peripheral atom in the ring were obtained from crystal coordinates, vectors thus obtained were converted into unit normal vectors. All of these unit normal vectors were approximately perpendicular to the plane of the aromatic ring. These unit normal vectors were averaged to represent the aromatic plane with a single unit vector that is perpendicular to the aromatic ring. Distances between central carbon atoms and each of peripheral atoms in the aromatic ring were also calculated from their coordinates. The central aromatic core was assumed to be a circle of radius (R). The circle was taken to be the average distance between the central carbon atom and each of peripheral atoms in the ring.

2.9.1.1 Dihedral angle (Θ_d)

Dihedral angle (Θ_d) is the angle between planes of two aromatic cores. Thus, $\Theta_d = 0$ is desired for better face-to-face (**FF**) stacking of molecules. Any deviation from this ideal situation will decrease **FF** interactions. When the dihedral angle reaches 90^o, there is no more **FF** stacking and the interaction is termed as edge-to-face (**EF**). The dihedral angle between two planes (Say, circles M and N in the above diagram) was calculated by

taking the dot product of the unit normal vectors of two aromatic planes. So, if C_1E = (X_1, Y_1, Z_1) and C_2F = (X_2, Y_2, Z_2) in the above diagram, the dihedral angle between two aromatic planes is given by,

(Θ_d) = ACOS $\{(C_1E \bullet C_2F) / |C_1E|\,|C_2F|$

= ACOS $[(X_1*X_2 + Y_1*Y_2 + Z_1*Z_2) / \{(X_1^2 + Y_1^2 + Z_1^2)\}^{0.5} X \{(X_2^2 + Y_2^2 + Z_2^2)\}^{0.5}]$

2.9.1.2 Vertical Displacement (D_v) and Horizontal Displacement (D_h)

Vertical displacement (D_v) is the distance between the planes of two interacting aromatic moieties along a normal vector of an aromatic plane. For effective interaction between two aromatic moieties, d_v should be less than sum of Van der Waal's radii of two carbon atoms (3.4 Å). Similarly, horizontal displacement (D_h) is the distance between centres of two interacting aromatic moieties along a vector 90° to the normal of one of the aromatic planes. D_h would be zero for perfect overlap of two interacting aromatics where two interacting partners would be one above another.

The following mathematical procedures were followed to calculate d_v as described in the above diagram; 1) Distances and vectors between centres of two aromatic moieties were calculated from the crystal coordinates of central carbon atoms. 2) Angle between vectors C_1E and C_1C_2 was calculated. The angle is represented as 'a' in the diagram above. 3) D_v and D_h were then calculated using simple trigonometry from the known value of angle 'a' and distance between C_1 and C_2.

2.9.1.3 Area of overlap (A_o)

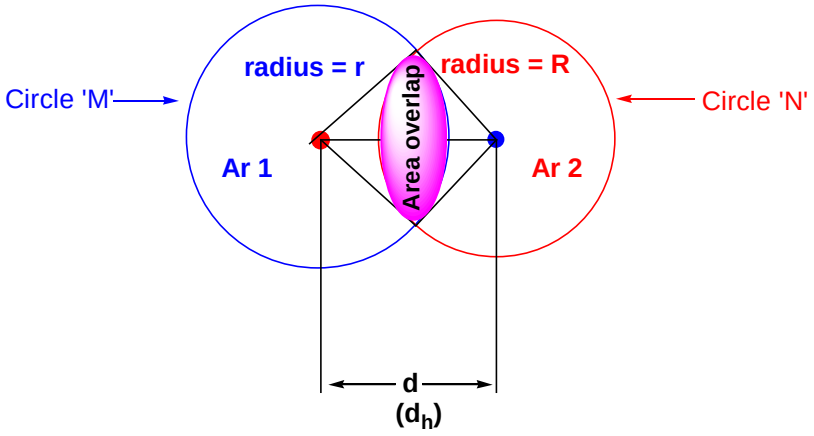

Figure 2.15. Area of overlap (A_o) between two aromatic moieties (Ar 1 and Ar 2) with radii r & R respectively. Distance between two aromatic centres, d is also the horizontal displacement (D_h).

In the above diagram (Figure 2.15), if vertical displacement (D_v) was set to zero, two interacting aromatic moieties (being represented as circles M & N) would position next to each other in the same horizontal line. In that case, some area of the circles M and N may overlap with each other. This, what is called as the area of overlap (A_o) depends on horizontal displacement (D_h) and can be calculated mathematically from the known value of d_h and average radii of the interacting aromatic moieties. The average radius of the aromatic core was assumed to be the average of distances between the central carbon atom and each non – central atom.

The area of overlap (A_o) was then calculated[193] using the following mathematical equation;

$$\text{Area of overlap } (A_o) = r^2 \cos^{-1}\left(\frac{d^2 + r^2 - R^2}{2\,d\,r}\right) + R^2 \cos^{-1}\left(\frac{d^2 + R^2 - r^2}{2\,d\,R}\right) - \frac{1}{2}\sqrt{(-d + r + R)\,(d + r - R)\,(d - r + R)\,(d + r + R)}\,.$$

2.9.2 Molecular Orbital (MO) Calculations

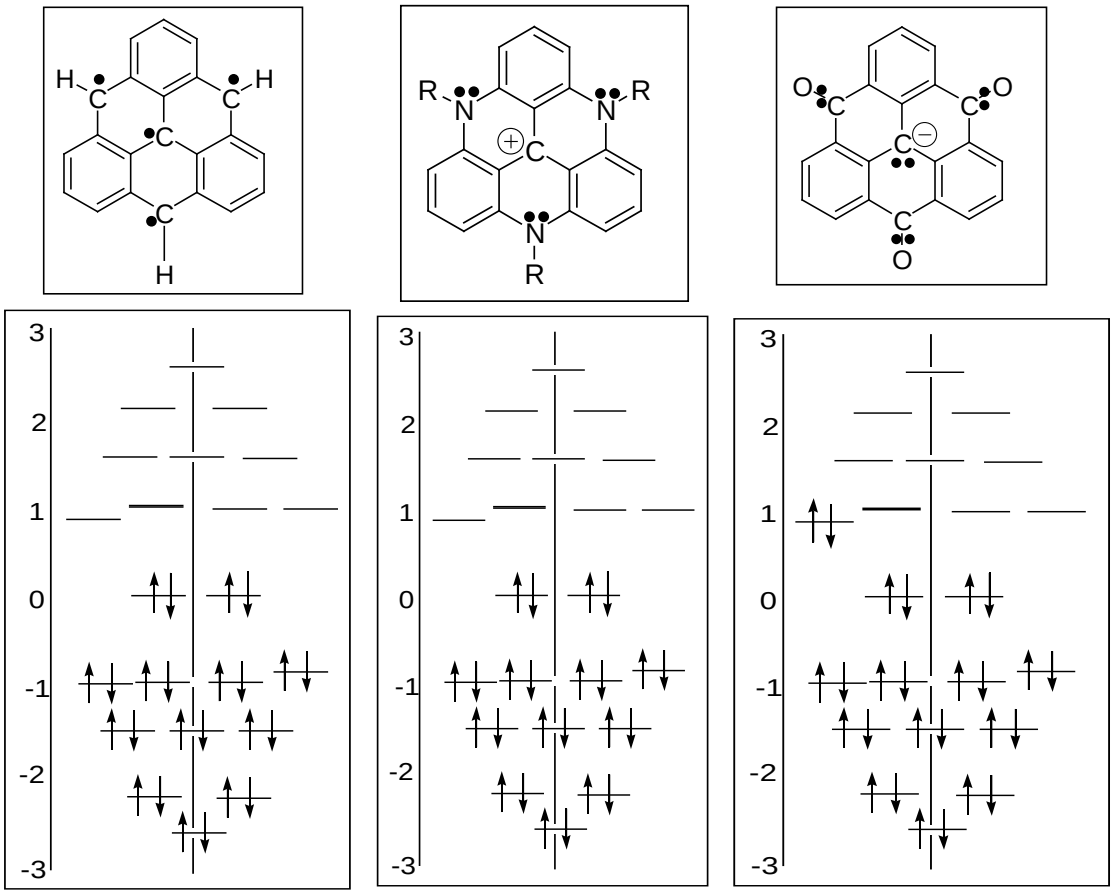

Figure 2.16. Above; delocalized π-framework of parent triangulene (left), aromatic cation (middle) and aromatic anion (righ) and below; their respective Huckel energy diagram. The purpose of showing paired / unpaired electrons is for accounting of π-electrons.

As described previously, triangulene hydrocarbon diradical[186] is the parent molecule of all aromatic cations and anions under study. To get better idea of electronic constructions of aromatic cores of cations and anions from the parent triangulene, simple Huckel molecular orbital (SHMO) calculations were done. Software is available at http://www.chem.ucalgary.ca/SHMO/index.html. The electronic construction in molecular orbitals (MOs) and their predicted energies in terms of α (energy of electrons in 2p-orbital) and β (interaction energy between p-orbitals) were analyzed. The

theoretical aspects of the method have been published.[194] The results of these SHMO calculations are shown in Figure 2.16.

As mentioned above, the SHMO calculation was done only to get some insights on electronic constructions and energies of MO for parent triangulene and its all-carbon derivatives with specific number of electrons and charges. It was not done in any way to calculate the energy of actual aromatic cations and anions under study. The actual energies of molecular orbitals (MO) of an aromatic cation and an anion were approximated at "Restricted Hartree-Fock (RHF) / 3-21G", a low level of theory. Whether or not the formation of dimer (or n-mer) by aromatic cations and aromatic anions is energetically favorable process? To answer this question, energies of HOMO (highest occupied molecular orbital) and LUMO (lowest unoccupied molecular orbital) of an aromatic cation and an aromatic anion were compared with their FF-stacked dimers placed together within π-stacking distance(3.4 Å) found in crystal structures of cations under study.

2.10 Results and Discussion

Crystal structures of two triazatriangulenium cations ($[\mathbf{1}(NR)_3]^+ BF_4^-$, R = *n*-propyl and *n*-octyl) (Figure 2.1) were published in the chemical literature before the current project started.[74] Analyzing the published crystal structures and crystals of $[\mathbf{1}(NR)_3]^+$ revealed that triangulenium cations with *N*-ethyl (or longer aliphatic) side chains packed as polymer of **FF**-staggered-dimer (Figure 2.17, left) with side chains of one stacking partner pointing above the aromatic plane and the other pointing below the plane (Figure 2.18). Since alkyl side chains are not perturbing the interaction between two Ar-cations in a dimer, one would expect dimers of alkyl-substituted Ar-cations, $[\mathbf{1}(NR)_3]^+$ to have similar vertical displacement (d_v) but this is not the case. The vertical displacement (d_v), which is only 3.29 Å for $[\mathbf{1}(NEt)_3]^+BF_4^-$**,** increases with increasing length of alkyl side chains and reaches 3.35 Å in $[\mathbf{1}(NDec)_3]^+BF_4^-$ and $[\mathbf{1}(NDodec)_3]^+BF_4^-$. It again increases with further increase in the length of side chains (d_v=3.41 Å in $[\mathbf{1}(NHexadec)_3]^+BF_4^-$). This is probably due to increased interactions between alkyl side chains of vicinal dimers in long chain Ar-cations which causes cationic discs of the dimer to pull apart from each other with increase in its size. The

interaction between alkyl side chains of vicinal dimers is caused by interdigitation of alkyl groups of one dimer with those of other (Figure 2.18). There should be a limit for the effect of size of side chains on d_v of cationic dimers. However, since d_v in $[\mathbf{1}(NHexadec)_3]^+BF_4^-$ (R = *n*-$C_{16}H_{33}$) is already outside the pi-stacking distance (> 3.4 Å), we didn't try to synthesize Ar-cations with R > *n*-$C_{16}H_{33}$.

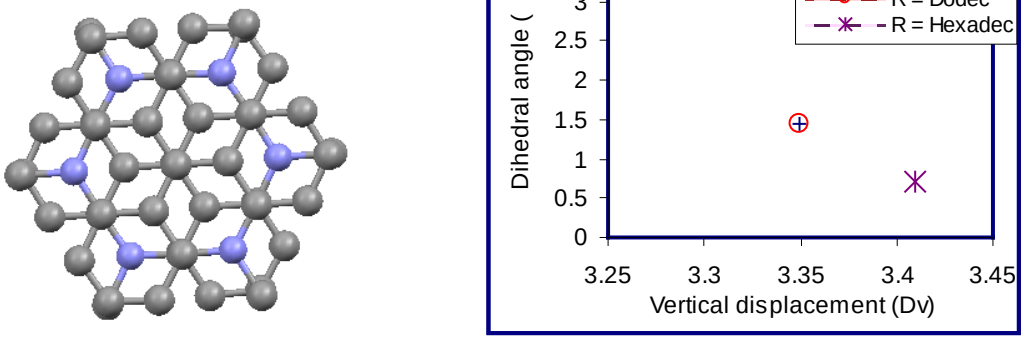

Figure 2.17. (left) Ball & stick model of staggered dimer of $[\mathbf{1}(NMe)_3]^+NCO^-$ representing general trend in the crystal structure of $[\mathbf{1}(NR)_3]^+BF_4^-$ dimer. Grey represents carbon atoms and blue represents Nitrogen atoms. Alkyl side chains and anions were not shown for clarity. (Right) Θ_d vs. d_v showing inverse relationship between the two. Angle measured in degree and distance in Å.

Analysis of crystal structures shows that there is an inverse relationship between the dihedral angle (Θ_d) and vertical displacement (d_v) in the Ar-cations, $[\mathbf{1}(NR)_3]^+$ with R ≥ Et. $[\mathbf{1}(NEt)_3]^+BF_4^-$ with smallest d_v (3.29 Å) has the biggest dihedral angle (Θ_d = 3.51°). As seen in the plot of Θ_d vs. d_v in Figure 2.17 (right), the dihedral angle (Θ_d) decreases with increase in d_v; 1.44 deg. for cations with R = decyl (*n*-$C_{10}H_{21}$) and dodecyl (*n*-$C_{12}H_{25}$) and 0.72 deg. for the one with R = hexadecyl (*n*-$C_{16}H_{33}$) which has highest d_v. Although Θ_d & d_v are two independent parameters of solid state structures, the dependence of Θ_d with d_v in the crystals of Ar- cations, $[\mathbf{1}(NR)_3]^+$ with R ≥ Et is

most probably due to increased electrostatic repulsion between two cationic discs as d_v decreases. This repulsion between two cationic discs of a dimer pushes individual Ar-cation out of the stacking plane at some points leading to the increase in dihedral angle (Θ_d) between two Ar-cations of the dimer. However, the dihedral angle noticed in the dimers of Ar-cations under study is still low and it ranges from 0.72° – 3.5°.

Aromatic cations	$(D_v)_1$	$(D_h)_1$	$(\Theta_d)_1$	$(\Theta_c)_1$	$(A_o)_1$
[**1**$(O)_3(OH)_3]^+$ BF_4^-	3.25	4.83	1.92	34.0	8.52
[**1**$(O)_3(OH)_3]^+$ SiF_6^{2-}	3.32	1.32	1.07	68.3	71.5
[**1**$(NMe)]^+$ PF_6^-	3.46	1.82	2.59	62.3	61.4
[**1**$(NMe)]^+$ NCO^-	3.35	0.19	3.06	86.8	95.9
[**1**$(NEt)_3]^+$ BF_4^-	3.29	0.17	3.51	87.1	96.4
[**1**$(NDec)_3]^+$ BF_4^-	3.35	0.3	1.44	84.9	93.6
[**1**$(NDodec)_3]^+$ BF_4^-	3.35	0.29	1.44	85.0	93.7
[**1**$(NHexadec)_3]^+$ BF_4^-	3.41	0.29	0.72	85.1	93.7

Aromatic cations	$(D_v)_2$	$(D_h)_2$	$(\Theta_d)_2$	$(\Theta_c)_2$	$(A_o)_2$
[**1**$(O)_3(OH)_3]^+$ BF_4^-	3.22	5.64	1.9	29.7	0.78
[**1**$(O)_3(OH)_3]^+$ SiF_6^{2-}	3.33	1.44	1.1	66.0	69
[**1**$(NMe)]^+$ PF_6^-	3.36	1.92	2.0	60.3	59.34
[**1**$(NMe)]^+$ NCO^-	3.47	1.96	3.1	60.6	58.59

Table 2.1. Parameters of crystals of Ar-cations under study. Lengths measured in Å, angles in degree and ring overlap (A_o) in %.

Another important crystal parameter to describe stacking is the horizontal displacement (d_h), the distance between two Ar-centers if they were next to one another in the same horizontal plane. If other parameters stay the same, effective **FF**-stacking is observed when two stacking aromatic centers are one above another ($d_h = 0$). But the centers of $[\mathbf{1}(NR)_3]^+$ with R ≥ Et in their dimers are not one above another in the same vertical plane causing these dimers to have none zero value for d_h. The d_h seems to be have direct relationship with the size of alkyl side chains in Ar-cations. $[\mathbf{1}(NEt)_3]^+BF_4^-$ with ethyl side chains has the lowest value (d_h = 0.17 Å) and it remains constant in the cations with alkyl side chains ≥ octyl as found in crystals of $[\mathbf{1}(NR)_3]^+$ with R = decyl, dodecyl and hexadecyl and also in the triazatrioctyltriangulenium tetrafluoroborate[74] (R = Oct). Triazatripropyltriangulenium tetrafluoroborate[74](R = Pr) has exceptionally small value for d_h (d_h = 0.07 Å). The Horizontal displacement (d_h) can be correlated with an angle (Θ_c) between two Ar-centers. For optimal **FF**-stacking, the angle (Θ_c) would be equal to 90 degree for $d_h = 0$. Since crystals of $[\mathbf{1}(NR)_3]^+$ with R ≥ Et have none zero d_h, the angle between two Ar-centers is deviated from 90 degree such that greater the deviation in d_h from zero, the greater will be the deviation of Θ_c from 90 degree. Very similar to the trend in d_h, the aromatic cation with ethyl side chains (R = Et) has the least deviation in Θ_c (Θ_c = 87. 13 deg.) and the deviation increases and stays constant (~ 85 deg.) for the cations with alkyl side chains ≥ octyl as found in crystals of $[\mathbf{1}(NR)_3]^+$ and also in the triazarioctyltriangulenium tetrafluoroborate[74] (R = Oct). The anomalous behavior of triazatripropyltriangulenium tetrafluoroborate[74] is due to its anomalous d_h.

From the observed values of d_h and average radii (r) of Ar-cores of stacking dimers, areas of overlap (A_o) between two stacking aromatics was calculated (Figure 2.15). Although, bigger A_o means better **FF**-stacking for the given value of d_v, it should never be assumed that bigger A_o alone means better stacking because d_v is an important crystal parameter to study stacking. Following the trend in d_h, $[\mathbf{1}(NEt)_3]^+BF_4^-$ has the highest overlap (% A_o = 96.4) between stacking partners and decreases to stay constant (% A_o = ~93.5) for the cations with alkyl side chains ≥ octyl as found in crystals of $[\mathbf{1}(NR)_3]^+$ and also in the triazarioctyltriangulenium tetrafluoroborate[74] (R = Oct). Again, the anomalous behavior of triazatripropyltriangulenium tetrafluoroborate[74] is due to its anamolous value of d_h.

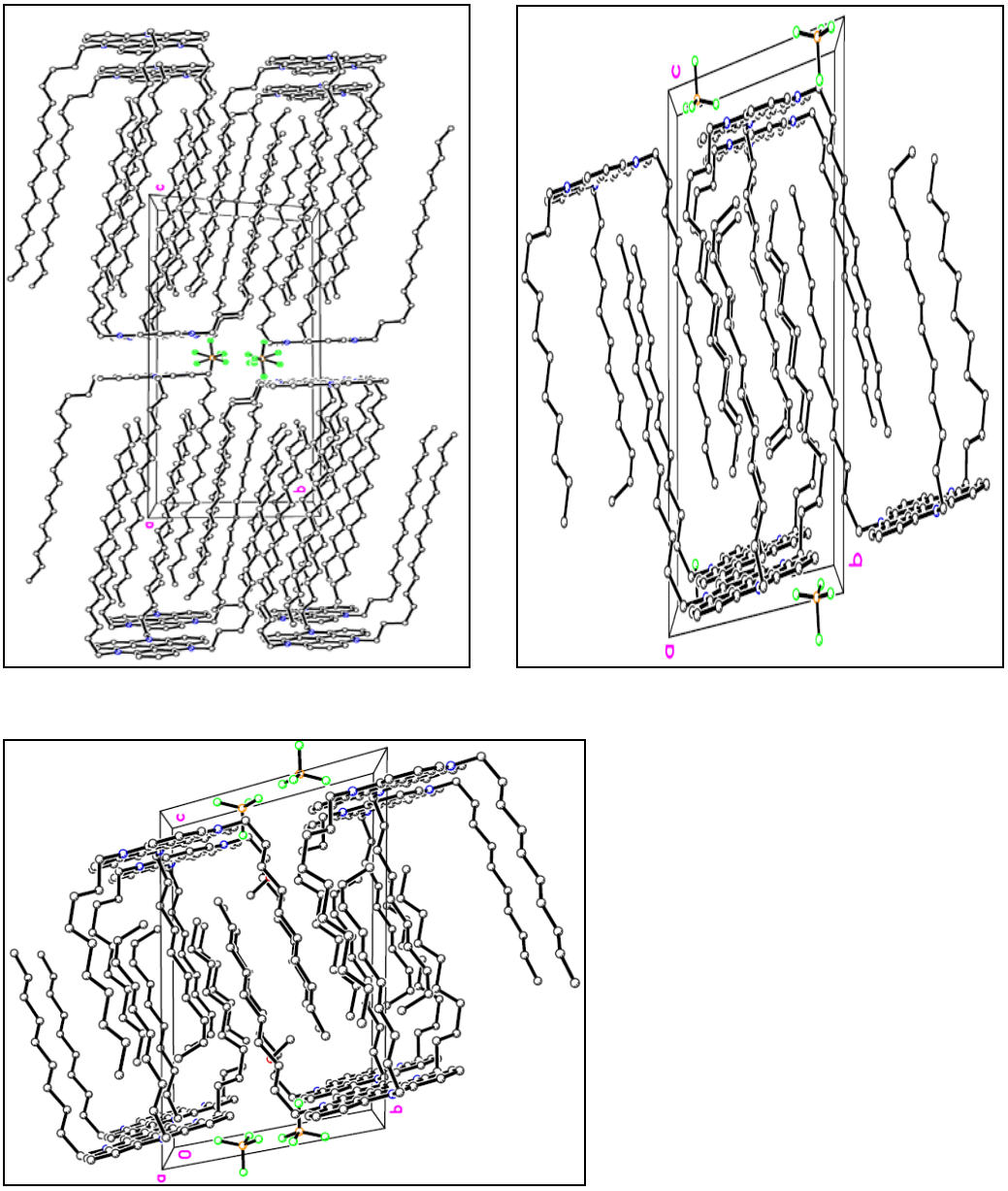

Figure 2.18. Crystal structures of [**1**$(NR)_3]^+BF_4^-$. Top left: R = hexadecyl, top right: R = dodecyl and bottom: R = decyl viewed down a-axis. Some anions are omitted.

As stated above, from the crystal structures of alkyl substituted triazatriangulenium cations, distances between two aryl components in the homodimers decreases with decreasing size of side chans. [**1**$(NR)_3]^+BF_4^-$ with R = *n*-$C_{16}H_{33}$ has short

distance between dimers of 22.2 Å which decreases with decrease in the size of alkyl substitutions and reaches 5.5 Å and 4.5 Å in the crystals of tripropyltriazatriangulenium tetrafluoroborate[74] (R = *n*-C_3H_7) and [**1**$(NR)_3]^+$ with R = C_2H_5 respectively.

From the crystal structures of alkyl-substuted [**1**$(NR)_3]^+$ with R ≥ C_2H_5, it is clear that alkyl side chains prevent polymeric arrangement of cations in 1D column. This came out to be true as cations with reduced steric parameters (R = Me) crystallize in a polymeric arrangement of cations in 1D column with alternate stack of more intimate and less intimate dimers. These more- and less intimate association can also be understood as the interactions within a dimer and between two dimers respectively. In absence of steric in the stacking direction, one would expect [**1**$(NMe)_3]^+$ not to have two different interactions between any two Ar-units positioned next to each other.

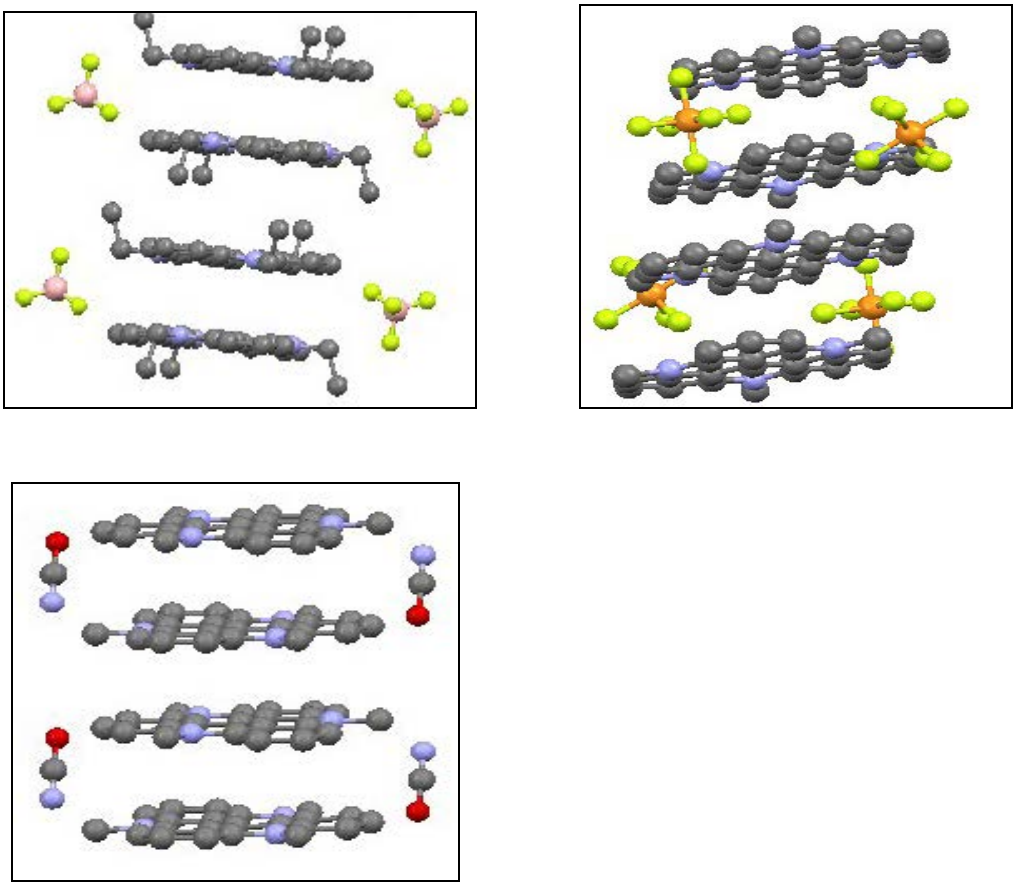

Figure 2.19. Crystal structures of [**1**$(NEt)_3]^+BF_4^-$ (top left), [**1**$(NMe)_3]^+PF_6^-$ (top right) and [**1**$(NMe)_3]^+NCO^-$ (bottom) showing arrangement of dimers in the solid states.

Arrangement of counter anions in the crystals may modulate the intimacy of the Ar-Ar interactions. As seen in the crystal of $[\mathbf{1}(NMe)_3]^+PF_6^-$ (Figure 2.19), the anions which are positioned at the peripheries of cations are close to the dimer. It is probably the strong electrostatic attraction between unit charges of reverse signs that results more intimate association in the dimer. The less intimate interaction between two dimers may be under the control of a) electrostatic repulsion between two positively charged Ar-cations. The repulsion in case of dimer is probably compensated by the strong electrostatic attraction between two cations and each of two anions; b) decreased electrostatic attraction between cations and anions of different dimers.

Big shifts in vertical displacement (d_v) are observed when ethyl side chains (R = Et) are replaced with methyl groups (R = Me) in the cations, $[\mathbf{1}(NR)_3]^+$. Close interaction between two cations within dimer decreases greatly going from C_2H_5 to CH_3 side chains. The vertical displacement (d_v) in dimer of $[\mathbf{1}(NEt)_3]^+BF_4^-$ is only 3.29 Å which increases to 3.35 Å & 3.36 Å as seen in the more intimate dimer of $[\mathbf{1}(NMe)_3]^+$ with PF_6^- and NCO^- respectively. This is probably due to increased interaction between dimers as side chains become smaller and there is compensation between decreased interaction within a dimer and increased interaction between two dimers. The reason behind overall better stacking in $[\mathbf{1}(NMe)_3]^+NCO^-$ than in $[\mathbf{1}(NMe)_3]^+PF_6^-$ is attributed to the size & shape of counter anion. We think that perturbation in Ar-interactions by a planar and small NCO^- is smaller than PF_6^-. The less intimate interactions between two dimers of $[\mathbf{1}(NMe)_3]^+$ are beyond Van der Walls' interactions.

Another shift in solid state is observed when N-atoms of Ar-cations are replaced with O-atoms. Literature reports crystal structures of trioxatriangulenium cation,[75] $[\mathbf{1}(O)_3]^+$ with anions of various size, shape and valences (Figure 2.20). Although herringbone like zigzag packing pattern seems to be dominated in the solid state of trioxatriangulenium cation, considerable amount of facial stacking between two cationic discs can be achieved by crystallizing it with relatively small divalent anion ($S_2O_6^{2-}$).[75] As seen in the crystal structure (5 in Figure 2.20), each dianion positions the periphery of two dimers that are next to each other. It is probably the strong electrostatic interaction between each cation in the dimer and each peripheral dianion that overcomes the

repulsion between two like charge cations and hence stabilizes the **FF**-stacked dimer. Since another dimer in the stacking plane sits above the peripheral anions of the aforementioned dimers, polymeric arrangement of cations is not possible. Presence of bulky *t*-butyl groups on peripheries of the cation puts two cationic discs one above another cofacially in a dimer with ~ 3.35 Å of separation between two discs. However, the distance between two adjacent dimers is quite big because of the position of counter anions between the two (4 in Figure 2.20).[75]

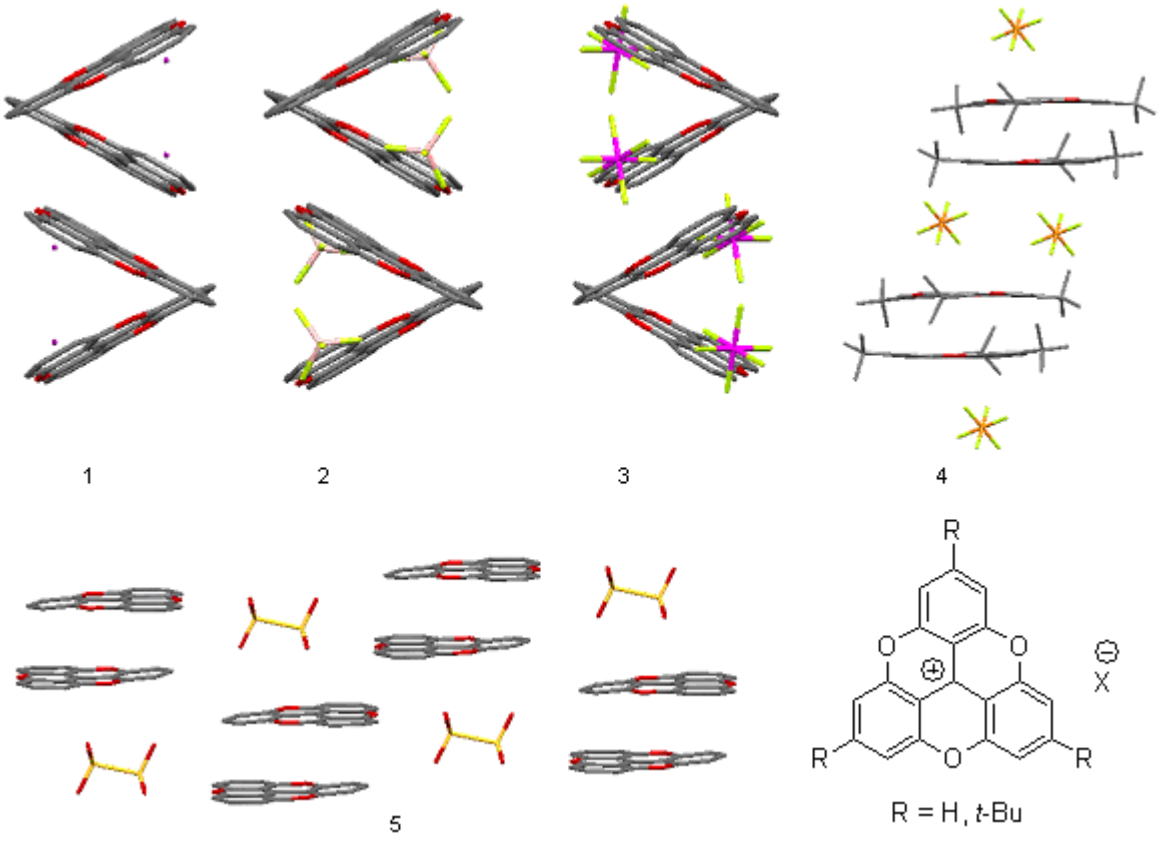

Figure 2.20. Literature examples of crystals of trioxatriangulenium cation, with various anions; 1 (R = H, X = Cl), 2 (R = H, X = BF_4), 3 (R = H, X = PF_6), 4 (R = t-Bu, X = PF_6) and 5 (R = H, X = $S_2O_6^-$).

Compared to trioxatriangulenium cations, trihydroxy derivatives of trioxatriangulenium cations, $[\mathbf{1}(O)_3(OH)_3]^+$ show better **FF**-stacking in the solid states (Figure 2.21). Crystal structure of $[\mathbf{1}(O)_3(OH)_3]^+BF_4^-$ shows two dimensional arrangements of aromatic discs (Figure 2.21, top) but there is no ring overlap between discs of cross dimension. Similar to the crystal structure of $[\mathbf{1}(NMe)_3]^+$, there are two different types of interactions in the solid state of $[\mathbf{1}(O)_3(OH)_3]^+BF_4^-$; more intimate and less intimate interactions. Although, the % overlap between two Ar-discs is very small (% Å = 0.78 & 8.52) due to high value of d_h (5.64 Å, 4.83 Å), the best intimacy between two neighboring Ar-discs is found in $[\mathbf{1}(O)_3(OH)_3]^+BF_4^-$ among all Ar-cations under study as predicted by single crystal analysis. Vertical displacements of 3.22 Å & 3.25 Å found in the solid state of $[\mathbf{1}(O)_3(OH)_3]^+BF_4^-$ are the more intimate and less intimate distance between two stacking units. Switching from mono-valent anion (BF_4^-) to divalent anion (SiF_6^{2-}) brought large changes in the solid state of $[\mathbf{1}(O)_3(OH)_3]^+$.

As seen in the crystal structure of $[\mathbf{1}(O)_3(OH)_3]^+SiF_6^{2-}$, there is almost no difference between stacking cations making it very difficult to Figure out distinction between more intimate and less intimate interactions (Figure 2.21, bottom). The two d_v values found in the crystal (3.32 Å & 3.33 Å) are within 0.01 Å to each other and both are within the Van der Waals' interaction distance. The average ring overlap between two adjacent cations in a column was 70% with average horizontal displacement (d_h) equal to 1.38 Å. Among all the Ar-cations studied in this research, $[\mathbf{1}(O)_3(OH)_3]^+SiF_6^{2-}$, is the only example having truly polymeric arrangement of cationic disc in the solid state. To the best of our knowledge, this is the first and only example of ionic π-stacking with truly polymeric arrangement of like charge π-ions in the literature of solid state organic chemistry.

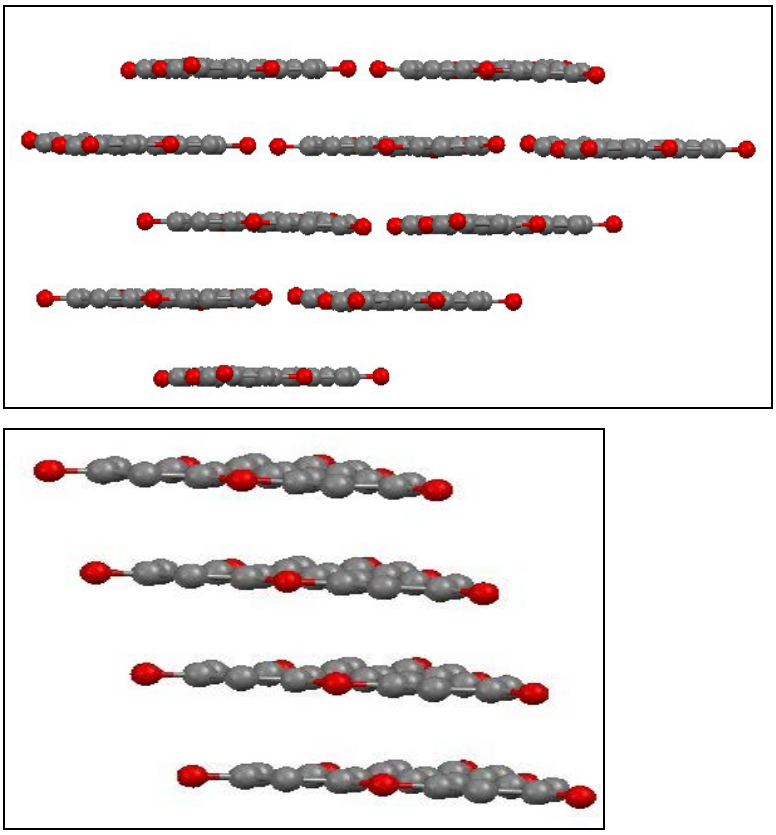

Figure 2.21. Crystal structures of $[\mathbf{1}(O)_3(OH)_3]^+BF_4^{2-}$ (top) and $[\mathbf{1}(O)_3(OH)_3]^+SiF_6^{2-}$ (bottom). Solvent molecules and counter anions are also not shown for clarity.

The steric effect of alkyl side chains in **FF**-stacking of triazatriangulenium cations, $[\mathbf{1}(NR)_3]^+$ is further clarified in the crystal structure of $[\mathbf{1}(NPh)_3]^+BF_4^-$ where all alkyl side chains are replaced with phenyl groups (Figure 2.22, left). Similar to the crystal structures of ethyl (or longer chains) substituted triazatriangulenium cations, $[\mathbf{1}(NPh)_3]^+BF_4^-$ has these phenyl groups positioned out of the plane of central Ar-core. But, unlike ethyl (or longer chains) substituted triangulenium cations where all three side chains of a cationic unit are pointed to the same direction, each phenyl group in $[\mathbf{1}(NPh)_3]^+BF_4^-$ is pointed above and below the central Ar-plane. These phenyl side chains block the way of incoming cationic partner to stack from above and below the plane. So, **FF**-stacking between central Ar-cores of two adjacent units is not observed in the solid state of $[\mathbf{1}(NPh)_3]^+BF_4^-$.

When one NPh group is replaced with oxygen atom ([**1**$(NPh)_2O]^+BF_4^-$**,** Figure 2.22, middle), faces of two T-stacked dimers seem to interact with each other. Although the mathematical calculation as describes already doesn't show any indication of ring overlap between the two t-stacked dimers in [**1**$(NPh)_2O]^+BF_4^-$**,** a close distance of 3.08 Å is found between them. The closest distance between two Ar-units in a t-stacked dimer is 3.28 Å. When two NPh groups are substituted with oxygen atoms ([**1**$(NPh)(O)_2]^+BF_4^-$**,** Figure 2.22, right) to give enough space for stacking, **FF**-stacked dimers are noticed with t-staking between two dimers. The closest distance between two **FF**-stacked Ar-units is found to be 3.28 Å in [**1**$(NPh)(O)_2]^+BF_4^-$**.** Although the crystal structure of [**1**$(NPh)(O)_2]^+BF_4^-$ is reported in the literature,[74] the one described here was grown by us in ethanol.

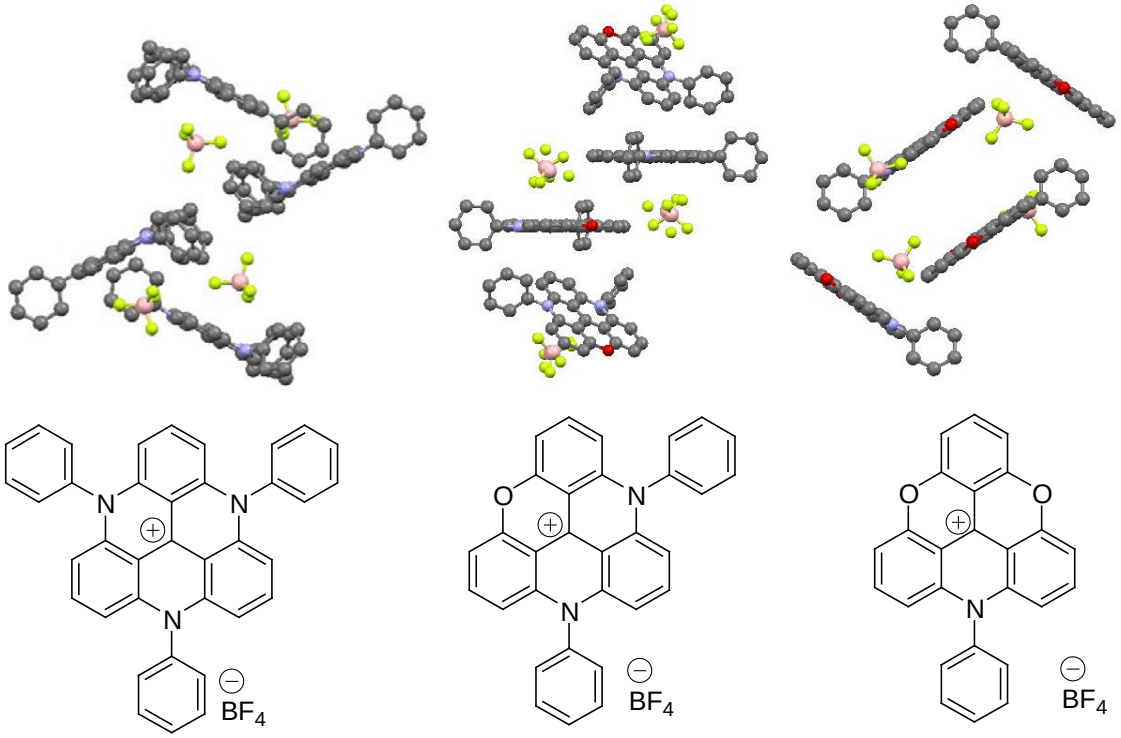

Figure 2.22. Above: Crystal structures of [**1**$(NPh)_3]^+BF_4^-$ (left), [**1**$(NPh)_2O]^+BF_4^-$ (middle) and [**1**$(NPh)(O)_2]^+BF_4^-$ (right) showing steric effect of phenyl substitution in **FF**-stacking. Below: Their corresponding molecular structures.

Literature reports crystal structure of triangulene anion,[76] (**2**)$^{-}$$Bu_4N^+$ where there is no facial staking between Ar-anions. The crystal of this compound grown by us in acetonitrile doesn't indicate any facial contact between anions either. The only interaction between two anions is t-stacking. Increasing the size of counter cation brings all anionic Ar-units parallel to each other ((**2**)$^{-}$$Hex_4N^+$ in Figure 2.23) but due to intervention by big cation/s, faces of two adjacent Ar-moieties are well separated from each other. Ar-anions and counter cations are arranged alternatively in a column. Dianion, (**3**)$^{2-}$ has structural similarities with (**2**)$^{-}$$Hex_4N^+$ in the solid state. Like (**2**)$^{-}$$Hex_4N^+$, faces of aromatic anions in the dianion are separated from each other by counter cations. The anions studied in this research have big counter cations.

Would there be facial stacking in the solid state of these anions if crystallized with small cations? We tried to co-crystallize the anion, (**2**)$^{-}$ with variety of small cations but unfortunately, we were not able to get diffractable quality crystals. The cations tried were Me_4N^+, Et_4N^+, K^+ & Li^+. Getting excited from the solid state of [**1**$(O)_3(OH)_3]^+SiF_6^{2-}$ where divalent counter anion may have brought truly polymeric arrangement of Ar-cations in the crystal, we tried to co-crystallize the anion (**2**)$^{-}$ with small divalent cation (Ca^{2+}) but diffractable quality crystals were never obtained.

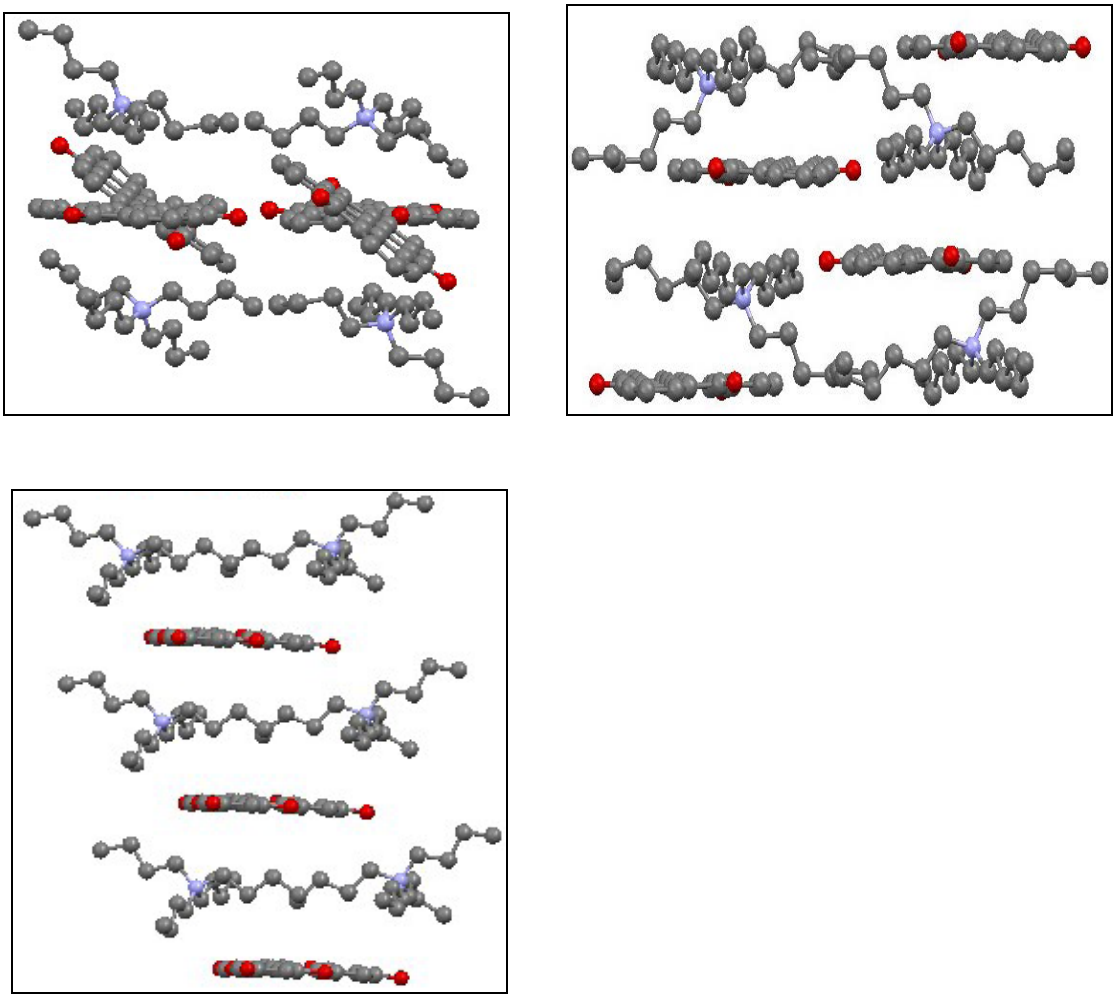

Figure 2.23. Crystal structure of aromatic anions. (**2**)$^{-}$$Bu_4N^+$ (top left), (**2**)$^{-}$$Hex_4N^+$ (top right) and (**3**)$^{2-}$$2Bu_4N^+$ (bottom). Solvents molecules are not shown for clarity.

Literature reports **FF**-stacking between two anion-π moieties[153,161] but the interaction is assisted by unpaired spin (radical) in the interacting units and is best described as pancake bonding;[153-162] a long range $2e^-$, multi-centre bonding. The strong interactions between two unpaired spin & π- π must have overcome the repulsion between two like charges leading to the stacking between two radical π-anions. But this is not the case in the anions we studied. There appears to be no additional attractive force between two Ar-units other than π- π interaction which may have undermined by a strong repulsive force between two like charges. There is a cation mediated indirect association between faces of two Ar-anions but the position of big cation doesn't let Ar-units come closer to each other.

Huckel molecular Orbital (HMO) calculations (Figure 2.16) for all-carbon analogue of Ar-cations and anions under study shows that energy of highest occupied molecular orbitals (HOMO) of Ar-anion is much higher than that of Ar-cation. One can assume this energy difference between HOMO of Ar-cation and Ar-anion to further increase, if you consider the real molecules. Similarly, although the energy difference between lowest unoccupied molecular orbital (LUMO) of all carbon-analogue of Ar-cation and Ar-anion is low, it should increase in the calculation for the real molecules. Just by analyzing the HMO of all carbon analogues of Ar-ions, it wouldn't be hard for chemists to believe that Ar-cations have low-energy LUMOs capable of accepting π-electron while corresponding anion has these orbitals filled. These assumptions were further studied by approximating the energies of HOMO and LUMO of the parent Ar-cation, $[\mathbf{1}(NH)_3]^+$ and the Ar-anion $(\mathbf{2})^-$ at "Restricted Hartree-Fock (RHF) / 3-21G", a low level of theory. The results are presented in the table 2.2 below.

MO	Energy of parent Ar-cation, $[\mathbf{1}(NH)_3]^+$ in ev	Energy of Ar-anion, $(\mathbf{2})^-$ in ev	Monomer / dimer
HOMO	-6.35	-3.02	Monomer
	-13.16	-0.03	Dimer
LUMO	-5.53	4.64	Monomer
	-5.36	6.94	Dimer

Table 2.2. Energies of HOMO and LUMO of Ar-ions and their FF-stacked homo-dimers approximated at RHF / 3-21G.

As seen in the table 2.2, energies of both HOMO and LUMO of Ar-anion are much higher than corresponding cation in their monomeric as well as dimeric forms. Centers of two **FF**-stacked Ar-units in the homo-dimer of cations and anions were placed 3.415 Å apart from each other. While going from monomer to homo-dimer of the Ar-cation, a huge decrease (diff. is 6.81 ev) in energy of HOMO is noticed, thus stabilizing the electrons in HOMO. Although the energy of LUMO slightly increases in homo dimer

of Ar-cation, it is still much lower than the LUMO of Ar-anion. Overall huge decrease in energies of HOMO & LUMO of the dimer supports that practical observation of **FF**-stacking in the Ar-cations is energetically favorable process. The low-energy LUMO of dimer can still accept the electron density from the HOMO of monomer leading to the formation of trimer (or n-mers) by Ar-cations if the process is sterically allowed. The dimer formation by Ar-anions is not an energetically favorable process as indicated by increase in energy of both HOMO & LUMO while going from monomer to dimer.

The overall observation is that triangulenium Ar-cations studied in this research along with the similar ones mentioned in the literature[74,75] do stack their π-faces in the solid state but the Ar-anions don't. The fundamental difference in stacking of Ar-cation and Ar-anions can be further understood in different ways other than MO calculation just described above;

As discussed earlier (sections **2.3.5.1** and **2.3.5.2**), π -electrons have better affinity with cations than anions. This is also evident from the mechanism of ionic, addition reaction of HCl to a π-bond where H^+ (not Cl^-) is added to the π-bond in the first step (Figure 2.24).

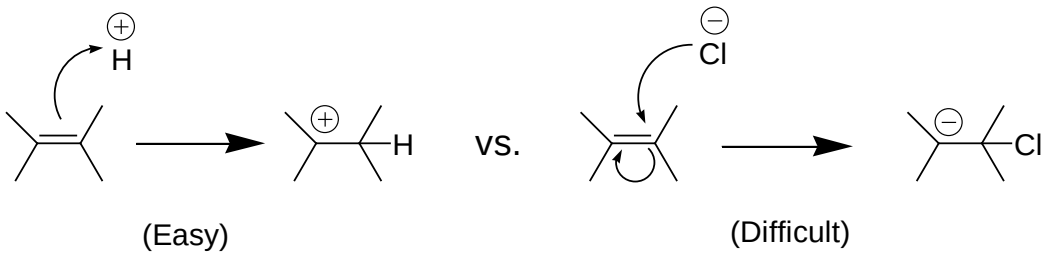

Figure 2.24. Reaction showing preference of a π-bond with a cation over with an anion.

In a **FF**-stacked dimer of Ar-cation, there are i) attraction between a cation of Ar-ring 1 and π-electrons of Ar-ring 2 ii) attraction between a cation of Ar-ring 2 and π-electrons of Ar-ring 1 iii) repulsion between two cations (Ar-ring 1 & Ar-ring 2). In a hypothetical **FF**-stacked dimer of Ar-anion, there would be all repulsive forces between two discs; repulsion between each of the anions and each of the Ar-rings as well as repulsion between two like charge anions. There are ionic interactions between opposite

charges in the FF-stacked dimer of Ar-cation as well as Ar-anion. So, compared with Ar-anion, Ar-cation is expected to have **FF**-stacking of ions easily.

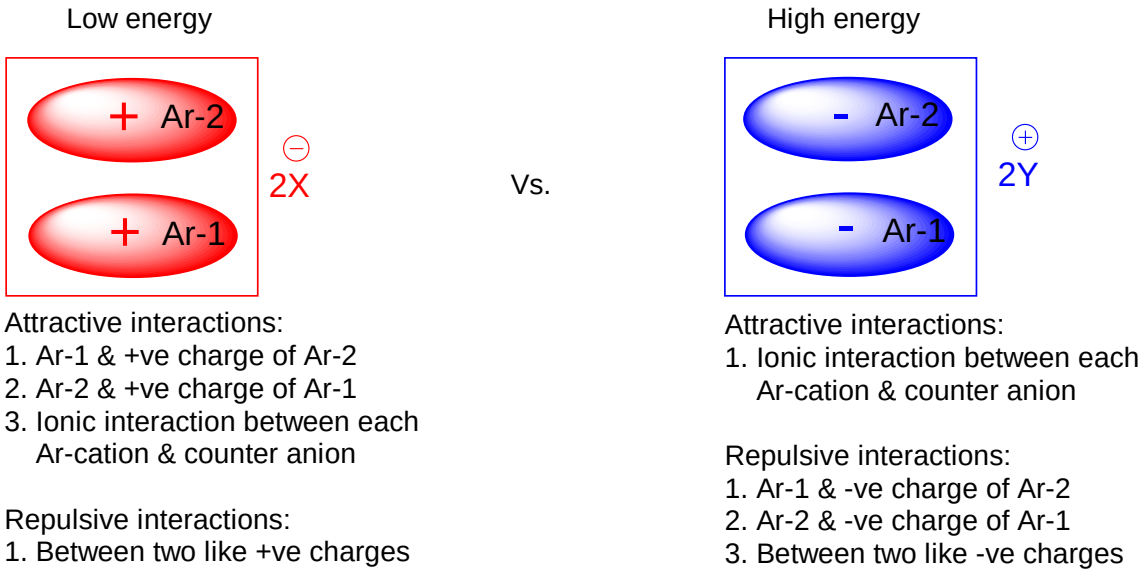

Figure 2.25. Comparing attractive and repulsive forces in **FF**-stacked dimer of Ar-cation vs. Ar-anion. **FF**-stacked dimer of Ar-cation is more favorable than Ar-anion.

Let's consider different ways of condensing ionic species together in the solid state that are relevant to the crystal structures of triangulene cations and anions studied in this research. When two similarly charged monopoles condensed in the solid state, they repel each other but two oppositely charged monopoles attract each other and form a dipole. When two dipoles condense in the solid state, there may be proximal like charged triangulene disc (cation or anion) which is represented in the following Figure (Figure 2.26).

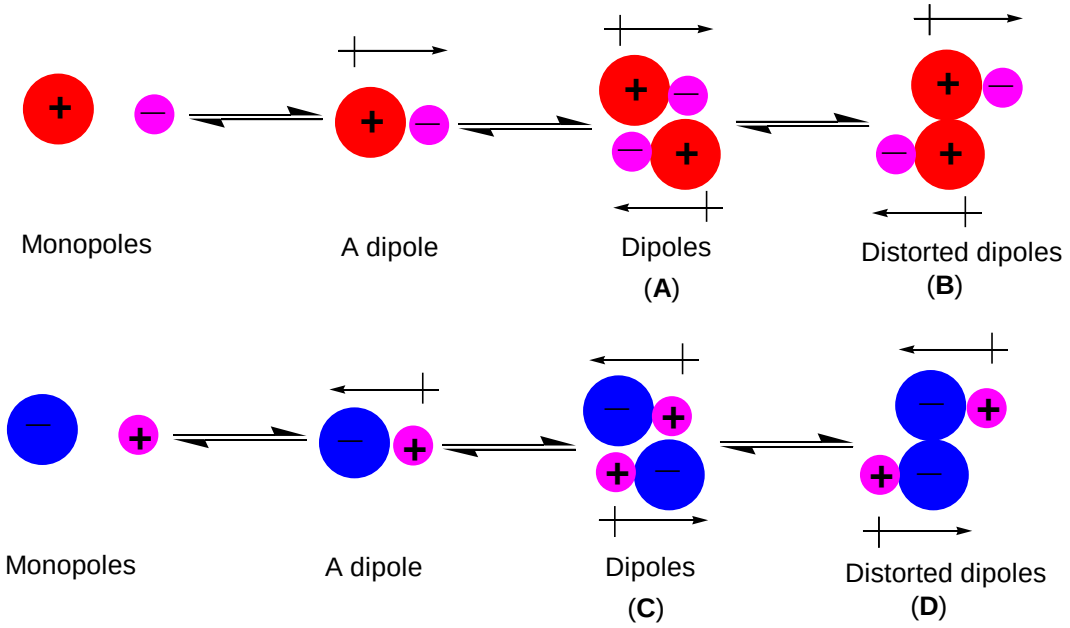

Figure 2.26. Representing various ways of putting two dipoles in the solid state that are relevant to the crystal structures Ar-cations (top) and Ar-anions (bottom) under study.

The condensed dipoles shown above summarize the stacking (or not stacking) behavior of Ar-ions in their solid states. Actual position of Ar-ions and counter anions may change slightly and depends on several factors like nature /size of side chains on Ar-ions, size and valency of couner ions etc. Models '**A'** and **'C'** (Figure 2.26) are observed in the solid state of trioxatriangulenium cations[75] (Figure 2.20) and triangulene anions (Figure 2.23) respectively. These arrangements of ions are expected and self explanatory; counter ions are at the faces of Ar-cations and Ar-anions. The observed arrangement of ions in case of triazatriangulenium cations (Figures 2.18 and 2.19) is represented by the model '**B**'. Shifting of ionic arrangement '**A**' to '**B**' with the replacement of three oxygen atoms in trioxatriangulenium cations by three –NR groups in triazatriangulenium cations, $[\mathbf{1}(NR)_3]^+$ can be described in terms of stability of the Ar-cations and their electrophilicities: a) Lone pair of electrons of N-atom are more accessible than the those of O-atom. So, replacing 3O-atoms with 3NR groups gives extra stability to triazatriangulenium cations and put them among the most stable cations known so far.[74] These highly stable triazatriangulenium cations do not seek added stability by putting counter anions at their faces as compared with relatively less stable trioxatriangulenium

cations which seek some stability by putting counter anions at their faces. b) For the same reason, trioxatriangulenium cations are stronger electrophile than triazatriangulenium cations. So, trioxatriangulenium cation probably satisfies its electrophilicity by putting a nucleophile (i.e.counter anion) at its face. Compared with this, weakly electrophilic triazatriangulenium cation doesn't seek to satisfy its electrophilicity by putting the counter anion at its face.

As stated already, the local repulsive electrostatic interactions as represented in the model '**B**' and found in solid state of triazatriangulenium cations are overcome by several attractive interactions including the bonding energy in the dimer and multiple opposed dipoles in the 3D matrix. Following the similar trend that is observed in the solid state of Ar-cations, substituting 3H of trioxatriangulenium cations with 3OH groups (as in $[(\mathbf{1}(O)_3(OH)_3]^+$) shifts packing pattern from '**A**' to '**B**'. We reasoned this to be because of increased stability and decreased electrophilicity of $[(\mathbf{1}(O)_3(OH)_3]^+$) due to added 3OH groups; lone pairs of electrons in each O-atom can be delocalized to stabilize the positive charge. Ionic arrangement as represented in the model '**D**' was never observed in the solid state of triangulene anions. It is probably because of greater repulsive electrostatic force dominating in the triangulene anion which can't be overcome by other attractive forces therein.

2.11 Conclusion and Further Studies

Although, the Coulomb equation ($E = q^2/\varepsilon r^2$) for electrostatic repulsion energies generated when two like charges are brought into proximity should not depend on the sign of the charge, this study found otherwise; the interactions in the crystalline state indicated that energies between aromatic faces of the same charge at close distances depend greatly whether the charge is positive or negative. Discotic cations exhibit dimeric or polymeric arrangement in the crystalline state but the discotic anions do not.

As supported by MO calculations, this is likely because large π-system cations have low-energy LUMOs capable of accepting π-face electron density at close distances and these more intimate interactions conquer electrostatic repulsion. The corresponding anion has these orbitals filled and thus even at close distances repels the π-faces. Crystal structure analyses indicate the **FF**-stacking in discotic cation is greatly supported by the

strong electrostatic attraction between each cationic disc and a relatively small counter anion positioned at the edge of the disc. This unit charged electrostatic attraction combined with attraction between cations and π- moieties and π-π moieties may have undermined the electrostatic repulsion between two like charged cationic discs. But, the counter cations in the solid state of anionic discs sit at the faces of Ar-discs or between the discs blocking FF-stacking between Ar-discs. The electrostatic repulsion between two anionic discs may have dominated the π- π interaction between them not to enable aromatic anions to stack co-facially. This basic difference in the solid state proved that triangulene cations are cohesive at their faces but triangulene anions are not. The superiority of Ar-cations over analogous anion in **FF**-stacking is clearly evident from the solid state structures of the Ar-cation, $[\mathbf{1}(O)_3(OH)_3]^+SiF_6^{2-}$ and its fully deprotonated form $(\mathbf{3})^{2-}$; while $[\mathbf{1}(O)_3(OH)_3]^+SiF_6^{2-}$ is found to have 1D **FF**-stack of Ar-cations in the solid state, the Ar-anion, $(\mathbf{3})^{2-}$ doesn't indicate any facial stacking between Ar-discs in the solid state. The difference in facial cohesiveness between trioxatriangulenium cations and triazatriangulenium cations was explained based on the difference in their stability and electrophilicity; while less stable and more electrophilic trioxatriangulenium cation prefers counter anion to position at its face, highly stable and weakly electrophilic triazatriangulenium cation prefers counter anion to position at its edge so as to enable **FF**-stacking between Ar-discs.

As described above and in chapter 1, there are many examples in the literature that requires at least one electron-deficient group for favorable intermolecular aromatic interactions.[71-73] This chapter reported **FF**-stacking between two positively charged aromatics, probably be guided by electrostatic attraction between a positively charged aromatic moiety and its counter anion. What if these stacking aromatics are unit but oppositely charged? Would there be strong synergy between unit charged electrostatic and π-π interactions? How would these aromatic cations and aromatic anions arrange in the solid states? Would we get any interactions in the solution states? To answer all these questions, we co-crystallized triangulene - based aromatic cations and aromatic anions and studied the interactions between them in solid states as well as solution states. The studies of these interactions are described in chapter 3.

2.12 Experimental

4,8,12-trimethyl-4,8,12-triazatriangulenium hexafluorophosphate $[1(NMe)_3]^+PF_6^-$

It is a known compound[189] and was synthesized by following the same procedure mentioned in the literature.[189] MS (ESI) *m/z 324* $[M\text{-}PF_6]^+$. ^1H NMR & ^{13}C NMR data of the title compound, $[\mathbf{1}(NR)_3]^+PF_6^-$ were indistinguishable to the ones reported in the literature. Diffraction-quality crystals of this compound were grown as follow; $[\mathbf{1}(NR)_3]^+PF_6^-$ (~ 20 mg) was taken in a 250 mL RB flask and dissolved in DMSO (20 mL) followed by addition of water just enough to start precipitation. Minimum quantity of methanol was then added to the flask to dissolve the precipitate. Slow evaporation of methanol at an ambient temperature resulted in crystalline dark red needles.

4,8,12-trimethyl-4,8,12-triazatriangulenium cyanate $[1(NMe)_3]^+NCO^-$

The title compound was prepared by exchanging anion of $[\mathbf{1}(NMe)_3]^+PF_6^-$ with cyanate ion. A solution of potassium cyanate (15 mg, 0.185 mmol) in water (0.5 mL) was added to the solution of $[\mathbf{1}(NMe)_3]^+PF_6^-$ [189] (40 mg, 0.085 mmol) in DMSO (20 mL) and agitated for 1 h at room temperature. Upon the addition of water (50mL), a red precipitate formed which was filtered and washed with water. Desiccation under vacuum followed by dissolution in warm acetonitrile and slow evaporation of the solvent from hot solution gave red needle-like crystal (28 mg, 89.7 %). X-ray analysis of the crystal thus obtained confirmed the presence of cyanate ion. MS (ESI) *m/z 324* $[M\text{-}NCO]^+$. ^{1}HNMR (400 MHz, D_6-DMSO): δ 7.94 (t, J = 8.8, 3H), 7.18 (d, J = 8.8, 6H), 3.6 (s, 9H); ^{13}C NMR (100 MHz, D_6-DMSO): δ 139.847, 139.820, 137.244, 108.716, 105.246, 35.065.

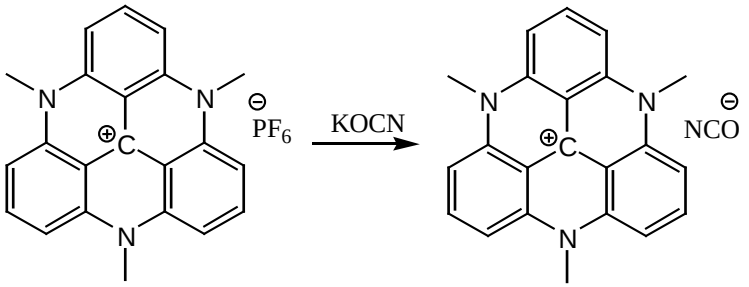

$[\mathbf{1}(NMe)_3]^+ PF_6^-$ $[\mathbf{1}(NMe)_3]^+ NCO^-$

Figure 2.27. Anion exchange between PF_6^- and NCO^- in preparation of $[\mathbf{1}(NMe)_3]^+NCO^-$

4,8,12-triethyl-4,8,12-triazatriangulenium tetrafluoroborate $[1(NEt)_3]^+BF_4^-$

A mixture of 1.0 g (1.96 mmol) of tris-(2,6-dimethoxyphenyl) carbenium tetrafluoroborate[188] and 3.58 g (29.34 mmol) of benzoic acid were taken up in 20 mL of NMP (N-methylpyrollidinone). Ethylamine (1.27 g, 28.2 mmol) gas was bubbled through the reaction mixture; the exact weight of ethylamine used in the reaction was indicated by the differences in weight of reaction mixture before and after passing ethylamine gas. The reaction flask was fitted with a dry ice condenser and the flask was heated (150 ^oC - 155 ^oC) for 26 h. under nitrogen. Cold water (200 mL) was added to the reaction mixture at 25 °C and the precipitate formed was washed with water. The crude product was dried, redissolved in acetonitrile (20 mL) and crystallized by adding 48 % aq. HBF_4 (2 mL) followed by water (50 mL). Solid thus obtained was again washed thoroughly with water, dried and washed with Et_2O (20 mL x 10). The compound was purified by recrystallizing it from slow evaporation of 1:1 mixture of methanol and dichloromethane to give orange-red crystal of the title compound (0.25 g, 28 %). X-Ray diffraction analysis of the crystal thus obtained confirmed atomic connectivity and presence of tetrafluoroborate ion. MS (ESI) *m/z 366* $[M\text{-}BF_4]^+$. ^1H NMR (400 MHz, D_6-DMSO): δ 8.05 (t, *J* = 8.4 Hz, 3H), 7.39 (d, *J* = 8.4 Hz, 6H), 4.44 (q, *J* = 6.8 Hz, 6H), 1.38 (t, *J* = 6.8 Hz, 9H); ^{13}C NMR (100 MHz, D_6-DMSO): δ 139.797, 139.729, 137.782, 110.016, 104.916, 42.299, 10.221.

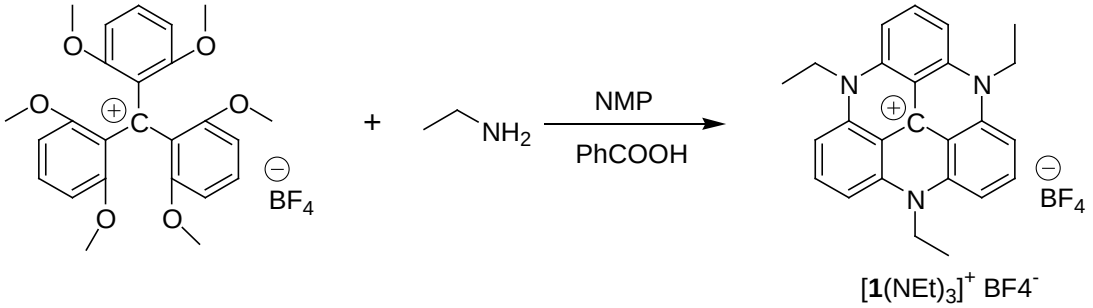

Figure 2.28. Syntheis of $[\mathbf{1}(NEt)_3]^+BF_4^-$

4,8,12-triphenyl-4,8,12-triazatriangulenium tetrafluoroborate $[1(NPh)_3]^+BF_4^-$

0.3 g (0.58 mmol) of *tris*-(2, 6-dimethoxyphenyl) carbenium tetrafluoroborate[188] was dissolved in 10 mL NMP (N-methyl-2-pyrrolidinone). Freshly distilled aniline (12 mL) and benzoic acid (0.25g, 2 mmol) were added. The mixture was agitated and refluxed 60 h. at 190-195 ^oC under nitrogen. The contents of the reaction vessel at 25 °C was poured into 300 mL of Et_2O and a dark red solid was filtered out and washed with Et_2O (3 x 20 mL), dried and was subjected to column chromatography (SiO_2, chloroform). The material was dissolved in EtOH and MeCN, 1:1. Slow evaporation gave red, needle crystals (70 mg, 20 %) of the title compound which upon analyzed by X-Ray diffraction confirmed atomic connectivity and presence of tetrafluoroborate ion. The title compound decomposed at 361 ^oC (DSC, 10 ^oC / min) before melting. MS (MALDI-TOF) *m/z 510* $[M\text{-}BF_4^-]^+$; ATR-IR (ν_{max}/cm^{-1}): 1610 (C=N), 1596 and 1526 (Ar C=C); ^1H NMR (400 MHz, $CDCl_3$): δ 7.79 (t, *J* = 7.6 Hz, 6H), 7.69 (t, *J* = 7.2 Hz, 3H), 7.54 (t, *J* = 8.8 Hz, 3H), 7.44 (d, *J* = 7.2 Hz, 6H), 6.35 (d, *J* = 8.8 Hz; 6H); ^{13}C NMR (100 MHz, $CDCl_3$): δ 142.538, 142.113, 137.900, 137.343, 132.474, 130.864, 128.772, 110.456, 107.463.

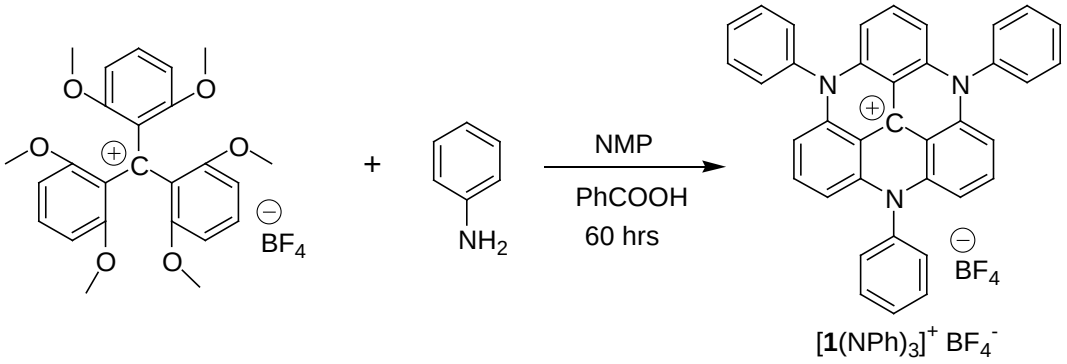

Figure 2.29. Synthesis of $[\mathbf{1}(NPh)_3]^+BF_4^-$

4,8,12-tri-*n*-decyl-4,8,12-triazatriangulenium tetrafluoroborate $[1(NDec)_3]^+BF_4^-$

A mixture of of tris-(2,6-dimethoxyphenyl) carbenium tetrafluoroborate[188] (0.27 g, 0.53 mmol) and *n*-decylamine (3.0 g, 19.01 mmol) were taken up in a 100 mL RB flask. 30 mL of NMP (N-methylpyrollidinone) was then added to the reaction flask. The reaction flask was fitted with a water-condenser and heated (160^oC -170^oC) for 24 h.

under nitrogen. Cold water (100 mL) was added to the reaction mixture at 25 °C and the precipitate formed was washed thoroughly with water. The crude product was dried, washed with diethyl ether (20 mL X 5) and ice-cold ethanol (2 mL X 3), dried again and then subjected to column chromatography (SiO_2, chloroform). The title compound (165 mg, 39.5 %) was obtained as dark-red needles when its solution in hot methanol was allowed to cool at the ambient temperature. MS (ESI) *m/z 702* $[M\text{-}BF_4]^+$; ATR-IR (ν_{max}/cm^{-1}): 2923, 2853 (sp^3 C-H), 1610 (C=N), 1535 (C=C); ^1H NMR (400 MHz, $CDCl_3$): δ 8.03 (t, *J* = 8.4 Hz, 3H), 7.12 (d, *J* = 8.4 Hz, 6H), 4.23 (t, *J* = 7.2 Hz, 6H), 1.83 (m, 6H), 1.56 (m, 6H), 1.21-1.43 (m, 36 H), 0.86 (t, J = 6.8 Hz 9H); ^{13}C NMR (100 MHz, $CDCl_3$): δ 140.689, 140.387, 138.370, 110.695, 105.375, 48.350, 32.103, 29.776, 29.761, 29.663, 29.511, 26.965, 25.366, 22.880, 14.272. Atomic connectivity and presence of tetrafluoroborate ion (BF_4^-) was confirmed by single crystal X-ray analysis.

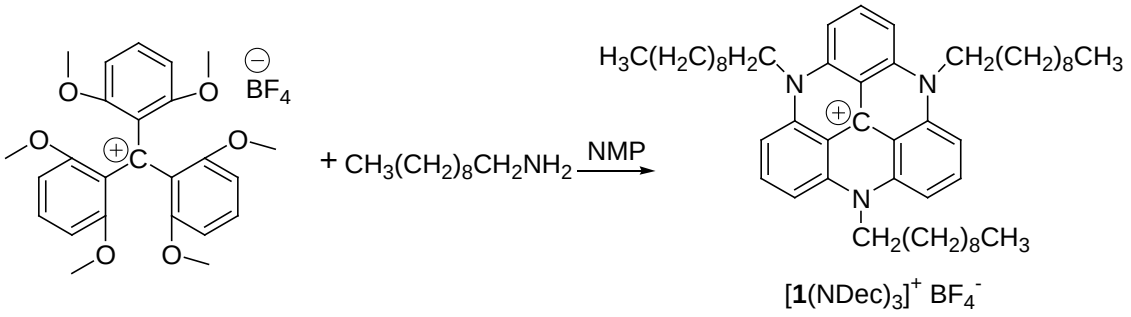

Figure 2.30. Syntheis of $[1(NDec)_3]^+BF_4^-$

4,8,12-tri-*n*-dodecyl-4,8,12-triazatriangulenium tetrafluoroborate $[1(NDodec)_3]^+BF_4^-$

A mixture of tris-(2,6-dimethoxyphenyl) carbenium tetrafluoroborate[188] (0.20 g, 0.39 mmol) and *n*-dodecylamine (2.33 g, 12.59 mmol) in 20 mL NMP (N-methylpyrollidinone) was taken up in a 50 mL RB flask. The reaction flask was fitted with a water-condenser and heated (160°C -170°C) for 35 h. under nitrogen. Cold water (30 mL) was added to the reaction mixture at 25 °C and the precipitate formed was washed thoroughly with water. The crude product was dried, washed with ice-cold diethyl ether (20 mL X 5) and the dried mass was subjected to column chromatography (SiO_2, chloroform). The title compound (105 mg, 34 %) was obtained as dark-red needles when its solution in 1:1 mixture of methanol and dichloromethane was allowed to

evaporate slowly at the ambient temperature. MS (ESI) *m/z 786* $[M\text{-}BF_4]^+$; ATR-IR (ν_{max}/cm^{-1}): 2921, 2852 (sp^3 C-H), 1610 (C=N), 1535 (C=C); ^1H NMR (400 MHz, $CDCl_3$): δ 8.03 (t, *J* = 8.4 Hz, 3H), 7.12 (d, *J* = 8.4 Hz, 6H), 4.24 (t, *J* = 7.2 Hz, 6H), 1.85 (m, 6H), 1.55 (m, 6H), 1.18-1.44 (m, 48 H), 0.86 (t, J = 6.8 Hz 9H); ^{13}C NMR (100 MHz, $CDCl_3$): δ 140.711, 140.404, 138.358, 110.725, 105.375, 48.377, 32.148, 29.871, 29.841, 29.814, 29.795, 29.670, 29.556, 26.984, 25.373, 22.899, 14.279. Atomic connectivity and presence of tetrafluoroborate ion (BF_4^-) was confirmed by single crystal X-ray analysis.

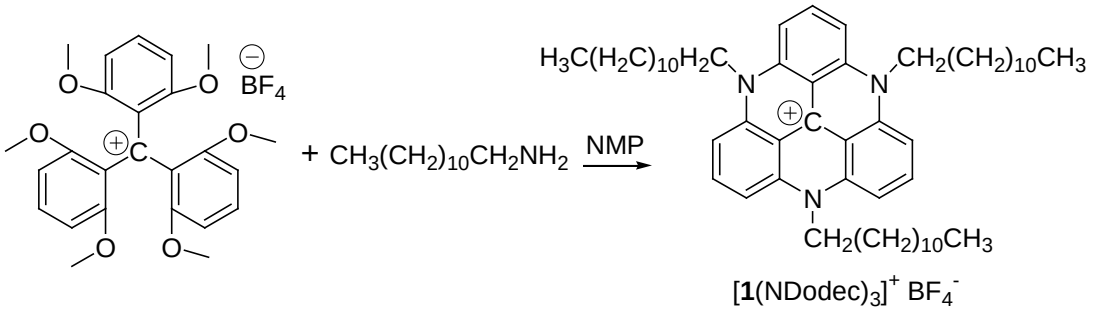

Figure 2.31. Syntheis of $[\mathbf{1}(NDodec)_3]^+BF_4^-$

4,8,12-tri-n-hexadecyl-4,8,12-triazatriangulenium tetrafluoroborate $[1(NHexadec)_3]^+BF_4^-$

A mixture of tris-(2,6-dimethoxyphenyl) carbenium tetrafluoroborate[188] (0.25 g, 0.49 mmol) and *n*-hexadecylamine (3.10 g, 12.86 mmol) in10 mL NMP (N-methylpyrollidinone) was taken up in a 25 mL RB flask. The reaction flask was fitted with a water-condenser and heated (160°C -170°C) for 48 h. under nitrogen. Cold water (30 mL) was added to the reaction mixture at 25 °C and the precipitate formed was washed thoroughly with water. The crude product was dried, washed with ice-cold diethyl ether (20 mL X 5) and the dried mass was subjected to column chromatography (SiO_2, chloroform) to get the title compound (112 mg, 21.9 %). Methanol (1 mL) was added to a small amount (~10 mg) of the title compound followed by addition of dichloromethane (DCM) just enough to dissolve the compound. Slow evaporation of the solvent mixture at an ambient temperature gave dark-red needle like crystals. MS (ESI) *m/z 954* $[M\text{-}BF_4]^+$; ATR-IR (ν_{max}/cm^{-1}): 2920, 2851 (sp^3 C-H), 1610 (C=N), 1535 (C=C); ^1H NMR (400 MHz, $CDCl_3$): δ 8.03 (t, *J* = 8.4 Hz, 3H), 7.15 (d, *J* = 8.4 Hz, 6H),

4.30 (t, *J* = 7.2 Hz, 6H), 1.89 (m, 6H), 1.58 (m, 6H), 1.15-1.45 (m, 72 H), 0.857 (t, J = 6.8 Hz 9H); ^{13}C NMR (100 MHz, $CDCl_3$): δ 140.836, 140.700, 138.283, 110.778, 105.261, 48.407, 32.152, 29.954, 29.935, 29.920, 29.909, 29.901, 29.890, 29.875, 29.818, 29.644, 29.591, 26.995, 25.245, 22.918, 14.355. Atomic connectivity and presence of tetrafluoroborate ion (BF_4^-) was confirmed by single crystal X-ray analysis.

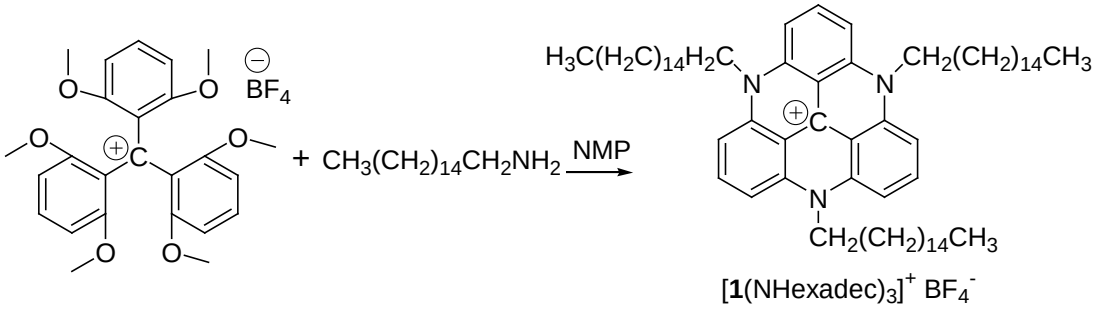

Figure 2.32. Syntheis of [**1**$(NHexadec)_3]^+BF_4^-$

4, 8-diphenyl-4, 8-diaza-12-oxatriangulenium tetrafluoroborate [1$(NPh)_2(O)]^+BF_4^-$

0.3 g (0.58 mmol) of tris (2,6-dimethoxyphenyl) carbenium tetrafluoroborate[188] was dissolved in 10 mL NMP (1-methyl-2-pyrrolidinone) in a 100 mL round bottom flask and an excess of aniline (10 mL) was added. The mixture was refluxed at 180^{o}C over silicon oil bath for 36 hours under nitrogen atmosphere. The mixture was constantly shaken by the magnetic stirrer throughout the experiment. After the mixture was cooled down, it was poured into a big beaker containing 300 mL of anhydrous diethyl ether. The mixture was filtered and dark orange-red solid obtained was washed with more anhydrous ether (3 x 20 mL), dried and subjected to aluminum oxide column chromatography. Non polar compounds were eluted with ethyl acetate and chloroform. Finally orange red compound was eluted with 1%-5% methanol in chloroform. Red needle crystals of the compound were obtained by refrigerating the quite concentrated ethanol solution to give 100 mg (32.5 %) of the title compound. MS (MALDI-TOF) *m/z 435* [M-$BF_4^-]^+$; ^{1}H NMR (400 MHz,): δ 8.04 (t, *J* = 8.41 Hz, 2H), 7.94 (t, *J* = 8.41 Hz, 1H), 7.91 (t, *J* = 7.46 Hz, 4H), 7.83 (t, *J* = 7.32 Hz, 2H), 7.65 (d, *J* = 7.52 Hz, 4H), 7.54 (d, *J* = 8.22 Hz, 2H), 6.63 (d, *J* = 8.6 Hz, 2H), 6.52 (d, *J* = 8.41 Hz, 2H); ^{13}C NMR (100 MHz,): δ 152.778, 142.545, 141.756, 139.987, 137.740, 132.829, 131.592, 128.965,

111.089, 109.472, 108.060, 107.635, 79.822. Single crystal x-ray analysis of the crystal grown in ethanol confirmed connectivity and the presence of tetrafluoroborate ion (BF_4^-).

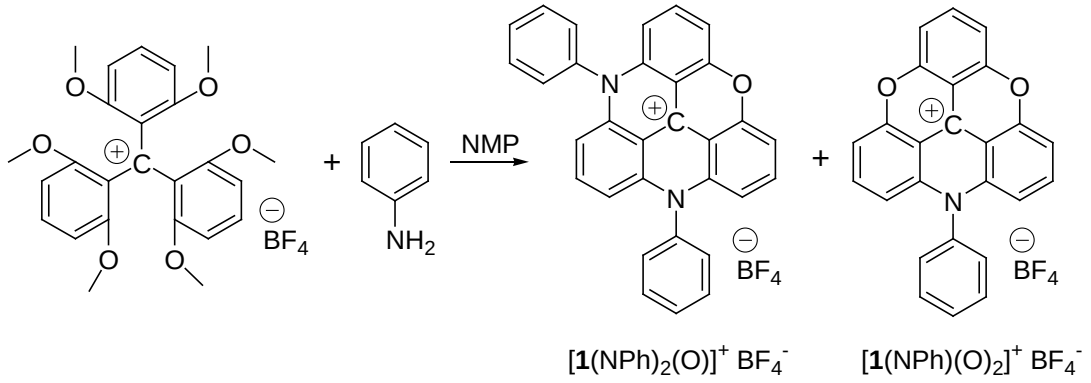

Figure 2.33. Synthesis of $[\mathbf{1}(NPh)_2(O)]^+BF_4^-$ and $[\mathbf{1}(NPh)(O)_2]^+BF_4^-$

4-phenyl-4-aza-8, 12-dioxatriangulenium tetrafluoroborate $[1(NPh)(O)_2]^+BF_4^-$

This is a known compound[74] but was synthesized and isolated in our lab along with $[\mathbf{1}(NPh)_2(O)]^+BF_4^-$ (see above for detailed procedure) as an orange red solid. The compound was eluted from column after $[\mathbf{1}(NPh)_2(O)]^+BF_4^-$ and diffractable quality crystals were obtained by refrigerating quite concentrated solution of the title compound in ethanol. Yield 52.6 mg (20%); MS (MALDI-TOF) *m/z 360* $[M\text{-}BF_4]^+$; ^{1}HNMR (400 MHz, DMSO): δ 8.26 (m, 3H), 7.91 (m, 3H), 7.75 (d, *J* = 8.41 Hz, 4H), 7.69 (d, *J* = 7.05 Hz, 2H), 6.87 (d, J = 8.73 Hz, 2H); Atomic connectivity and presence of tetrafluoroborate anion (BF_4^-) was confirmed by single crystal X-ray analysis of the crystal grown in ethanol.

4,8,12-trioxa-2,6,10-trihydroxytriangulenium tetrafluoroborate $[1(O)_3(OH)_3]^+BF_4^-$

A mixture of tris-(2,4,6-trimethoxyphenyl) carbenium tetrafluoroborate[191] (2.0 g, 3.33 mmol) and pyridine hydrochloride (6.0 g, 51.95 mmol) in 5 mL NMP (N-methylpyrollidinone) was taken in a 50 mL round bottom flask fitted with water condenser. The reaction flask was then heated to about 180 ^oC for 3 hours under nitrogen. Methanol (30 mL) was added to the cold reaction mixture and solid precipitates thus obtained were washed with acetonitrile (5 mL X 10) and then dried under vacuum to get dihydroxy ketone derivative of trioxatriangulene, 10 (1.07 g, 94.8 %) which was very

difficult to characterize due to its low solubility in common organic solvents. A small amount of the compound, 10 was mixed with DMSO (0.5 mL) and added molar excess of 48 % aq. HBF_4 to it followed by addition of water (5 mL). Slow evaporation of water at an ambient temperature gave yellow crystals of the title compound. Atomic connectiveity and the presence of tetrafluoroborate (BF_4^-) ion was confirmed by single crystal X-ray analysis of the crystal thus obtained.

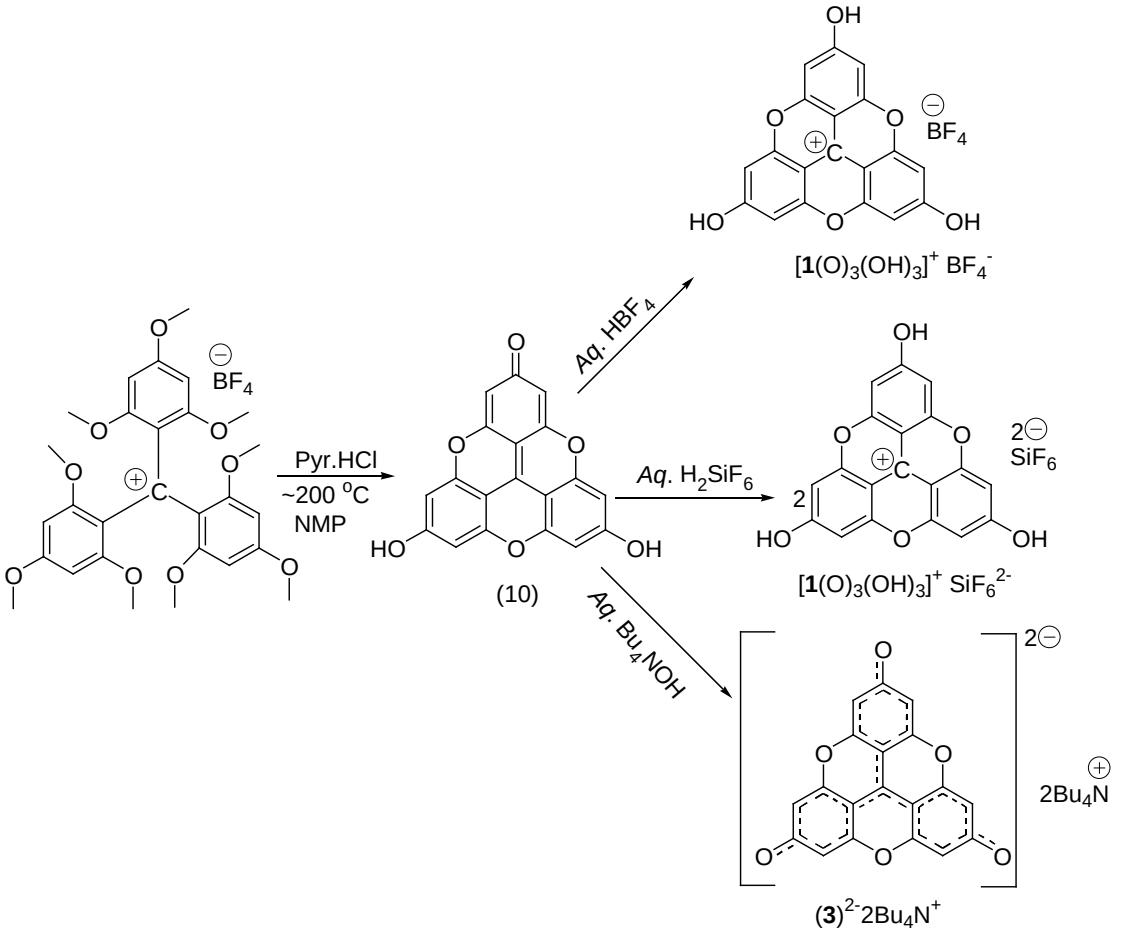

Figure 2.34. Synthesis of $[\mathbf{1}(O)_3(OH)_3]^+BF_4^-$, $[\mathbf{1}(O)_3(OH)_3]^+SiF_6^{2-}$ and $(\mathbf{3})^{2-}2Bu_4N^+$

4,8, 12-trioxa-2,6,10-trihydroxytriangulenium hexafluorosilicate $[\mathbf{1(O)_3(OH)_3}]^+\mathbf{SiF_6^{2-}}$

The procedure was same as above mentioned procedure for $[\mathbf{1}(O)_3(OH)_3]^+BF_4^-$. The title compound, $[\mathbf{1}(O)_3(OH)_3]^+SiF_6^{2-}$ was crystallized from aq. acidic (H_2SiF_6) solution of **10** by slow evaporation of water at an ambient temperature. Atomic

connectivity and presence of SiF_6^{2-} ion was confirmed by single crystal X-ray analysis of the crystal thus obtained.

Tetrabutylammonium 4, 8, 12-trioxotriangulenium [76] (2)$^-Bu_4N^+$

The title compound, (**2**)$^-Bu_4N^+$ is the known compound and was synthesized following the procedure mentioned in the literature.[76] The only difference is that the sodium amalgam used in the reduction steps was replaced by zinc powder activated with copper to avoid the use of mercury.[81] The obtained yield of the title compound was only 3%. The solid state structure of the title compound was elucidated by examining the crystals grown in dichloromethane (DCM).[76] We re-examined the solid state structure of the title compound by analyzing its crystal grown in acetonitrile. MS (ESI) *m/z 321* [M-Bu_4N^+]$^-$; ^{1}H NMR (400 MHz, d_6-DMSO): δ 8.75 (d, *J* = 7.6 Hz, 6H), 7.51 (t, *J* = 7.6 Hz, 3H), 3.12 (t, *J* = 8.0 Hz, 8H), 1.52 (m, 8H), 1.27 (m, 8H), 0.91 (t, *J* = 7.2 Hz, 12 H); ^{13}C NMR (100 MHz, d_6-DMSO): δ 180.544, 132.360, 132.333, 126.930, 120.288, 90.878, 57.477, 23.024, 19.190, 13.483. Atomic connectivity and presence of tetrabutylammonium ion was confirmed by single crystal X-ray analysis.

Tetrahexylammonium 4, 8, 12-trioxotriangulenium (2)$^-Hex_4N^+$

The title compound, (**2**)$^-Hex_4N^+$ was prepared by the cationic exchange of (**2**)$^-$ Bu_4N^+ with tetrahexylammonium bromide. A mixture of tetrabutylammonium 4, 8, 12-trioxotriangulenium[76] (40 mg, 0.071 mmol) and tetrahexylammonium bromide (123.34 mg, 0.28 mmol) was dissolved in the hot mixture of acetonitrile and chloroform (1:3). The resultant solution was filtered while hot and the filtrate was allowed to cool to room temperature. Dark blue crystals thus obtained were washed with cold acetonitrile (1mL X 5) to give the title compound (38 mg, 79.25 %). MS (ESI) *m/z 321* [M-Hex_4N^+]$^-$; ^{1}H NMR (400 MHz, d_6-DMSO): δ 8.75 (d, *J* = 6.4 Hz, 6H), 7.51 (t, *J* = 6.4 Hz, 3H), 3.12 (br, 8H), 1.53 (br, 8H), 1.27 (br, 24H), 0.86 (br, 12 H); ^{13}C NMR (100 MHz, d_6-DMSO): δ 180.499, 132.326, 132.280, 126.900, 120.239, 90.828, 57.576, 30.522, 25.383, 21.838, 20.898, 13.767. Atomic connectivity and presence of tetrahexylammonium ion (Hex_4N^+) was confirmed by single crystal X-ray analysis.

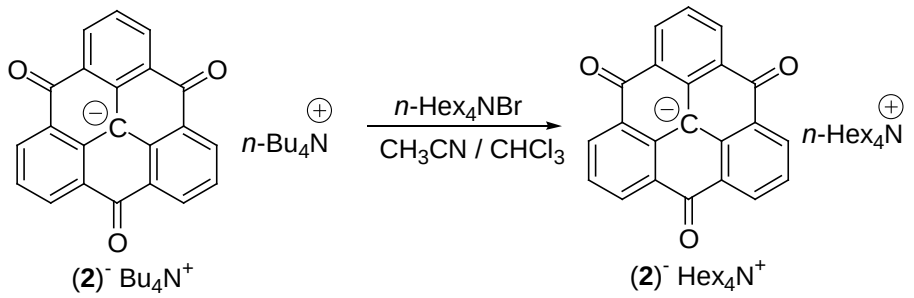

Figure 2.35. Cationic exchange in synthesis of $(\mathbf{2})^{-}Hex_4N^{+}$ from $(\mathbf{2})^{-}Bu_4N^{+}$

Bis (tetrabutylammonium)-2,6,10-trioxo-4,8,12-trioxatriangulenium $(3)^{2-}2Bu_4N^{+}$

The procedure for making the title compound was published in a recent literature[192] after we synthesized this compound in our laboratory. The title compound was prepared by deprotonation of both acidic hydrogens of **10.** See experimental of $[\mathbf{1}(O)_3(OH)_3]^{+}BF_4^{-}$ above for the synthetic details of **10**. Aq. 46 % tetrabutylammonium hydroxide (1mL) was added to the heterogeneous mixture of **10** (55 mg, 0.165 mmol) and DMSO (5 mL). The resultant solution was stirred for 5 minutes at an ambient temperature and then filtered. Acetonitrile (20 mL) was added to the filtrate followed by excess diethyl ether (200 mL) to cause precipitation of the yellow solid which was further washed with diethyl ether (5 mL X 5) and dried to give dianion, **6** (110 mg, 82 %). MS (ESI) *m/z 165* $[M\text{-}Bu_4N^{+}]^{-}$, *m/z 331* $[MH\text{-}Bu_4N^{+})$; ^{1}H NMR (400 MHz, d_6-DMSO): δ 5.63 (s, 6H), 3.14 (t, *J* = 8.4 Hz, 16H), 1.54 (m, 16H), 1.29 (m, 16H), 0.92 (t, *J* = 7.2 Hz, 24 H); ^{13}C NMR (100 MHz, d_6-DMSO): δ 179.632, 153.921, 127.877, 101.202, 87.682, 57.501, 23.045, 19.197, 13.488. Atomic connectivity was confirmed by single crystal X-ray analysis of the crystals grown in acetonitrile.

Chapter 3

Interactions between Ionic Aromatics: Synergy between Unit Charge Electrostatics and π-π Stacking

Subsequent to the solid state structure of benzene / fluorobenzene hetero-dimer,[195] the chemical literature reports many examples of face-to-face (**FF)**-stacking between two π moieties driven by electrostatics,[16,145,149-151,163] and quadrupolar interactions.[195,196] It is the directional nature of electrostatic attractions[140] that determine the disposition of the interactions between π moieties; CH-π or π-π interactions. Chapter 1 showed that positive charges were important for intra-molecular aromatic interactions in a conformationally flexible molecule where a triad of 'π^+-π-π^+' was observed.[5] Chapter 2 showed that large polycyclic aromatic cations were cohesive at their faces whereas the corresponding aromatic anions were apparently repulsive.

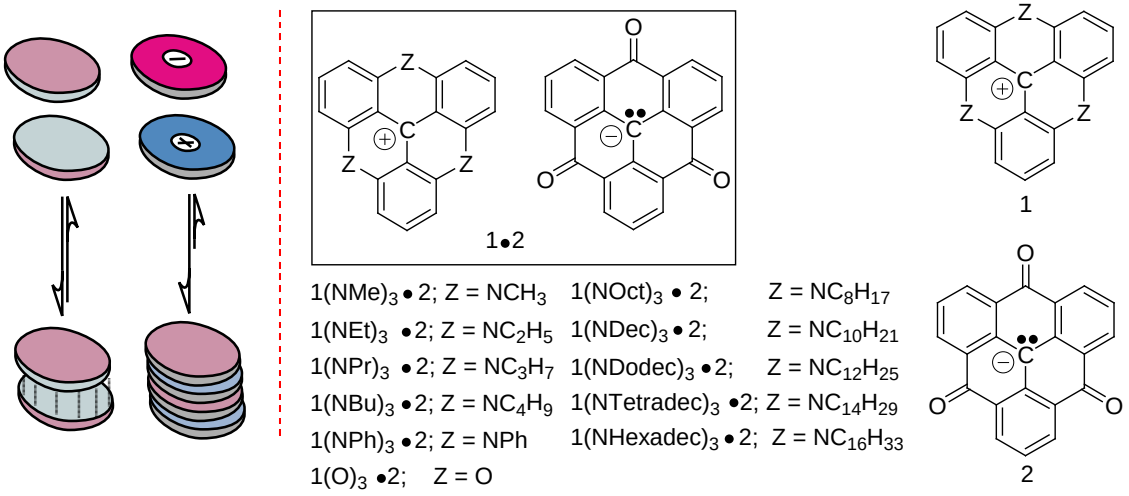

(a) (b)

Figure 3.1. (a) Cartoon showing π-stacking dependence on weak quadrupolar interactions (left) versus cartoon of putative, strong synergy between stacking and electrostatics in aromatic monopoles (right). (b) Structures of aromatic ion-pairs under study.

This chapter discusses the solid- and solution-state interactions between big, polycyclic aromatic cations and iso-structural anion in the aromatic ion-pairs **1•2** to examine possible synergy between unit charge electrostatic and the aromatic interactions; the unit charge electrostatics should direct the aromatic moieties to stack co-facially. The interaction discussed here is towards the extreme end of electrostatic driven π-π stacking. This contribution is novel to the chemical literature because no previous examples of such interactions between ionic aromatics have been reported.

3.1 Major Findings

Evidence will be presented below that paints an interesting picture of the interactions between the oppositely charged aromatic discotic molecules studied herein. This work was initiated to search for synergy or to describe the interaction between the strongest non-covalent force and the weakest non-covalent force: ionic bonding and π-stacking, respectively.

The synergy between monopole charges and π-stacking that we thought we would discover is only evident when there are no steric encumbrances to face-to-face interactions. Very favorable interactions appear to result only when near covalent bonding distances are achieved. Likely these interactions involve some covalent component with optimization of molecular orbital interactions in the ion pairing between discotic cations **1** and discotic anion **2**.

This chapter consists of the examination of crystalline state structures, UV-vis ion-pairing studies to measure ion-pairing energy, differential scanning calorimetry, electrochemistry and electrospray mass spectrometry studies. They all indicate that ion pairing interactions in **1**$(O)_3$•**2** and **1**$(NMe)_3$•**2** are in a class by themselves whereas analogous interactions in other **1**$(NAlkyl)_3$•**2** had more moderate affinity for each other.

Notably, a large difference in ion-pairing affinities was observed for **1**$(NMe)_3$•**2** vs. **1**$(NEt)_3$•**2**. These two substituents (*Me* and *Et*) are close in size when other standards of measure are employed such as the A-values in cyclohexanes,[197] and of Taft steric parameters (E_s).[198] This result corroborates the structural difference in face-to-face interactions of **1**$(NMe)_3$•X(-) vs. **1**$(NEt)_3$•X(-) where X(-) was a small non-discotic anion. In the Chapter 2, polymeric face-to-face π interactions were noted for the

crystalline states of **1**$(NMe)_3$•X(-) whereas the crystalline state of **1**$(NEt)_3$•X(-) featured dimeric face-to-face interactions.

Another discovery in the current chapter concerns bands in the near infrared that are characteristic of strongly interacting π-faces. The chemical literature regarding 'pancake bonding'[153-162] such as that observed in the crystalline states of the radical anion tetracyanoethylene [TCNE(•)][153,161] cite these near-IR bands as a new spectral feature that results upon complex formation.[199]

In chemistry there are two basic ways to form a bond: (1) with radicals A• + B• → A─B, and (2) with charged species A(+) + B:(−) → A─B. In these two broad groups there are many details and distinctions that enrich the discipline of mechanistic chemistry. Analogously, there are now also two ways to form strong π-system interactions, namely spin assisted and charge-assisted stacking. The spin assisted formation in the conversion of doublet spin states to ground state singlets is discussed in the 'pancake bonding' literature.[153-162] Some details of the novel charge-assisted π-π interactions are described in this chapter.

3.2 Introduction

Readers are referred to section 2.4 of chapter two to get detailed information and discussion on electrostatic arguments of solid-state π-π interactions. Great attention has been paid to π-π interactions in the chemical literature probably because of its diverse application in various fields such as biochemistry,[6-9] molecular self assembly,[10,11] molecular recognition,[15,16] supramolecular design, crystal engineering,[17-19,166-168] molecular conductors,[169-171] molecular machines,[172,173] electronics, [174,175] and discotic liquid crystals.[176,177] The extent of π-π interaction is a key for investigating the electric properties of organic materials[180] because π-stacked materials act as medium for the electron /energy processes.[200] However, the π-π interaction itself, without getting any synergistic effects from other forces, is a weak non-covalent force. [201,202] Gas phase calculations show that the binding energy of the benzene dimer (−2.8 kcal / mole)[202] is less than the pentane dimer (−3.9 kcal / mole),[203] both having the same number of electrons. Also, the interaction energies of the π-face benzene dimer and naphthalene dimer are found to be very similar to the interaction energies of their corresponding

saturated hydrocarbons. [201] These literature observations don't categorize the π-π interaction as a special interaction in small aromatic hydrocarbons. However, π-π interaction becomes a distinguished force of attraction when number of delocalized π electrons increases in fused or condensed, polycyclic aromatic hydrocarbons.[131,201]

Literature indicates that spin-assisted π-dimers of neutral, anionic, cationic or mix π-radical is the most effective way of designing strong π-π interactions in the solid states as evident from the small π-face separation.[199,204] The distance between two π-faces is as low as 2.87 Å as observed in the crystal of [TCNE(•)].[199] The Van der Waals distance is approximately 3.4 Å, so this decreased interaction and spin pairing are indicative of covalent bond formation. The π-π interaction in these spin assisted dimers is best described as 'pancake bonding'; [153-162] a long range, $2e^{-}$ / multi-centered bond. The radical / radical attraction combined with anions / counter cations attraction[161] contribute to the close interaction in these dimers but the disability to form a strong covalent bond is attributed to the electrostatic repulsion between bonded electrons, the delocalized π electrons in two π-faces.[153] Some structures of π-radicals capable of forming stable π-dimers in the solid states are given in Figure 3.2 below. The distance between the π-faces of these dimers are 2.9 Å [CA(•)],[199] ≈ 3.2 Å [TCNQ(•)],[205-207] ≈ 2.9 Å [DDQ(•)],[208-210] ≈ 3.22 Å [PHEN(•)],[199,211,212] and 3.2 Å [OMB(•+)].[213] These spin-assisted π-stacking interactions are also observed in the solution states. [23]

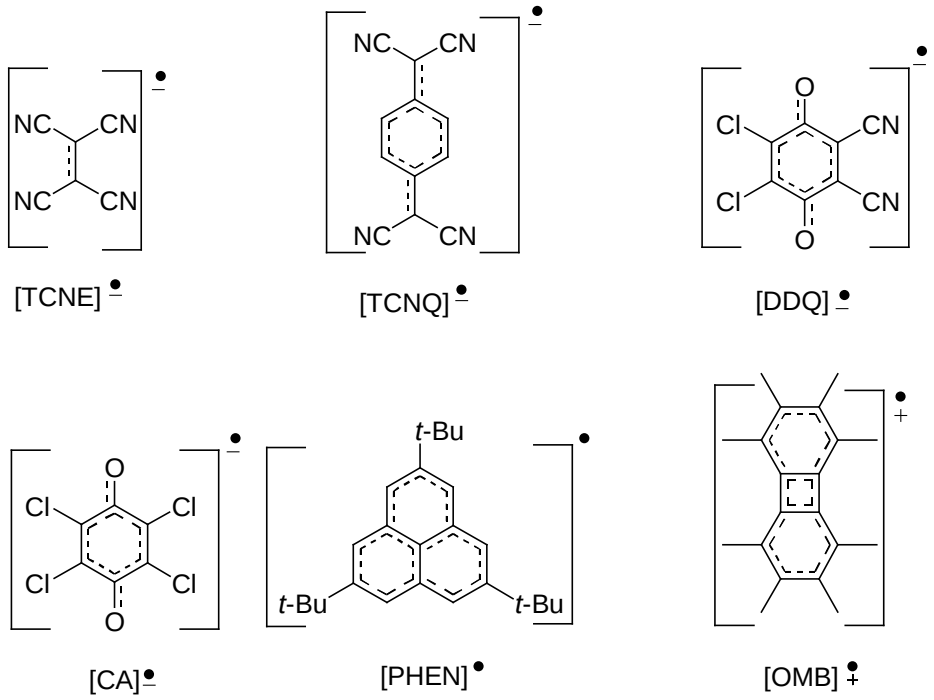

Figure 3.2. Literature examples of π-radicals capable of forming stable π-dimers.

An effective way of observing strong π-π interactions is by mixing an organic donor (electron rich π-molecule) and an organic acceptor (electron acceptor) to give so called donor-acceptor (DA) complex or charge-transfer (CT) complex.[214-223] A fraction of electronic charge from the donor molecule (D) is transferred to the acceptor molecule (A) and the partial electrostatic generated therein stabilize the DA (or $D^{\delta+}A^{\delta-}$) complex. The donor and acceptor π molecules should have low ionization potential and high electron affinity respectively to be able to form the effective CT complex.[217] As evident from UV-Vis studies, the π-stacking interactions in these CT complexes are characterized by absorption at longer λ than the individual donor (D) or acceptor (A) in the solution states.[223-228] Solid state π-stacking in these complexes are characterized by close distance[214,219,229] (shorter than the sum of Van der Walls' radii of two carbon atoms) between any two adjacent π-faces in these complexes. The CT complex formed between DDQ and TMDO (DDQ, TMDO) and between *o*-CA and TTF (*o*-CA, TTF) have π-face distance of 2.95 Å and 3.25 Å respectively in the solid state.[222] Literature reports that the energy of solution-state π-stacking in these CT complexes can be as high as −6.79 kcal / mole (Binding constant = 96000 M^{-1}).[230]

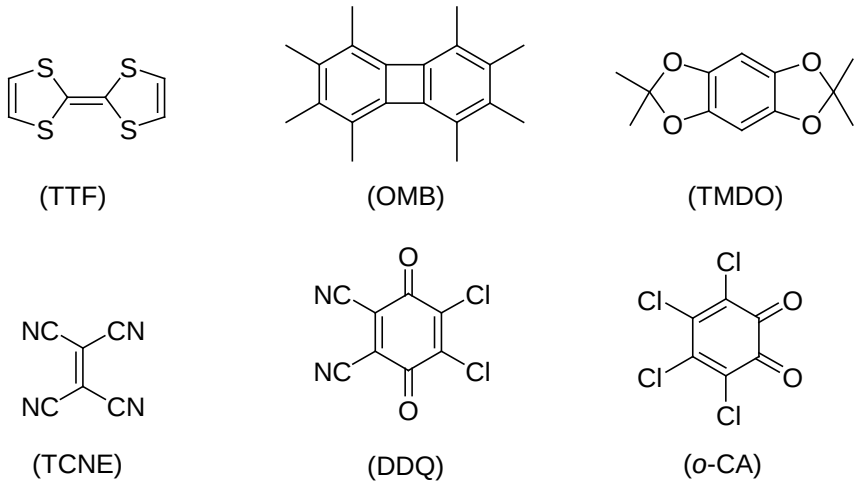

Figure 3.3. Literature examples of good donors (top) and acceptors (bottom) π-systems. These associate as π-dimers as their corresponding radical cations and anions after electron transfer.

3.3 Methods

In the following section the methods used to study the ion-pairing between triangulene cations (**1**) and anion (**2**) are described. The results of these experiments and interpretations of these appear in the next sections.

3.3.1. Solid-States

3.3.1.1 Crystal Structure Analysis

Single crystals of aromatic ion-pairs **1•2** were grown by various procedures and in different solvent systems. The experimental section at the end of this chapter includes detailed procedures for the crystallization of these aromatic ion-pairs. Quick view of crystals of aromatic ion-pairs showed the **FF**-stacking of aromatic cations and aromatic anions alternatively in a 1D column. Different aspects of interaction between aromatic cores of cations **1** anion **2** in the solid-state were studied by calculating a) dihedral angle (Θ_d): the angle between planes of two aromatic cores b) vertical displacement of the centers of two aromatic cores (D_v): the distance between the planes of two interacting aromatic moieties along a normal vector of an aromatic plane and c) horizontal displacement of the centers of two aromatic cores (D_h): the distance between centres of two interacting aromatic moieties along a vector 90° to the normal of one of the aromatic

planes. Finally area of overlap (A_o) between two adjacent aromatic cores was calculated from average radii (R_1 and R_2) of two adjacent aromatic cores and D_h. Horizontal displacement (D_h) can also be correlated with the angle between two aromatic centres (Θ_c). The detailed procedure of the method of the crystal structure analysis is described in chapter 2 (section **2.9.1**).

3.3.1.2 Powder X-ray Diffraction (PXRD)

PXRD spectra of the aromatic ion-pairs **1•2** were obtained and the results were compared with the results obtained from single crystal analysis to verify the workability of the PXRD technique to determine the π-stacking distance. Once comparable results were obtained, the technique was utilized to estimate the π-stacking distance in the aromatic ion-pairs for which single crystal analyses were not possible.

3.3.1.3 Differential Scanning Calorimetry (DSC)

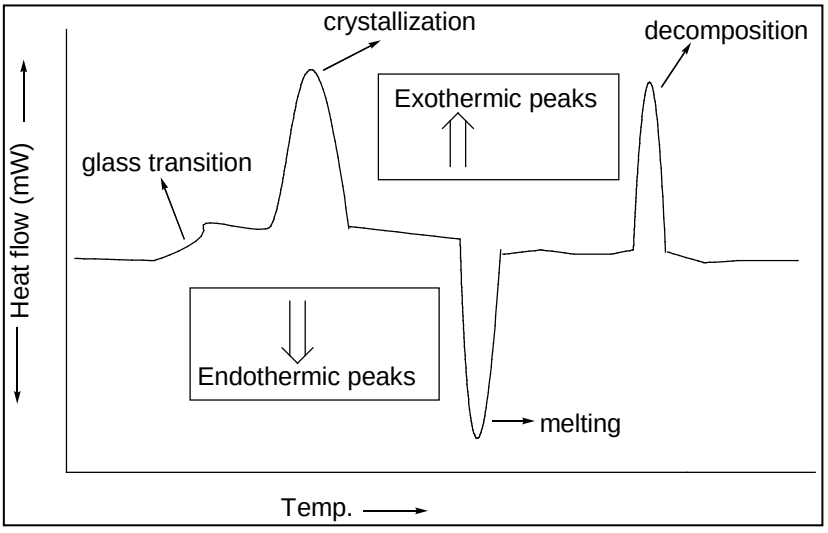

Figure 3.4. Typical DSC curves.

Developed by E.S. Watson and M.J. O'Neill in 1960, the DSC technique is used to study the phase transition temperatures of the molecules. In this technique, sample and reference are maintained at the same temperature. The temperature of the sample and reference is increased with time during the experiment. This rise in temperature causes

the sample to undergo various phase transitions (melting, decomposition etc.) while the stable reference molecule stays unaffected. These transitions change the temperature of the sample and there has to be flow of heat energy to (or from) the sample to maintain the zero (0) temperature difference between the sample and the reference molecule. The flow of heat energy is displayed as the ordinate of the DSC curves. Melting temperature / decomposition temperature of the aromatic ion-pairs **1•2** and the enthalpy of their melting were studied to observe possible synergy between aromatic interactions and unit charged electrostatics in these ion-pairs.

3.3.2 Solution States

3.3.2.1. UV-Vis Spectroscopy

UV-Vis spectroscopy was carried out to investigate the interaction between the aromatic cations **1** and the aromatic anion **2** in solution-state. Absorbencies due to a certain concentration of **1**•X($^-$) and same concentration of **2**•Y($^+$) were subtracted from the absorbance of equal concentration of 1:1 mixture of the two (equation 3.1) to see if there were any interactions between **1** and **2**.

$$A_{(\mathbf{1}\cdot\mathbf{2})} = A_{(1\text{--}2\ mix)} - [A_{\{\mathbf{1}\cdot X(-)\}} + A_{\{\mathbf{2}\cdot Y(+)\}}] \quad \text{.....Eq. 3.1}$$

Where $A_{\{\mathbf{1}\cdot X(-)\}}$, $A_{\{2\cdot Y(+)\}}$ and $A_{(1\text{--}2\ mix)}$ are the experimental absorbencies of **1**•X(−), **2**•Y(+) and 1:1 mixture of the two respectively. $A_{(\mathbf{1}\cdot\mathbf{2})}$ is the calculated absorbance of the hypothetical **1•2** complex.

In absence of any interactions between **1** and **2**, one would expect to see a straight line without any peaks. If there were any interactions between the two, one would expect to see some positive peaks as well as negative peaks. The positive peaks would be possibly due to **1•2** complex formed between aromatic cation and aromatic anion and the negative peaks must be due to decrease in the concentration of free aromatic cation **1** and aromatic anion **2** in the 1:1 mixture. Equation 3.1 resulted non zero absorbance showing that there were some interactions between the aromatic cation and the aromatic anions.

3.3.2.1.1 Ion Pairing Association Constant / Ion Pairing Association Energy

Once UV-Vis spectroscopy studies confirmed that there were interactions between the aromatic cations and the aromatic anions in the solution states, the strengths of these associations were investigated in terms of ion pairing association constant (K_{eq}) and ion pairing association energy (ΔG) as follows;

$$\text{Cation (1)} + \text{Anion (2)} \underset{}{\overset{K_{eq}}{\rightleftharpoons}} [1\bullet 2]$$

Initial conc	[1]	[2]	0
After mixing	[1] Y	[2] Y	(1 - Y)[1•2]

Where,

Y = Fraction of free ions (unassociated)

$$K_{eq} = \frac{(1 - Y)[1\bullet 2]}{[1]\ Y\ \ [2]\ Y}$$

$$\text{Ion pairing energy } (\Delta G) = -RT\ln(K_{eq})$$

As seen in the above mathematical equations, the initial concentration of hypothetical complex [**1•2**] between aromatic cation **1** and the anion **2** is zero. When equal concentration of aromatic cation [**1**] and the anion [**2**] are mixed, some fraction associates, this fraction = (1-Y).

Absorbance due to **1•2** at a particular wavelength (λ) is given by;

$A_{\mathbf{1\cdot 2}(\lambda)} = A_{(\lambda)} - \{A_{\mathbf{1}(\lambda)} + A_{\mathbf{2}(\lambda)}\}Y$……..(3.2)

1•2 was assumed to be the single species and not a polymeric complex. Further experimentation to elucidate stoichiometry at high concentration (see next section) indicates that this is a good approximation at low concentration. The mathematical crux to the evalation of the equilibrium constant is the absence of a UV spectrum of pure **1•2**. A system of equations for absorbance at various concentrations is solvable however. Ratios of absorbencies of **1•2** at two different wavelengths should remain constant with change in concentration.

$A_{(\lambda 1)} = \varepsilon_1 lC$

$A_{(\lambda 2)} = \varepsilon_2 lC$

$A_{(\lambda 1)} / A_{(\lambda 2)} = \varepsilon_1/\varepsilon_2 =$ **Constant**

$\varepsilon_{1 \text{ and }} \varepsilon_2$ are constants for the given wavelengths and called molar absorptivity of the solution.

We iteratively converged on values for 'Y' to get a self-consistent association constant in different concentrations. The best value of 'Y' that gives the same value for the equilibrium constant of ion pairing was then determined by plotting 'Y' against the standard deviation of various $A_{(\lambda 1)}/ A_{(\lambda 2)}$ values over all the concentrations investigated. Ratios of absorptions at 4-pairs of wavelengths were used to determine association.

We chose wavelengths that mainly belonged to one species or the other to maximize the importance of these numbers to the solution. Choosing an isosbestic point would be useless because the wavelength associated with the isosbestic point would have similar absorbances from the species present.

The detailed step-wise procedure for the estimation of ion pairing and hence ion-pairing energy is presented below;

Step 1

Three different concentrations of **1**$(NOct)_3 \bullet BF_4^-$, **2**$\bullet Bu_4N^+$ and 1:1 mixture of the aromatic cation and the aromatic anion are made in acetonitrile. The concentrations prepared were $1.25X10^{-5}$ M, $5X10^{-5}$ M and $2X10^{-4}$ M. Most of the ion-pairing studies involved 4 or 5 concentrations.

Step 2

UV-Vis absorption data of all 3 species were collected at different concentrations. Absorption due to free cation and anion were subtracted from that of the 1:1 mixture at each concentration to get the absorbance due only to the hypothetical complex formed between **1**$(NOct)_3$ and **2**.

$A_{\{\mathbf{1}(NOct)3 \bullet \mathbf{2}\ (\lambda)\}} = A_{(\lambda)} - [A_{\{\mathbf{1}(NOct)3 \bullet BF4^-\ (\lambda)\}} + A_{\{\mathbf{2} \bullet Bu4N^+\ (\lambda)\}}]Y$ …….(3.3)

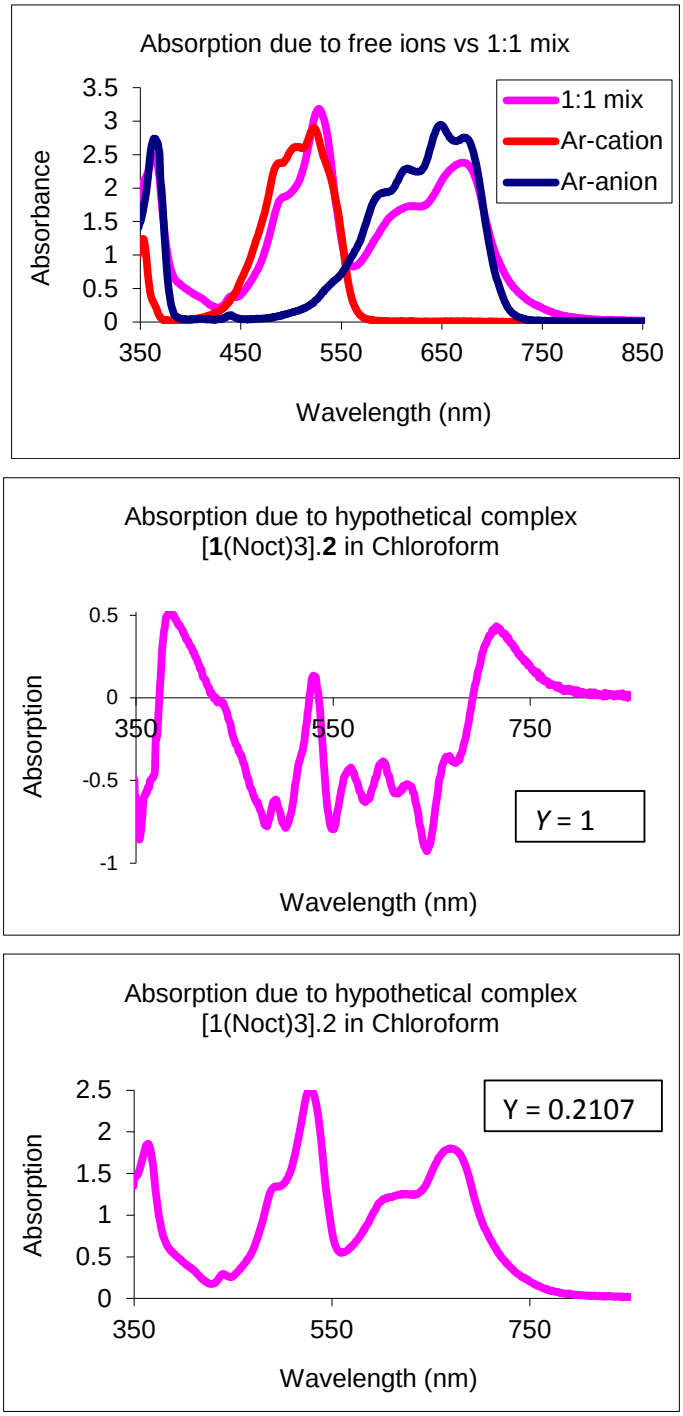

Figure 3.5. (Top) Red, blue and pink curves represent the absorptions due to **1**$(NOct)_3$•$BF4^-$, **2**•Bu_4N^+ and 1:1 mixture of the two respectively. (Bottom two) Absorption due to hypothetical **1**$(NOct)_3$•**2** at two different Y according to eq. 3.3. Concentration of each solution was $2X10^{-4}$ M $CHCl_3$.

This absorption can not be negative. The negative peaks in the resultant spectrum as shown in Figure 3.5 are due to greater concentration of unassociated **1** and **2** in individual solutions than in the mixture. So, by inputting suitable value for 'Y', the residual peaks due to complex rise above the zero line. The value for 'Y' was found to be 0.6 for the 1.25 X 10^{-5} M solution, the lowest concentration used for this particular example that brought residual peaks due to the complex to the zero line. This means that when $Y \leq 0.6$, equation 3.3 gives all positive peaks. This is the starting point for the iterative approximation of Y with the criterion of self-consistence in the equilibrium constant for ion-pairing at all concentrations.

Step 3

Choose different pairs of wavelengths such that at least a member of each pair has some absorbance from individual Ar-ions. Four different pairs of wavelengths were chosen for ion-pairing studies of all ion-pairs presented in this chapter. The pairs of wavelengths (nm) chosen for this particular example were 450/556, 670/724, 400/740 and 385/410.

Step 4

Input a value of Y for a particular concentration, possible values are from some maximum value that gives a positive spectrum to zero; with this Y, calculate the corresponding ion-pairing constant. Compute the ion-pairing constant for the other concentrations at this Y value. Exhaustively repeat for other Y values.

Step 5

How can we be sure which ion-pairing constant is the right one? Input a set of values for 'Y' in equation 3.3 to get different values of absorbence due to 1•2 at different concentrations. The correct ion-pairing constant will minimize the differences in the values for ratios of absorbencies at different wavelengths as a function of concentration. Standard deviations for the ratios of absorbencies in different concentrations are calculated. The ratio of absorbencies at two different wavelengths should be independent of concentration for the **1**$(NOct)_3$•**2**. So, the concentration-dependent values of Y that minimizes the average standard deviation of ratios of absorbencies for **1**$(NOct)_3$•**2** determine the ion-pairing constant. In Figure 3.6, it is clear that the ratios of absorbencies

for three hypothetical Y values, change the least when the ion-pairing equilibrium constant = 3.0 x 10^7 M^{-1} (Y = 0.05 for 1.25E^{-05} M solution), the graph at the bottom left.

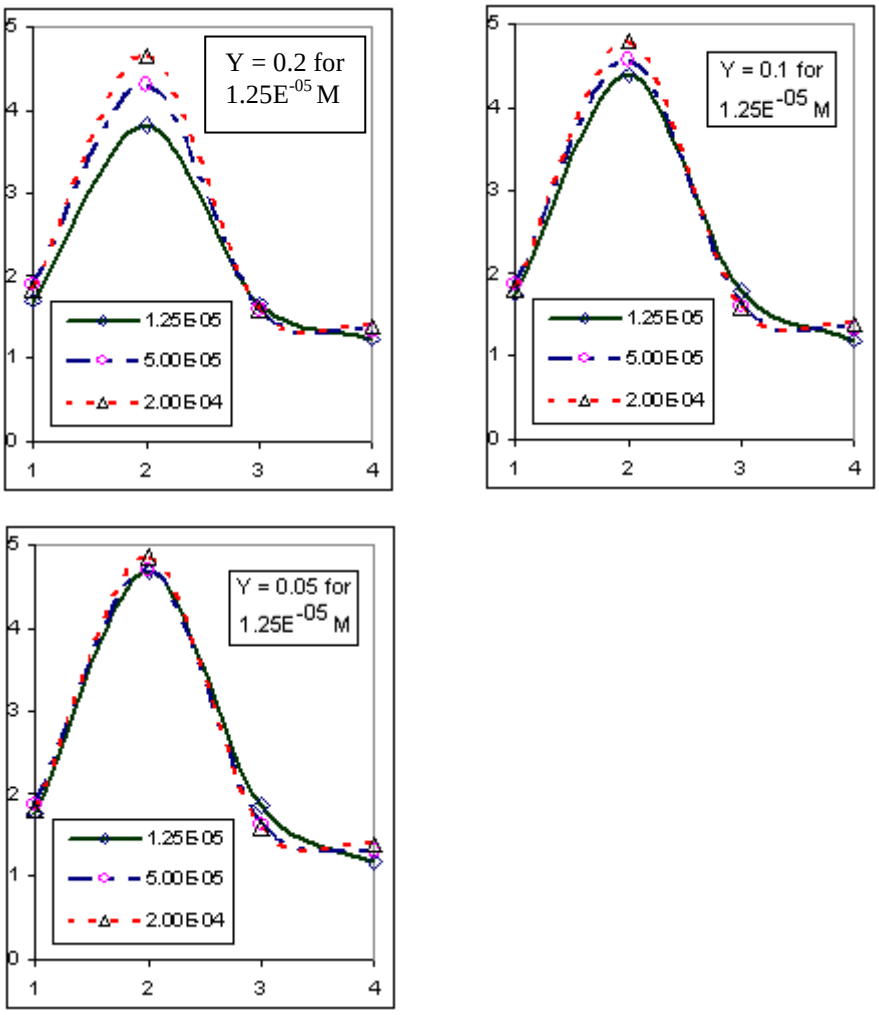

Figure 3.6. Four ratios of absorbencies (absorbance is y-axis) at fixed wavelengths with changes in concentrations of **1**$(NOct)_3$•BF_4^-, **2**•Bu_4N^+ in $CHCl_3$. Numbers (1-4) on x-axis represent the four ratios of wavelengths mentioned in step 3.

Step 6

The average standard deviations in the ratios of wavelengths were plotted against 'Y'. The value of 'Y' that corresponded to the minimum standard deviation value was considered to best represent the fraction of unassociated Ar-ions, **1**$(NOct)_3$ and **2.** The

plot of average standard deviation vs. ‘Y’ should give a curve with the minimum value as a function of ‘Y’.

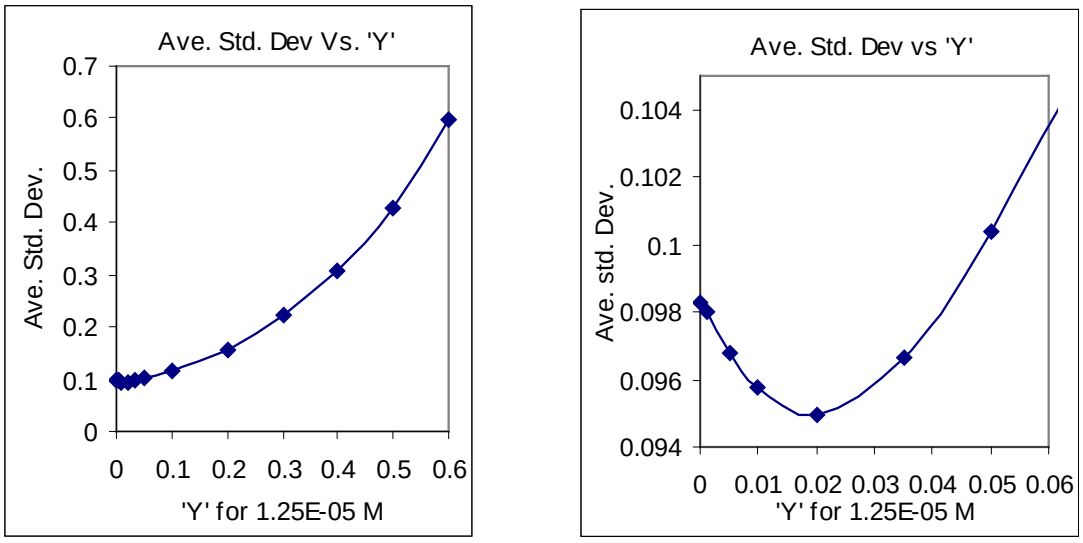

Fraction of unassociated ions (Y)	Average standard deviation	Fraction of unassociated ions (Y)	Average standard deviation	Fraction of unassociated ions (Y)	Average standard deviation
0.5	0.429	0.1	0.117	0.01	0.0957
0.4	0.308	0.05	0.101	0.005	0.0968
0.3	0.221	0.035	0.096	0.001	0.0979
0.2	0.156	0.02	0.095	0.0001	0.0982

Figure 3.7. (Top) Graphical representation of average standard deviation of ratios of absorbencies at different wavelengths plotted against fraction (‘Y’) of unassociated ions in **1**$(NOct)_3$•**2** based on eq. 3.3. Full scale (left) and magnified scale at a certain region (right). (Bottom) Actual average standard deviation values for different values of ‘Y’.

From the above graphs, the value of the fraction (Y) of unassociated **1**$(NOct)_3$ and **2** in the 1:1 mixture in this particular example converged on 0.02. With this value of ‘Y’ and known concentrations of solutions, the ion-pairing association constant and ion-pairing energy were calculated to be 1.96 X 10^{08} M^{-1} and −11.38 kcal/ mol respectively.

3.3.2.1.2 Stoichiometry of '1•2 Complex'

As described above, the ion-pairing studies of the association between aromatic cation **1** and aromatic anion **2** in solution-state assumed the '**1•2** complex' to be a single species and the association to be of 1:1 in nature. Is this the only type of association observed between aromatic cation and aromatic anion in the solution states? Are there any higher orders of association? To answers these questions, Job's method[231,232] of continuous variation was employed in UV-Vis studies to determine the stoichiometry of the complex formed between Ar-ions in solutions.

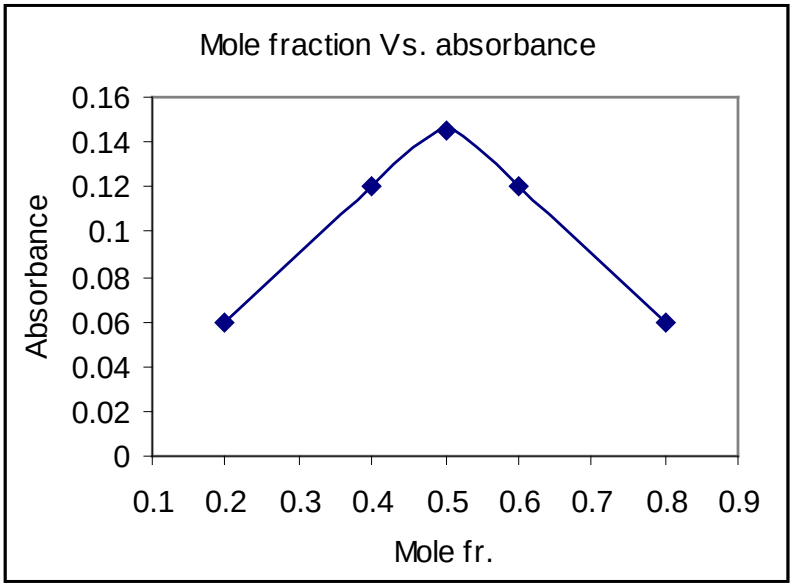

Figure 3.8. Typical Job's plot for 1:1 associated complex.

As suggested by the method, the mole fractions of aromatic cation and the aromatic anion in the mixture are changed keeping the final total concentration constant. Uv-Vis data were collected for each mixture and mole fraction is plotted against absorbencies at different wavelengths. The stoichiometry of the '**1•2** complex' was then determined from the inflection points in the Job's plots. A typical Job's plot (Figure 3.8) consists of two straight lines meeting at a point of inflection.

3.3.2.2 Electro Spray Ionization – Mass Spectroscopy (ESI-MS)

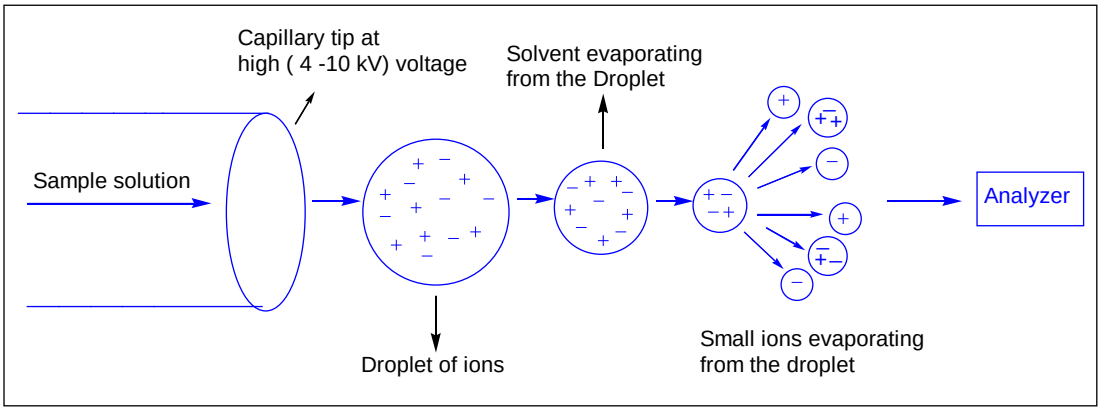

Figure 3. 9. Typical electro-spray ionization (ESI) process.

Electro spray ionization (ESI) is a soft way of ionization where ionization occurs at atmospheric pressure. In this process, the solution of the sample in polar, volatile solvent system (the most common being the mixture of CH_3CN and H_2O) is passed through a small capillary tube at a certain flow rate. The tip of the tube is maintained at high voltage (4-10 kV)[233] and the tube is surrounded by a cylindrical electrode maintained at 500-600 V.[233] Due to this high voltage at the tip of the tube, when the sample solution passes through it, the solution is sprayed into small droplets. Each droplet consists of solvent and ions of analyte. N_2 flow directs these droplets to the mass analyzer as well as diminishes the size by evaporating solvent molecules. The solvent shells around free and associated ions get evaporated and these ultimately reach the analyzer.

Due to its soft nature of ionization, ESI-MS can transform the solution phase information to the gas phase to some extent. So, the non covalent interactions or aggregation in the solution states can be studied by analyzing the ESI-MS data. Literature reports several studies that involve ESI-MS to investigate several non covalent interactions such as self-aggregation, [233] interaction of cationic porphyrin with double-stranded oligodeoxynucleotides, [234] catechin-peptide complexes, [235] protein-ligand complexes,[236] DNA-metal complexes,[237] peptide-polyphenols supramolecular

assemblies,[238] and others. [239-245] We studied the non-covalent interactions between aromatic cations **1** and aromatic anion **2** in the solution of aromatic ion-pairs, **1(**Z**)**$_3$•**2** by collecting ESI-MS data and compared the results.

3.3.2.3 Electrochemical Studies

Electrochemistry has been one of the very effective techniques to study solution-state interactions between electron donor and electron acceptor molecules in charge-transfer complexes.[246-250] The technique involves measuring the oxidation potential of the donor molecule or the reduction potential of the acceptor molecule (or both) individually as well as in presence of their interacting partners. The difference in potentials thus obtained is a measure of stability gained by the analyte due to interaction. Compounds with high positive oxidation potential and high negative reduction potential are more difficult to oxidize and reduce respectively.[250,251]

We studied the interaction between **2** and **1**(NR)$_3$ by measuring the oxidation potential of **2** in absence and presence of different **1**(NR)$_3$. Any stability gained by **2** due to its interaction with **1**(NR)$_3$ should be reflected by shifting its oxidation potential to more positive side when measured in presence of **1**(NR)$_3$. We chose to investigate electrochemical properties of **2** because it's the only species common in all ion-pairs, **1**(NR)$_3$•**2**. The increased oxidation potential of **2** in **1**(NR)$_3$•**2** will conservatively estimate the interaction energy, given that a hypothetical bond exists between **1** and **2**. The bond between the two species is the HOMO (Highest Occupied Molecular orbital). Oxidation will subtract an electron from this bond. Thus the difference in the oxidation potentials of **2** and **1**(NR)$_3$•**2** will indirectly measure the energy difference (ΔG) of the HOMO of **2** and the HOMO of **1**(NR)$_3$•**2**. This electrochemically derived $\Delta G_{(ox)}$ has to be less than the $\Delta G_{(ion\ pairing)}$ because oxidation leaves a multi-centered, one-electron HOMO that stabilizes [**1**(NR)$_3$•**2]**(•+) relative to 'free' **2**.

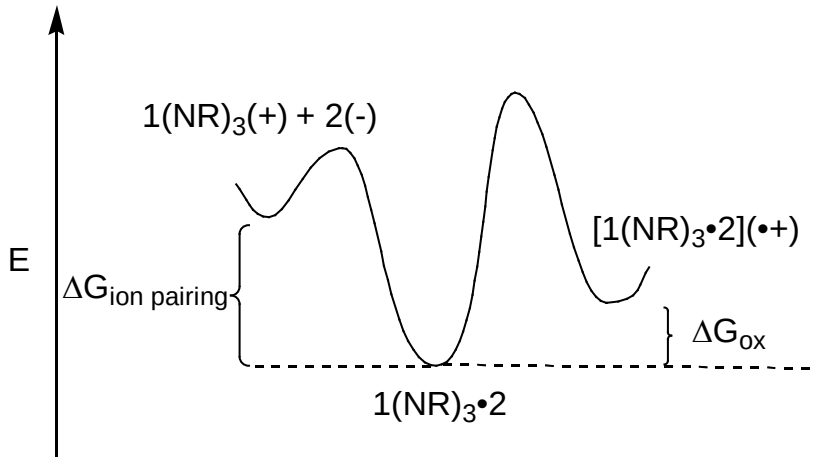

Figure 3.10. Energy diagram showing $\Delta G_{(\text{ion pairing})}$ and $\Delta G_{(\text{oxidation})}$

The Differential Pulse Voltammetry (DPV) technique was used to make these electrochemical measurements with a BAS 100B/W voltammeter. Electrolyte and solvent used were 0.1M tetra-*n*-butylammonium hexafluorophosphate ($TBAPF_6$) and CH_3CN respectively. A platinum rod, a platinum wire and a silver wire were employed as the working electrode, the counter electrode and the reference electrode respectively. Fc / Fc^+ was used as an internal reference for all measurements.

3.3.3 Molecular Orbital (MO) Calculations

Crude calculations were done to gain a fundamental understanding of the MO of the cation **1** and anion **2**. As described in the chapter 2, electronic construction in MOs of the π-framework of all-carbon analogues of aromatic cations and aromatic anion was studied using "Simple Huckel Molecular Orbital (SHMO) theory calculator". The software is available free of charge at http://www.chem.ucalgary.ca/SHMO/index.html. More advanced calculations were performed at higher levels of theory to appreciate the extent of the MO interaction in the ion pairs, **1**$(Z)_3$•2. The actual energies of molecular orbitals (MO) of the parent ion pairs, **1**$(NH)_3$•2 and **1**$(O)_3$•2 were approximated at "Restricted Hartree-Fock (RHF) / 3-21G", a low level of theory.

3.4 Results and Discussions

3.4.1 Single Crystal X-ray Diffraction

Crystal structure of **1**$(NPr)_3$•**2** was obtained by Dr. Jing Chen,[52] a previous lab member of our research group. This study elucidated the crystal structures for three more crystal structures of ion-pairs, **1**$(NOct)_3$•**2**, **1**$(NDec)_3$•**2** and **1**$(NPh)_3$•**2**. A quick view of these crystal structures revealed that these ion pairs were alternate stacks of aromatic cations and aromatic ions in a1D column.

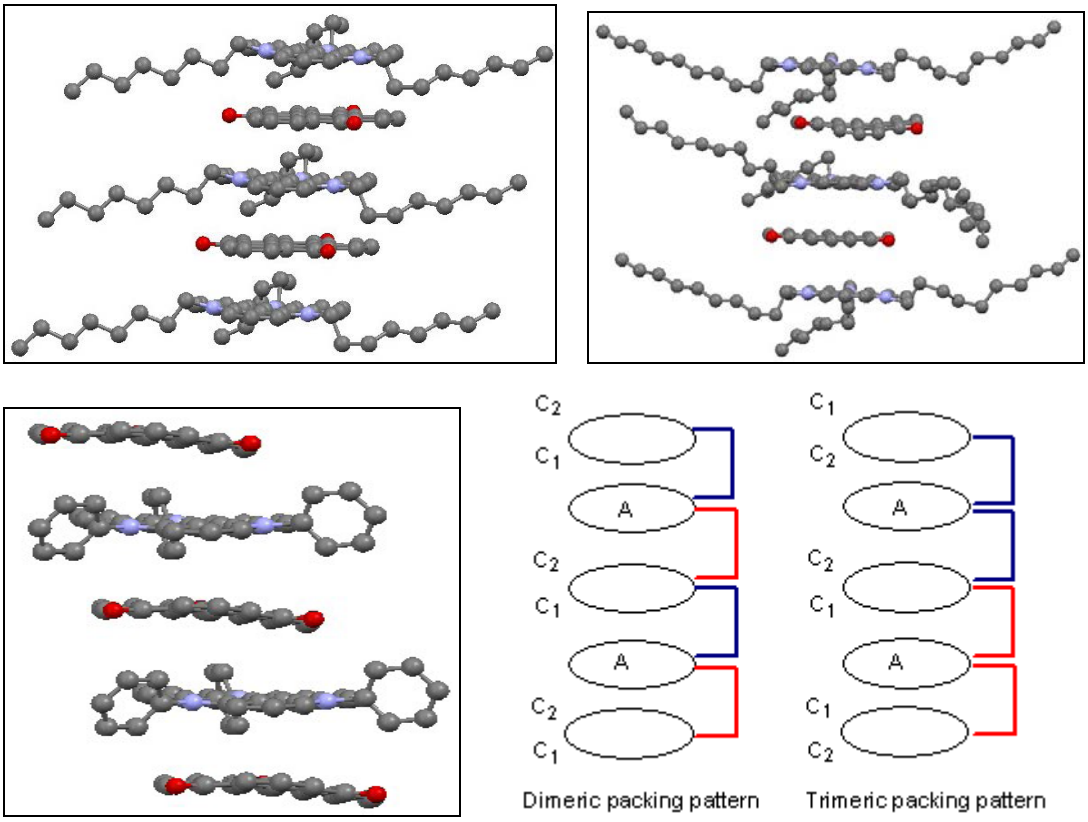

Figure 3.11. Above: Crystal structures of **1**$(NOct)_3$•**2** (left) and **1**$(NDec)_3$•**2** (right). Below: Crystal structure of **1**$(NPh)_3$•**2** (left) and different arrangement of ions in solid states; polymer of dimers and polymer of trimers (right). 'A' represents the anion and 'C_1' and 'C_2' represent two faces of the cation. The red and blue lines indicate the more intimate and the less intimate interactions between Ar-ions.

.

Detailed analysis of the crystal structures showed that the out-of-plane alkyl or phenyl groups in the cationic counter part were unsymmetrically placed above and below the aromatic plane; two groups pointing to one direction and the remaining one pointing to the other direction. This unsymmetrical distribution of side groups above and below the aromatic plane made the two faces of the cation different which led to two different types of interactions with the anion; a more intimate and a less intimate interaction

Crystals of **1**$(NPr)_3$•**2**, **1**$(NOct)_3$•**2** and **1**$(NPh)_3$•**2** were also found to have alternate stacks of more intimate and less intimate dimers. The arrangement of Ar-ions in the solid state of **1**$(NDec)_3$•**2** was found to be trimeric; more intimate and less intimate trimers arranged alternatively in 1D stacks. As shown in Figure 3.11 (dimeric packing paern), each anion in the crystal structure of **1**$(NPr)_3$•**2**, **1**$(NOct)_3$•**2** and **1**$(NPh)_3$•**2** associated with two different faces of cation from above and below leading to the dimeric arrangement of ions in 1D columns. Each anion in the crystal of **1**$(NDec)_3$•**2** associated with two similar faces of the cation leading to the trimeric arrangement of ions ($C_1AC_1.C_2AC_2$) in the 1D column.

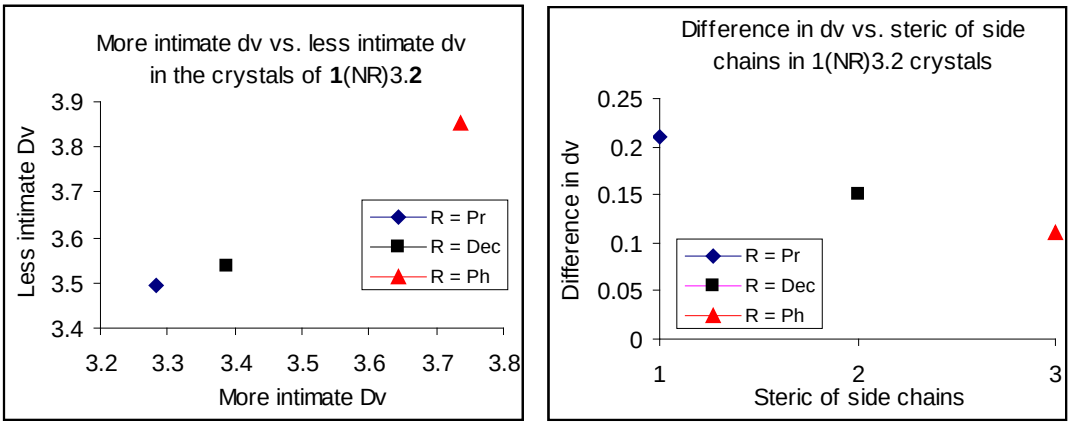

Figure 3.12. (Left) Plot of more intimate D_v vs. less intimate D_v in the crystals of **1**$(NR)_3$•**2**. (Right) Plot showing inverse relationship between sterics of side chains and the difference in more intimate and less intimate D_v. Numbers on x-axis represent the qualitative measure of sterics of alkyl and phenyl side chains.

The vertical displacement (D_v) in the crystal of **1**$(NR)_3$•**2** was found to increase with increase in the size of alkyl side groups. It was 3.28 Å for the more intimate dimer in the crystal of **1**$(NPr)_3$•**2** which increased and remained almost the same (~3.39 Å) for the more intimate dimer (or trimer) in the crystals of **1**$(NR)_3$•**2** with R ≥ C_8H_{17}. This trend resembled the change in D_v with the size of alkyl side chains in the crystal structures of aromatic cations described in the chapter 2. The trend would be better studied if we had some more crystal structures with small alkyl side chains but the efforts to crystallize these ion-pairs from various solvent systems had been fruitless. Both, the more intimate and less intimate D_v increase with increase in the steric of alkyl (or aryl) side chains in the cations (Figure 3.12, left). It looks like there is a steric dependent give and take relationship between d_v of more intimate and less intimate dimers (or trimers) of ion pairs and ; the less steric are the side chains, the smaller is the D_v for the more intimate dimer and the larger is its value for less intimate dimer. Thus, the difference between less intimate D_v and more intimate D_v increases with increase in bulkiness of the side chains in the cations (Figure 3.12, right).

As seen in the above plot (Figure 3.12, left), there is a linear relationship between more intimate D_v and less intimate D_v in the crystals of **1**$(NR)_3$•**2** such that both increase with increase in the steric of alkyl (or aryl) side chains in the cations but the difference between more intimate D_v and less intimate D_v has inverse relationship (Figure 3.12, right) with the steric of side chains; while the difference in more intimate D_v and less intimate D_v in **1**$(NPh)_3$•**2**, the ion-pair with the bulkiest phenyl side chains was only 0.11 Å, it increased to 0.15 Å in **1**$(NDec)_3$•**2** and further increased to 0.21 Å in **1**$(NPr)_3$•**2,** the ion pair with least steric side chains. Due to much greater steric effects of phenyl side chains over alkyl chains in the stacking plane, the vertical displacement (D_v) in both – more intimate and less intimate –dimers of **1**$(NPh)_3$•**2** were found to increase beyond the van der Waals radii of 3.4 Å; these were 3.74 Å and 3.85 Å for more and less intimate dimers respectively.

Aromatic ion pairs	$(D_v)_1$	$(D_h)_1$	$(\Theta_d)_1$	$(\Theta_c)_1$	$(A_o)_1$
1$(NPr)_3$•**2**	3.28	1.38	3.83	67.18	75.91
1$(NOct)_3$•**2**	3.4	2.2	2.31	57.01	58.14
1$(NDec)_3$•**2**	3.39	1.31	1.57	68.92	77.1
1$(NPh)_3$•**2**	3.74	1.39	6.35	69.67	75.6

Aromatic ion pairs	$(D_v)_2$	$(D_h)_2$	$(\Theta_d)_2$	$(\Theta_c)_2$	$(A_o)_2$
1$(NPr)_3$•**2**	3.49	3.36	3.83	46.13	35.75
1$(NOct)_3$•**2**	3.39	3.05	2.31	48.01	41.24
1$(NDec)_3$•**2**	3.54	1.87	3.96	62.19	65.08
1$(NPh)_3$•**2**	3.85	1.9	6.35	63.73	64.64

Table 3.1. Parameters of crystals of Ar-cations under study. Lengths measured in Å, angles in degree and ring % overlap.

Table 3.1 lists some important solid-state parameters for known crystals of aromatic ion pairs. The detailed procedure of the method to calculate these crystal-parameters is described in the "*Methods*" section of the chapter 2 and also defined previously in this chapter. For the better **FF** π-stacking between two aromatic cores, it is desired that a) vertical displacement (D_v) and horizontal displacement (D_h) between centers of two stacking aromatic cores and angle between two aromatic planes (Θ_d) to be as minimum as possible b) ring overlap or % area of one aromatic core that is overlapped with aromatic core of another stacking partner (A_o) to be as maximum as possible and c) angle between centers of two stacking aromatic cores (Θ_c) to be more close to 90°.

In terms of horizontal displacement (D_h), trimeric arrangement of ions in the crystal of **1**$(NDec)_3$•**2** seems to be more effective than the dimeric arrangement in other three known crystals of **1**$(NR)_3$•**2.** Although **1**$(NDec)_3$•**2** contained the biggest alkyl groups in the cation, it had the lowest value of D_h among all four known crystals. Due to the small value of D_h, **1**$(NDec)_3$•**2** had the maximum ring overlap (average A_o = 71.1 %) between aromatic ions among crystals of all four ion pairs. Despite the large value of D_v due to greater steric hindrance of phenyl groups in the stacking plane, the area of ring overlap in **1**$(NPh)_3$•**2** was comparable to **1**$(NDec)_3$•**2** because of low value of D_h.

As stated already, the dihedral angle (Θ_d) between stacking planes should be minimum for the effective **FF** interaction. The dihedral angle (Θ_d) was found to be similar for the all dimers of **1**$(NPr)_3$•**2** (Θ_d = 3.83 deg.), **1**$(NOct)_3$•**2** (Θ_d = 2.31 deg.) and **1**$(NPh)_3$•**2** (Θ_d = 6.35 deg.) irrespective of the difference in their vertical displacements. The dihedral angle in alkyl substituted ion pairs, **1**$(NAlkyl)_3$•**2** found to increase slightly with decrease in size of alkyl side chains but the dihedral angle (Θ_d) observed in the known crystals of aromatic ion pairs in this study is still low ($\leq$ 6.35). The ion pair, **1**$(NPh)_3$•**2** had relatively high (6.35 degree) value of Θ_d. After analyzing the crystal structure, we came to the point that the anomalous Θ_d in **1**$(NPh)_3$•**2** could be most possibly due to unevenly distributed effects of phenyl side chains over the stacking of Ar-core of the cation with that of anion. Due to none-zero D_h, some parts of the anion in **1**$(NPh)_3$•**2** pushed more towards the Ph groups than the remaining parts. The part of the anion which situated close to the Ph groups of the cation pushed away from the stacking plane whereas the part that situated away from the Ph groups of the cation pushed down the plane. Since this steric effect of Ph groups in the crystal of **1**$(NPh)_3$•**2** seemed to be much greater than the corresponding alkyl groups in the alkyl substituted ion-pairs, the dihedral angle angle in **1**$(NPh)_3$•**2** was very high.

If D_h were zero, the centers of aromatic cation and aromatic anion would be one above another in the same vertical line, the angle between two aromatic centers (Θ_c) would be 90 degree and the maximum (ideally 100 %) overlap would have been achieved between Ar-cores of cation and anion (Figure 3.13). The non-zero D_h in the ion pairs caused the Θ_c to deviate from 90 degree. The mathematical equation, $\Theta_c = Tan^{-1}(D_v / D_h)$ clearly indicates that it depends on D_v as well. The angle between any two adjacent

centers in the crystal of **1**$(NDec)_3$•**2** (Θ_c = 65.56 deg.) was found to be least deviated from 90 degree among all alkyl substituted ion-pairs. This could be probably due to very low value of D_h. The comparable value (Θ_c = 65.56 deg.) in **1**$(NPh)_3$•**2** must be due to high value of D_v.

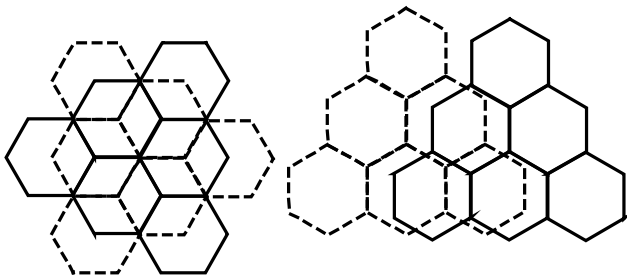

Figure 3.13. Optimal molecular alignment (left) and actual alignment in the ion pair, **1**$(NPh)_3$•**2** (right). Dotted line represents anion. Phenyl side chains are omitted for clarity.

Analyzing the known crystals of **1**$(NR)_3$•**2** clearly indicated that the non-optimal association of Ar-ions in these ion pairs was due to the steric effect of alkyl (or phenyl) groups in the stacking plane. If there were no steric effects in the stacking plane, optimal synergistic effects between unit-charge electrostatic and aromatic interactions would have likely resulted. **1**$(NMe)_3$•**2** and **1**$(O)_3$•**2** were the only two candidates in this category but diffraction-quality crystals were not obtained. However, the average distances between two adjacent aromatic layers in these ion pairs were estimated from powder diffraction analysis.

3.4.2 Powder X-ray Diffraction (PXRD)

D-spacing obtained from powder x-ray diffraction (PXRD) was compared with the vertical displacement obtained from single crystal analysis for the ion pairs of known crystal structures. The PXRD peaks in the π-stacking region of **1**$(NR)_3$•**2** (R = Pr, Oct, Dec and Ph) were comparable to the results obtained from single crystal analysis. Once PXRD peaks due to D_v were identified, the technique was applied to get some insight on the solid state of ion pairs with unknown crystal structures; **1**$(NMe)_3$•**2** and **1**$(O)_3$•**2**, both

of which were thought to have the optimum synergy between unit-charge electrostatic and aromatic interactions in absence of any steric effects in the stacking plane.

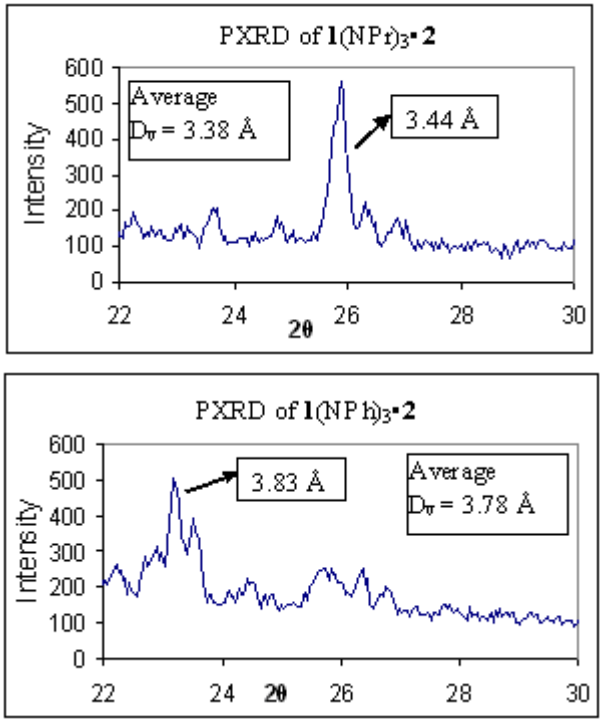

Figure 3.14. Comparison of d-spacing obtained from PXRD with vertical displacement (D_v) obtained from single crystal analysis.

As seen in the Figure above (Figure 3.14), similar trend was obtained for the d-spacing obtained from PXRD and single crystal analysis although the results obtained from PXRD were a little bit higher than the single crystal analysis. While **1**$(NMe)_3$•**2** showed a broad peak (not shown) in PXRD, a well defined single peak (Figure 3.15, top) was obtained for **1**$(O)_3$•**2** in the region that corresponds to 3 Å – 4 Å. The broad peak (not shown) in **1**$(NMe)_3$•**2** might include several closely related peaks which would indicate several closely related vertical displacements (D_v) in the solid state. Due to the absence of a well defined peak, d-spacing between aromatic ions (hence, the vertical displacement, D_v) couldn't be estimated for **1**$(NMe)_3$•**2.** However, d-spacing for **1**$(NMe)_3$•**2** was distinctly greater than that for **1**$(O)_3$•**2.** The sharp peak seen in **1**$(O)_3$•**2** had d-spacing equal to 3.26 Å which when plotted against more intimate D_v for known single crystals, corresponds to 3.06 Å (Figure 3.15, bottom).

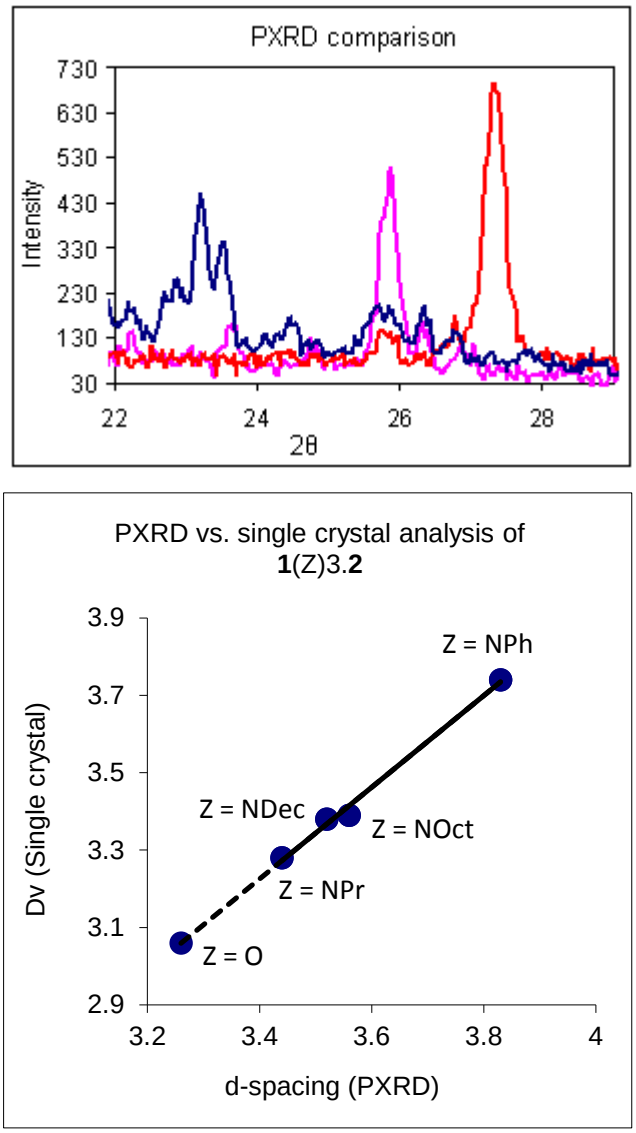

Figure 3.15. Top: PXRD data for **1**$(NPr)_3$•**2** (pink), **1**$(NPh)_3$•**2** (blue), and **1**$(O)_3$•**2** (red) with calculated d-spacing value for peaks of interest. Bottom: Graphical estimation of more intimate D_v in **1**$(O)_3$•**2** by extra-plotting d-spacing (PXRD) against known D_v. All distances were measured in Å**.**

The low value of calculated D_v in **1**$(O)_3$•**2** was expected because we thought there would be a strong synergy between ionic interaction and π-π interaction in absence of any steric effects in the stacking plane. The interaction in solid state of **1**$(O)_3$•**2** seemed to be stronger than the solid state of **1**$(NMe)_3$•**2** in terms of d-spacing and hence D_v. We reasoned this to be because of greater π-acidity and electrophilicity of **1**$(O)_3$ than **1**$(NMe)_3$; **1**$(O)_3$ being more electrophilic than **1**$(NMe)_3$, should have better contact with the anion **2**.

Literature reports the reduction potentials of **1**$(O)_3$ and **1**$(NR)_3$ with small, non-aromatic anions to be 0.106 V (vs. SCE)[252] and −1.40 V (vs. SCE)[253] respectively. Compounds with more positive (or less negative) reduction potential are easier to reduce; they have better affinity with electrons and are more electrophilic than the ones with more negative (or less positive) reduction potential which have less affinity with electrons and hence are less electrophilic. The positive value of the reduction potential for **1**$(O)_3$ proves that it is more electrophilic than **1**$(NR)_3$ with negative value for the reduction potential. We also collected the data for reduction potentials for **1**$(O)_3$• BF_4^- and **1**$(NMe)_3$• BF_4^- and obtained the similar results. Literature also puts **1**$(NR)_3$ among the most stable[74] cations indicating these to be weak electrophiles. Preliminary results for the stability gained by **2** when interacting with **1**$(NR)_3$ are presented under separate heading, "electrochemical studies"

3.4.3 Differential scanning calorimetry (DSC)

Differential scanning calorimetry (DSC) revealed that the ion pairs **1**$(NR)_3$•**2** with long alkyl chains ($R \geq C_8H_{17}$) had reversible melting transitions whereas the ion pairs with short alkyl ($R \leq C_4H_9$) or Phenyl (R = Ph) chains decomposed while or before melting. The DSC data showed a general trend in MP / decomposition temperature of alkyl substituted ion pairs; melting transition temperature increased with decrease in the length of side chains as expected. A big shift was noticed in the MP of short chain (or no side chains) ion pairs. The **1**$(NR)_3$•**2** ion pairs with R = Et decomposed while melting and R = Pr and Bu decomposed followed by melting. The ion pairs, **1**$(NMe)_3$•**2** and **1**$(O)_3$•**2** with no steric effects in the stacking planes decomposed before melting. Decomposition temperatures of these ion pairs were considered also as their minimum

MP transition temperatures for comparison with other ion pairs. DSC curves of some ion pairs are shown in Figure 3.16 below.

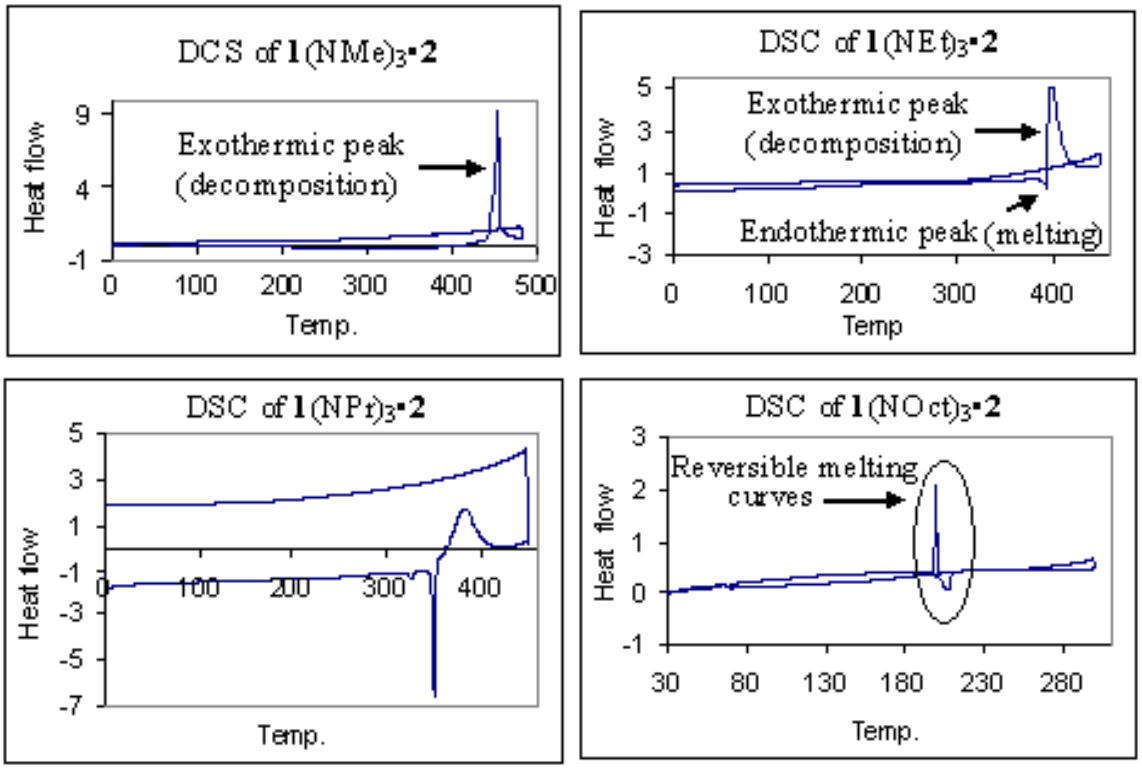

Figure 3.16. DSC curves of some ion pairs under study showing the effects of alkyl chain length in melting / decomposition transitions.

In DSC a) Forward direction (left to right) is heating and the reverse direction is the cooling process b) Endothermic peaks in the heating process are due to solid → liquid transition. The solid → liquid transition may be mediated with solid → liquid crystalline phase in some type of compounds called liquid crystals c) Exothermic peak in the heating process are due to decomposition d) For each peak that shows up in the heating process, there should be an exothermic peak in the cooling process. The melting / decomposition temperatures of **1**$(Z)_3$•**2** ion pairs under study are given in table 3.2. As seen in the table, a big shift in MP temperature of alkyl substituted ion pairs occurred while changing R in **1**$(NR)_3$•**2** from C_3H_7 to C_2H_5 and finally to CH_3; while there was only 9 °C difference in the melting temperatures of ion pairs with C_4H_9 and C_3H_7 groups, the difference increased to 43 °C with C_3H_7 and C_2H_5 groups and further increased to > 60 °C in the

ion pairs with C_2H_5 and CH_3 groups. These big shifts in melting transitions of **1**$(NR)_3$•**2** with C_2H_5 and CH_3 side chains were thought to be due to strong synergistic effects of ionic and aromatic interactions in absence of π-face steric interactions.

1$(Z)_3$•**2**	Melting temp.	**1**$(Z)_3$•**2**	Melting temp.
Z = NCH_3	453*	Z = NC_8H_{17}	208
Z = NC_2H_5	393	Z = $NC_{10}H_{21}$	184
Z = NC_3H_7	351	Z = $NC_{12}H_{25}$	170
Z = NC_4H_9	342	Z = $NC_{14}H_{29}$	170
Z = NC_6H_5	433	Z = $NC_{16}H_{33}$	170
Z = O	389*		

Table 3.2. Melting transitions (°C) of ion pairs under study. * Decomposed before melting.

Generally the steric effects of two adjacent alkyl homologues (say, *Me* vs. *Et*) are not very different. The dramatic difference found in the study of these ion pairs was due to a strong effect of ionic interactions added to π-π stacking; the synergy between ionic and π-π interactions. The π-π interactions need to be within bonding distances to be active. At or near the VW radius is the distance that MO interacts. Such shifts wouldn't be observed in the neutral aromatics. **1**$(O)_3$•**2** couldn't be compared with **1**$(NR)_3$•**2** because of structural differences; nitrogen (N) vs. oxygen (O) – substitution in the aromatic ring. However, it seemed to follow the same trend observed in N-substituted ion pairs**;** like **1**$(NR)_3$•**2** with no π-face steric interactions, it also decomposed before melting. The high melting point of **1**$(NPh)_3$•**2** could be attributed to the overall packing of ions in the solid state. The extra stability gained by the synergistic effect of ionic and aromatic interactions in **1**$(NPh)_3$•**2** could be explained based on the big difference in decomposition temperature of the ion pair (433 °C) vs. **1**$(NPh)_3$•BF_4^- (361 °C).

The steric dependent synergistic effects of ionic – and π – π interactions in the alkyl substituted aromatic ion pairs, **1**$(NR)_3$•**2** can also be explained on the basis of enthalpy change (ΔH) of their melting transitions. Table 3.3 lists ΔH values for the

melting transitions of some alkyl substituted ion pairs which had distinct melting curves in DSC. The table clearly indicates that there is an inverse relationship between ΔH of melting and size of alkyl side chains in **1**$(NR)_3$•**2**; more energy is required to melt the ion pairs with short alkyl chains. The result is also an indicative of better synergy between ionic – and π – π interactions in ion pairs with short alkyl chains; short alkyl chains have less steric effects on π faces to allow close proximity between aromatic ions. One would guess that **1**$(NMe)_3$•**2** and **1**$(O)_3$•**2** with no π – face steric effects would have relatively very high value for ΔH but the experimental value couldn't be achieved because of their decomposition prior to melting.

1$(NR)_3$•**2**	ΔH (kcal / mole)
R = C_3H_7	−12
R = C_4H_9	−11
R = C_8H_{17}	−4.2
R = $C_{10}H_{21}$	−3.8
R = $C_{12}H_{25}$	−3.1

Table 3.3. Enthalpy (ΔH) of melting for some alkyl substituted ion pairs.

3.4.4 UV-Vis Ion-Pairing Studies

The UV-Vis absorption spectra of individual cation (**1**•BF_4^- or **1**•PF_6^-) and anion (**2**•Bu_4N^+) was compared with that of a 1:1 mixture of the two (or pure **1**•**2**) to see whether there were any association between aromatic ions in the solution states. Following the trend in the solid state, ion pairs showed more distinct association with decrease in size of alkyl side chains.

Absorption at near IR region in ion pairs with no π – face steric [**1**$(NMe)_3$•**2** and **1**$(O)_3$•**2**] indicated a very strong association between cation and anion in these ion pairs even in the solution-states. These near IR absorptions were totally absent in the spectra of other ion pairs. These shifts were presumably because **1**$(NMe)_3$•**2** and **1**$(O)_3$•**2** could

allow close approach between the aromatic discs but other ion pairs couldn't. As shown in Figure 3.17, while the absorption due to sum of individual cation and anion in **1**$(NEt)_3$•**2** was similar to the one due to 1:1 mixture of the two, they were very different in **1**$(NMe)_3$•**2** and **1**$(O)_3$•**2**. There is literature that these near IR absorptions indicate strong $\pi - \pi$ interactions.[204,222]

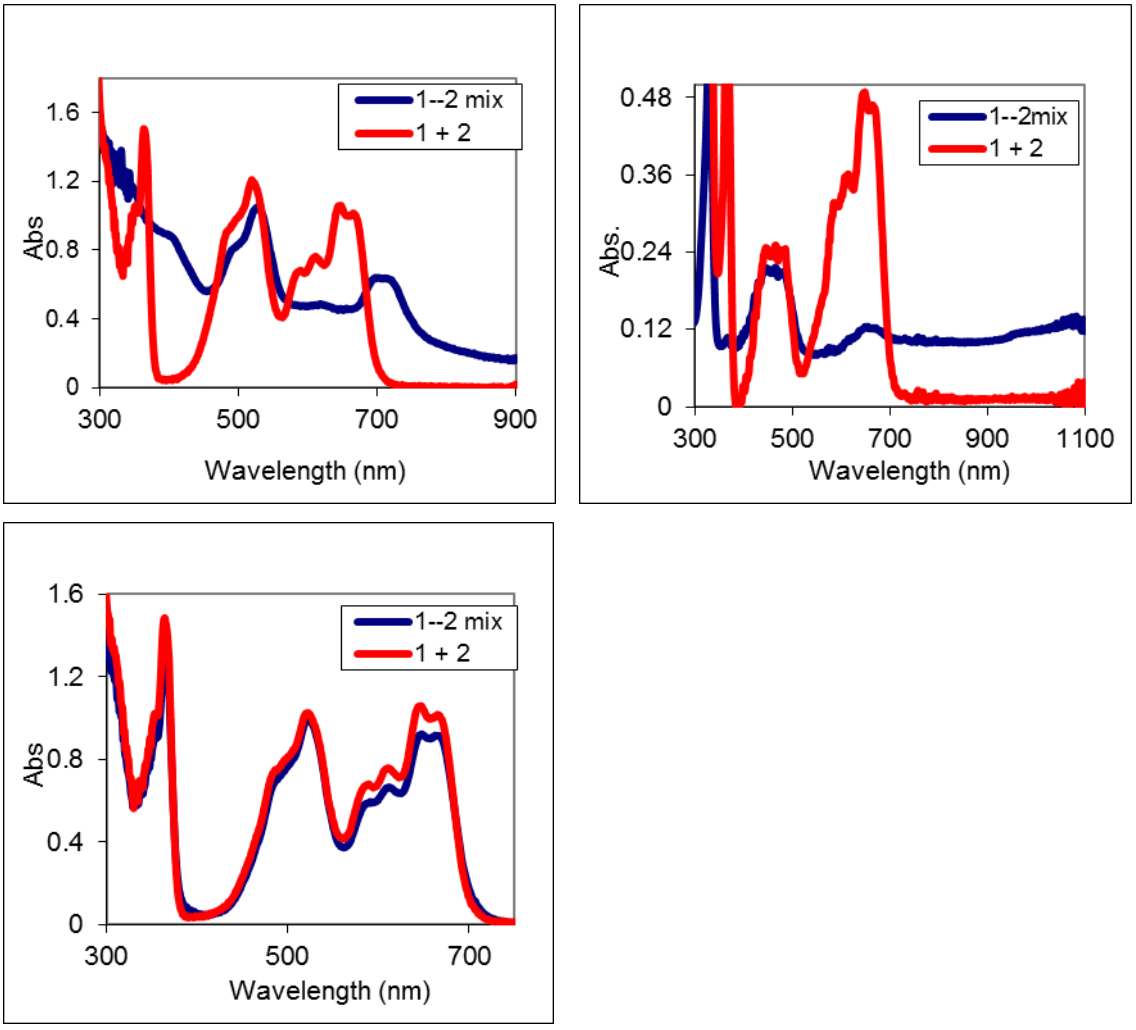

Figure 3.17. Association of aromatic cation and anion in ion pairs. Sum of absorption due to individual cation **1** and anion **2** (**1** + **2**) vs. 1:1 mixture of the two (**1**--**2** mix) at the same concentration; **1**$(NMe)_3$•**2** (top left) and **1**$(NEt)_3$•**2** (bottom) in 5 X 10^{-5} M and **1**$(O)_3$•**2** (top right) in 2.5 X 10^{-5} M in CH_3CN.

The steric effect of the side chains on π-face cohesion predicted by the crystal structure analysis was also unveiled by simple solution state UV-Vis ion-pairing studies. Ion-pairing association energy and association constant of the association between cation and anion in the ion pairs were calculated assuming that the complexes were single species of 1:1 (cation / anion) association. As expected the ion-pairing association energies and association constant of ion pairing increased with decreasing size of the alkyl side chains (Table 3.4).

1$(NR)_3$•**2**	Ion-pairing energy (kcal/mol)	Ion-pairing association constant (M^{-1})
R = Me	14.96	8.00×10^{10}
R = Et	10.06	2.16×10^{07}
R = Pr	9.22	5.22×10^{06}
R = Bu	8.62	1.90×10^{06}
R = Oct	8.1	8.00×10^{05}
R = Ph	7.76	4.49×10^{05}

Ion-pairing energy (kcal/mol)	Ion-pairing association constant (M^{-1})	Solvent	Dielectric (ε)	1/ε
11.38	1.90×10^{08}	$CHCl_3$	4.81	0.208
9.0	3.60×10^{06}	$(CH_3)_2CO$	20.7	0.048
8.1	8.00×10^{05}	CH_3CN	37.5	0.027
7.27	2.00×10^{05}	DMSO	46.7	0.021

Table 3.4. (Above): Ion-pairing energy and ion-pairing association constant of **1**$(NR)_3$•**2** in CH_3CN and (Below) dependence of ion pairing of **1**$(NOct)_3$•**2** on solvent-dielectric**.**

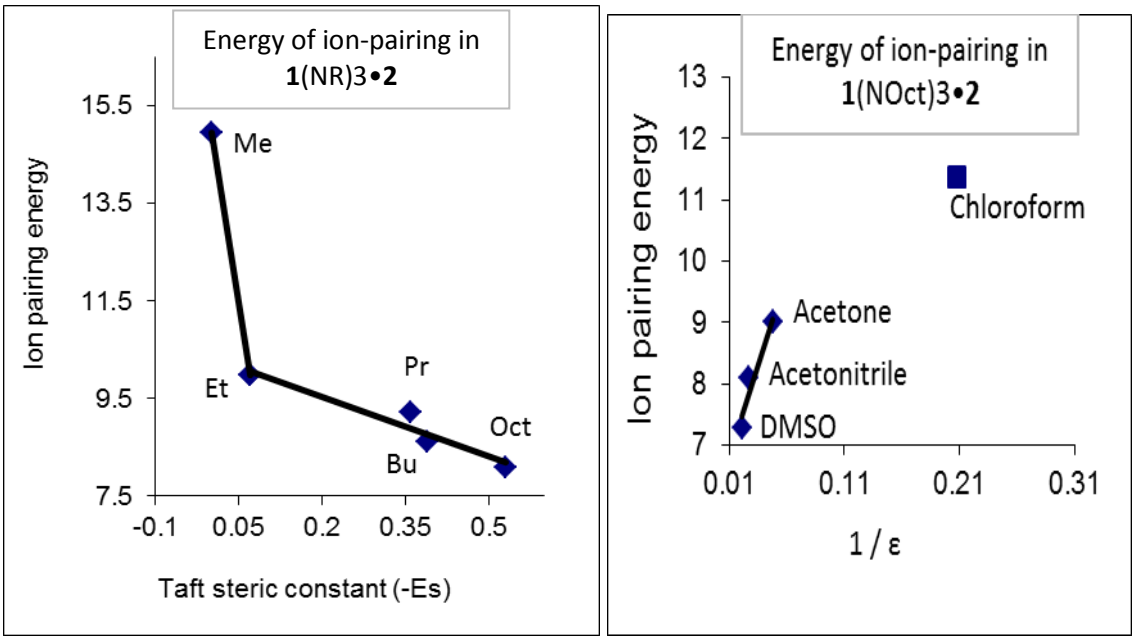

Figure 3.18. (Left): Energy of ion-pairing (kcal/mole) of **1**$(NR)_3$•**2** complex in CH_3CN as a function of Taft steric constant ($-E_s$) of the alkyl side chains[198] and (right): Association energy of **1**$(NOct)_3$•**2** as a function of solvent dielectric. All ion pairing energies were within ± 0.3 kcal / mole

As represented graphically in Figure 3.18, association energies of aromatic ions in alkyl substituted ion pairs (R = Et – Oct) in CH_3CN showed a more or less continuous line when plotted against the Taft steric constant ($-E_s$)[198] of the alkyl side chains. The big shift observed in the ion-pairing energy of ions in **1**$(NMe)_3$•**2** must be because of very strong interaction between oppositely charged aromatic discs in absence of any steric interaction in the stacking plane.

As mentioned previously, the size effects of *Me* and *Et* are very similar in most quantitative measurements such as the A-values in cyclohexanes,[197] and the Taft steric constant (E_s).[198] The angularity of *Et* group vs. non-angularity of *Me* group combined with arrangements of ionic discs as predicted by solid state studies rationalizes the big difference between *Me* and *Et* observed in this research. The lowest value for calculated association energy of ions in **1**$(NPh)_3$•**2** also corroborated the solid state findings of steric dependent π-stacking even in the solution states. Although it is obvious from Figure 3.17,

it is worth mentioning that **1**$(NMe)_3$•**2** had almost all (98.9 %) ions in the bound form at the lowest concentration (6.25 X 10^{-6} M) studied. The strong ion-pairing energy of ions in **1**$(NMe)_3$•**2** gives birth to the notion that **1**$(NMe)_3$•**2** is polymeric with 1:1 stoichiometry of cation and anion. The polymeric structure is blocked by the angularity in the alkyl chains longer than *Me*.

As expected, the association energies of ion pairs showed strong dependences on solvent dielectric. Association energy of ion pairing in **1**$(NMe)_3$•**2** was measured to be 8.17 kcal / mol in DMSO, which was 45 % decrease from the ion-pairing energy in CH_3CN and the fraction of ions associated in the complex was found to be only 65.8 % at the concentration of 6.25 X 10^{-6} M. The dependence of ion-pairing on the solvent dielectric is given in table 3.4 for the ion-pair, **1**$(NOct)_3$•**2**. When plotted against reciprocal of dielectric (1/ ε), association energy showed a linear decrease with increase in solvent dielectric (Figure 3.18, right). The deviation from linearity in $CHCl_3$ with a very low dielectric (4.81) could be due to expected non-linear effect of π-face bonding in a solvent of decrease dielectric. The low dielectric permits close approach of the discotic molecules and molecular orbital effects and the inverse quadratic dependence 'r' of the electrostatic potential might contribute to $CHCl_3$ as an outlier on the graph.

3.4.4.1 Error Analysis of the Ion-Pairing Studies

The results obtained from ion pairing studies are consistent with those obtained from other solution-state studies as well as solid-state studies. However, there are some errors associated with it; a) As mentioned previously; the complex formed between the aromatic cation **1** and the anion **2** was assumed to be 1:1. The assumption was made to simplify the calculations. Although the 1:1 complex seems to be predominant (see stoichiometric studies in the following paragraph and Figure 3.19) in these ion pairs, there are higher orders of aggregation. b) Graphical estimation of the fraction of unassociated ions ('Y' in Figure 3.7, right) in the 1:1 mixture of **1** and **2** considered the values of 'Y' to be in an increment order of 0.01. This gives error of ± 0.1 kcal / mole for the association energy. c) Human error (sample preparation for example) combined with instrumental error was estimated by repeating the complete procedure multiple times with freshly prepared solutions every time. The error was found to be ± 0.2 kcal / mole for

association energy as calculated by performing 4 repetitions of ion pairing studies of **1**$(NEt)_3$ and **2**. So, a total known error in the ion pairing study experiment was calculated to be ± 0.3 kcal / mole for ion pairing association energy.

3.4.5 Stoichiometry of the Association

Completely different spectral signatures of **1**$(NMe)_3$•**2** and **1**$(O)_3$•**2** from those of other ion pairs indicated that the complexes of ion pairs were not all single species of 1:1 (cation / anion) association. The assumption of 1:1 stoichiometry in the ion pairing was made to simplify the calculations. The stoichiometry of the association was further explored by using Job's method[231,232] of continuous variation.

Mole fractions of **1** and **2** in each ion pair were varied keeping final total concentration constant in CH_3CN solutions and the stoichiometry of the complex formed was determined from the inflection points (maxima or minima) in the Job's plots (Figure 3.19) of absorbance vs. mole fraction at a particular wavelength. The wavelengths chosen had no absorbance from the individual cationic and anionic solutions and were higher than the λ_{max} of individual cation and anion. As seen in the plot (Figure 3.19), only 1:1 dimeric complex, **1•2** was obvious in **1**$(NPh)_3$•**2** which had the biggest D_v in the crystalline state. When phenyl substituents were replaced with propyl groups, more than one type of complex was noticed which absorbed at the same wavelength range used to study stoichiometry of the complex.

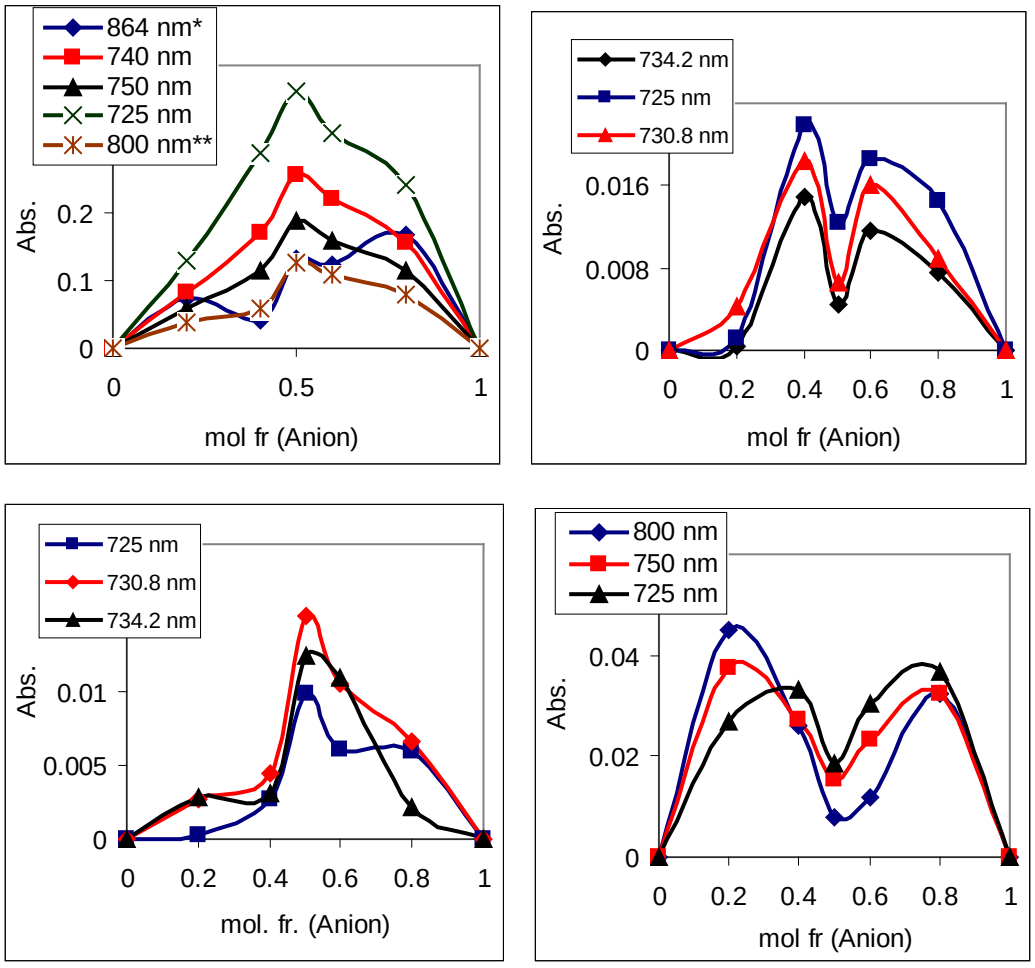

Figure 3.19. Job's plots for the determination of stoichiometry of the complex formed between cation **1** and anion **2** of aromatic ion pairs **1**$(Z)_3$•**2** in CH_3CN. Z = NMe (top left), NPr (top right), NPh (bottom left) and O (bottom right) Notes: *absorbance multiplied by 10 and **absorbance multiplied by 2.

1$(NPr)_3$•**2** had two symmetrically placed 2:3 complexes on either side of the 1:1 complex. The maxima due to **1•2•1•2•1** and **2•1•2•1•2** indicate, as expected that the anions in these pentamers have different molar absorptivities than the absorptivities of the anion in **1•2** dimeric complex. These differences in the molar absorptivities are more accentuated at longer wavelengths. The pentamers are expected to absorb more at longer wavelengths than the dimers or trimers due to increased MO interactions.

The ion pairs with no steric hindrance in the π face showed even higher order of molecularity in ion pairing. **1**$(NMe)_3$•**2** had predominantly 1:1 complex (**1•2**) between cation and anion even at very high wavelength. There were **1•2•1•2•1**, **2•1•2•1•2** and other pentameric complexes in **1**$(NMe)_3$•**2**. Similar type of complexes (1:1, 2:3 and 1:4) were observed also in **1**$(O)_3$•**2**.

There is no way to tell the difference between **1•2** and $(\mathbf{1•2})_n$. Both have 1:1 stoichiometry. Same is true for all other complexes observed in the solution-states. However, the observation of **1•2•1•2•1** and **2•1•2•1•2** in Jobs plot and the large λ – absorptions of all complexes mainly in the ion pairs with no π face steric hindrance suggested a polymeric arrangement of ions even in the solution states. The observation of $(\mathbf{1•2})_n$ in the crystalline phase and the observation of **1•2•1** and **2•1•2** in the mass spectrometry provide strong evidence for polymeric structure in pairing.

Figure 3.19 clearly indicated that complexes of ions of **1**$(NMe)_3$•**2** and **1**$(O)_3$•**2** absorbed in the near IR (800 – 864 nm). As discussed previously, this was probably a clue for the strong solution – state π – π interaction which was aided by unit charge electrostatic and also supported by the absence of π face steric hindrance in these ion pairs. Remember that solutions of **1**•BF_4^- and **2**•Bu_4N^+ had no absorption above 720 nm. Such a big shift in absorption would have never been observed in the association between neutral aromatics. The reason for predominantly observed $(\mathbf{1•2})_n$ complex in **1**$(NMe)_3$•**2** and **1**$(O)_3$•**2** could be because the cationic counter parts (**1**) in these ion pairs – unlike other alkyl substituted ion pairs don't have facial discrimination to associate with its anionic part (**2**).

3.4.6 Electro-Spray Ionization – Mass Spectrometry (ESI-MS)

ESI-MS detected a peak for aromatic cation ($\mathbf{1}^+$) and aromatic anion ($\mathbf{2}^-$) in each aromatic salt, **1**$(Z)_3$•**2** when data were collected at positive and negative mode respectively. The cationic trimer $(\mathbf{1•2•1})^+$ was detected in all aromatic salts except in **1**$(NPh)_3$•**2**. When MS-MS experiment was performed on the trimeric peak $(\mathbf{1•2•1})^+$, each aromatic salt gave respective peak for $\mathbf{1}^+$ as expected. Although the ESI-MS is a gas-phase experiment, literature reports its application to get the information about non-covalent interactions in the solution states. [233-245] We tried to understand the aggregations

between cation (**1**) and anion (**2**) and their relative strength in the solution states by comparing the abundance of $(\mathbf{1{\bullet}2{\bullet}1})^+$ peak relative to that of $\mathbf{1}^+$ peak in various aromatic salts. All physical and instrumental parameters were kept constant for each set of the experiment.

In one experiment, ESI-MS data for $\mathbf{1}(O)_3{\bullet}\mathbf{2}$, $\mathbf{1}(NPh)_3{\bullet}\mathbf{2}$ and $\mathbf{1}(NR)_3{\bullet}\mathbf{2}$ (where R $\leq C_8H_{17}$) were collected by spraying their very dilute solutions in CH_3CN / H_2O, one at a time. The results of relative abundance of $(\mathbf{1{\bullet}2{\bullet}1})^+$ with that of respective $\mathbf{1}^+$ are represented in table 3.5 below.

$\mathbf{1}(Z)_3{\bullet}\mathbf{2}$	Abundance of $(\mathbf{1{\bullet}2{\bullet}1})^+$ relative to $\mathbf{1}^+$
Z = NMe	42
Z = NEt	21
Z = Npr	2.5
Z = NBu	1.5
Z = NOct	1
Z = NPh	0
Z = O **	18 (36*)

Table 3.5. Abundance of $(\mathbf{1{\bullet}2{\bullet}1})^+$ relative to that of respective $\mathbf{1}^+$ in different aromatic salts as estimated by ESI-MS. * Abundance of $(\mathbf{2{\bullet}1{\bullet}2})^-$ relative to that of $\mathbf{2}^-$**. **** Only salt in which $(\mathbf{2{\bullet}1{\bullet}2})^-$ was observed.

As seen in the table 3.5, relative abundance (hence relative stability) of $(\mathbf{1{\bullet}2{\bullet}1})^+$ of alkyl substituted salts increased continuously with decrease in steric effects of side groups. The big shift in stability / abundance noticed in $\mathbf{1}(NMe)_3{\bullet}\mathbf{2}$ and $\mathbf{1}(NEt)_3{\bullet}\mathbf{2}$ was indicative of a close association of ions in the cationic trimers of these salts. ESI-MS didn't detect such a trimer in $\mathbf{1}(NPh)_3{\bullet}\mathbf{2}$. The low stability of such trimers in the phenyl substituted salt was obvious from the high value of D_v in the solid – state; the phenyl rings maintain a non-zero dihedral angle between two stacking planes and block the π face interactions.

1$(O)_3$•**2** showed a high value not only for the relative abundance of cationic trimer, $(\mathbf{1}\bullet\mathbf{2}\bullet\mathbf{1})^+$ but also for anionic trimer, $(\mathbf{2}\bullet\mathbf{1}\bullet\mathbf{2})^-$. This O-substituted salt was the only one that showed $(\mathbf{2}\bullet\mathbf{1}\bullet\mathbf{2})^-$ as detected by ESI-MS and when combined together, the relative abundance / stability of trimers in **1**$(O)_3$•**2** was much greater than that in **1**$(NMe)_3$•**2**; the trend also found in solid-state and other solution-state methods. The difference in stability of $(\mathbf{1}\bullet\mathbf{2}\bullet\mathbf{1})^+$ vs. $(\mathbf{2}\bullet\mathbf{1}\bullet\mathbf{2})^-$ between aza salts (N-substituted) and oxa salt (O-substituted) is explained in the following paragraph. **1**$(NMe)_3$•**2** and **1**$(O)_3$•**2** were considered for the comparison because of their similarities in terms of both not having π face steric hindrance.

Chapter 2 discussed the solid-state stacking of aromatic cations vs. aromatic anions when crystallized with small non-aromatic counter ions. As described therein, $[\mathbf{1}(NMe)_3]^+$ stacked co-facially to give polymeric arrangement of homo-dimer with counter anions positioning at the edges. However, such stacking was not observed in $[\mathbf{1}(O)_3]^+$; aromatic cations has facial contact with counter anions. This means that $[\mathbf{1}(O)_3]^+$ has better affinity than $[\mathbf{1}(NMe)_3]^+$ with counter anion. This explains that why $[\mathbf{1}(O)_3]^+$ can form complex with two aromatic anions $(\mathbf{2})^-$ easier than $[\mathbf{1}(NMe)_3]^+$. Literature reports that trioxa cation (E_{Red} = 0.106 V vs. SCE) [252] is better electron receptor than triaza cation (E_{Red} = −1.40 V vs. SCE)[253] supporting the fact that formation of $[\mathbf{2}\bullet\mathbf{1}(O)_3\bullet\mathbf{2}]^-$ is easier than $[\mathbf{2}\bullet\mathbf{1}(NMe)_3\bullet\mathbf{2}]^-$. Better facial cohesiveness of $[\mathbf{1}(NMe)_3]^+$ than $[\mathbf{1}(O)_3]^+$ also supports the finding from ESI-MS studies that formation of cationic trimer, $[\mathbf{1}(NMe)_3\bullet\mathbf{2}\bullet\mathbf{1}(NMe)_3]^+$ is easier than $[\mathbf{1}(O)_3\bullet\mathbf{2}\bullet\mathbf{1}(O)_3]^+$.

Overall, exceptionally high relative abundance / stability of trimers in **1**$(NMe)_3$•**2** and **1**$(O)_3$•**2** suggested that π-π and ionic interactions must have synergized optimally even in the solution states to establish close contacts between aromatic cation and aromatic anions in these salts which corroborated the solid state findings. **1**$(NR)_3$•**2** with R ≥ C_8H_{17} didn't show any trimeric peaks in CH_3CN / H_2O solvent system. However, qualitative data were obtained when 1,4-dioxane was used instead of CH_3CN. Cationic trimer, $(\mathbf{1}\bullet\mathbf{2}\bullet\mathbf{1})^+$ was observed in all (R = C_8H_{17} to $C_{16}H_{33}$) aromatic salts in dioxane / H_2O showing the greater interactions between Ar-ions in solvents of low dielectric which supported the findings from UV-vis ion-pairing studies.

3.4.7 Electrochemical Studies

A detailed study of electrochemical stability gained by **2** when interacting with **1**$(NR)_3$ couldn't be carried out due to a) poor solubility of the ion-pairs in the solvent (CH_3CN) used in this study and b) complex phenomena of the interactions between aromatic radicals and aromatic cations that are formed as a result of first oxidation; remember that all three different combinations (two aromatic radicals, two aromatic cations and aromatic radical-aromatic cation pair) have π-face interactions. However, we were able to gather some important information regarding the steric effects of **R** side chains to the stacking of ionic aromatics in **1**$(NR)_3$•**2**. The first oxidation potential curves for 10^{-5} M solutions of the triangulene anion**, 2** with Bu_4N^+, [**1**$(NPh)_3]^+$, and [**1**$(NMe)_3]^+$ are given in Figure 3.20. The oxidation potential of **2** with Bu_4N cation is -150 mV (Vs. Fc/Fc^+). When measurement was done in presence of equimolar solution of [**1**$(NPh)_3]^+$, the oxidation potential of **2** was shifted by 85 mV. This positive shift in oxidation potential means that **2** is more difficult to oxidize in presence of [**1**$(NPh)_3]^+$ than Bu_4N^+. Gibb's free energy change (ΔG) of the shift in potential (ΔE) is given by;

2•$Bu_4N \rightarrow$ (**2**$^{+\bullet}$)•$Bu_4N + e^-$; oxidation potential = $E_{1(ox)}$

2•**1**$(NR)_3 \rightarrow$ (**2**$^{+\bullet}$)•**1**$(NR)_3 + e^-$; oxidation potential = $E_{2(ox)}$

$\Delta E = E_{2(ox)} - E_{1(ox)}$

$\Delta G = -nF\Delta E$.

In the equation, $\Delta G = -nF\Delta E$: 'n' is number of electron involved in the electrochemical transformation (here, n = 1), 'F' is Faraday constant and ΔE is the potential shift. The above equation calculates that 85 mV shift in potential is equivalent to -1.96 kcal/mol of free energy change (ΔG). This means that [**1**$(NPh)_3]^+$ stabilizes **2** by 1.96 kcal/mol more than Bu_4N^+ does. All other measurements found the π-face interaction between **2** and [**1**$(NPh)_3]^+$ to be the weakest one due to strong steric encumbrance of three phenyl groups in the stacking plane. However, notable interaction between **2** and [**1**$(NPh)_3]^+$ observed in the electrochemical studies is indicative of strong interaction between **2** and sterically unencumbered aromatic caions, [**1**$(NMe)_3]^+$ and [**1**$(O)_3]^+$. The oxidation of **2** in presence of equimolar solution of [**1**$(NMe)_3]^+$ resulted in a broad peak (Figure 3.20) with peak potential of 10 mV (Vs. Fc/Fc^+). The broad peak

likely indicates multiple aggregation states of 1•2 involving perhaps tetrameric and trimeric anions and cations in multiple solvation states.

So, presence of $[\mathbf{1}(NMe)_3]^+$ brought a positive shift in oxidation potential of **2** by 160 mV (ΔG = -3.69 kcal/mol) making it more difficult to oxidize by 3.69 kcal/mole. The electrochemical results are preliminary and the detailed study is to follow. However, the greater shift in oxidation potential of **2** by $[\mathbf{1}(NMe)_3]^+$ than by $[\mathbf{1}(NPh)_3]^+$ suggests that the interaction of **2** is stronger with $[\mathbf{1}(NMe)_3]^+$ than with $[\mathbf{1}(NPh)_3]^+$. The result corroborates the findings from other solid- and solution-state studies.

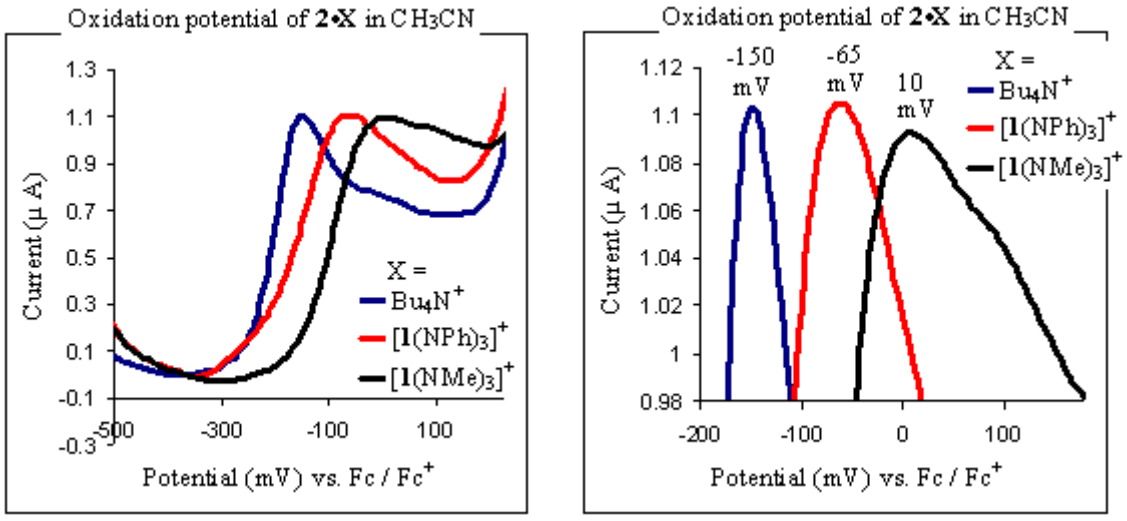

Figure 3.20. DPV Curves representing first oxidation potentials of 10^{-5}M CH_3CN solutions of **2** containing equimolar solutions of Bu_4N^+ and $[\mathbf{1}(NR)_3]^+$ scanned at the rate of 25 mV/sec. (Left): full curves and (right): magnified at the peak regions. Peak values were considered for the comparison.

3.4.8 MO Calculations

SHMO (Simple Huckel Molecular Orbital) analysis of the π-framework of aromatic cation and aromatic anion of the aromatic salts revealed the LUMO (Lowest Unoccupied Molecular Orbital) of the cation and the HOMO (Highest Occupied Molecular Orbital) of the anion to be iso-symmetric. See Figure 2.16 in chapter 2 and the

text that follow for the details on SHMO method of orbital calculations. The high compatibility between LUMO of the cation and HOMO of the anion should give optimal π-π overlap in the aromatic salts under study. The difference in interactions between cation and anion in the solid state and solution state of the aromatic salts, [**1**$(Z)_3$•**2**] was mostly due to the difference in steric effects of their side groups in the π faces. Pictorial representation of the LUMO of the parent triaza cation, **1**$(NH)_3^+$ and the HOMO of the anion estimated at "Restricted Hartree-Fock (RHF) / 3-21G", a low level of theory are shown in Figure 3.21. When placed one above another, lobes of one sign should overlap with lobes of other sign.

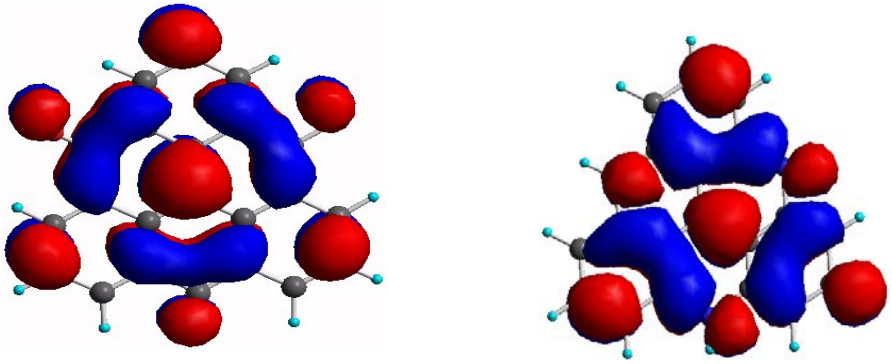

Figure 3.21. Showing lobes of HOMO of $(\mathbf{2})^-$ and LUMO of **1**$(NH)_3^+$ calculated at RHF / 3-21G.

Calculation at the same level of theory indicated that the trioxa aromatic salt, **1**$(O)_3$•**2** had more intimate association between cation and anion than the parent triaza salt, **1**$(NH)_3$•**2**; the optimum distances between aromatic ions in **1**$(O)_3$•**2** and **1**$(NH)_3$•**2** were estimated to be 3.416 Å and 3.44 Å respectively. The strong interaction between Ar-ions in **1**$(O)_3$•**2** was further supported by the observation that HOMO of this salt had some fraction of π-lobes of anion overlapped with the empty orbital of cation in a head-to-head manner (Figure 3.22). We termed this σ – type of bonding between two flat π-systems an σ-π bond and the observation is very similar to the one observed in the bonding MO of face-to-face dimer of [TCNE(•)] radical anion.[153] Such strong interactions in neutral aromatics are never observed. The level of theory used in the

calculation was low and the results should be used only to grossly compare the relative energies of the gas monomers versus the ion-pair. However, the results obtained from MO calculation were consistent with those obtained from solid and solution state methods.

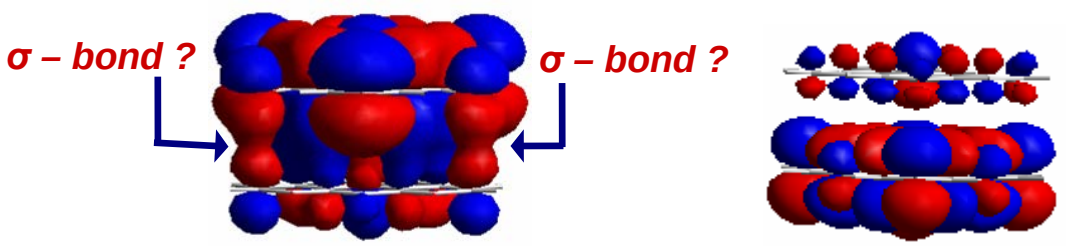

Figure 3.22. Sigma-like bonding, HOMO (left) and LUMO (right) of **1**$(O)_3$•**2** calculated at **"**RHF / 3-21G".

Despite the great attention being paid to the π-π interaction in the chemical literature, it's a weak force of interaction. [201,202] Literature indicates the spin assisted π-stacking as most effective way of observing strong π-system interaction in the solid states.[199,204] As indicated by the single crystal XRD, the distance between two π faces of the spin-assisted dimer of cationic, anionic or neutral π radical is about 3.0 Å which is very similar to the distance observed in the solid state of ion pairs with no π –face steric interactions and is much shorter (and hence stronger) than the sum of VW radii (3.4 Å) of two carbon atoms. So, the charge assisted π-stacking explored in this research seems to be as strong as the spin assisted[199,204] π-stacking in terms of the π –face distance between the two (or more) stacking partners.

However, in terms of overall interaction charge-assisted π-stacking explored in this research seems to be more effective than spin-assisted π-stacking as the former gives the polymeric arrangement of dimers in the solid state while the latter gives only dimeric arrangement of species. [199,204] The polymeric arrangement of ions as observed in the solid state studies of **1**$(Z)_3$•**2** is also supported from the calculation of electrostatic potential on the surface of **1**$(O)_3$•**2**. The calculation shows that the cation and anion have some residual charges (See Figure 3.23) in the dimer separated by 3.4 Å from each other which

allows incoming cations and anions to be attracted towards the anionic and cationic faces of the dimer respectively to give polymeric arrangement of ions.

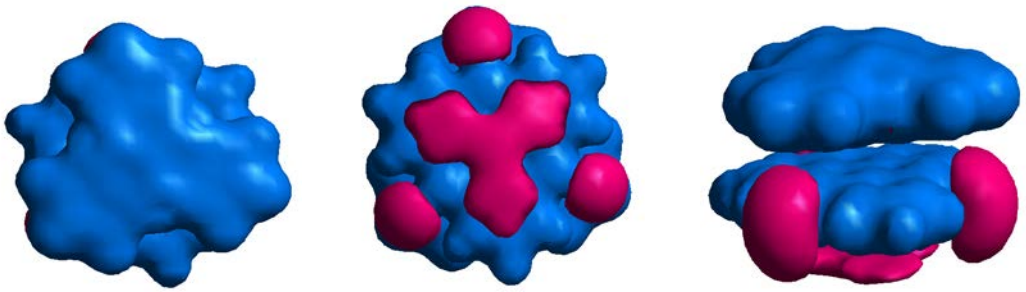

Figure 3.23. Electrostatic potential surfaces of **1**$(O)_3$•**2** calculated at RHF / 3-21G. Left: cationic face, middle: anionic face and right: side view showing both faces. Blue: electropositive surface and red: electronegative surface.

The weak π-π interaction, in general, is difficult[254] to study in the solution state because the interaction is further undermined by the intervention due to solvent molecules. However, the interaction can be studied in the π-systems where these interactions are amplified [254] by increasing total π-surface area in the planar and rigid π-framework,[254,255] incorporating electrostatic component[143] or unpaired spin in the stacking partners.[199,222] Experimental NMR studies show that the energy of π-π interaction, as indicated by the free energy change (ΔG) of the dimerization (homo or hetero) is only a few kcal / mole in $CDCl_3$.[143,254] Refer to Figure 3.24 for the molecular structures of π-systems capable of forming π face dimers in solution. This study found that the energy of ion pairing of sterically encumbered cation, [**1**$(NOct)_3$] with the anion (**2**) is −11.38 kcal / mole in the same solvent, $CHCl_3$; the value is > 3 times the one mentioned in the literature. Although the energy of ion pairing of sterically unencumbered cation, [**1**$(NMe)_3$] with the anion, (**2**) couldn't be calculated in $CDCl_3$ due to solubility issues, it was calculated to be ~ −15 kcal / mole even in the solvent (CH_3CN) of high dielectric than $CDCl_3$.

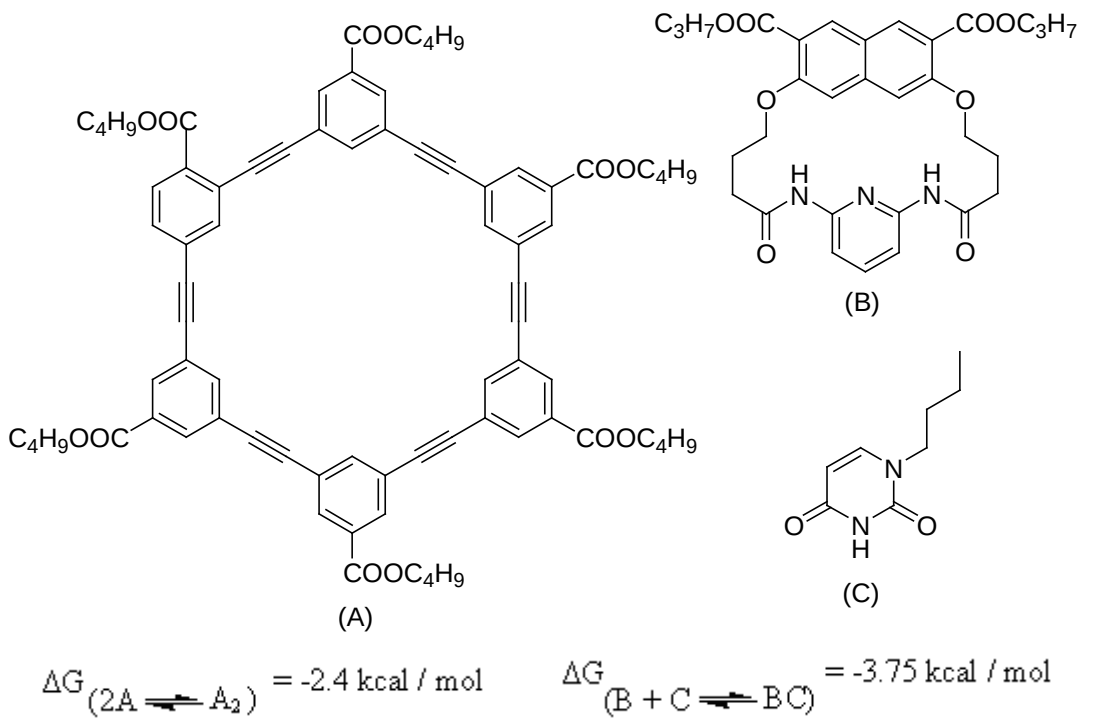

Figure 3.24. Literature examples of molecules capable of forming π-stacked dimers in $CDCl_3$.

Literature indicates that the charge-transfer complexes (donor-acceptor complexes)[223] formed between an organic donor (electron rich aromatic) and an acceptor (electron poor aromatic) is another way of designing observable π-stacked interactions in solution states.[223-228] Geometry optimized calculation (MP2/6-31*g** method) estimates high energy for these CT complex.[256] The same level of theory calculates the binding energy of CT complex between *p*-xylene (PX) and 1,2-dichloro-5,6-dicyano-*p*-benzoquinone (DDQ) to be as high as −15.47 kcal / mole[256] while experimental value for the same complex is found to be −0.15 kcal/ mole (association constant K = 1.29 M^{-1}). [256] As indicated by low binding constant, the solution state π-π interactions in CT complexes is weak. [256,257] Binding constant in these complexes can be increased by tuning electronic properties of donor or acceptor,[230,258] increasing number of binding sites,[226,230] and MO compatibility[230] of the donor and acceptor. We reason that the very high value of association constant for binding (96000 M^{-1}) [230] and corresponding binding energy (−6.79 kcal / mole) reported in the literature is due to the synergistic effects of

increased binding sites and compatibility of donor-acceptor molecular orbital to the π-stacking. Analogously, the very high value of ion-pairing association constant constant ($4.5\ E^{05}\ M^{-1}$ to $8.0\ E^{10}\ M^{-1}$) observed in our studies is attributed to synergistic effects of energy compatible MO and unit charge electrostatics to the π-stacking interactions.

The radical-assisted π stacked dimer has high stabilization energy ($\Delta H = -9.8$ kcal/mole)[199] in CH_2Cl_2 at 298 K. The high value of ΔH (change in enthalpy of monomer → dimer formation) in these dimers is attributed to existence of some covalent character which is definitely an indication of strong interaction between π-monomers. However, the association constant for the formation of these dimers from monomers is very low[199] and in some cases there is no any association between monomers even at very low temperature (183 K).[204] The exceptionally high value of association constant [$8.0E^{10}$ for **1**$(NMe)_3$•**2** in CH_3CN] in the current study suggests that the charge-assisted π-stacking in solution is much stronger than the radical-assisted π-dimerization[199,204] or any other solution-state π-stacking mentioned in the literature.[143,223-228,254,259]

3.5 Conclusions

We successfully designed, synthesized, and studied the solid- and the solution-state properties of the aromatic ion pairs, **1**$(Z)_3$•**2** having symmetry compatible MO (molecular orbital). The work presented here is towards the extreme end of electrostatic driven π-π stacking where unit – charge electrostatic was combined with π-π interaction and explored the synergy between the two in the form of aromatic ion pairs.

Crystal structure studies gave the hints that interactions in these ionic aromatics were dependent on the bulkiness of the alkyl (or aryl) side groups which interrupted the association by projecting into the stacking plane. DSC results were consistent with the crystalline state prediction of optimal synergy between ionic and π-π interactions in **1**$(NMe)_3$•**2** and **1**$(O)_3$•**2** where there is no π face steric hindrance. Although diffraction quality crystals of these ion pairs with no π face steric hindrance were not obtained, powder x-ray diffraction (PXRD) technique estimated the inter-planar distance between aromatic ions in these ion pairs to be much smaller than the others. PXRD also suggested the inter-planar distance in **1**$(O)_3$•**2** to be smaller than in **1**$(NMe)_3$•**2** which was supported by MO calculation that the HOMO of **1**$(O)_3$•**2** showed a fraction of σ – type of bonding

between two flat (no ring deformation) aromatics but no such observation was made in the HOMO of **1**$(NMe)_3$•**2**.

Corroborating the findings from the solid state studies and the MO calculations, the solution-state analysis also showed a steric dependent association between oppositely charged aromatics. While the energy of association between Ar-ions linearly increased with the decrease in the size of substituents, the big shift / difference observed between the ***methyl*** [ion-pairing energy = 14.96 kcal/mol] vs. ***ethyl*** [ion-pairing energy = 10.06 kcal/mol] substituted ion pairs was due to the optimal synergy between ionic and π-π interactions in **1**$(NMe)_3$•**2** even in the solution state. The steric effects of ***methyl*** vs. ***ethyl*** groups are not very dramatic in the quantitative organic chemistry such as the A-values in cyclohexanes,[197] and of Taft steric parameters (E_s).[198] The big shift observed in the current study was due to angurality of ***ethyl*** vs. non-angularity of ***methyl*** groups (Figure 3.25) that block / unblock the path of stacking Ar-ions to come to close proximity. The strong synergy of electrostatic with π-π interactions in the ion pairs with no π face steric hindrance was further clarified by the near IR absorbance of these ion pairs and also supported by relatively very high abundance / stability of trimeric peaks, $(\mathbf{1•2•1})^+$ and $(\mathbf{2•1•2})^-$ observed in ESI-MS of these ion pairs.

It is obvious that the interaction between aromatic ions (**1** and **2**) of salts (**1•2**) with *Et* or longer side chains is frustrated (not optimal) because of the angularity of the side chains in the π faces. Although there are no π face steric effect in the salts with *Me* or *O*-substitution, the interaction between aromatic ions is still frustrated (not optimal) probably because of electronic repulsion between two large aromatic discs at very close distances.

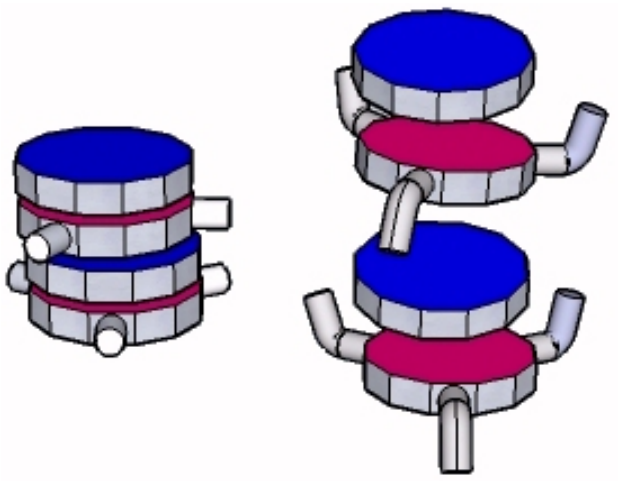

Figure 3.25. Cartoon showing difference in the steric effects of *methyl* (left) vs. *ethyl* (right) side groups. Non-angular *methyl* groups allow close association between aromatic discs to optimize synergy between ionic and π-π interactions but angular *ethyl* and longer chains don't. Red and blue rings represent the aromatic cation **1** and anion **2** respectively.

The attractions due to unit-charge electrostatics (ionic interaction) and the π-π interaction are the strongest and the weakest among all non-covalent interactions. The work presented in this research clearly investigated the novel method of designing aromatics with a strong synergy between ionic and π-π interactions situated at two extreme ends of the non-covalent interaction. Literature shows that radical π faces of the cationic, anionic or neutral π radical can form stable π dimers[199,204] in the solid states. Analogously, our study shows that similar complexes can be formed by oppositely charged, triangulene based aromatics. While, these spin-assisted dimers[199,204] are separated from each other by ≈ 10 Å,[199] the distance between any two adjacent dimers in our studies is found within Van der Walls' distance (3.4 Å) indicating the superiority of charge-assisted π-stacking explored in this research over the spin assisted π-stacking. [199,204]

Literature reports the donor-acceptor based CT complexes[223-228,230,258] as an effective way designing strong π-stacked interactions in the solution states and energy / symmetry compatible MO[230] as the synergistic factor to the π-stacking. Our investigation proves that aromatic ion pairs, where synergy of MO compatibility to the π-stacking

interactions is amplified by unit-charge electrostatic in the stacking partners, is the most effective way of designing strong π-system interactions in the solution states as indicated by exceptionally high value of ion-pairing association constant.

3.6 Future Studies

Solid-state studies of the aromatic cations with small, non-aromatic counter anions (as discussed in the chapter 2) indicated that stacking in aromatic cations depends on reduction potential such that the cations with low reduction potential have overall better stacking than the ones with high reduction potential. General applicability of this reduction potential based aromatic stacking needs to be studied in details with varieties of iso-structural aromatic cations. One way could be by introducing different electron donating and electron withdrawing groups in the aromatic cations studied in the present work. Substitution should change electronic nature of the aromatic cations and hence reduction potential should also change. Whether solid-state stacking changes with the change in reduction potential could be studied.

The chapter 2 also explored the better facial cohesiveness of the aromatic cations over the iso-structural anions when individual aromatic ions were crystallized in presence of a non-aromatic counter anion. Single crystal XRD of **1**$(NMe)_3$•X (X = NCO^- and PF_6^-) was also evident of better FF-stacking in the aromatic cation when counter ion was smaller and planar. The counter ions for aromatic cations studied in the present work, however, were much smaller than the ones for aromatic anions. Our efforts of crystallizing the aromatic anions with small counter ions were unproductive. This should be followed up to explore the effects of size / shape of counter ions in the stacking of aromatic anions experimentally while keeping in mind that the logic presented in this work and the calculations don't support FF-stacking in the aromatic anions.

Chapter 3 was very clear evident of optimum overlap between aromatic cation and aromatic anion in the aromatic ion-pairs [**1**$(Z)_3$•**2**] when there were no steric encumbrances of side chains in the stacking plane. For this reason, ion-pairs with Z = *N*Me and *O* (oxygen) seemed to have much better overlap (later being superior) between aromatic ions than the ones with Z = *N*Et and longer alkyl chains. However, diffractable quality single crystals of these ion-pairs (Z=*N*Me and *O*) couldn't be grown due to

solubility problems associated with these ion-pairs. To overcome this solubility problem of the optimally overlapped ion-pairs, we propose the general structure of aromatic cations (Figure 3.26) that should be synthesized and co-crystallized with the aromatic anion, **2**. Introduction of long, alkyl chains should increase solubility without projecting into the stacking plane as they are away from the central aromatic core being separated by planar alkynyl groups. The alkynyl groups also increase the total π-surface area in the aromatic cation which creates enough room for the aromatic anion allowing the anion to come to the close proximity of the aromatic cation.

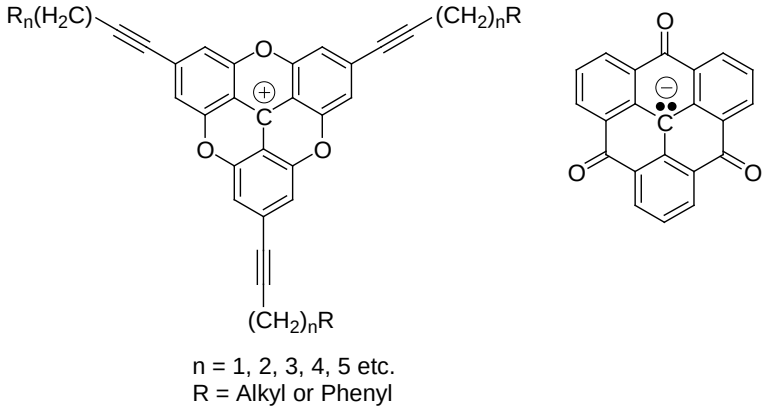

Figure 3.26. General structure of the aromatic cation (left) which is proposed to be synthesized and co-crystallized with the aromatic anion (right).

The *N*-substituted aromatic ion-pairs, [**1**$(NR)_3$•**2**] with R ≥ *n*-$C_{10}H_{21}$ showed LC (liquid crystalline) transition[176,177] as indicated by the DSC curves where distinct reversible curves were obtained before melting curves. Although LC (Liquid crystal) properties of these ion-pairs were poorly studied and hence not discussed in the main contents of this dissertation, such LC transitions indicated by the DSC curves were confirmed by examining the crystals of these ion-pairs under hot Polarized Optical Microscope (POM). DSC curves of these ion-pairs that show LC transitions are shown in figure 3.27. Structural features of these ion-pairs put themselves in the family of discotic liquid crystals[176,177] although exact nature of these LC remained unexplored. Such discotic liquid crystals where there is alternate stack of aromatic cations and aromatic

anions have never been reported to the literature of liquid crystals. These novel LCs and their possible applications should be explored systematically.

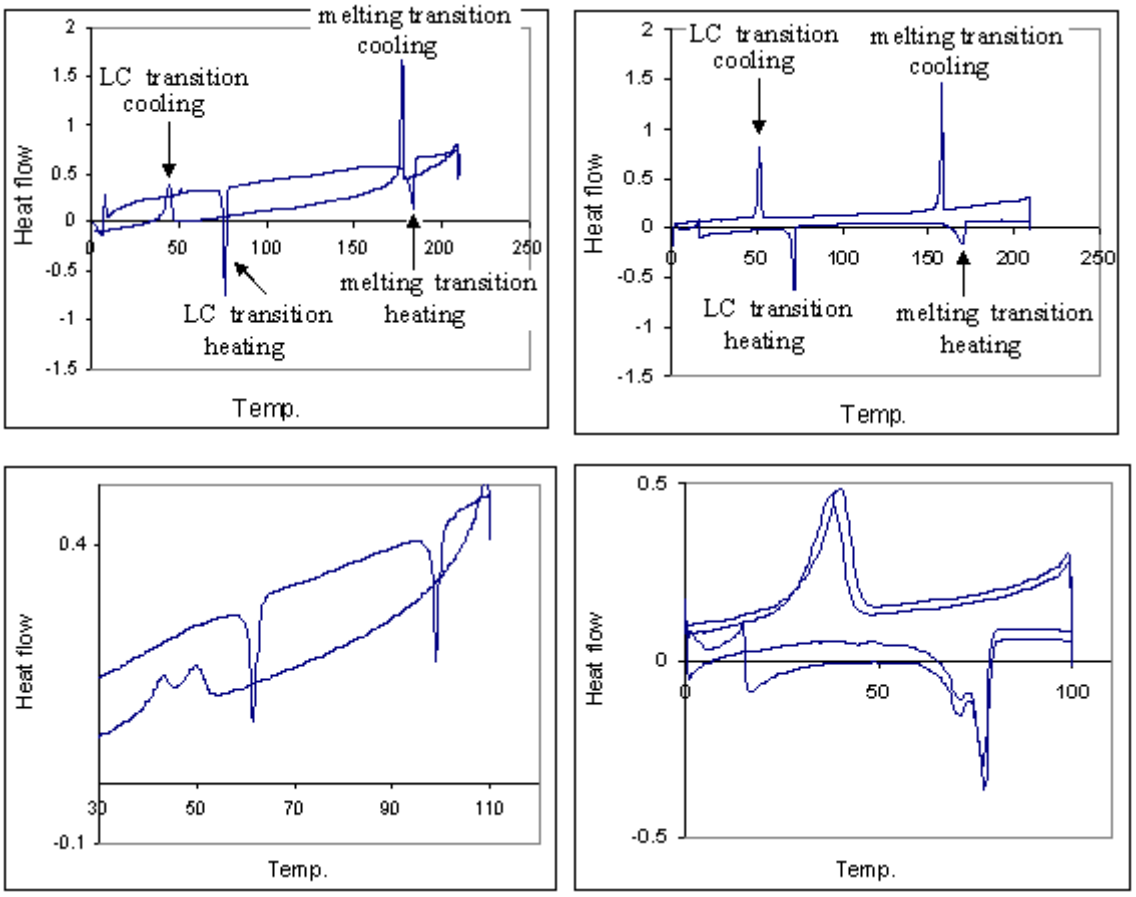

Figure 3.27. DSC curves of ion-pairs, [**1**$(NR)_3$•**2**] capable of forming liquid crystalline phase. Top left: R = *n*-$C_{10}H_{21}$, top right: R = *n*-$C_{12}H_{25}$, bottom left: R = *n*-$C_{14}H_{29}$ and bottom right: R = *n*-$C_{16}H_{33}$. Top: showing both melting and LC transitions. Bottom: showing only LC transitions.

3.7 Experimental

3.7.1 Instruments / Techniques

Nuclear magnetic Resonance (NMR): Varian INOVA 400 MHz spectrometer was used to record ^{1}H and ^{13}C NMR spectra. The NMR spectrometer was purchased under the CRIF program of the NSF, grant CHE-9974810.

Differential Scanning Calorimetry (DSC): DSC 822 ^{e} (Mettler) was used to study the melting / decomposition transitions of the ion pairs under study. Melting points were reported as the endothermic maxima of first order transitions as detected by DSC. The samples were heated at the rate of 2-5 ^{o}C / min under N_2.

UV-Vis spectroscopy: All UV-Vis-NIR data including those for ion pairing and stoichiometry studies of the association between the aromatic cation (C) and the aromatic anion (A) were made using either an Agilent Technologies 8453 spectrophotometer or Varian Cary 1 UV-Vis spectrometer.

Differential Pulse Voltametry (DPV): All electrochemical measurements were carried out using DPV techniques with a BAS 100B/W voltammeter. Electrolyte and solvent used were 0.1M tetra-*n*-butylammonium hexafluorophosphate and CH_3CN respectively. A platinum rod, a platinum wire and a silver wire were employed as the working electrode, the counter electrode and the reference electrode respectively. Fc / Fc^{+} was used as an internal reference for all measurements.

Single Crystal analysis: Unless otherwise noted, X-ray diffraction data were collected at 90.0 K on either a Nonius kappa CCD diffractometer or a Bruker-Nonius X8 Proteum diffractometer with graded-multilayer focusing optics.[260] Raw data were integrated, scaled, merged and corrected for Lorentz-polarization effects using either the HKL-SMN package[261] or the APEX2 package.[260] Structures were solved by direct methods (SHELXL97)[262] and refined by against F^2 by weighted full-matrix least-squares (SHELXL97).[262] Where possible, hydrogen atoms were found in difference maps but subsequently placed at calculated positions and refined using appropriate riding models. Non-hydrogen atoms were refined with anisotropic displacement parameters. Atomic scattering factors were taken from the International Tables for Crystallography (vol.C).[263]

Powder x-Ray Diffraction (PXRD): Powder diffraction data were collected by using a Multiflex (Rigaku) diffractrometer. Cu Kα radiation was used to scan the samples in the 2θ range of 2° – 40° with scan rate of 2° 2θ min^{-1}.

Mass Spectrometry (MS): Mass specra were acquired by the University of Kentucky Mass Spectrometry Facility (UKMSF). Elecrospray ionization (ESI) mass spectra were obtained on a ThermoFinnigan LCQ. Samples were diluted in CH_3CN / H_2O and introduced into the ESI source of the LCQ via syringe pump at 3 μL / min.

Molecular Orbital (MO) Calculations: Levels of calculation higher than Extended Huckle were run with Gaussian 03 at the University of Kentucky Center for Computational Sciences.

3.7.2 Synthesis

General Procedure: BF_4^- or PF_6^- salt solution of the aromatic cation $[\mathbf{1}(Z)_3]^+$ was mixed with the solution of aromatic anion $\mathbf{2}\bullet Bu_4N^+$ in more soluble organic solvents. In most of the cases, solid precipitate resulted which was filtered, washed and recrystallized. Detail of synthesis of individual cation is described below.

4,8,12-trimethyl-4,8,12-triazatriangulenium trioxytriangulenate [1(NMe)$_3$•2]

Acetonitrile (MeCN) solutions of 4,8,12-trimethyl-4,8,12-triazatriangulenium hexafluorophosphate, $\mathbf{1}(NMe)_3\bullet PF_6^-$ (75 mg, 0.16 mmol) in 15 mL and tertrabutylammonium trioxytriangulenate, $\mathbf{2}\bullet Bu_4N^+$ (61 mg, 0.10 mmol) in 15 mL were mixed. The dark ppt. immediately obtained was washed with MeCN (10 mL), EtOH (10 mL), chloroform (10 mL) and Et_2O (10 mL) and the precipitate put under vacuum, 53 mg (92.5 %). The compound had very little solubility in common organic solvents, but had moderate solubility in hot DMSO and good solubility in *N*,*N*-dimethylacetoacetamide. Recrystallization from different solvents (hot DMSO, hot DMF, hot aniline and *N*,*N*-dimethylacetoacetamide) failed to give diffraction quality material. Decomposed at 453 °C (DSC, 10 °C / min) before melting; ATR-IR (ν_{max}/cm^{-1}): 1609 (C=N), 1593 (C=O) 1577 and 1550 (Ar C=C); MS (ESI): *m*/*z* 321 [Anion], 324 [Cation], 969 [Cation-anion-cation]; ^{1}H NMR (400 MHz, D_6-DMSO, 80 °C): δ 8.72 (d, J = 7.6 Hz, 6H), 8.07 (t, J = 8.4 Hz, 3H), 7.46 (t, J = 7.6 Hz, 3H), 7.43 (d, J = 8.4 Hz, 6H), 3.90 (s, 9H). ^{13}C NMR

could not be collected due to its poor solubility in NMR solvents. Elemental analysis calculated (%) for $C_{44}H_{27}N_3O_3.0.5H_2O$: C 80.71, H 4.31, N 6.41; found C 80.43, H 4.39, N 6.39.

4,8,12-triethyl-4,8,12-triazatriangulenium trioxytriangulenate [1(NEt)$_3$•2]

Solution of 65 mg (0.14 mmol) of 4,8,12-triethyl-4,8,12-triazatriangulenium tetrafluoroborate, **1**(NEt)$_3$•BF_4^- in 15 mL of acetonitrile was added to solution of 60 mg (0.1 mmol) of tetrabutylammonium trioxytriangulenate, **2**•Bu_4N^+ in 15 mL of acetonitrile. Reaction mixture was stirred for 10 minutes at room temperature and volume reduced to 10 mL. Solid thus obtained was washed with acetonitrile (2mL X 5) and dried to get 62 mg (84.6 %) of the title compound which melted at 393 °C (DSC, 10 °C / min) followed by decomposition. ATR-IR (ν_{max}/cm^{-1}): 2974 (SP^2 C-H), 2932 (SP^3 C-H), 1609 (C=N), 1593 (C=O), 1552 (Ar C=C); MS (ESI): *m*/*z* 321 [Anion], 366 [Cation], 1053 [Cation-anion-cation]; ^{1}H NMR (400 MHz, D_6-DMSO): δ 8.63 (d, J = 7.2, 6H), 7.96 (t, J = 8.4, 3H), 7.41 (t, J = 7.2, 3H), 7.29 (d, J = 8.4, 6H), 4.38 (q, J = 6.8, 6H), 1.36 (t, J = 6.8, 9H); ^{13}C NMR (400 MHz, D_6-DMSO): δ 180.167, 139.395, 139.275, 137.292, 131.968, 131.929, 126.593, 119.979, 109.702, 104.599, 93.903, 42.224, 10.119.

4,8,12-tripropyl-4,8,12-triazatriangulenium trioxytriangulenate [1(NPr)$_3$•2]

MeCN (15 mL) solutions of 4,8,12-tripropyl-4,8,12-triazatriangulenium tetrafluoroborate, **1**(NPr)$_3$•BF_4^- (77 mg, 0.15 mmol) and tetrabutylammonium trioxytriangulenate, **2**•Bu_4N^+ (61 mg, 0.09 mmol) were mixed. The dark ppt. thus obtained was washed with acetone (5 x 10 mL), 57.6 mg (89 %). Small amount of this compound was recrystallized from its saturated solution in hot DMSO. X-ray diffraction of the crystal thus obtained confirmed connectivity. Material melted at 350 °C (DSC, 10 °C/min) followed by decomposition. ATR-IR (ν_{max}/cm^{-1}): 2934 and 2871 (SP^3 C-H), 1611 (C=N), 1592 (C=O), 1551 (Ar C=C); MS (ESI): *m*/*z* 321 [Anion], 408 [Cation], 1137 [Cation-anion-cation]; ^{1}H NMR (400 MHz, D_6-DMSO): δ 8.69 (d, J = 7.6, 6H), 8.01 (t, J = 8.4, 3H), 7.46 (t, J = 7.6, 3H), 7.36 (d, J = 8.4, 6H), 4.33 (t, J = 8.0, 6H), 1.81 (m, 6H), 1.12 (t, J = 7.4, 9H); ^{13}C NMR (100 MHz, D_6-DMSO): δ 180.063, 139.644,

139.328, 137.022, 131.938, 131.585, 126.559, 119.516, 109.604, 104.688, 90.384, 48.190, 17.735, 10.262.

4,8,12-tributyl-4,8,12-triazatriangulenium trioxytriangulenate [1(NBu)$_3$•2]

MeCN (15 mL) solutions of 4,8,12-tributyl-4,8,12-triazatriangulenium tetrafluoroborate, **1**(NBu)$_3$•BF_4^-, (45 mg, 0.083 mmol) and trioxytriangulene anion, **2**•Bu_4N^+ (37 mg, 0.065 mmol) were mixed in a 50 mL RB flask. No visible ppt. was obtained. Solvent was evaporated completely and the solid thus obtained was washed with diethyl ether (1mL X 5) and cold acetonitrile (0.5mL X 5). The dried purple solid weighed 47.4 mg (93.5%) which melted at 341 °C (DSC, 10 °C/min) followed by decomposition. ATR-IR (ν_{max}/cm^{-1}): 2954, 2930, 2870 (SP^3 C-H), 1607 (C=N), 1593 (C=O), 1552 (Ar C=C); MS (ESI): *m*/*z* 321 [Anion], 450 [Cation], 1092 [Anion-cation-anion] 1221 [Cation-anion-cation]; ^{1}H NMR (400 MHz, D_6-DMSO): δ 8.62 (d, J = 7.2 Hz, 6H), 7.93 (t, J = 8.4, 3H), 7.40 (t, J = 7.2 Hz, 3H), 7.20 (d, J = 8.4, 6H), 4.24 (t, J = 7.2, 6H), 1.71 (m, 6H), 1.56 (m, 6H), 1.01 (t, J = 7.2 Hz, 9H); ^{13}C NMR (100 MHz, D_6-DMSO): δ 179.954, 139.434, 139.015, 136.902, 131.829, 131.476, 126.473, 119.430, 109.475, 104.462, 90.338, 46.660, 26.280, 18.927, 13.224.

4,8,12-trioctyl-4,8,12-triazatriangulenium trioxytriangulenate [1(NOct)$_3$•2]

MeCN (15 mL) solutions of 4,8,12-trioctyl-4,8,12-triazatriangulenium tetrafluoroborate, **1**(NOct)$_3$•BF_4^- (30.04 mg, 0.043 mmol) and trioxytriangulene anion, **2**•Bu_4N^+ (20 mg, 0.036 mmol) were mixed in a 50 mL RB flask. The resultant mixture was agitated for 10 minutes at an ambient temperature and solvent was evaporated at reduced pressure. Solid thus obtained was washed with cold acetonitrile (1mL X 10). The dried brown-purple solid weighed 29.0 mg (87 %) which melted at 200 °C (DSC, 5 °C/min). ATR-IR (ν_{max}/cm^{-1}): 2927, 2856 (SP^3 C-H), 1612 (C=N), 1604 (C=O), 1555 (Ar C=C); MS (ESI): *m*/*z* 321 [anion], 618 [cation], 1557 [cation-anion-cation]; ^{1}H NMR (400 MHz, D_6-DMSO): δ 8.59 (d, J = 7.6 Hz, 6H), 7.91 (t, J = 8.4, 3H), 7.38 (t, J = 7.6 Hz, 3H), 7.17 (d, J = 8.4, 6H), 4.21 (t, 6H), 1.72 (m, 6H), 1.53-1.29 (m, 30H), 0.88 (t, J = 6.4 Hz, 9H). A small amount of the title compound was dissolved in hot DMSO. Slow cooling of the hot solution to an ambient temperature gave diffractable quality crystals

which upon analyzing with x-ray confirmed atomic connectivity and presence of Ar-cations and Ar-anions in the solid state.

4,8,12-tridecyl-4,8,12-triazatriangulenium trioxytriangulenate [1(NDec)$_3$•2]

A solution of 4,8,12-tridecyl-4,8,12-triazatriangulenium tetrafluoroborate, **1**(NDec)$_3$•BF_4^- (59.0 mg, 0.075 mmol) in hot MeCN (15 mL) was mixed with a solution of tetrabutylammonium trioxytriangulenate, **2**•Bu_4N^+ (32 mg, 0.057 mmol) in MeCN (20 mL) in a 50 mL RB flask. The resultant mixture was agitated for 10 minutes at an ambient temperature and solvent was evaporated at reduced pressure. Solid thus obtained was washed with distilled H_2O (1 mL X 5) and then cold acetonitrile (1mL X 10). The dried solid was then mixed with warm diethyl ether (100 mL) and filtered. The red solid on the filter paper was washed with diethyl ether until the colorless filtrate was obtained. The volume of the filtrate was reduced to ~ 5 mL under reduced pressure and excess hexane was added to undergo complete precipitation. The dried dark-purple solid weighed 52.0 mg (89.4 %) which melted at 177.16 °C (DSC, 5 °C/min). ATR-IR (ν_{max}/cm^{-1}): 2926, 2855 (SP^3 C-H), 1614 (C=N), 1606 (C=O), 1555 (Ar C=C); MS (ESI): *m*/*z* 321 [anion], 702 [cation], 1725 [cation-anion-cation]; ^{1}H NMR (400 MHz, D_6-DMSO): δ 8.55 (d, J = 7.2 Hz, 6H), 7.84 (t, J = 8.4, 3H), 7.32 (br, 3H), 7.06 (d, J = 8.4, 6H), 4.12 (t, J = 7.2 Hz, 6H), 1.71 (m, 6H), 1.56-1.24 (m, 42 H), 0.86 (t, 9H, J = 6.4Hz); ^{13}C NMR (100 MHz, D_6-DMSO, 70 °C): δ 180.056, 139.585, 139.237, 137.031, 131.943, 131.579, 126.562, 119.496, 109.614, 104.609, 90.381, 46.853, 30.848, 28.545, 28.457, 28.355, 28.215, 25.563, 24.282, 21.603, 13.419. A small amount of the title compound was dissolved in hot NMP (N-methyl pyrrolidinone). Slow cooling of the hot solution to an ambient temperature gave diffractable quality crystals which upon analyzing with x-ray confirmed atomic connectivity and presence of Ar-cations and Ar-anions in the solid state.

4,8,12-tridodecyl-4,8,12-triazatriangulenium trioxytriangulenate [1(NDodec)$_3$•2]

A solution of 4,8,12-tridodecyl-4,8,12-triazatriangulenium tetrafluoroborate, **1**(NDodec)$_3$•BF_4^- (56.5 mg, 0.065 mmol) in hot MeCN (15 mL) was mixed with a solution of tetrabutylammonium trioxytriangulenate, **2**•Bu_4N^+ (25 mg, 0.044 mmol) in

MeCN (25 mL) in a 50 mL RB flask. The resultant mixture was agitated for 10 minutes at an ambient temperature and solvent was evaporated at reduced pressure. Solid thus obtained was washed with distilled H_2O (1 mL X 5) and then cold acetonitrile (1mL X 10). The dried solid was then mixed with warm diethyl ether (100 mL) and filtered. The red solid on the filter paper was washed with diethyl ether until the colorless filtrate was obtained. The volume of the filtrate was reduced to ~ 5 mL under reduced pressure and excess hexane was added to undergo complete precipitation. The dried dark-purple solid weighed 52.0 mg (89.4 %) which melted at 177.16 °C (DSC, 5 °C/min). ATR-IR (ν_{max}/cm^{-1}): 2926, 2855 (SP^3 C-H), 1614 (C=N), 1606 (C=O), 1555 (Ar C=C); MS (ESI): *m*/*z* 321 [anion], 870 [cation], 2061 [cation-anion-cation]; ^{1}H NMR (400 MHz, D_6-DMSO, 80 ºC): δ 8.61 (d, *J* = 7.6 Hz, 6H), 7.92 (t, *J* = 8.4, 3H), 7.36 (t, *J* = 7.6, 3H), 7.18 (d, *J* = 8.4, 6H), 4.24 (t, *J* = 7.6 Hz, 6H), 1.77 (m, 6H), 1.53 (m, 6H), 1.42-1.26 (m, 48 H), 0.86 (t, 9H, J = 6.4 Hz). A small amount of the title compound was dissolved in hot NMP (N-methyl pyrrolidinone). Slow cooling of the hot solution to an ambient temperature gave diffractable quality crystals which upon analyzing with x-ray confirmed atomic connectivity and presence of Ar-cations and Ar-anions in the solid state.

4,8,12-tritetradecyl-4,8,12-triazatriangulenium trioxytriangulenate [1(NTetradec)$_3$•2]

A solution of 4,8,12-tritetradecyl-4,8,12-triazatriangulenium tetrafluoroborate, **1**(NTetradec)$_3$•BF_4^- (55.9 mg, 0.059 mmol) in the 1:1 mixture of MeCN and DCM (20 mL) was added to the solution of tetrabutylammonium trioxytriangulenate, **2**•Bu_4N^+ (27 mg, 0.048 mmol) in MeCN (15 mL) in a 50 mL RB flask. A dark purple brown precipitate was obtained immediately. Solvent was completely evaporated at reduced pressure followed by addition of MeCN (0.5 mL) and diethyl ether (50 mL). The resultant mixture was filtered and the red solid left on the filter paper was washed with diethyl ether (2 mL X 5) until the colorless filtrate was obtained. Solvent was evaporated at the reduced pressure and the dried solid was washed with MeCN several times (1 mL X 10) before it was vacuum dried to get purple brown solid (50 mg, 87.7 %) of the title compound which melted at 162.75 °C (DSC, 5 °C/min). ATR-IR (ν_{max}/cm^{-1}): 2923, 2852 (SP^3 C-H), 1614 (C=N), 1604 (C=O), 1556 (Ar C=C); MS (ESI): *m*/*z* 321 [anion], 870

[cation], 2061 [cation-anion-cation]; ^{1}H NMR (400 MHz, D_6-DMSO, 80 ºC): δ 8.61 (d, *J* = 7.6 Hz, 6H), 7.92 (t, *J* = 8.4, 3H), 7.36 (t, *J* = 7.6, 3H), 7.17 (d, *J* = 8.4, 6H), 4.24 (t, *J* = 7.6 Hz, 6H), 1.77 (m, 6H), 1.53 (m, 6H), 1.41-1.25 (m, 60 H), 0.86 (t, 9H, J = 6.4 Hz). Re-crystallization from several solvent systems failed to give diffracttion quality crystals.

4,8,12-trihexadecyl-4,8,12-triazatriangulenium trioxytriangulenate [1(NHexadec)$_3$•2]

A solution of 4,8,12-trihexadecyl-4,8,12-triazatriangulenium tetrafluoroborate, **1**(NHexadec)$_3$•BF_4^- (51.22 mg, 0.049 mmol) in DCM (20 mL) was added to the solution of tetrabutylammonium trioxytriangulenate, **2**•Bu_4N^+ (25 mg, 0.044 mmol) in MeCN (30 mL) in a 100 mL RB flask. A dark purple brown precipitate was obtained immediately. Solvent was completely evaporated at reduced pressure followed by addition of diethyl ether (20 mL) and the mixture was filtered. The red solid left on the filter paper was washed with warm diethyl ether (2 mL X 5) until the colorless filtrate was obtained. Solvent was evaporated at the reduced pressure and the dried solid was washed with MeCN several times (1 mL X 5) before it was vacuum dried to get purple brown solid (48.8 mg, 86.22 %) of the title compound which melted at 162.99 °C (DSC, 5 °C/min). ATR-IR (ν_{max}/cm^{-1}): 2923, 2852 (SP^3 C-H), 1614 (C=N), 1604 (C=O), 1556 (Ar C=C); MS (ESI): *m*/*z* 321 [anion], 954 [cation], 2229 [cation-anion-cation]; ^{1}H NMR (400 MHz, D_6-DMSO, 80 ºC): δ 8.67 (d, *J* = 7.6 Hz, 6H), 7.99 (t, *J* = 8.4, 3H), 7.41 (t, *J* = 7.6, 3H), 7.28 (d, *J* = 8.4, 6H), 4.34 (t, *J* = 7.6 Hz, 6H), 1.81 (m, 6H), 1.55 (m, 6H), 1.44-1.24 (m, 72 H), 0.85 (t, 9H, J = 6.4 Hz). Re-crystallization from several solvent systems failed to give diffractable quality crystals.

4,8,12-triphenyl-4,8,12-triazatriangulenium trioxytriangulenate [1(NPh)$_3$•2]

MeCN solutions 2 mL each of 4,8,12-triphenyl-4,8,12-triazatriangulenium tetrafluoroborate, **1**(NPh)$_3$•BF_4^- (19.9 mg, 0.033 mmol) and tetrabutylammonium trioxytriangulenate, **2**•Bu_4N^+ (18.76 mg, 0.033 mmol) were mixed. The dark brown precipitate was filtered and washed with 3 x 1 mL MeCN, dried and recrystallized by slow cooling in DMSO/ CH_3CN (1:1), (22 mg, 79.4%) needles were obtained which upon examined by X-Ray diffraction confirmed atomic connectivity. Compound melted

at 432 °C (DSC, 10 °C/min) followed by decomposition. ATR-IR (ν_{max}/cm^{-1}): 3035 (SP^2 C-H), 1606 (C=N), 1593 (C=O), 1551 and 1526 (Ar C=C); MS (ESI): *m*/*z* 321 [Anion], 510 [Cation]; ^{1}HNMR (400 MHz, D_6-DMSO): δ 8.71 (d, *J* = 7.6 Hz, 6H), 7.88 (t, *J* = 7.6 Hz, 6H), 7.79 (t, *J* = 7.6 Hz, 3H), 7.70 (t, *J* = 8.4 Hz, 3H), 7.59 (d, *J* = 7.6 Hz, 6H), 7.46 (t, *J* = 7.6 Hz, 3H), 6.26 (d, *J* = 8.4 Hz, 6H); ^{13}CNMR (DMSO, 100 MHz): δ 180.482, 141.470, 141.460, 137.596, 137.481, 132.290, 132.275, 132.256, 130.600, 128.500, 126.863, 120.235, 109.630, 106.633, 90.853.

4,8,12-trioxatriangulenium trioxytriangulenate [1(O)$_3$•2]

Mixing two 15 mL MeCN solutions of 4,8,12-trioxatriangulenium tetrafluoroborate, **1**(O)$_3$•BF_4^- (40 mg, 0.1 mmol) and tetrabutylammonium trioxytriangulenate, **2**•Bu_4N^+ (46 mg, 0.08 mmol) gave a dark blue precipitate. After washing with MeCN, MeOH and CH_2Cl_2, the title compound was obtained (48.5 mg, 98%) which decomposed at 388 °C (DSC, 10 °C/min) before melting. The material had very little solubility in common organic solvents, sparing solubility in hot DMSO, but good solubility in N,N-dimethylacetoacetamide and fluorinated alcohols like 2,2,2-trifluoroethanol. ATR-IR (ν_{max}/cm^{-1}): 3080 (SP^2 C-H), 1627 (C=O$^+$), 1597 (Anion C=O), 1557 (Ar C=C); MS (ESI): *m*/*z* 285 [Cation], 321 [Anion], 891 [Cation-anion-cation]; ^{1}HNMR (400 MHz, D_6-DMSO, 80 °C): δ 8.74 (d, *J* = 7.6 Hz, 6H), 7.50 (t, *J* = 7.6 Hz, 3H), 7.46 (t, *J* = 8.4 Hz, 3H), 7.14 (d, *J* = 8.4 Hz, 3H). ^{13}C NMR data couldn't be collected for this compound due to its very low solubility in NMR solvents.

4,8,12-tributyl-4,8,12-triazatriangulenium tetrafluoroborate [1(NBu)$_3$•BF_4^-]

A mixture of 0.5 g (0.98 mmol) of tris-(2,6-dimethoxyphenyl) carbenium tetrafluoroborate[188] and an excess *n*-Butylamine (5 mL) were taken up in 20 mL of NMP (N-methylpyrollidinone). The reaction flask was fitted with a H_2O- condenser and the flask was heated (160^{o}C-170^{o}C) for 26 h. under nitrogen. To prevent loss from evaporation, *n*-Butylamine (0.2 mL X 3) was further added during the course of the reaction and the mixture was stirred with a magnetic stirrer throughout. Cold water (100 mL) was added to the reaction mixture at 25 °C and the precipitate formed was washed with water. The crude product was dried, washed with diethyl ether (5 mL X 20) and re-

dissolved in minimum amount of hot acetonitrile. Slow evaporation of MeCN gave dark-red crystal of the title compound (0.263 g, 50 %). MS (ESI) *m/z 408* $[M\text{-}BF_4]^+$; ^{1}H NMR (400 MHz, D_6-DMSO): δ 8.02 (t, *J* = 8.8 Hz, 3H), 7.29 (d, *J* = 8.8 Hz, 6H), 4.26 (q, *J* = 7.2 Hz, 6H), 1.7 (m, 6H), 1.56 (m, 6H), 1.0 (t, *J* = 7.2 Hz, 9H); ^{13}C NMR (100 MHz, D_6-DMSO): δ 139.744, 139.555, 137.676, 109.758, 105.030, 46.770, 26.582, 19.246, 13.760.

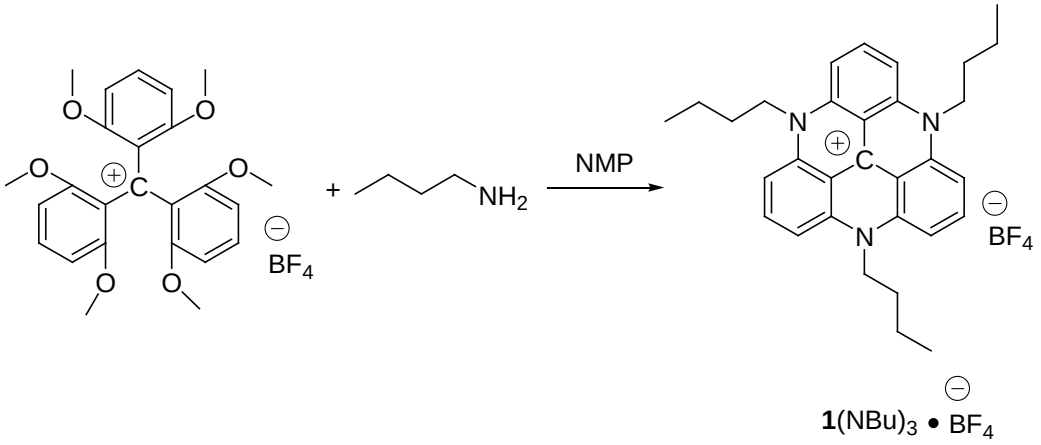

Figure 3.28. Synthesis of **1**$(NBu)_3$•BF_4^-

4,8,12-tri-*n*-tetradecyl-4,8,12-triazatriangulenium tetrafluoroborate [1(NTetradec)$_3$•BF_4^-]

A mixture of tris-(2,6-dimethoxyphenyl) carbenium tetrafluoroborate[188] (0.50 g, 0.98 mmol) and *n*-tetradecylamine (2.9 g, 13.61 mmol) in 20 mL NMP (N-methylpyrollidinone) was taken up in a 50 mL RB flask. The reaction flask was fitted with a water-condenser and heated (160^{o}C-170^{o}C) for 48 h. under nitrogen. Cold diethyl ether (100 mL) was added to the reaction mixture at 25 °C and the precipitate formed was washed thoroughly with diethyl ether (10 mL X 10). Dichloromethane (50 mL) was added to the solid left on the filter paper and the mixture was filtered. Solvent was evaporated from the filtrate under reduced pressure and the dried solid was subjected to column chromatography (SiO_2, chloroform) to get the title compound (250 mg, 26.65 %) as a dark-red solid. MS (ESI) *m/z 870* $[M\text{-}BF_4]^+$; ATR-IR (ν_{max}/cm^{-1}): 2920, 2851 (sp^3 C-H), 1610.7 (C=N), 1535 (C=C); ^{1}H NMR (400 MHz, $CDCl_3$): δ 8.03 (t, *J* = 8.4 Hz, 3H), 7.12 (d, *J* = 8.4 Hz, 6H), 4.24 (t, *J* = 8.0 Hz, 6H), 1.83 (m, 6H), 1.57 (m, 6H), 1.53-1.25 (m, 60 H), 0.86 (t, J = 6.8 Hz 9H); ^{13}C NMR (100 MHz, $CDCl_3$): δ 140.651,

140.332, 138.377, 110.642, 105.382, 48.327, 32.148, 29.913, 29.890, 29.875, 29.852, 29.822, 29.791, 29.678, 29.572, 26.957, 25.366, 22.888, 14.272. Re-crystallization from varieties of solvent systems failed to give diffractable quality crystals.

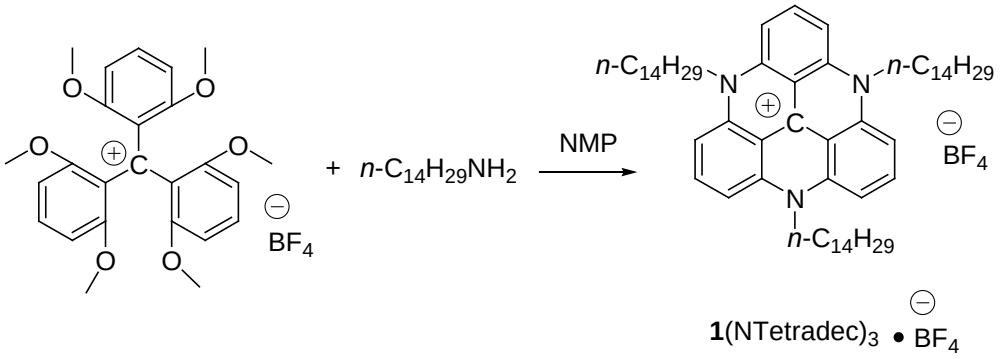

Figure 3.29. Synthesis of **1**(NTetradec)$_3$•BF_4^-.

Appendices

Crystallographic Information File (CIF) for each crystal is given. Readers are suggested to go through the following steps to visualize the individual crystal;

a) Copy the text below dotted line for each CIF file. [Please copy text only. Don't copy the dotted line]
b) Save it as "Plain Text" file.
c) Open it with crystal visualizing software like "mercury" or any other suggested software.

A-1: Crystallographic Information File (CIF) for 1a-2PF_6

……

_chemical_name_systematic	m-xylylene-N,N'-bis-2-phenylpyridinium dihexafluorophosphate
_chemical_formula_moiety	C_{30} H_{26} N_2, 2(F_6 P)
_symmetry_cell_setting	orthorhombic
_symmetry_space_group_name_H-M	'I b c a'

loop_
_symmetry_equiv_pos_as_xyz
'x, y, z'
'-x+1/2, -y, z+1/2'
'-x, y+1/2, -z+1/2'
'x+1/2, -y+1/2, -z'
'x+1/2, y+1/2, z+1/2'
'-x+1, -y+1/2, z+1'
'-x+1/2, y+1, -z+1'
'x+1, -y+1, -z+1/2'
'-x, -y, -z'
'x-1/2, y, -z-1/2'
'x, -y-1/2, z-1/2'
'-x-1/2, y-1/2, z'
'-x+1/2, -y+1/2, -z+1/2'
'x, y+1/2, -z'
'x+1/2, -y, z'
'-x, y, z+1/2'

_cell_length_a 12.7804(8)
_cell_length_b 29.868(2)
_cell_length_c 31.617(2)
_cell_angle_alpha 90.00
_cell_angle_beta 90.00
_cell_angle_gamma 90.00
_cell_formula_units_Z 16

loop_
 _atom_site_label
_atom_site_type_symbol
 _atom_site_fract_x
_atom_site_fract_y
 _atom_site_fract_z
_atom_site_U_iso_or_equiv
 _atom_site_adp_type
_atom_site_occupancy
 _atom_site_symmetry_multiplicity
_atom_site_calc_flag
 _atom_site_refinement_flags
_atom_site_disorder_assembly
 _atom_site_disorder_group
N1 N -0.08011(19) 0.35997(9) 0.09283(9) 0.0278(6) Uani 1 1 d . . .
N2 N 0.3220(2) 0.33664(10) 0.14850(9) 0.0312(6) Uani 1 1 d . . .
C1 C -0.0639(2) 0.38033(12) 0.05465(11) 0.0313(7) Uani 1 1 d . . .
C2 C -0.0708(3) 0.35503(13) 0.01851(12) 0.0370(8) Uani 1 1 d . . .
H2 H -0.0582 0.3686 -0.0082 0.044 Uiso 1 1 calc R . .
C3 C -0.0957(3) 0.31028(13) 0.02044(12) 0.0367(8) Uani 1 1 d . . .
H3 H -0.1012 0.2932 -0.0048 0.044 Uiso 1 1 calc R . .
C4 C -0.1126(3) 0.29055(13) 0.05885(12) 0.0354(8) Uani 1 1 d . . .
H4 H -0.1298 0.2597 0.0606 0.042 Uiso 1 1 calc R . .
C5 C -0.1042(2) 0.31598(12) 0.09480(11) 0.0316(8) Uani 1 1 d . . .
H5 H -0.1155 0.3024 0.1216 0.038 Uiso 1 1 calc R . .
C6 C -0.0738(2) 0.38555(13) 0.13332(10) 0.0318(8) Uani 1 1 d . . .
H6A H -0.0868 0.3649 0.1572 0.038 Uiso 1 1 calc R . .
H6B H -0.1295 0.4086 0.1336 0.038 Uiso 1 1 calc R . .
C7 C 0.0302(2) 0.40790(12) 0.13954(10) 0.0302(7) Uani 1 1 d . . .
C8 C 0.1231(2) 0.38461(12) 0.13376(10) 0.0296(7) Uani 1 1 d . . .
H8 H 0.1213 0.3538 0.1263 0.036 Uiso 1 1 calc R . .
C9 C 0.2182(2) 0.40609(12) 0.13878(10) 0.0301(7) Uani 1 1 d . . .
C10 C 0.3186(2) 0.38192(12) 0.12984(11) 0.0322(8) Uani 1 1 d . . .
H10A H 0.3279 0.3795 0.0988 0.039 Uiso 1 1 calc R . .
H10B H 0.3776 0.3997 0.1412 0.039 Uiso 1 1 calc R . .
C11 C 0.3277(3) 0.30161(13) 0.12206(12) 0.0369(8) Uani 1 1 d . . .
H11 H 0.3298 0.3068 0.0924 0.044 Uiso 1 1 calc R . .
C12 C 0.3306(3) 0.25881(14) 0.13665(13) 0.0429(9) Uani 1 1 d . . .

H12 H 0.3344 0.2344 0.1174 0.051 Uiso 1 1 calc R . .
C13 C 0.3279(3) 0.25129(14) 0.17967(13) 0.0427(9) Uani 1 1 d . . .
H13 H 0.3297 0.2216 0.1905 0.051 Uiso 1 1 calc R . .
C14 C 0.3227(3) 0.28757(13) 0.20670(12) 0.0374(8) Uani 1 1 d . . .
H14 H 0.3209 0.2829 0.2364 0.045 Uiso 1 1 calc R . .
C15 C 0.3201(2) 0.33024(12) 0.19087(11) 0.0318(8) Uani 1 1 d . . .
C16 C 0.3166(3) 0.36971(12) 0.21936(11) 0.0327(8) Uani 1 1 d . . .
C17 C 0.4041(3) 0.39663(14) 0.22399(11) 0.0384(9) Uani 1 1 d . . .
H17 H 0.4668 0.3898 0.2092 0.046 Uiso 1 1 calc R . .
C18 C 0.3996(3) 0.43344(15) 0.25027(13) 0.0455(9) Uani 1 1 d . . .
H18 H 0.4591 0.4522 0.2533 0.055 Uiso 1 1 calc R . .
C19 C 0.3095(3) 0.44320(15) 0.27216(13) 0.0452(9) Uani 1 1 d . . .
H19 H 0.3069 0.4687 0.2900 0.054 Uiso 1 1 calc R . .
C20 C 0.2227(3) 0.41587(14) 0.26821(12) 0.0416(9) Uani 1 1 d . . .
H20 H 0.1607 0.4225 0.2836 0.050 Uiso 1 1 calc R . .
C21 C 0.2260(3) 0.37905(13) 0.24193(11) 0.0367(8) Uani 1 1 d . . .
H21 H 0.1666 0.3602 0.2393 0.044 Uiso 1 1 calc R . .
C22 C -0.0348(3) 0.42808(12) 0.05358(11) 0.0326(8) Uani 1 1 d . . .
C23 C 0.0675(3) 0.43893(13) 0.04309(11) 0.0357(8) Uani 1 1 d . . .
H23 H 0.1159 0.4160 0.0361 0.043 Uiso 1 1 calc R . .
C24 C 0.0988(3) 0.48312(14) 0.04288(12) 0.0435(9) Uani 1 1 d . . .
H24 H 0.1690 0.4906 0.0360 0.052 Uiso 1 1 calc R . .
C25 C 0.0284(3) 0.51640(14) 0.05268(12) 0.0473(10) Uani 1 1 d . . .
H25 H 0.0504 0.5468 0.0530 0.057 Uiso 1 1 calc R . .
C26 C -0.0742(3) 0.50573(14) 0.06204(12) 0.0450(9) Uani 1 1 d . . .
H26 H -0.1228 0.5289 0.0681 0.054 Uiso 1 1 calc R . .
C27 C -0.1064(3) 0.46177(13) 0.06264(11) 0.0373(8) Uani 1 1 d . . .
H27 H -0.1770 0.4545 0.0692 0.045 Uiso 1 1 calc R . .
C28 C 0.0341(3) 0.45274(13) 0.15128(11) 0.0334(8) Uani 1 1 d . . .
H28 H -0.0292 0.4687 0.1558 0.040 Uiso 1 1 calc R . .
C29 C 0.1288(3) 0.47422(13) 0.15638(11) 0.0361(8) Uani 1 1 d . . .
H29 H 0.1307 0.5049 0.1642 0.043 Uiso 1 1 calc R . .
C30 C 0.2207(3) 0.45083(13) 0.15009(11) 0.0342(8) Uani 1 1 d . . .
H30 H 0.2861 0.4656 0.1535 0.041 Uiso 1 1 calc R . .
P1 P 0.61608(6) 0.36841(3) 0.11280(3) 0.0321(2) Uani 1 1 d . . .
F1 F 0.52239(14) 0.38066(8) 0.08170(6) 0.0409(5) Uani 1 1 d . . .
F2 F 0.70907(15) 0.35541(8) 0.14405(7) 0.0430(5) Uani 1 1 d . . .
F3 F 0.54241(15) 0.33425(7) 0.13749(7) 0.0413(5) Uani 1 1 d . . .
F4 F 0.57969(16) 0.40741(8) 0.14404(7) 0.0455(5) Uani 1 1 d . . .
F5 F 0.69059(15) 0.40260(8) 0.08876(8) 0.0512(6) Uani 1 1 d . . .
F6 F 0.65208(17) 0.32972(8) 0.08136(7) 0.0463(6) Uani 1 1 d . . .
P2 P 0.0000 0.2500 0.19469(4) 0.0341(3) Uani 1 2 d S . .
F7 F 0.06118(16) 0.27682(8) 0.15873(7) 0.0445(5) Uani 1 1 d . . .
F8 F 0.06110(17) 0.27714(8) 0.23000(7) 0.0460(5) Uani 1 1 d . . .
F9 F 0.08999(15) 0.21261(7) 0.19437(7) 0.0413(5) Uani 1 1 d . . .
P3 P 0.7500 0.17803(5) 0.0000 0.0348(3) Uani 1 2 d S . .

F10 F 0.68009(18) 0.14083(9) 0.02170(7) 0.0523(6) Uani 1 1 d . . .
F11 F 0.82446(16) 0.17804(8) 0.04076(7) 0.0462(6) Uani 1 1 d . . .
F12 F 0.6803(2) 0.21583(9) 0.02142(7) 0.0620(7) Uani 1 1 d . . .

A-2: Crystallographic Information File (CIF) for 1b-2PF_6

.....

_chemical_name_systematic	m-xylylene-N,N'-bis-2-methylpyridinium dihexafluorophosphate
_chemical_formula_moiety	C_{20} H_{22} N_2, 2(F_6 P)
_symmetry_cell_setting	triclinic
_symmetry_space_group_name_H-M	'P -1'

loop_
_symmetry_equiv_pos_as_xyz
'x, y, z'
'-x, -y, -z'

_cell_length_a	6.5862(4)
_cell_length_b	13.6774(8)
_cell_length_c	13.9306(8)
_cell_angle_alpha	64.645(3)
_cell_angle_beta	89.598(3)
_cell_angle_gamma	82.241(3)
_cell_formula_units_Z	2

loop_
_atom_site_label
_atom_site_type_symbol
_atom_site_fract_x
_atom_site_fract_y
_atom_site_fract_z
_atom_site_U_iso_or_equiv
_atom_site_adp_type
_atom_site_occupancy
_atom_site_symmetry_multiplicity
_atom_site_calc_flag
_atom_site_refinement_flags
_atom_site_disorder_assembly
_atom_site_disorder_group
N1 N 0.4330(6) 0.9969(3) 0.7640(3) 0.0236(8) Uani 1 1 d . . .
N2 N 0.9831(6) 0.5168(3) 0.7672(3) 0.0264(8) Uani 1 1 d . . .
C1 C 0.2710(7) 1.0690(3) 0.7655(3) 0.0252(9) Uani 1 1 d . . .
C2 C 0.2938(7) 1.1257(3) 0.8255(4) 0.0282(10) Uani 1 1 d . . .
H2 H 0.1811 1.1751 0.8289 0.034 Uiso 1 1 calc R . .
C3 C 0.4750(8) 1.1122(4) 0.8798(4) 0.0305(10) Uani 1 1 d . . .

H3 H 0.4896 1.1535 0.9190 0.037 Uiso 1 1 calc R . .
C4 C 0.6371(8) 1.0378(4) 0.8772(4) 0.0297(10) Uani 1 1 d . . .
H4 H 0.7645 1.0269 0.9145 0.036 Uiso 1 1 calc R . .
C5 C 0.6100(7) 0.9800(4) 0.8198(3) 0.0258(9) Uani 1 1 d . . .
H5 H 0.7188 0.9269 0.8194 0.031 Uiso 1 1 calc R . .
C6 C 0.4084(7) 0.9347(4) 0.6994(4) 0.0274(10) Uani 1 1 d . . .
H6A H 0.3521 0.9870 0.6271 0.033 Uiso 1 1 calc R . .
H6B H 0.3075 0.8840 0.7323 0.033 Uiso 1 1 calc R . .
C7 C 0.6050(7) 0.8701(4) 0.6902(3) 0.0252(9) Uani 1 1 d . . .
C8 C 0.6539(7) 0.7595(4) 0.7573(3) 0.0252(9) Uani 1 1 d . . .
H8 H 0.5633 0.7240 0.8103 0.030 Uiso 1 1 calc R . .
C9 C 0.8355(7) 0.7006(4) 0.7471(4) 0.0258(9) Uani 1 1 d . . .
C10 C 0.8911(8) 0.5818(4) 0.8229(4) 0.0321(10) Uani 1 1 d . . .
H10A H 0.9899 0.5748 0.8795 0.038 Uiso 1 1 calc R . .
H10B H 0.7664 0.5526 0.8569 0.038 Uiso 1 1 calc R . .
C11 C 0.8527(7) 0.5105(4) 0.6942(4) 0.0289(10) Uani 1 1 d . . .
H11 H 0.7155 0.5468 0.6833 0.035 Uiso 1 1 calc R . .
C12 C 0.9146(8) 0.4541(4) 0.6377(4) 0.0326(10) Uani 1 1 d . . .
H12 H 0.8216 0.4492 0.5886 0.039 Uiso 1 1 calc R . .
C13 C 1.1164(9) 0.4032(4) 0.6522(4) 0.0373(12) Uani 1 1 d . . .
H13 H 1.1639 0.3625 0.6137 0.045 Uiso 1 1 calc R . .
C14 C 1.2465(8) 0.4128(4) 0.7236(4) 0.0337(11) Uani 1 1 d . . .
H14 H 1.3860 0.3802 0.7324 0.040 Uiso 1 1 calc R . .
C15 C 1.1788(7) 0.4690(4) 0.7830(4) 0.0312(10) Uani 1 1 d . . .
C16 C 1.3174(9) 0.4763(5) 0.8628(5) 0.0457(13) Uani 1 1 d . . .
H16A H 1.3238 0.5534 0.8448 0.069 Uiso 1 1 calc R . .
H16B H 1.4552 0.4391 0.8624 0.069 Uiso 1 1 calc R . .
H16C H 1.2645 0.4414 0.9336 0.069 Uiso 1 1 calc R . .
C17 C 0.0794(7) 1.0875(4) 0.7009(4) 0.0319(10) Uani 1 1 d . . .
H17A H 0.1055 1.1234 0.6251 0.048 Uiso 1 1 calc R . .
H17B H -0.0272 1.1341 0.7177 0.048 Uiso 1 1 calc R . .
H17C H 0.0335 1.0171 0.7170 0.048 Uiso 1 1 calc R . .
C18 C 0.7354(7) 0.9209(4) 0.6111(4) 0.0279(10) Uani 1 1 d . . .
H18 H 0.7009 0.9961 0.5636 0.033 Uiso 1 1 calc R . .
C19 C 0.9163(8) 0.8615(4) 0.6017(4) 0.0299(10) Uani 1 1 d . . .
H19 H 1.0071 0.8966 0.5487 0.036 Uiso 1 1 calc R . .
C20 C 0.9651(7) 0.7520(4) 0.6688(4) 0.0283(10) Uani 1 1 d . . .
H20 H 1.0883 0.7117 0.6611 0.034 Uiso 1 1 calc R . .
P1 P 0.12911(19) 0.76019(9) 0.98885(9) 0.0271(4) Uani 1 1 d . . .
F1 F -0.1040(5) 0.7501(3) 1.0174(3) 0.0548(9) Uani 1 1 d . . .
F2 F 0.1991(6) 0.7069(3) 1.1117(2) 0.0518(9) Uani 1 1 d . . .
F3 F 0.0967(5) 0.8785(3) 0.9868(3) 0.0481(8) Uani 1 1 d . . .
F4 F 0.3604(5) 0.7730(3) 0.9601(2) 0.0436(8) Uani 1 1 d . . .
F5 F 0.0598(4) 0.8137(2) 0.8656(2) 0.0356(7) Uani 1 1 d . . .
F6 F 0.1570(7) 0.6422(3) 0.9915(3) 0.0612(11) Uani 1 1 d . . .
P2 P 0.40993(18) 0.71356(9) 0.48429(10) 0.0276(4) Uani 1 1 d DU . .

F7 F 0.1829(4) 0.6847(3) 0.4918(2) 0.0436(8) Uani 1 1 d DU A .
F8 F 0.6369(5) 0.7418(3) 0.4781(3) 0.0541(9) Uani 1 1 d DU A .
F9 F 0.4254(6) 0.6770(5) 0.6090(3) 0.0571(14) Uani 0.841(8) 1 d PDU A 1
F10 F 0.3124(7) 0.8318(3) 0.4619(6) 0.075(2) Uani 0.841(8) 1 d PDU A 1
F11 F 0.3934(6) 0.7416(4) 0.3602(3) 0.0603(15) Uani 0.841(8) 1 d PDU A 1
F12 F 0.5042(6) 0.5926(3) 0.5052(4) 0.0484(12) Uani 0.841(8) 1 d PDU A 1
F9' F 0.445(4) 0.6227(17) 0.6025(13) 0.058(7) Uiso 0.159(8) 1 d PD A 2
F10' F 0.357(3) 0.8016(13) 0.5369(14) 0.032(5) Uiso 0.159(8) 1 d PD A 2
F11' F 0.379(3) 0.8205(12) 0.3727(11) 0.035(5) Uiso 0.159(8) 1 d PD A 2
F12' F 0.470(3) 0.6393(17) 0.4316(18) 0.052(6) Uiso 0.159(8) 1 d PD A 2

A-3: Crystallographic Information File (CIF) for $[1(NMe)_3]^+PF_6^-$

.....

_chemical_name_common	Trimethyltriazatriangulenium Hexafluorophosphate
_chemical_formula_moiety	C_{22} H_{18} F_6 N_3 P
_symmetry_cell_setting	monoclinic
_symmetry_space_group_name_H-M	P 21/n

loop_
 _symmetry_equiv_pos_as_xyz
 'x, y, z'
 '-x+1/2, y+1/2, -z+1/2'
 '-x, -y, -z'
 'x-1/2, -y-1/2, z-1/2'

_cell_length_a	13.4672(8)
_cell_length_b	21.0848(12)
_cell_length_c	13.7867(7)
_cell_angle_alpha	90.00
_cell_angle_beta	101.027(3)
_cell_angle_gamma	90.00
_cell_formula_units_Z	8

loop_
 _atom_site_type_symbol
 _atom_site_fract_x
 _atom_site_fract_y
 _atom_site_fract_z
 _atom_site_U_iso_or_equiv
 _atom_site_adp_type
 _atom_site_occupancy
 _atom_site_symmetry_multiplicity
 _atom_site_calc_flag

_atom_site_refinement_flags
_atom_site_disorder_assembly
_atom_site_disorder_group

P 0.47069(16) 0.17763(9) 0.21014(15) 0.0512(6) Uani 1 1 d . . .
P 0.00428(17) 0.37472(9) 0.25624(18) 0.0598(6) Uani 1 1 d . . .
C 0.6050(5) 0.4542(3) 0.4062(4) 0.0332(14) Uani 1 1 d . . .
C 0.7132(5) 0.4503(3) 0.4257(4) 0.0380(15) Uani 1 1 d . . .
C 0.6167(5) 0.5679(3) 0.3804(4) 0.0355(14) Uani 1 1 d . . .
C 0.6044(6) 0.4831(3) 0.1468(5) 0.0424(16) Uani 1 1 d . . .
N 0.5524(5) 0.4273(3) 0.1498(4) 0.0473(16) Uani 1 1 d . . .
N 0.7678(5) 0.5051(3) 0.4265(4) 0.0426(13) Uani 1 1 d . . .
N 0.4422(4) 0.4040(2) 0.3890(4) 0.0378(13) Uani 1 1 d . . .
C 0.5504(6) 0.5400(3) 0.1224(4) 0.0386(15) Uani 1 1 d . . .
C 0.5583(5) 0.5132(3) 0.3837(4) 0.0329(14) Uani 1 1 d . . .
C 0.3934(6) 0.4611(3) 0.3665(4) 0.0376(15) Uani 1 1 d . . .
C 0.4447(6) 0.5390(3) 0.1039(4) 0.0374(15) Uani 1 1 d . . .
N 0.5471(5) 0.6528(3) 0.0923(4) 0.0428(14) Uani 1 1 d . . .
C 0.7236(5) 0.5639(3) 0.4013(5) 0.0390(15) Uani 1 1 d . . .
C 0.4432(6) 0.6540(3) 0.0783(5) 0.0430(17) Uani 1 1 d . . .
C 0.4516(5) 0.5168(3) 0.3634(4) 0.0343(14) Uani 1 1 d . . .
C 0.4048(5) 0.5764(3) 0.3408(4) 0.0379(15) Uani 1 1 d . . .
C 0.6018(6) 0.5981(3) 0.1176(5) 0.0433(17) Uani 1 1 d . . .
C 0.3900(6) 0.5962(3) 0.0821(4) 0.0398(16) Uani 1 1 d . . .
C 0.4486(6) 0.4248(3) 0.1337(5) 0.0425(17) Uani 1 1 d . . .
C 0.3928(6) 0.4822(3) 0.1093(5) 0.0418(16) Uani 1 1 d . . .
C 0.5681(6) 0.6272(3) 0.3563(5) 0.0397(15) Uani 1 1 d . . .
C 0.5458(5) 0.3985(3) 0.4077(4) 0.0367(15) Uani 1 1 d . . .
N 0.4644(5) 0.6301(2) 0.3409(4) 0.0405(13) Uani 1 1 d . . .
C 0.7106(7) 0.4851(4) 0.1680(5) 0.0518(19) Uani 1 1 d . . .
C 0.2851(6) 0.4813(3) 0.0912(5) 0.0481(18) Uani 1 1 d . . .
F 0.3652(4) 0.2002(3) 0.1473(4) 0.0716(14) Uani 1 1 d . . .
C 0.7603(6) 0.3912(3) 0.4447(5) 0.0490(18) Uani 1 1 d . . .
N 0.2346(5) 0.5374(3) 0.0665(5) 0.0510(16) Uani 1 1 d . . .
C 0.3786(6) 0.3472(3) 0.3948(6) 0.0507(18) Uani 1 1 d . . .
C 0.5945(6) 0.3401(3) 0.4280(5) 0.0467(18) Uani 1 1 d . . .
C 0.2885(6) 0.4663(3) 0.3452(5) 0.0438(16) Uani 1 1 d . . .
C 0.6288(6) 0.6811(3) 0.3490(5) 0.0458(17) Uani 1 1 d . . .
F 0.4144(4) 0.1392(2) 0.2822(4) 0.0705(14) Uani 1 1 d . . .
C 0.2834(6) 0.5948(3) 0.0655(5) 0.0467(17) Uani 1 1 d . . .
F 0.5760(4) 0.1547(2) 0.2701(4) 0.0723(14) Uani 1 1 d . . .
C 0.7323(6) 0.6740(4) 0.3680(5) 0.0507(18) Uani 1 1 d . . .
C 0.2290(7) 0.6526(4) 0.0489(6) 0.055(2) Uani 1 1 d . . .
C 0.3963(8) 0.3684(3) 0.1409(5) 0.057(2) Uani 1 1 d . . .
C 0.6030(7) 0.7117(3) 0.0770(6) 0.0534(19) Uani 1 1 d . . .
C 0.2996(5) 0.5802(3) 0.3175(5) 0.0443(16) Uani 1 1 d . . .

F 0.4722(4) 0.2392(2) 0.2760(4) 0.0775(16) Uani 1 1 d . . .
C 0.7074(6) 0.5987(4) 0.1397(5) 0.0502(18) Uani 1 1 d . . .
C 0.6121(7) 0.3683(4) 0.1739(6) 0.058(2) Uani 1 1 d . . .
C 0.6981(7) 0.3379(3) 0.4447(5) 0.0516(19) Uani 1 1 d . . .
C 0.7823(6) 0.6182(3) 0.3949(5) 0.0477(17) Uani 1 1 d . . .
C 0.2443(6) 0.5251(4) 0.3206(6) 0.0514(18) Uani 1 1 d . . .
C 0.3886(7) 0.7106(3) 0.0620(5) 0.0497(19) Uani 1 1 d . . .
C 0.2920(8) 0.3694(4) 0.1242(6) 0.064(2) Uani 1 1 d . . .
F 0.4672(4) 0.1169(2) 0.1410(4) 0.0755(15) Uani 1 1 d . . .
F 0.5272(4) 0.2161(2) 0.1362(4) 0.0715(14) Uani 1 1 d . . .
C 0.2845(7) 0.7082(4) 0.0492(6) 0.059(2) Uani 1 1 d . . .
C 0.2338(7) 0.4245(4) 0.0999(6) 0.060(2) Uani 1 1 d . . .
C 0.4147(6) 0.6927(3) 0.3267(6) 0.0532(19) Uani 1 1 d . . .
C 0.7588(7) 0.5421(4) 0.1653(6) 0.059(2) Uani 1 1 d . . .
C 0.8794(6) 0.5018(4) 0.4562(7) 0.059(2) Uani 1 1 d . . .
F -0.0314(5) 0.3065(3) 0.2720(6) 0.103(2) Uani 1 1 d . . .
C 0.1226(7) 0.5356(5) 0.0390(9) 0.075(3) Uani 1 1 d . . .
F 0.1158(5) 0.3466(3) 0.2720(7) 0.112(3) Uani 1 1 d . . .
F -0.1009(5) 0.4033(4) 0.2488(7) 0.123(3) Uani 1 1 d . . .
F 0.0199(9) 0.3834(6) 0.3687(7) 0.187(6) Uani 1 1 d . . .
F 0.0453(8) 0.4414(3) 0.2406(14) 0.221(8) Uani 1 1 d . . .
F -0.0054(9) 0.3625(7) 0.1452(6) 0.195(6) Uani 1 1 d . . .

A-4: Crystallographic Information File (CIF) for $[1(NMe)_3]^+NCO^-$

.....

_chemical_name_common	Trimethyltriazatriangulenium Cyanate
_chemical_formula_moiety	$C_{22}H_{18}N_3$, CNO, H_2O
_symmetry_cell_setting	monoclinic
_symmetry_space_group_name_H-M	P 21/n

loop_
_symmetry_equiv_pos_as_xyz
'x, y, z'
'-x+1/2, y+1/2, -z+1/2'
'-x, -y, -z'
'x-1/2, -y-1/2, z-1/2'

_cell_length_a	7.1272(4)
_cell_length_b	20.6211(12)
_cell_length_c	12.1963(8)
_cell_angle_alpha	90.00
_cell_angle_beta	103.290(3)
_cell_angle_gamma	90.00
_cell_formula_units_Z	4

```
loop_
 _atom_site_label
 _atom_site_type_symbol
 _atom_site_fract_x
 _atom_site_fract_y
 _atom_site_fract_z
 _atom_site_U_iso_or_equiv
 _atom_site_adp_type
 _atom_site_occupancy
 _atom_site_symmetry_multiplicity
 _atom_site_calc_flag
 _atom_site_refinement_flags
 _atom_site_disorder_assembly
 _atom_site_disorder_group
N1 N 0.9033(3) 0.36318(9) 0.09995(18) 0.0300(5) Uani 1 1 d . . .
C1 C 0.9227(3) 0.41322(13) 0.2823(2) 0.0341(6) Uani 1 1 d . . .
H1 H 0.9728 0.3746 0.3204 0.041 Uiso 1 1 calc R . .
N2 N 0.7194(3) 0.58758(9) 0.12001(18) 0.0299(5) Uani 1 1 d . . .
C2 C 0.8899(3) 0.46715(14) 0.3424(2) 0.0377(6) Uani 1 1 d . . .
H2 H 0.9156 0.4640 0.4222 0.045 Uiso 1 1 calc R . .
N3 N 0.6853(3) 0.48665(10) -0.24194(17) 0.0307(5) Uani 1 1 d . . .
C3 C 0.8217(3) 0.52538(13) 0.2928(2) 0.0337(6) Uani 1 1 d . . .
H3 H 0.8003 0.5612 0.3375 0.040 Uiso 1 1 calc R . .
C4 C 0.5892(3) 0.64813(11) -0.0519(2) 0.0349(6) Uani 1 1 d . . .
H4 H 0.5661 0.6851 -0.0104 0.042 Uiso 1 1 calc R . .
C5 C 0.5437(3) 0.64872(13) -0.1687(3) 0.0396(7) Uani 1 1 d . . .
H5 H 0.4880 0.6870 -0.2057 0.048 Uiso 1 1 calc R . .
C6 C 0.5740(3) 0.59744(13) -0.2342(2) 0.0349(6) Uani 1 1 d . . .
H6 H 0.5420 0.6006 -0.3141 0.042 Uiso 1 1 calc R . .
C7 C 0.7644(3) 0.37263(13) -0.2532(2) 0.0357(6) Uani 1 1 d . . .
H7 H 0.7325 0.3738 -0.3332 0.043 Uiso 1 1 calc R . .
C8 C 0.8276(3) 0.31625(13) -0.1967(2) 0.0398(7) Uani 1 1 d . . .
H8 H 0.8390 0.2788 -0.2401 0.048 Uiso 1 1 calc R . .
C9 C 0.8754(3) 0.31059(12) -0.0813(2) 0.0351(6) Uani 1 1 d . . .
H9 H 0.9189 0.2704 -0.0464 0.042 Uiso 1 1 calc R . .
C10 C 0.8818(3) 0.41619(11) 0.16571(19) 0.0257(5) Uani 1 1 d . . .
C11 C 0.8127(3) 0.47548(10) 0.11126(18) 0.0227(5) Uani 1 1 d . . .
C12 C 0.7850(3) 0.53057(11) 0.1757(2) 0.0260(5) Uani 1 1 d . . .
C13 C 0.6699(3) 0.59196(11) 0.0033(2) 0.0263(5) Uani 1 1 d . . .
C14 C 0.6987(3) 0.53733(10) -0.06164(19) 0.0239(5) Uani 1 1 d . . .
C15 C 0.6527(3) 0.54048(11) -0.1811(2) 0.0281(5) Uani 1 1 d . . .
C16 C 0.7478(3) 0.42833(11) -0.1904(2) 0.0276(5) Uani 1 1 d . . .
C17 C 0.7935(3) 0.42453(11) -0.07108(19) 0.0241(5) Uani 1 1 d . . .
C18 C 0.8587(3) 0.36522(11) -0.0165(2) 0.0272(5) Uani 1 1 d . . .
C19 C 0.7700(3) 0.47936(10) -0.00673(19) 0.0214(5) Uani 1 1 d . . .
```

C20 C 0.9617(4) 0.30030(13) 0.1537(3) 0.0485(7) Uani 1 1 d . . .
H20A H 1.0131 0.3067 0.2347 0.073 Uiso 1 1 calc R . .
H20B H 1.0613 0.2809 0.1205 0.073 Uiso 1 1 calc R . .
H20C H 0.8498 0.2714 0.1418 0.073 Uiso 1 1 calc R . .
C21 C 0.6986(4) 0.64620(13) 0.1846(2) 0.0406(7) Uani 1 1 d . . .
H21A H 0.7697 0.6407 0.2629 0.061 Uiso 1 1 calc R . .
H21B H 0.5619 0.6535 0.1823 0.061 Uiso 1 1 calc R . .
H21C H 0.7503 0.6836 0.1516 0.061 Uiso 1 1 calc R . .
C22 C 0.6421(4) 0.49026(15) -0.3655(2) 0.0408(7) Uani 1 1 d . . .
H22A H 0.7271 0.4606 -0.3942 0.061 Uiso 1 1 calc R . .
H22B H 0.6629 0.5347 -0.3887 0.061 Uiso 1 1 calc R . .
H22C H 0.5074 0.4779 -0.3961 0.061 Uiso 1 1 calc R . .
N1A N 0.6474(14) 0.3262(19) 0.478(3) 0.045(2) Uani 0.769(15) 1 d PDU A 1
C1A C 0.7979(10) 0.3115(11) 0.4737(14) 0.0347(10) Uani 0.769(15) 1 d PDU A 1
O1A O 0.9642(5) 0.29376(18) 0.4643(6) 0.0480(14) Uani 0.769(15) 1 d PDU A 1
N1B N 0.991(2) 0.3056(8) 0.519(2) 0.0480(14) Uani 0.231(15) 1 d PDU A 2
C1B C 0.832(3) 0.310(4) 0.478(5) 0.0347(10) Uani 0.231(15) 1 d PDU A 2
O1B O 0.652(4) 0.321(5) 0.466(7) 0.045(2) Uani 0.231(15) 1 d PDU A 2
O1W O 0.6962(3) 0.62752(10) 0.47432(18) 0.0500(5) Uani 1 1 d D . .
H1W H 0.589(4) 0.6474(17) 0.496(3) 0.075 Uiso 1 1 d D . .
H2W H 0.799(5) 0.6585(16) 0.489(3) 0.075 Uiso 1 1 d D . .

A-5: Crystallographic Information File (CIF) for $[1(NEt)_3]^+BF_4^-$

.....

_chemical_name_common	triethyltriazatriangulenium tetrafluoroborate
_chemical_formula_moiety	C_{25} H_{24} N_3, B F_4
_symmetry_cell_setting	triclinic
_symmetry_space_group_name_H-M	P -1

loop_
 _symmetry_equiv_pos_as_xyz
 'x, y, z'
 '-x, -y, -z'

_cell_length_a	8.7342(3)
_cell_length_b	11.1919(3)
_cell_length_c	12.3100(4)
_cell_angle_alpha	113.2440(14)
_cell_angle_beta	101.3644(14)
_cell_angle_gamma	101.5848(14)
_cell_formula_units_Z	2

loop_
 _atom_site_label
 _atom_site_type_symbol

_atom_site_fract_x
_atom_site_fract_y
_atom_site_fract_z
_atom_site_U_iso_or_equiv
_atom_site_adp_type
_atom_site_occupancy
_atom_site_symmetry_multiplicity
_atom_site_calc_flag
_atom_site_refinement_flags
_atom_site_disorder_assembly
_atom_site_disorder_group
N1 N 0.6719(4) 0.4453(3) 0.7295(3) 0.0407(8) Uani 1 1 d . . .
N2 N 0.8329(4) 0.6382(3) 0.4647(3) 0.0399(8) Uani 1 1 d . . .
N3 N 0.4250(4) 0.1944(3) 0.2834(3) 0.0390(8) Uani 1 1 d . . .
C1 C 0.3556(5) 0.0908(4) 0.4154(4) 0.0410(10) Uani 1 1 d . . .
H1 H 0.2846 0.0092 0.3453 0.049 Uiso 1 1 calc R . .
C2 C 0.3753(5) 0.1035(4) 0.5337(4) 0.0429(10) Uani 1 1 d . . .
H2 H 0.3160 0.0289 0.5428 0.051 Uiso 1 1 calc R . .
C3 C 0.4758(5) 0.2180(4) 0.6389(4) 0.0406(10) Uani 1 1 d . . .
H3 H 0.4840 0.2224 0.7186 0.049 Uiso 1 1 calc R . .
C4 C 0.8912(5) 0.6611(4) 0.8210(4) 0.0477(11) Uani 1 1 d . . .
H4 H 0.9058 0.6677 0.9020 0.057 Uiso 1 1 calc R . .
C5 C 0.9865(6) 0.7630(5) 0.8025(4) 0.0506(11) Uani 1 1 d . . .
H5 H 1.0656 0.8397 0.8728 0.061 Uiso 1 1 calc R . .
C6 C 0.9712(5) 0.7577(4) 0.6871(4) 0.0470(11) Uani 1 1 d . . .
H6 H 1.0394 0.8297 0.6794 0.056 Uiso 1 1 calc R . .
C7 C 0.7177(5) 0.5098(4) 0.2403(4) 0.0443(10) Uani 1 1 d . . .
H7 H 0.7830 0.5799 0.2285 0.053 Uiso 1 1 calc R . .
C8 C 0.6102(6) 0.3946(5) 0.1397(4) 0.0504(11) Uani 1 1 d . . .
H8 H 0.6027 0.3876 0.0592 0.060 Uiso 1 1 calc R . .
C9 C 0.5116(6) 0.2879(4) 0.1490(4) 0.0458(11) Uani 1 1 d . . .
H9 H 0.4383 0.2098 0.0767 0.055 Uiso 1 1 calc R . .
C10 C 0.4416(5) 0.1998(4) 0.4000(4) 0.0372(9) Uani 1 1 d . . .
C11 C 0.5491(5) 0.3177(4) 0.5066(4) 0.0354(9) Uani 1 1 d . . .
C12 C 0.5662(5) 0.3285(4) 0.6273(4) 0.0360(9) Uani 1 1 d . . .
C13 C 0.7746(5) 0.5498(4) 0.7186(4) 0.0395(10) Uani 1 1 d . . .
C14 C 0.7570(5) 0.5399(4) 0.5979(4) 0.0381(9) Uani 1 1 d . . .
C15 C 0.8578(5) 0.6488(4) 0.5828(4) 0.0393(10) Uani 1 1 d . . .
C16 C 0.7315(5) 0.5241(4) 0.3591(4) 0.0380(9) Uani 1 1 d . . .
C17 C 0.6318(5) 0.4141(4) 0.3727(4) 0.0363(9) Uani 1 1 d . . .
C18 C 0.5222(5) 0.2973(4) 0.2669(4) 0.0395(10) Uani 1 1 d . . .
C19 C 0.6456(5) 0.4262(4) 0.4927(4) 0.0347(9) Uani 1 1 d . . .
C20 C 0.6898(6) 0.4512(5) 0.8533(4) 0.0479(11) Uani 1 1 d . . .
H20A H 0.5818 0.4061 0.8561 0.057 Uiso 1 1 calc R . .
H20B H 0.7270 0.5479 0.9170 0.057 Uiso 1 1 calc R . .
C21 C 0.8127(6) 0.3809(5) 0.8830(4) 0.0556(12) Uani 1 1 d . . .

H21A H 0.7755 0.2849 0.8205 0.083 Uiso 1 1 calc R . .
H21B H 0.8215 0.3857 0.9653 0.083 Uiso 1 1 calc R . .
H21C H 0.9203 0.4268 0.8823 0.083 Uiso 1 1 calc R . .
C22 C 0.9222(5) 0.7560(4) 0.4493(4) 0.0472(11) Uani 1 1 d . . .
H22A H 0.9413 0.8421 0.5242 0.057 Uiso 1 1 calc R . .
H22B H 0.8536 0.7598 0.3772 0.057 Uiso 1 1 calc R . .
C23 C 1.0852(6) 0.7441(5) 0.4297(5) 0.0594(13) Uani 1 1 d . . .
H23A H 1.1590 0.7530 0.5056 0.089 Uiso 1 1 calc R . .
H23B H 1.1345 0.8169 0.4102 0.089 Uiso 1 1 calc R . .
H23C H 1.0679 0.6549 0.3608 0.089 Uiso 1 1 calc R . .
C24 C 0.3121(6) 0.0707(4) 0.1729(4) 0.0487(11) Uani 1 1 d . . .
H24A H 0.2700 0.0957 0.1067 0.058 Uiso 1 1 calc R . .
H24B H 0.2172 0.0317 0.1944 0.058 Uiso 1 1 calc R . .
C25 C 0.3971(7) -0.0356(5) 0.1251(4) 0.0609(14) Uani 1 1 d . . .
H25A H 0.4945 0.0043 0.1079 0.091 Uiso 1 1 calc R . .
H25B H 0.3216 -0.1137 0.0485 0.091 Uiso 1 1 calc R . .
H25C H 0.4303 -0.0664 0.1878 0.091 Uiso 1 1 calc R . .
B1 B 0.8288(10) 0.8536(8) 0.1699(7) 0.0520(12) Uani 0.809(7) 1 d PDU A 1
F1 F 0.8484(7) 0.9361(3) 0.2916(3) 0.0748(15) Uani 0.809(7) 1 d PDU A 1
F2 F 0.7008(8) 0.7350(4) 0.1238(5) 0.0841(19) Uani 0.809(7) 1 d PDU A 1
F3 F 0.8057(6) 0.9232(4) 0.1014(4) 0.0694(14) Uani 0.809(7) 1 d PDU A 1
F4 F 0.9628(7) 0.8144(8) 0.1603(6) 0.130(2) Uani 0.809(7) 1 d PDU A 1
B1' B 0.836(3) 0.843(2) 0.1675(19) 0.0520(12) Uani 0.191(7) 1 d PDU A 2
F1' F 0.955(3) 0.905(2) 0.2798(16) 0.084(5) Uani 0.191(7) 1 d PDU A 2
F2' F 0.671(2) 0.785(3) 0.140(3) 0.081(6) Uani 0.191(7) 1 d PDU A 2
F3' F 0.893(3) 0.890(2) 0.0916(17) 0.086(5) Uani 0.191(7) 1 d PDU A 2
F4' F 0.871(3) 0.7229(19) 0.1254(18) 0.088(4) Uani 0.191(7) 1 d PDU A 2

A-6: Crystallographic Information File (CIF) for $[1(NPh)_3]^+BF_4^-$

.....

_chemical_name_common	triphenyltriazatriangulenium tetrafluoroborate
_chemical_formula_moiety	$C_{37}\ H_{24}\ N_3,\ BF_4$
_symmetry_cell_setting	monoclinic?
_symmetry_space_group_name_H-M	P 21/n

loop_
 _symmetry_equiv_pos_as_xyz
 'x, y, z'
 '-x+1/2, y+1/2, -z+1/2'
 '-x, -y, -z'
 'x-1/2, -y-1/2, z-1/2'

_cell_length_a 14.6290(4)
_cell_length_b 10.6080(3)
_cell_length_c 18.3220(5)
_cell_angle_alpha 90.00
_cell_angle_beta 98.9540(10)
_cell_angle_gamma 90.00
_cell_formula_units_Z 4

loop_
 _atom_site_label
 _atom_site_type_symbol
 _atom_site_fract_x
 _atom_site_fract_y
 _atom_site_fract_z
 _atom_site_U_iso_or_equiv
 _atom_site_adp_type
 _atom_site_occupancy
 _atom_site_symmetry_multiplicity
 _atom_site_calc_flag
 _atom_site_refinement_flags
 _atom_site_disorder_assembly
 _atom_site_disorder_group
F6 F 0.42240(19) 0.3409(3) 0.24311(16) 0.0487(8) Uani 1 1 d . . .
F3 F 0.50842(19) 0.5139(2) 0.28318(14) 0.0453(8) Uani 1 1 d . . .
F4 F 0.5779(2) 0.3315(3) 0.2589(2) 0.0692(10) Uani 1 1 d . . .
F5 F 0.5030(3) 0.3451(3) 0.35766(17) 0.0891(13) Uani 1 1 d . . .
B2 B 0.5036(4) 0.3832(5) 0.2863(3) 0.0374(15) Uani 1 1 d . . .
C34 C 0.5575(3) 0.5391(4) 0.1224(2) 0.0291(12) Uani 1 1 d . . .
N9 N 0.6224(3) 0.3536(4) 0.0758(2) 0.0331(10) Uani 1 1 d . . .
C16 C 0.4567(3) 0.3702(4) 0.0683(2) 0.0307(12) Uani 1 1 d . . .
N8 N 0.4904(3) 0.7200(3) 0.17498(19) 0.0302(10) Uani 1 1 d . . .
C31 C 0.4030(3) 0.6674(4) 0.1609(2) 0.0312(12) Uani 1 1 d . . .
C33 C 0.4690(3) 0.4879(4) 0.1049(2) 0.0263(11) Uani 1 1 d . . .
N7 N 0.2946(3) 0.3759(4) 0.07612(19) 0.0340(10) Uani 1 1 d . . .
C35 C 0.6354(3) 0.4711(4) 0.1089(2) 0.0313(12) Uani 1 1 d . . .
C36 C 0.7247(3) 0.5199(5) 0.1290(2) 0.0371(13) Uani 1 1 d . . .
C18 C 0.3552(4) 0.2018(5) 0.0119(3) 0.0405(14) Uani 1 1 d . . .
C17 C 0.3692(3) 0.3162(5) 0.0525(2) 0.0347(13) Uani 1 1 d . . .
C15 C 0.5356(3) 0.3045(4) 0.0515(2) 0.0311(12) Uani 1 1 d . . .
C39 C 0.5692(3) 0.6595(4) 0.1586(2) 0.0316(12) Uani 1 1 d . . .
C27 C 0.3030(3) 0.4912(4) 0.1122(2) 0.0330(12) Uani 1 1 d . . .
C32 C 0.3922(3) 0.5510(4) 0.1238(2) 0.0304(12) Uani 1 1 d . . .
C19 C 0.4336(4) 0.1441(5) -0.0080(3) 0.0400(13) Uani 1 1 d . . .
C38 C 0.6566(3) 0.7111(5) 0.1773(3) 0.0356(13) Uani 1 1 d . . .
C40 C 0.5016(3) 0.8340(5) 0.2196(3) 0.0339(12) Uani 1 1 d . . .
C37 C 0.7333(4) 0.6411(5) 0.1620(3) 0.0409(13) Uani 1 1 d . . .

C20 C 0.5239(4) 0.1906(4) 0.0114(3) 0.0359(13) Uani 1 1 d . . .
C30 C 0.3252(4) 0.7297(5) 0.1830(3) 0.0393(13) Uani 1 1 d . . .
C29 C 0.2393(3) 0.6675(5) 0.1719(3) 0.0376(13) Uani 1 1 d . . .
C28 C 0.2268(3) 0.5479(5) 0.1367(2) 0.0379(13) Uani 1 1 d . . .
C21 C 0.2108(4) 0.3014(5) 0.0748(3) 0.0385(13) Uani 1 1 d . . .
C11 C 0.7456(3) 0.2509(5) 0.0184(3) 0.0425(14) Uani 1 1 d . . .
C1 C 0.7140(4) 0.1820(5) 0.1383(3) 0.0402(13) Uani 1 1 d . . .
C41 C 0.5235(3) 0.8198(5) 0.2961(3) 0.0382(13) Uani 1 1 d . . .
C42 C 0.5305(3) 0.9287(5) 0.3397(3) 0.0389(13) Uani 1 1 d . . .
C10 C 0.6980(3) 0.2639(5) 0.0791(3) 0.0377(13) Uani 1 1 d . . .
C14 C 0.7770(4) 0.0841(5) 0.1391(3) 0.0417(14) Uani 1 1 d . . .
C12 C 0.8091(4) 0.1499(5) 0.0186(3) 0.0456(14) Uani 1 1 d . . .
C13 C 0.8230(4) 0.0660(5) 0.0791(3) 0.0446(14) Uani 1 1 d . . .
C45 C 0.4865(3) 0.9506(5) 0.1867(3) 0.0410(13) Uani 1 1 d . . .
C44 C 0.4932(4) 1.0572(5) 0.2301(3) 0.0470(14) Uani 1 1 d . . .
C22 C 0.2129(4) 0.2089(5) 0.1300(3) 0.0471(15) Uani 1 1 d . . .
C25 C 0.1393(4) 0.1256(5) 0.1278(3) 0.0534(16) Uani 1 1 d . . .
C23 C 0.1389(4) 0.3147(5) 0.0173(3) 0.0457(15) Uani 1 1 d . . .
C26 C 0.0644(4) 0.1370(6) 0.0703(3) 0.0542(16) Uani 1 1 d . . .
C43 C 0.5154(3) 1.0462(5) 0.3071(3) 0.0409(13) Uani 1 1 d . . .
C24 C 0.0630(4) 0.2311(6) 0.0169(3) 0.0582(17) Uani 1 1 d . . .

A-7: Crystallographic Information File (CIF) for $[1(NDec)_3]^+BF_4^-$

.....

_chemical_name_common	triazatri-*n*-decyltriangulenium tetrafluoroborate
_chemical_formula_moiety	$C_{49}H_{72}N_3$, BF_4, 0.836(CH_4O)
_symmetry_cell_setting	triclinic
_symmetry_space_group_name_H-M	'P -1'

loop_
_symmetry_equiv_pos_as_xyz
'x, y, z'
'-x, -y, -z'

_cell_length_a	11.9763(2)
_cell_length_b	12.4531(3)
_cell_length_c	17.9813(5)
_cell_angle_alpha	75.7584(9)
_cell_angle_beta	84.2537(10)
_cell_angle_gamma	64.3295(10)
_cell_formula_units_Z	2

```
loop_
 _atom_site_label
 _atom_site_type_symbol
 _atom_site_fract_x
 _atom_site_fract_y
 _atom_site_fract_z
 _atom_site_U_iso_or_equiv
 _atom_site_adp_type
 _atom_site_occupancy
 _atom_site_symmetry_multiplicity
 _atom_site_calc_flag
 _atom_site_refinement_flags
 _atom_site_disorder_assembly
 _atom_site_disorder_group
N1 N 1.20395(18) 0.01819(18) 0.09814(11) 0.0273(5) Uani 1 1 d . . .
N2 N 1.02795(17) -0.26493(17) 0.09063(10) 0.0232(5) Uani 1 1 d . . .
N3 N 0.75804(17) 0.15498(16) 0.10134(10) 0.0241(5) Uani 1 1 d . . .
C1 C 0.8447(2) 0.2951(2) 0.11094(13) 0.0296(6) Uani 1 1 d . . .
H1 H 0.7645 0.3579 0.1149 0.036 Uiso 1 1 calc R . .
C2 C 0.9483(3) 0.3156(2) 0.11184(13) 0.0332(6) Uani 1 1 d . . .
H2 H 0.9375 0.3942 0.1159 0.040 Uiso 1 1 calc R . .
C3 C 1.0685(2) 0.2270(2) 0.10711(13) 0.0309(6) Uani 1 1 d . . .
H3 H 1.1374 0.2455 0.1077 0.037 Uiso 1 1 calc R . .
C4 C 1.3399(2) -0.1918(2) 0.09027(13) 0.0286(6) Uani 1 1 d . . .
H4 H 1.4113 -0.1772 0.0907 0.034 Uiso 1 1 calc R . .
C5 C 1.3518(2) -0.3054(2) 0.08593(13) 0.0299(6) Uani 1 1 d . . .
H5 H 1.4326 -0.3678 0.0829 0.036 Uiso 1 1 calc R . .
C6 C 1.2519(2) -0.3326(2) 0.08573(12) 0.0280(6) Uani 1 1 d . . .
H6 H 1.2644 -0.4123 0.0830 0.034 Uiso 1 1 calc R . .
C7 C 0.8043(2) -0.1980(2) 0.09659(13) 0.0256(6) Uani 1 1 d . . .
H7 H 0.8131 -0.2773 0.0960 0.031 Uiso 1 1 calc R . .
C8 C 0.6879(2) -0.1045(2) 0.09922(13) 0.0278(6) Uani 1 1 d . . .
H8 H 0.6177 -0.1216 0.1003 0.033 Uiso 1 1 calc R . .
C9 C 0.6688(2) 0.0126(2) 0.10037(13) 0.0268(6) Uani 1 1 d . . .
H9 H 0.5871 0.0744 0.1018 0.032 Uiso 1 1 calc R . .
C10 C 0.8588(2) 0.1810(2) 0.10412(12) 0.0241(6) Uani 1 1 d . . .
C11 C 0.9807(2) 0.0874(2) 0.10000(12) 0.0217(5) Uani 1 1 d . . .
C12 C 1.0862(2) 0.1118(2) 0.10159(12) 0.0252(6) Uani 1 1 d . . .
C13 C 1.2215(2) -0.0983(2) 0.09403(12) 0.0252(6) Uani 1 1 d . . .
C14 C 1.1168(2) -0.1235(2) 0.09327(12) 0.0218(6) Uani 1 1 d . . .
C15 C 1.1315(2) -0.2417(2) 0.08962(12) 0.0227(6) Uani 1 1 d . . .
C16 C 0.9087(2) -0.1751(2) 0.09483(12) 0.0223(6) Uani 1 1 d . . .
C17 C 0.8924(2) -0.0552(2) 0.09693(12) 0.0203(5) Uani 1 1 d . . .
C18 C 0.7708(2) 0.0393(2) 0.09937(12) 0.0234(6) Uani 1 1 d . . .
C19 C 0.9966(2) -0.0299(2) 0.09653(12) 0.0206(5) Uani 1 1 d . . .
C20 C 1.3148(2) 0.0390(2) 0.10499(14) 0.0302(6) Uani 1 1 d . . .
```

H20A H 1.2919 0.1280 0.0907 0.036 Uiso 1 1 calc R . .
H20B H 1.3783 0.0005 0.0684 0.036 Uiso 1 1 calc R . .
C21 C 1.3710(2) -0.0133(3) 0.18673(14) 0.0400(7) Uani 1 1 d . . .
H21A H 1.4121 -0.1036 0.1956 0.048 Uiso 1 1 calc R . .
H21B H 1.4358 0.0150 0.1894 0.048 Uiso 1 1 calc R . .
C22 C 1.2797(3) 0.0213(3) 0.25110(14) 0.0434(7) Uani 1 1 d . . .
H22A H 1.2083 0.0042 0.2445 0.052 Uiso 1 1 calc R . .
H22B H 1.2482 0.1102 0.2475 0.052 Uiso 1 1 calc R . .
C23 C 1.3365(3) -0.0478(3) 0.33032(15) 0.0435(7) Uani 1 1 d . . .
H23A H 1.3954 -0.0172 0.3414 0.052 Uiso 1 1 calc R . .
H23B H 1.3838 -0.1356 0.3304 0.052 Uiso 1 1 calc R . .
C24 C 1.2394(3) -0.0338(3) 0.39352(15) 0.0450(8) Uani 1 1 d . . .
H24A H 1.1989 0.0530 0.3969 0.054 Uiso 1 1 calc R . .
H24B H 1.1751 -0.0548 0.3789 0.054 Uiso 1 1 calc R . .
C25 C 1.2902(3) -0.1123(3) 0.47207(14) 0.0439(7) Uani 1 1 d . . .
H25A H 1.3478 -0.0854 0.4894 0.053 Uiso 1 1 calc R . .
H25B H 1.3382 -0.1982 0.4678 0.053 Uiso 1 1 calc R . .
C26 C 1.1904(3) -0.1067(3) 0.53212(15) 0.0448(7) Uani 1 1 d . . .
H26A H 1.1292 -0.1273 0.5130 0.054 Uiso 1 1 calc R . .
H26B H 1.1468 -0.0219 0.5393 0.054 Uiso 1 1 calc R . .
C27 C 1.2405(3) -0.1931(3) 0.60964(15) 0.0463(8) Uani 1 1 d . . .
H27A H 1.2998 -0.1706 0.6294 0.056 Uiso 1 1 calc R . .
H27B H 1.2868 -0.2774 0.6020 0.056 Uiso 1 1 calc R . .
C28 C 1.1407(3) -0.1915(3) 0.66991(16) 0.0494(8) Uani 1 1 d . . .
H28A H 1.0747 -0.2020 0.6476 0.059 Uiso 1 1 calc R . .
H28B H 1.1776 -0.2615 0.7140 0.059 Uiso 1 1 calc R . .
C29 C 1.0842(3) -0.0748(3) 0.69792(16) 0.0516(8) Uani 1 1 d . . .
H29A H 1.1486 -0.0654 0.7216 0.077 Uiso 1 1 calc R . .
H29B H 1.0202 -0.0777 0.7358 0.077 Uiso 1 1 calc R . .
H29C H 1.0469 -0.0052 0.6545 0.077 Uiso 1 1 calc R . .
C30 C 1.0477(2) -0.3893(2) 0.08710(13) 0.0259(6) Uani 1 1 d . . .
H30A H 1.1137 -0.4191 0.0496 0.031 Uiso 1 1 calc R . .
H30B H 0.9707 -0.3855 0.0686 0.031 Uiso 1 1 calc R . .
C31 C 1.0841(2) -0.4803(2) 0.16460(13) 0.0291(6) Uani 1 1 d . . .
H31A H 1.1126 -0.5637 0.1561 0.035 Uiso 1 1 calc R . .
H31B H 1.1552 -0.4762 0.1855 0.035 Uiso 1 1 calc R . .
C32 C 0.9830(2) -0.4615(2) 0.22463(13) 0.0312(6) Uani 1 1 d . . .
H32A H 0.9133 -0.4702 0.2056 0.037 Uiso 1 1 calc R . .
H32B H 0.9517 -0.3773 0.2323 0.037 Uiso 1 1 calc R . .
C33 C 1.0280(2) -0.5523(2) 0.30160(14) 0.0371(7) Uani 1 1 d . . .
H33A H 1.0626 -0.6365 0.2934 0.045 Uiso 1 1 calc R . .
H33B H 1.0956 -0.5412 0.3215 0.045 Uiso 1 1 calc R . .
C34 C 0.9267(3) -0.5378(2) 0.36128(14) 0.0403(7) Uani 1 1 d . . .
H34A H 0.8630 -0.5567 0.3434 0.048 Uiso 1 1 calc R . .
H34B H 0.8865 -0.4514 0.3656 0.048 Uiso 1 1 calc R . .
C35 C 0.9723(3) -0.6193(2) 0.44051(14) 0.0428(7) Uani 1 1 d . . .

H35A H 1.0318 -0.5968 0.4601 0.051 Uiso 1 1 calc R . .
H35B H 1.0169 -0.7054 0.4360 0.051 Uiso 1 1 calc R . .
C36 C 0.8676(3) -0.6088(3) 0.49812(15) 0.0449(8) Uani 1 1 d . . .
H36A H 0.8192 -0.5216 0.4994 0.054 Uiso 1 1 calc R . .
H36B H 0.8115 -0.6367 0.4800 0.054 Uiso 1 1 calc R . .
C37 C 0.9104(3) -0.6818(3) 0.57919(14) 0.0454(8) Uani 1 1 d . . .
H37A H 0.9622 -0.7685 0.5779 0.055 Uiso 1 1 calc R . .
H37B H 0.9626 -0.6509 0.5987 0.055 Uiso 1 1 calc R . .
C38 C 0.8038(3) -0.6745(3) 0.63394(15) 0.0505(8) Uani 1 1 d . . .
H38A H 0.7486 -0.5874 0.6321 0.061 Uiso 1 1 calc R . .
H38B H 0.7551 -0.7109 0.6164 0.061 Uiso 1 1 calc R . .
C39 C 0.8447(3) -0.7390(3) 0.71575(15) 0.0554(9) Uani 1 1 d . . .
H39A H 0.8957 -0.8263 0.7185 0.083 Uiso 1 1 calc R . .
H39B H 0.7718 -0.7289 0.7483 0.083 Uiso 1 1 calc R . .
H39C H 0.8933 -0.7038 0.7336 0.083 Uiso 1 1 calc R . .
C40 C 0.6317(2) 0.2515(2) 0.10590(13) 0.0282(6) Uani 1 1 d . . .
H40A H 0.5730 0.2383 0.0782 0.034 Uiso 1 1 calc R . .
H40B H 0.6302 0.3323 0.0806 0.034 Uiso 1 1 calc R . .
C41 C 0.5899(2) 0.2513(2) 0.18956(13) 0.0314(6) Uani 1 1 d . . .
H41A H 0.5915 0.1705 0.2149 0.038 Uiso 1 1 calc R . .
H41B H 0.6484 0.2647 0.2173 0.038 Uiso 1 1 calc R . .
C42 C 0.4601(2) 0.3504(2) 0.19412(14) 0.0400(7) Uani 1 1 d . . .
H42A H 0.4004 0.3286 0.1742 0.048 Uiso 1 1 calc R . .
H42B H 0.4551 0.4283 0.1604 0.048 Uiso 1 1 calc R . .
C43 C 0.4217(3) 0.3700(2) 0.27520(14) 0.0404(7) Uani 1 1 d . . .
H43A H 0.4858 0.3840 0.2968 0.049 Uiso 1 1 calc R . .
H43B H 0.3434 0.4450 0.2718 0.049 Uiso 1 1 calc R . .
C44 C 0.4034(3) 0.2650(2) 0.33035(14) 0.0406(7) Uani 1 1 d . . .
H44A H 0.4805 0.1889 0.3329 0.049 Uiso 1 1 calc R . .
H44B H 0.3364 0.2530 0.3106 0.049 Uiso 1 1 calc R . .
C45 C 0.3705(3) 0.2880(2) 0.41091(14) 0.0402(7) Uani 1 1 d . . .
H45A H 0.4379 0.3001 0.4301 0.048 Uiso 1 1 calc R . .
H45B H 0.2942 0.3649 0.4077 0.048 Uiso 1 1 calc R . .
C46 C 0.3502(3) 0.1867(2) 0.46865(15) 0.0421(7) Uani 1 1 d . . .
H46A H 0.4255 0.1092 0.4711 0.051 Uiso 1 1 calc R . .
H46B H 0.2810 0.1762 0.4505 0.051 Uiso 1 1 calc R . .
C47 C 0.3210(3) 0.2105(2) 0.54912(14) 0.0420(7) Uani 1 1 d . . .
H47A H 0.3898 0.2221 0.5668 0.050 Uiso 1 1 calc R . .
H47B H 0.2453 0.2878 0.5465 0.050 Uiso 1 1 calc R . .
C48 C 0.3016(3) 0.1105(3) 0.60779(15) 0.0454(8) Uani 1 1 d . . .
H48A H 0.3771 0.0330 0.6108 0.054 Uiso 1 1 calc R . .
H48B H 0.2323 0.0990 0.5906 0.054 Uiso 1 1 calc R . .
C49 C 0.2730(3) 0.1375(3) 0.68718(15) 0.0551(9) Uani 1 1 d . . .
H49A H 0.3421 0.1471 0.7051 0.083 Uiso 1 1 calc R . .
H49B H 0.2612 0.0698 0.7227 0.083 Uiso 1 1 calc R . .
H49C H 0.1973 0.2132 0.6849 0.083 Uiso 1 1 calc R . .

B1 B 0.6745(3) 0.6356(3) 0.01532(18) 0.0313(7) Uani 1 1 d U . .
F1 F 0.63017(13) 0.55665(12) 0.00290(8) 0.0369(4) Uani 1 1 d U A .
F2 F 0.5997(2) 0.75490(17) -0.0180(2) 0.0765(9) Uani 0.884(3) 1 d PU A 1
F3 F 0.6629(2) 0.6318(3) 0.09546(12) 0.0801(9) Uani 0.884(3) 1 d PU A 1
F4 F 0.79510(15) 0.60504(15) -0.00256(12) 0.0496(6) Uani 0.884(3) 1 d PU A 1
F2' F 0.6094(17) 0.7289(18) 0.0271(10) 0.048(4) Uiso 0.116(3) 1 d PU A 2
F3' F 0.7601(16) 0.5836(14) 0.0717(10) 0.060(4) Uiso 0.116(3) 1 d PU A 2
F4' F 0.7113(15) 0.6688(15) -0.0697(9) 0.067(4) Uiso 0.116(3) 1 d PU A 2
O1S O 0.6480(4) 0.5026(3) 0.2378(2) 0.0959(13) Uani 0.836(5) 1 d PU . .
H1S H 0.6558 0.5361 0.1922 0.144 Uiso 0.836(5) 1 calc PR . .
C1S C 0.5760(5) 0.5940(4) 0.2790(3) 0.0866(17) Uani 0.836(5) 1 d PU . .
H2S H 0.5795 0.5562 0.3339 0.130 Uiso 0.836(5) 1 calc PR . .
H3S H 0.4898 0.6333 0.2610 0.130 Uiso 0.836(5) 1 calc PR . .
H4S H 0.6091 0.6555 0.2704 0.130 Uiso 0.836(5) 1 calc PR . .

A-8: Crystallographic Information File (CIF) for $[1(NDodec)_3]^+BF_4^-$

.....

_chemical_name_common	triazatri-*n*-dodecyltriangulenium tetrafluoroborate
_chemical_formula_moiety	C_{55} H_{84} N_3, BF_4
_symmetry_cell_setting	triclinic
_symmetry_space_group_name_H-M	'P -1'

loop_
 _symmetry_equiv_pos_as_xyz
 'x, y, z'
 '-x, -y, -z'

_cell_length_a	11.9683(7)
_cell_length_b	12.3541(7)
_cell_length_c	20.1073(11)
_cell_angle_alpha	79.116(4)
_cell_angle_beta	87.642(4)
_cell_angle_gamma	64.684(4)
_cell_formula_units_Z	2

loop_
 _atom_site_label
 _atom_site_type_symbol
 _atom_site_fract_x
 _atom_site_fract_y
 _atom_site_fract_z
 _atom_site_U_iso_or_equiv

_atom_site_adp_type
_atom_site_occupancy
_atom_site_symmetry_multiplicity
_atom_site_calc_flag
_atom_site_refinement_flags
_atom_site_disorder_assembly
_atom_site_disorder_group
N1 N 0.73487(15) 0.33886(14) 0.91099(8) 0.0223(4) Uani 1 1 d . . .
N2 N 0.29215(15) 0.47337(15) 0.91466(8) 0.0243(4) Uani 1 1 d . . .
N3 N 0.46679(15) 0.75983(14) 0.91867(8) 0.0221(4) Uani 1 1 d . . .
C1 C 0.68865(19) 0.69403(18) 0.91265(10) 0.0261(4) Uani 1 1 d . . .
H1 H 0.6802 0.7742 0.9124 0.031 Uiso 1 1 calc R . .
C2 C 0.80416(19) 0.60015(18) 0.91077(10) 0.0263(4) Uani 1 1 d . . .
H2 H 0.8743 0.6176 0.9099 0.032 Uiso 1 1 calc R . .
C3 C 0.82296(19) 0.48277(18) 0.91009(10) 0.0257(4) Uani 1 1 d . . .
H3 H 0.9043 0.4209 0.9087 0.031 Uiso 1 1 calc R . .
C4 C 0.6478(2) 0.19652(18) 0.90398(10) 0.0282(5) Uani 1 1 d . . .
H4 H 0.7276 0.1332 0.9008 0.034 Uiso 1 1 calc R . .
C5 C 0.5443(2) 0.17513(19) 0.90364(11) 0.0305(5) Uani 1 1 d . . .
H5 H 0.5548 0.0955 0.9007 0.037 Uiso 1 1 calc R . .
C6 C 0.4261(2) 0.26315(19) 0.90741(10) 0.0291(5) Uani 1 1 d . . .
H6 H 0.3574 0.2439 0.9071 0.035 Uiso 1 1 calc R . .
C7 C 0.15787(19) 0.68313(19) 0.92102(10) 0.0289(5) Uani 1 1 d . . .
H7 H 0.0866 0.6678 0.9204 0.035 Uiso 1 1 calc R . .
C8 C 0.14599(19) 0.79747(19) 0.92514(10) 0.0287(5) Uani 1 1 d . . .
H8 H 0.0656 0.8592 0.9290 0.034 Uiso 1 1 calc R . .
C9 C 0.24475(19) 0.82670(18) 0.92400(10) 0.0267(4) Uani 1 1 d . . .
H9 H 0.2324 0.9074 0.9257 0.032 Uiso 1 1 calc R . .
C10 C 0.58473(18) 0.67070(17) 0.91494(9) 0.0216(4) Uani 1 1 d . . .
C11 C 0.60159(17) 0.54965(16) 0.91365(9) 0.0198(4) Uani 1 1 d . . .
C12 C 0.72155(18) 0.45544(17) 0.91137(9) 0.0218(4) Uani 1 1 d . . .
C13 C 0.63417(18) 0.31223(17) 0.90905(9) 0.0227(4) Uani 1 1 d . . .
C14 C 0.51356(18) 0.40521(17) 0.91227(9) 0.0215(4) Uani 1 1 d . . .
C15 C 0.40815(19) 0.38036(18) 0.91172(10) 0.0240(4) Uani 1 1 d . . .
C16 C 0.27464(18) 0.59058(18) 0.91783(9) 0.0236(4) Uani 1 1 d . . .
C17 C 0.37921(18) 0.61651(17) 0.91753(9) 0.0218(4) Uani 1 1 d . . .
C18 C 0.36358(18) 0.73569(17) 0.92035(9) 0.0219(4) Uani 1 1 d . . .
C19 C 0.49804(18) 0.52410(17) 0.91488(9) 0.0201(4) Uani 1 1 d . . .
C20 C 0.85928(19) 0.24180(18) 0.90681(10) 0.0262(4) Uani 1 1 d . . .
H20A H 0.8618 0.1625 0.9298 0.031 Uiso 1 1 calc R . .
H20B H 0.9203 0.2571 0.9307 0.031 Uiso 1 1 calc R . .
C21 C 0.89454(19) 0.23539(19) 0.83392(10) 0.0292(5) Uani 1 1 d . . .
H21A H 0.8955 0.3135 0.8115 0.035 Uiso 1 1 calc R . .
H21B H 0.8315 0.2237 0.8095 0.035 Uiso 1 1 calc R . .
C22 C 1.0205(2) 0.1319(2) 0.82942(11) 0.0367(5) Uani 1 1 d . . .
H22A H 1.0232 0.0563 0.8583 0.044 Uiso 1 1 calc R . .

H22B H 1.0844 0.1504 0.8479 0.044 Uiso 1 1 calc R . .
C23 C 1.0526(2) 0.1088(2) 0.75794(11) 0.0381(5) Uani 1 1 d . . .
H23A H 1.1286 0.0318 0.7606 0.046 Uiso 1 1 calc R . .
H23B H 0.9850 0.0972 0.7382 0.046 Uiso 1 1 calc R . .
C24 C 1.0728(2) 0.2089(2) 0.71042(11) 0.0345(5) Uani 1 1 d . . .
H24A H 1.1435 0.2179 0.7283 0.041 Uiso 1 1 calc R . .
H24B H 0.9984 0.2870 0.7088 0.041 Uiso 1 1 calc R . .
C25 C 1.0984(2) 0.1827(2) 0.63897(11) 0.0370(5) Uani 1 1 d . . .
H25A H 1.1717 0.1036 0.6412 0.044 Uiso 1 1 calc R . .
H25B H 1.0271 0.1743 0.6213 0.044 Uiso 1 1 calc R . .
C26 C 1.1211(2) 0.2789(2) 0.58948(11) 0.0357(5) Uani 1 1 d . . .
H26A H 1.1944 0.2855 0.6060 0.043 Uiso 1 1 calc R . .
H26B H 1.0490 0.3587 0.5879 0.043 Uiso 1 1 calc R . .
C27 C 1.1423(2) 0.2515(2) 0.51798(11) 0.0366(5) Uani 1 1 d . . .
H27A H 1.2129 0.1707 0.5199 0.044 Uiso 1 1 calc R . .
H27B H 1.0682 0.2469 0.5013 0.044 Uiso 1 1 calc R . .
C28 C 1.1684(2) 0.3451(2) 0.46790(11) 0.0363(5) Uani 1 1 d . . .
H28A H 1.2434 0.3490 0.4842 0.044 Uiso 1 1 calc R . .
H28B H 1.0984 0.4262 0.4664 0.044 Uiso 1 1 calc R . .
C29 C 1.1877(2) 0.3181(2) 0.39657(11) 0.0379(5) Uani 1 1 d . . .
H29A H 1.2567 0.2363 0.3983 0.046 Uiso 1 1 calc R . .
H29B H 1.1122 0.3158 0.3800 0.046 Uiso 1 1 calc R . .
C30 C 1.2161(2) 0.4098(2) 0.34671(12) 0.0426(6) Uani 1 1 d . . .
H30A H 1.2920 0.4119 0.3630 0.051 Uiso 1 1 calc R . .
H30B H 1.1473 0.4917 0.3449 0.051 Uiso 1 1 calc R . .
C31 C 1.2346(3) 0.3815(2) 0.27573(12) 0.0487(6) Uani 1 1 d . . .
H31A H 1.3036 0.3010 0.2769 0.073 Uiso 1 1 calc R . .
H31B H 1.2533 0.4435 0.2458 0.073 Uiso 1 1 calc R . .
H31C H 1.1590 0.3817 0.2587 0.073 Uiso 1 1 calc R . .
C32 C 0.1817(2) 0.4511(2) 0.90854(11) 0.0302(5) Uani 1 1 d . . .
H32A H 0.1201 0.4927 0.9404 0.036 Uiso 1 1 calc R . .
H32B H 0.2053 0.3626 0.9217 0.036 Uiso 1 1 calc R . .
C33 C 0.1228(2) 0.4962(2) 0.83712(11) 0.0355(5) Uani 1 1 d . . .
H33A H 0.0559 0.4698 0.8353 0.043 Uiso 1 1 calc R . .
H33B H 0.0844 0.5864 0.8278 0.043 Uiso 1 1 calc R . .
C34 C 0.2107(2) 0.4522(2) 0.78140(11) 0.0371(5) Uani 1 1 d . . .
H34A H 0.2397 0.3630 0.7863 0.045 Uiso 1 1 calc R . .
H34B H 0.2838 0.4681 0.7868 0.045 Uiso 1 1 calc R . .
C35 C 0.1518(2) 0.5137(2) 0.71055(11) 0.0386(5) Uani 1 1 d . . .
H35A H 0.0926 0.4814 0.7008 0.046 Uiso 1 1 calc R . .
H35B H 0.1046 0.6023 0.7091 0.046 Uiso 1 1 calc R . .
C36 C 0.2462(2) 0.4937(2) 0.65590(11) 0.0371(5) Uani 1 1 d . . .
H36A H 0.3115 0.5155 0.6691 0.044 Uiso 1 1 calc R . .
H36B H 0.2856 0.4059 0.6536 0.044 Uiso 1 1 calc R . .
C37 C 0.1931(2) 0.5662(2) 0.58622(11) 0.0362(5) Uani 1 1 d . . .
H37A H 0.1442 0.6528 0.5895 0.043 Uiso 1 1 calc R . .

H37B H 0.1360 0.5365 0.5703 0.043 Uiso 1 1 calc R . .
C38 C 0.2906(2) 0.5579(2) 0.53426(11) 0.0372(5) Uani 1 1 d . . .
H38A H 0.3511 0.5820 0.5518 0.045 Uiso 1 1 calc R . .
H38B H 0.3356 0.4720 0.5287 0.045 Uiso 1 1 calc R . .
C39 C 0.2388(2) 0.6371(2) 0.46567(11) 0.0383(5) Uani 1 1 d . . .
H39A H 0.1921 0.7227 0.4715 0.046 Uiso 1 1 calc R . .
H39B H 0.1798 0.6118 0.4477 0.046 Uiso 1 1 calc R . .
C40 C 0.3361(2) 0.6314(2) 0.41407(11) 0.0377(5) Uani 1 1 d . . .
H40A H 0.3796 0.5468 0.4062 0.045 Uiso 1 1 calc R . .
H40B H 0.3977 0.6524 0.4329 0.045 Uiso 1 1 calc R . .
C41 C 0.2834(2) 0.7165(2) 0.34669(12) 0.0405(6) Uani 1 1 d . . .
H41A H 0.2403 0.8011 0.3547 0.049 Uiso 1 1 calc R . .
H41B H 0.2210 0.6960 0.3283 0.049 Uiso 1 1 calc R . .
C42 C 0.3791(2) 0.7114(2) 0.29398(12) 0.0458(6) Uani 1 1 d . . .
H42A H 0.3410 0.7812 0.2559 0.055 Uiso 1 1 calc R . .
H42B H 0.4480 0.7201 0.3145 0.055 Uiso 1 1 calc R . .
C43 C 0.4302(2) 0.5953(2) 0.26689(12) 0.0475(6) Uani 1 1 d . . .
H43A H 0.4720 0.5261 0.3039 0.071 Uiso 1 1 calc R . .
H43B H 0.4895 0.5980 0.2323 0.071 Uiso 1 1 calc R . .
H43C H 0.3625 0.5858 0.2468 0.071 Uiso 1 1 calc R . .
C44 C 0.44638(19) 0.88578(16) 0.92064(10) 0.0264(4) Uani 1 1 d . . .
H44A H 0.5245 0.8849 0.9357 0.032 Uiso 1 1 calc R . .
H44B H 0.3839 0.9176 0.9543 0.032 Uiso 1 1 calc R . .
C45 C 0.4028(2) 0.97073(18) 0.85234(11) 0.0305(5) Uani 1 1 d . . .
H45A H 0.3306 0.9633 0.8352 0.037 Uiso 1 1 calc R . .
H45B H 0.3742 1.0556 0.8592 0.037 Uiso 1 1 calc R . .
C46 C 0.4981(2) 0.94895(18) 0.79831(11) 0.0304(5) Uani 1 1 d . . .
H46A H 0.5693 0.9596 0.8142 0.037 Uiso 1 1 calc R . .
H46B H 0.5286 0.8637 0.7917 0.037 Uiso 1 1 calc R . .
C47 C 0.4467(2) 1.0345(2) 0.73111(11) 0.0357(5) Uani 1 1 d . . .
H47A H 0.3782 1.0207 0.7143 0.043 Uiso 1 1 calc R . .
H47B H 0.4120 1.1196 0.7385 0.043 Uiso 1 1 calc R . .
C48 C 0.5417(2) 1.0190(2) 0.67737(11) 0.0368(5) Uani 1 1 d . . .
H48A H 0.5801 0.9326 0.6721 0.044 Uiso 1 1 calc R . .
H48B H 0.6077 1.0377 0.6931 0.044 Uiso 1 1 calc R . .
C49 C 0.4896(2) 1.0990(2) 0.60875(11) 0.0371(5) Uani 1 1 d . . .
H49A H 0.4279 1.0764 0.5912 0.045 Uiso 1 1 calc R . .
H49B H 0.4464 1.1851 0.6142 0.045 Uiso 1 1 calc R . .
C50 C 0.5887(2) 1.0872(2) 0.55766(11) 0.0384(5) Uani 1 1 d . . .
H50A H 0.6340 1.0002 0.5542 0.046 Uiso 1 1 calc R . .
H50B H 0.6484 1.1124 0.5749 0.046 Uiso 1 1 calc R . .
C51 C 0.5412(2) 1.1616(2) 0.48726(11) 0.0401(6) Uani 1 1 d . . .
H51A H 0.4850 1.1337 0.4686 0.048 Uiso 1 1 calc R . .
H51B H 0.4929 1.2483 0.4905 0.048 Uiso 1 1 calc R . .
C52 C 0.6445(2) 1.1510(2) 0.43928(11) 0.0411(6) Uani 1 1 d . . .
H52A H 0.6957 1.0635 0.4388 0.049 Uiso 1 1 calc R . .

H52B H 0.6980 1.1827 0.4572 0.049 Uiso 1 1 calc R . .
C53 C 0.6026(3) 1.2178(2) 0.36689(11) 0.0448(6) Uani 1 1 d . . .
H53A H 0.5518 1.1842 0.3480 0.054 Uiso 1 1 calc R . .
H53B H 0.5497 1.3050 0.3671 0.054 Uiso 1 1 calc R . .
C54 C 0.7089(3) 1.2078(2) 0.32154(12) 0.0485(7) Uani 1 1 d . . .
H54A H 0.7559 1.2469 0.3387 0.058 Uiso 1 1 calc R . .
H54B H 0.7653 1.1204 0.3243 0.058 Uiso 1 1 calc R . .
C55 C 0.6703(3) 1.2651(3) 0.24856(12) 0.0543(7) Uani 1 1 d . . .
H55A H 0.6260 1.2252 0.2306 0.082 Uiso 1 1 calc R . .
H55B H 0.7438 1.2555 0.2224 0.082 Uiso 1 1 calc R . .
H55C H 0.6158 1.3521 0.2450 0.082 Uiso 1 1 calc R . .
B1A B 0.1731(2) 0.1389(2) 1.00643(15) 0.0350(6) Uani 0.391(3) 1 d PDU A 1
F1A F 0.117(2) 0.0647(17) 1.0022(14) 0.0295(13) Uani 0.391(3) 1 d PDU A 1
F2A F 0.1773(6) 0.1258(6) 1.0839(2) 0.0635(14) Uani 0.391(3) 1 d PDU A 1
F3A F 0.2858(7) 0.1113(10) 0.9908(4) 0.047(2) Uani 0.391(3) 1 d PDU A 1
F4A F 0.0911(8) 0.2586(7) 0.9866(5) 0.052(2) Uani 0.391(3) 1 d PDU A 1
B1B B 0.1731(2) 0.1389(2) 1.00643(15) 0.0350(6) Uani 0.306(5) 1 d PDU B 2
F1B F 0.126(2) 0.056(2) 1.0077(15) 0.0295(13) Uani 0.306(5) 1 d PDU B 2
F2B F 0.2795(8) 0.0884(7) 1.0456(6) 0.063(2) Uani 0.306(5) 1 d PDU B 2
F3B F 0.0958(9) 0.2473(8) 1.0144(5) 0.0267(18) Uani 0.306(5) 1 d PDU B 2
F4B F 0.2113(8) 0.1551(7) 0.9343(3) 0.0526(18) Uani 0.306(5) 1 d PDU B 2
B1C B 0.1731(2) 0.1389(2) 1.00643(15) 0.0350(6) Uani 0.303(5) 1 d PDU C 3
F1C F 0.1403(18) 0.0489(15) 1.0007(14) 0.0295(13) Uani 0.303(5) 1 d PDU C 3
F2C F 0.3013(9) 0.0919(12) 1.0123(6) 0.030(2) Uani 0.303(5) 1 d PDU C 3
F3C F 0.1224(6) 0.2056(9) 1.0554(6) 0.052(2) Uani 0.303(5) 1 d PDU C 3
F4C F 0.1396(9) 0.2222(7) 0.9405(4) 0.059(2) Uani 0.303(5) 1 d PDU C 3

A-9: Crystallographic Information File (CIF) for [1(NHexadec)$_3$]$^+$BF$_4^-$

.....

_chemical_name_common	triazatri-*n*-hexadecyltriangulenium tetrafluoroborate
_chemical_formula_moiety	C_{67} H_{108} N_3, B F_4
_symmetry_cell_setting	triclinic
_symmetry_space_group_name_H-M	'P -1'

loop_
 _symmetry_equiv_pos_as_xyz
 'x, y, z'
 '-x, -y, -z'

_cell_length_a	11.9982(7)
_cell_length_b	12.7366(8)
_cell_length_c	25.4451(15)

_cell_angle_alpha 90.348(4)
_cell_angle_beta 93.934(4)
_cell_angle_gamma 117.721(3)
_cell_formula_units_Z 2

loop_
_atom_site_label
_atom_site_type_symbol
_atom_site_fract_x
_atom_site_fract_y
_atom_site_fract_z
_atom_site_U_iso_or_equiv
_atom_site_adp_type
_atom_site_occupancy
_atom_site_symmetry_multiplicity
_atom_site_calc_flag
_atom_site_refinement_flags
_atom_site_disorder_assembly
_atom_site_disorder_group
N1 N 0.7318(2) 0.52653(19) 0.93185(10) 0.0483(6) Uani 1 1 d . . .
N2 N 0.2842(2) 0.26529(18) 0.92567(9) 0.0478(6) Uani 1 1 d . . .
N3 N 0.4421(2) 0.68909(19) 0.94077(10) 0.0512(7) Uani 1 1 d . . .
C1 C 0.6684(3) 0.8207(2) 0.94609(12) 0.0549(8) Uani 1 1 d . . .
H1 H 0.6561 0.8882 0.9488 0.066 Uiso 1 1 calc R . .
C2 C 0.7867(3) 0.8326(3) 0.94691(12) 0.0559(8) Uani 1 1 d . . .
H2 H 0.8553 0.9095 0.9511 0.067 Uiso 1 1 calc R . .
C3 C 0.8118(3) 0.7395(3) 0.94194(12) 0.0545(8) Uani 1 1 d . . .
H3 H 0.8957 0.7526 0.9420 0.065 Uiso 1 1 calc R . .
C4 C 0.6524(3) 0.3138(3) 0.92348(14) 0.0616(9) Uani 1 1 d . . .
H4 H 0.7346 0.3228 0.9229 0.074 Uiso 1 1 calc R . .
C5 C 0.5506(3) 0.2031(3) 0.92021(14) 0.0664(10) Uani 1 1 d . . .
H5 H 0.5654 0.1371 0.9175 0.080 Uiso 1 1 calc R . .
C6 C 0.4281(3) 0.1831(2) 0.92062(13) 0.0558(8) Uani 1 1 d . . .
H6 H 0.3612 0.1053 0.9181 0.067 Uiso 1 1 calc R . .
C7 C 0.1377(3) 0.3466(3) 0.92753(13) 0.0572(8) Uani 1 1 d . . .
H7 H 0.0682 0.2702 0.9242 0.069 Uiso 1 1 calc R . .
C8 C 0.1193(3) 0.4434(3) 0.93185(14) 0.0631(9) Uani 1 1 d . . .
H8 H 0.0359 0.4316 0.9316 0.076 Uiso 1 1 calc R . .
C9 C 0.2160(3) 0.5577(3) 0.93654(13) 0.0597(9) Uani 1 1 d . . .
H9 H 0.1985 0.6221 0.9396 0.072 Uiso 1 1 calc R . .
C10 C 0.5649(3) 0.7077(2) 0.94122(11) 0.0456(7) Uani 1 1 d . . .
C11 C 0.5880(3) 0.6089(2) 0.93698(10) 0.0411(7) Uani 1 1 d . . .
C12 C 0.7123(3) 0.6249(2) 0.93675(11) 0.0458(7) Uani 1 1 d . . .
C13 C 0.6330(3) 0.4124(2) 0.92769(12) 0.0470(7) Uani 1 1 d . . .
C14 C 0.5083(3) 0.3954(2) 0.92812(11) 0.0412(7) Uani 1 1 d . . .
C15 C 0.4045(3) 0.2789(2) 0.92473(11) 0.0454(7) Uani 1 1 d . . .

C16 C 0.2586(3) 0.3607(2) 0.92802(11) 0.0473(7) Uani 1 1 d . . .
C17 C 0.3620(3) 0.4773(2) 0.93225(10) 0.0422(7) Uani 1 1 d . . .
C18 C 0.3395(3) 0.5769(2) 0.93672(11) 0.0468(7) Uani 1 1 d . . .
C19 C 0.4859(3) 0.4941(2) 0.93249(10) 0.0397(7) Uani 1 1 d . . .
C20 C 0.8626(3) 0.5476(3) 0.92776(13) 0.0583(9) Uani 1 1 d . . .
H20A H 0.8677 0.4749 0.9360 0.070 Uiso 1 1 calc R . .
H20B H 0.9188 0.6098 0.9539 0.070 Uiso 1 1 calc R . .
C21 C 0.9079(3) 0.5847(3) 0.87346(14) 0.0696(10) Uani 1 1 d . . .
H21A H 0.9118 0.6621 0.8673 0.084 Uiso 1 1 calc R . .
H21B H 0.9941 0.5950 0.8733 0.084 Uiso 1 1 calc R . .
C22 C 0.8295(4) 0.5013(3) 0.82879(14) 0.0771(10) Uani 1 1 d . . .
H22A H 0.7412 0.4826 0.8316 0.092 Uiso 1 1 calc R . .
H22B H 0.8349 0.4272 0.8324 0.092 Uiso 1 1 calc R . .
C23 C 0.8652(3) 0.5456(3) 0.77450(14) 0.0761(10) Uani 1 1 d . . .
H23A H 0.8717 0.6251 0.7726 0.091 Uiso 1 1 calc R . .
H23B H 0.9490 0.5533 0.7698 0.091 Uiso 1 1 calc R . .
C24 C 0.7764(4) 0.4698(4) 0.73031(15) 0.0927(13) Uani 1 1 d . . .
H24A H 0.6917 0.4572 0.7370 0.111 Uiso 1 1 calc R . .
H24B H 0.7748 0.3922 0.7312 0.111 Uiso 1 1 calc R . .
C25 C 0.8014(4) 0.5128(4) 0.67600(16) 0.0897(12) Uani 1 1 d . . .
H25A H 0.8092 0.5928 0.6755 0.108 Uiso 1 1 calc R . .
H25B H 0.8831 0.5193 0.6681 0.108 Uiso 1 1 calc R . .
C26 C 0.7057(5) 0.4389(4) 0.63325(16) 0.1032(14) Uani 1 1 d . . .
H26A H 0.6989 0.3592 0.6338 0.124 Uiso 1 1 calc R . .
H26B H 0.6240 0.4314 0.6419 0.124 Uiso 1 1 calc R . .
C27 C 0.7255(5) 0.4790(4) 0.57853(16) 0.0984(13) Uani 1 1 d . . .
H27A H 0.8058 0.4843 0.5693 0.118 Uiso 1 1 calc R . .
H27B H 0.7339 0.5593 0.5778 0.118 Uiso 1 1 calc R . .
C28 C 0.6258(5) 0.4039(4) 0.53722(16) 0.1077(15) Uani 1 1 d . . .
H28A H 0.6167 0.3234 0.5385 0.129 Uiso 1 1 calc R . .
H28B H 0.5458 0.3994 0.5465 0.129 Uiso 1 1 calc R . .
C29 C 0.6441(5) 0.4411(4) 0.48225(16) 0.1038(14) Uani 1 1 d . . .
H29A H 0.7237 0.4449 0.4729 0.125 Uiso 1 1 calc R . .
H29B H 0.6539 0.5219 0.4811 0.125 Uiso 1 1 calc R . .
C30 C 0.5437(5) 0.3664(4) 0.44106(17) 0.1122(16) Uani 1 1 d . . .
H30A H 0.5328 0.2854 0.4430 0.135 Uiso 1 1 calc R . .
H30B H 0.4646 0.3640 0.4503 0.135 Uiso 1 1 calc R . .
C31 C 0.5601(5) 0.3996(4) 0.38616(17) 0.1067(15) Uani 1 1 d . . .
H31A H 0.6392 0.4019 0.3769 0.128 Uiso 1 1 calc R . .
H31B H 0.5713 0.4807 0.3842 0.128 Uiso 1 1 calc R . .
C32 C 0.4608(5) 0.3259(4) 0.34527(18) 0.1192(17) Uani 1 1 d . . .
H32A H 0.3816 0.3230 0.3547 0.143 Uiso 1 1 calc R . .
H32B H 0.4502 0.2449 0.3470 0.143 Uiso 1 1 calc R . .
C33 C 0.4765(5) 0.3596(4) 0.28979(17) 0.1075(15) Uani 1 1 d . . .
H33A H 0.4867 0.4404 0.2879 0.129 Uiso 1 1 calc R . .
H33B H 0.5557 0.3627 0.2803 0.129 Uiso 1 1 calc R . .

C34 C 0.3769(6) 0.2850(5) 0.24923(19) 0.1323(19) Uani 1 1 d . . .
H34A H 0.3660 0.2040 0.2512 0.159 Uiso 1 1 calc R . .
H34B H 0.2977 0.2826 0.2584 0.159 Uiso 1 1 calc R . .
C35 C 0.3947(6) 0.3193(5) 0.19433(18) 0.1307(19) Uani 1 1 d . . .
H35A H 0.3974 0.3962 0.1906 0.196 Uiso 1 1 calc R . .
H35B H 0.3250 0.2606 0.1715 0.196 Uiso 1 1 calc R . .
H35C H 0.4734 0.3237 0.1845 0.196 Uiso 1 1 calc R . .
C36 C 0.1778(3) 0.1439(2) 0.92009(12) 0.0545(8) Uani 1 1 d . . .
H36A H 0.1047 0.1424 0.9357 0.065 Uiso 1 1 calc R . .
H36B H 0.2013 0.0897 0.9393 0.065 Uiso 1 1 calc R . .
C37 C 0.1424(3) 0.1019(3) 0.86255(13) 0.0660(9) Uani 1 1 d . . .
H37A H 0.1111 0.1516 0.8442 0.079 Uiso 1 1 calc R . .
H37B H 0.2179 0.1114 0.8462 0.079 Uiso 1 1 calc R . .
C38 C 0.0436(4) -0.0250(3) 0.85599(16) 0.0915(13) Uani 1 1 d . . .
H38A H -0.0381 -0.0302 0.8630 0.110 Uiso 1 1 calc R . .
H38B H 0.0635 -0.0709 0.8823 0.110 Uiso 1 1 calc R . .
C39 C 0.0318(5) -0.0804(3) 0.80179(17) 0.1060(15) Uani 1 1 d . . .
H39A H 0.1136 -0.0756 0.7955 0.127 Uiso 1 1 calc R . .
H39B H -0.0292 -0.1647 0.8023 0.127 Uiso 1 1 calc R . .
C40 C -0.0072(4) -0.0296(3) 0.75670(16) 0.0915(13) Uani 1 1 d . . .
H40A H 0.0559 0.0537 0.7547 0.110 Uiso 1 1 calc R . .
H40B H -0.0874 -0.0312 0.7633 0.110 Uiso 1 1 calc R . .
C41 C -0.0230(5) -0.0916(4) 0.70432(17) 0.0994(14) Uani 1 1 d . . .
H41A H 0.0600 -0.0818 0.6964 0.119 Uiso 1 1 calc R . .
H41B H -0.0773 -0.1767 0.7082 0.119 Uiso 1 1 calc R . .
C42 C -0.0755(4) -0.0554(4) 0.65836(17) 0.0975(13) Uani 1 1 d . . .
H42A H -0.0194 0.0288 0.6534 0.117 Uiso 1 1 calc R . .
H42B H -0.1572 -0.0624 0.6666 0.117 Uiso 1 1 calc R . .
C43 C -0.0942(5) -0.1216(4) 0.60754(16) 0.0974(13) Uani 1 1 d . . .
H43A H -0.0116 -0.1114 0.5988 0.117 Uiso 1 1 calc R . .
H43B H -0.1466 -0.2062 0.6132 0.117 Uiso 1 1 calc R . .
C44 C -0.1518(5) -0.0912(4) 0.56125(17) 0.1032(14) Uani 1 1 d . . .
H44A H -0.0985 -0.0071 0.5551 0.124 Uiso 1 1 calc R . .
H44B H -0.2337 -0.0999 0.5703 0.124 Uiso 1 1 calc R . .
C45 C -0.1728(5) -0.1589(4) 0.51071(16) 0.0982(13) Uani 1 1 d . . .
H45A H -0.0907 -0.1497 0.5017 0.118 Uiso 1 1 calc R . .
H45B H -0.2253 -0.2431 0.5171 0.118 Uiso 1 1 calc R . .
C46 C -0.2313(5) -0.1309(4) 0.46394(17) 0.1063(15) Uani 1 1 d . . .
H46A H -0.3134 -0.1400 0.4728 0.128 Uiso 1 1 calc R . .
H46B H -0.1787 -0.0468 0.4574 0.128 Uiso 1 1 calc R . .
C47 C -0.2516(5) -0.1988(4) 0.41435(17) 0.1002(14) Uani 1 1 d . . .
H47A H -0.1695 -0.1899 0.4056 0.120 Uiso 1 1 calc R . .
H47B H -0.3044 -0.2828 0.4210 0.120 Uiso 1 1 calc R . .
C48 C -0.3091(5) -0.1714(4) 0.36773(18) 0.1131(16) Uani 1 1 d . . .
H48A H -0.2548 -0.0880 0.3606 0.136 Uiso 1 1 calc R . .
H48B H -0.3899 -0.1776 0.3769 0.136 Uiso 1 1 calc R . .

C49 C -0.3338(5) -0.2413(4) 0.31794(17) 0.1073(15) Uani 1 1 d . . .
H49A H -0.2531 -0.2357 0.3089 0.129 Uiso 1 1 calc R . .
H49B H -0.3886 -0.3246 0.3251 0.129 Uiso 1 1 calc R . .
C50 C -0.3909(6) -0.2132(5) 0.2706(2) 0.1287(18) Uani 1 1 d . . .
H50A H -0.3328 -0.1322 0.2615 0.154 Uiso 1 1 calc R . .
H50B H -0.4684 -0.2127 0.2801 0.154 Uiso 1 1 calc R . .
C51 C -0.4232(5) -0.2916(5) 0.22233(19) 0.1312(19) Uani 1 1 d . . .
H51A H -0.3463 -0.2852 0.2092 0.197 Uiso 1 1 calc R . .
H51B H -0.4673 -0.2676 0.1956 0.197 Uiso 1 1 calc R . .
H51C H -0.4771 -0.3732 0.2308 0.197 Uiso 1 1 calc R . .
C52 C 0.4219(3) 0.7949(3) 0.94460(14) 0.0639(9) Uani 1 1 d . . .
H52A H 0.4856 0.8524 0.9705 0.077 Uiso 1 1 calc R . .
H52B H 0.3387 0.7712 0.9575 0.077 Uiso 1 1 calc R . .
C53 C 0.4289(4) 0.8542(3) 0.89336(16) 0.0799(11) Uani 1 1 d . . .
H53A H 0.4225 0.9270 0.9002 0.096 Uiso 1 1 calc R . .
H53B H 0.5124 0.8779 0.8809 0.096 Uiso 1 1 calc R . .
C54 C 0.3324(4) 0.7837(3) 0.85033(17) 0.0840(12) Uani 1 1 d . . .
H54A H 0.2489 0.7660 0.8613 0.101 Uiso 1 1 calc R . .
H54B H 0.3337 0.7079 0.8451 0.101 Uiso 1 1 calc R . .
C55 C 0.3504(4) 0.8442(4) 0.79803(17) 0.0922(13) Uani 1 1 d . . .
H55A H 0.3449 0.9180 0.8028 0.111 Uiso 1 1 calc R . .
H55B H 0.4355 0.8655 0.7880 0.111 Uiso 1 1 calc R . .
C56 C 0.2573(4) 0.7710(4) 0.75420(18) 0.0965(13) Uani 1 1 d . . .
H56A H 0.1732 0.7566 0.7630 0.116 Uiso 1 1 calc R . .
H56B H 0.2566 0.6939 0.7522 0.116 Uiso 1 1 calc R . .
C57 C 0.2787(4) 0.8221(4) 0.70052(18) 0.1016(14) Uani 1 1 d . . .
H57A H 0.2769 0.8982 0.7020 0.122 Uiso 1 1 calc R . .
H57B H 0.3633 0.8381 0.6918 0.122 Uiso 1 1 calc R . .
C58 C 0.1852(5) 0.7450(4) 0.65740(18) 0.1032(14) Uani 1 1 d . . .
H58A H 0.1841 0.6676 0.6575 0.124 Uiso 1 1 calc R . .
H58B H 0.1014 0.7322 0.6658 0.124 Uiso 1 1 calc R . .
C59 C 0.2052(5) 0.7883(4) 0.60328(18) 0.1053(14) Uani 1 1 d . . .
H59A H 0.2886 0.8004 0.5946 0.126 Uiso 1 1 calc R . .
H59B H 0.2067 0.8659 0.6029 0.126 Uiso 1 1 calc R . .
C60 C 0.1099(5) 0.7098(4) 0.56133(18) 0.1047(14) Uani 1 1 d . . .
H60A H 0.0269 0.6985 0.5701 0.126 Uiso 1 1 calc R . .
H60B H 0.1078 0.6320 0.5622 0.126 Uiso 1 1 calc R . .
C61 C 0.1287(5) 0.7508(4) 0.50607(19) 0.1100(15) Uani 1 1 d . . .
H61A H 0.1311 0.8288 0.5051 0.132 Uiso 1 1 calc R . .
H61B H 0.2114 0.7616 0.4972 0.132 Uiso 1 1 calc R . .
C62 C 0.0320(5) 0.6715(4) 0.46447(19) 0.1091(15) Uani 1 1 d . . .
H62A H -0.0506 0.6608 0.4735 0.131 Uiso 1 1 calc R . .
H62B H 0.0296 0.5936 0.4656 0.131 Uiso 1 1 calc R . .
C63 C 0.0492(5) 0.7109(4) 0.40900(19) 0.1106(15) Uani 1 1 d . . .
H63A H 0.0502 0.7882 0.4076 0.133 Uiso 1 1 calc R . .
H63B H 0.1322 0.7225 0.3999 0.133 Uiso 1 1 calc R . .

C64 C -0.0465(5) 0.6303(4) 0.36862(19) 0.1126(16) Uani 1 1 d . . .
H64A H -0.1292 0.6187 0.3781 0.135 Uiso 1 1 calc R . .
H64B H -0.0474 0.5531 0.3705 0.135 Uiso 1 1 calc R . .
C65 C -0.0341(5) 0.6650(4) 0.3129(2) 0.1157(16) Uani 1 1 d . . .
H65A H -0.0361 0.7409 0.3106 0.139 Uiso 1 1 calc R . .
H65B H 0.0495 0.6789 0.3035 0.139 Uiso 1 1 calc R . .
C66 C -0.1288(6) 0.5815(5) 0.2728(2) 0.138(2) Uani 1 1 d . . .
H66A H -0.2120 0.5681 0.2823 0.165 Uiso 1 1 calc R . .
H66B H -0.1270 0.5055 0.2755 0.165 Uiso 1 1 calc R . .
C67 C -0.1190(7) 0.6125(6) 0.2168(2) 0.166(3) Uani 1 1 d . . .
H67A H -0.1236 0.6861 0.2126 0.249 Uiso 1 1 calc R . .
H67B H -0.1880 0.5495 0.1954 0.249 Uiso 1 1 calc R . .
H67C H -0.0392 0.6222 0.2057 0.249 Uiso 1 1 calc R . .
B1 B 1.1703(8) 0.8494(7) 0.9983(4) 0.0693(19) Uani 0.688(5) 1 d PDU A 1
F1 F 1.1531(5) 0.8352(7) 0.9443(2) 0.149(2) Uani 0.688(5) 1 d PDU A 1
F2 F 1.0972(9) 0.8964(10) 1.0135(5) 0.104(3) Uani 0.688(5) 1 d PDU A 1
F3 F 1.2937(5) 0.9214(5) 1.0131(3) 0.099(2) Uani 0.688(5) 1 d PDU A 1
F4 F 1.1352(4) 0.7401(4) 1.0151(2) 0.1022(18) Uani 0.688(5) 1 d PDU A 1
B1' B 1.1658(17) 0.8535(16) 1.0056(7) 0.075(3) Uani 0.312(5) 1 d PDU A 2
F1' F 1.1243(8) 0.7524(8) 0.9769(6) 0.108(4) Uani 0.312(5) 1 d PDU A 2
F2' F 1.076(2) 0.888(2) 1.0007(9) 0.074(3) Uani 0.312(5) 1 d PDU A 2
F3' F 1.2744(12) 0.9310(11) 0.9863(6) 0.099(4) Uani 0.312(5) 1 d PDU A 2
F4' F 1.1825(9) 0.8372(11) 1.0580(4) 0.144(4) Uani 0.312(5) 1 d PDU A 2

A-10: Crystallographic Information File (CIF) for $[1(NPh)_2(O)]^+BF_4^-$

.....

_chemical_name_common	diazadiphenyloxatriangulenium tetrafluoroborate
_chemical_formula_moiety	C_{31} H_{19} N_2 O, B F_4
_symmetry_cell_setting	monoclinic
_symmetry_space_group_name_H-M	'P 21/c'

loop_
 _symmetry_equiv_pos_as_xyz
 'x, y, z'
 '-x, y+1/2, -z+1/2'
 '-x, -y, -z'
 'x, -y-1/2, z-1/2'

_cell_length_a	12.0712(10)
_cell_length_b	8.3175(6)
_cell_length_c	23.6419(17)
_cell_angle_alpha	90.00
_cell_angle_beta	104.330(3)

_cell_angle_gamma 90.00
_cell_formula_units_Z 4

loop_
 _atom_site_label
 _atom_site_type_symbol
 _atom_site_fract_x
 _atom_site_fract_y
 _atom_site_fract_z
 _atom_site_U_iso_or_equiv
 _atom_site_adp_type
 _atom_site_occupancy
 _atom_site_symmetry_multiplicity
 _atom_site_calc_flag
 _atom_site_refinement_flags
 _atom_site_disorder_assembly
 _atom_site_disorder_group
O1 O 0.67600(8) 0.18313(10) 0.65577(4) 0.0251(2) Uani 1 1 d . . .
N1 N 0.43002(9) 0.64352(12) 0.61690(4) 0.0221(2) Uani 1 1 d . . .
N2 N 0.76069(9) 0.64677(12) 0.77968(4) 0.0221(2) Uani 1 1 d . . .
C1 C 0.88610(11) 0.41270(16) 0.79817(6) 0.0253(3) Uani 1 1 d . . .
H1 H 0.9362 0.4630 0.8307 0.030 Uiso 1 1 calc R . .
C2 C 0.90776(11) 0.25894(16) 0.78195(6) 0.0274(3) Uani 1 1 d . . .
H2 H 0.9732 0.2045 0.8043 0.033 Uiso 1 1 calc R . .
C3 C 0.83826(11) 0.17956(15) 0.73434(6) 0.0270(3) Uani 1 1 d . . .
H3 H 0.8556 0.0737 0.7242 0.032 Uiso 1 1 calc R . .
C4 C 0.51265(11) 0.17364(15) 0.57770(6) 0.0263(3) Uani 1 1 d . . .
H4 H 0.5299 0.0658 0.5697 0.032 Uiso 1 1 calc R . .
C5 C 0.41781(11) 0.25194(16) 0.54355(6) 0.0274(3) Uani 1 1 d . . .
H5 H 0.3712 0.1960 0.5113 0.033 Uiso 1 1 calc R . .
C6 C 0.38818(11) 0.40673(16) 0.55421(5) 0.0259(3) Uani 1 1 d . . .
H6 H 0.3231 0.4565 0.5295 0.031 Uiso 1 1 calc R . .
C7 C 0.47509(11) 0.88388(15) 0.67619(5) 0.0231(3) Uani 1 1 d . . .
H7 H 0.4095 0.9382 0.6538 0.028 Uiso 1 1 calc R . .
C8 C 0.54886(11) 0.95975(15) 0.72258(5) 0.0241(3) Uani 1 1 d . . .
H8 H 0.5341 1.0687 0.7303 0.029 Uiso 1 1 calc R . .
C9 C 0.64296(11) 0.88576(15) 0.75838(5) 0.0236(3) Uani 1 1 d . . .
H9 H 0.6895 0.9414 0.7908 0.028 Uiso 1 1 calc R . .
C10 C 0.78976(10) 0.49332(15) 0.76621(5) 0.0221(3) Uani 1 1 d . . .
C11 C 0.71822(10) 0.41504(15) 0.71796(5) 0.0216(3) Uani 1 1 d . . .
C12 C 0.74434(11) 0.25938(15) 0.70284(5) 0.0233(3) Uani 1 1 d . . .
C13 C 0.58054(11) 0.25696(15) 0.62331(5) 0.0232(3) Uani 1 1 d . . .
C14 C 0.55258(10) 0.41326(15) 0.63643(5) 0.0216(3) Uani 1 1 d . . .
C15 C 0.45510(10) 0.48953(15) 0.60187(5) 0.0221(3) Uani 1 1 d . . .
C16 C 0.49849(10) 0.72724(15) 0.66295(5) 0.0211(3) Uani 1 1 d . . .
C17 C 0.59638(10) 0.64951(15) 0.69770(5) 0.0205(3) Uani 1 1 d . . .

C18 C 0.66818(10) 0.72910(15) 0.74623(5) 0.0213(3) Uani 1 1 d . . .
C19 C 0.62231(10) 0.49423(15) 0.68426(5) 0.0210(3) Uani 1 1 d . . .
C20 C 0.33242(10) 0.72408(15) 0.58047(5) 0.0226(3) Uani 1 1 d . . .
C21 C 0.34567(11) 0.80224(16) 0.53125(6) 0.0277(3) Uani 1 1 d . . .
H21 H 0.4178 0.8030 0.5219 0.033 Uiso 1 1 calc R . .
C22 C 0.25307(12) 0.87948(16) 0.49561(6) 0.0307(3) Uani 1 1 d . . .
H22 H 0.2610 0.9333 0.4614 0.037 Uiso 1 1 calc R . .
C23 C 0.14913(12) 0.87825(16) 0.50989(6) 0.0301(3) Uani 1 1 d . . .
H23 H 0.0856 0.9323 0.4856 0.036 Uiso 1 1 calc R . .
C24 C 0.13653(11) 0.79910(16) 0.55922(6) 0.0302(3) Uani 1 1 d . . .
H24 H 0.0645 0.7986 0.5687 0.036 Uiso 1 1 calc R . .
C25 C 0.22873(11) 0.72042(16) 0.59490(6) 0.0268(3) Uani 1 1 d . . .
H25 H 0.2206 0.6649 0.6288 0.032 Uiso 1 1 calc R . .
C26 C 0.83520(10) 0.72893(15) 0.82811(5) 0.0229(3) Uani 1 1 d . . .
C27 C 0.81494(11) 0.71898(16) 0.88289(6) 0.0277(3) Uani 1 1 d . . .
H27 H 0.7521 0.6586 0.8889 0.033 Uiso 1 1 calc R . .
C28 C 0.88755(12) 0.79830(17) 0.92892(6) 0.0323(3) Uani 1 1 d . . .
H28 H 0.8744 0.7935 0.9669 0.039 Uiso 1 1 calc R . .
C29 C 0.97893(12) 0.88424(16) 0.91951(6) 0.0336(3) Uani 1 1 d . . .
H29 H 1.0288 0.9384 0.9512 0.040 Uiso 1 1 calc R . .
C30 C 0.99884(12) 0.89251(16) 0.86458(6) 0.0324(3) Uani 1 1 d . . .
H30 H 1.0624 0.9514 0.8586 0.039 Uiso 1 1 calc R . .
C31 C 0.92611(11) 0.81486(15) 0.81838(6) 0.0275(3) Uani 1 1 d . . .
H31 H 0.9387 0.8207 0.7803 0.033 Uiso 1 1 calc R . .
B1 B 0.7973(7) -0.2283(10) 0.6081(4) 0.0254(15) Uani 0.573(5) 1 d PDU A 1
F1 F 0.6848(5) -0.1782(7) 0.5948(3) 0.0533(17) Uani 0.573(5) 1 d PDU A 1
F2 F 0.8230(6) -0.3134(6) 0.6596(2) 0.0367(9) Uani 0.573(5) 1 d PDU A 1
F3 F 0.81649(18) -0.3222(3) 0.56370(7) 0.0626(11) Uani 0.573(5) 1 d PDU A 1
F4 F 0.86774(17) -0.0973(3) 0.61576(13) 0.0649(10) Uani 0.573(5) 1 d PDU A 1
B1' B 0.7831(10) -0.2588(13) 0.6072(5) 0.029(2) Uani 0.427(5) 1 d PDU A 2
F1' F 0.6834(4) -0.1726(6) 0.5940(2) 0.0165(11) Uani 0.427(5) 1 d PDU A 2
F2' F 0.8254(9) -0.2690(10) 0.6668(4) 0.065(2) Uani 0.427(5) 1 d PDU A 2
F3' F 0.7572(2) -0.4127(3) 0.58665(13) 0.0607(12) Uani 0.427(5) 1 d PDU A 2
F4' F 0.8626(2) -0.1933(4) 0.58194(14) 0.0563(14) Uani 0.427(5) 1 d PDU A 2

A-11: Crystallographic Information File (CIF) for $[1(NPh)(O)_2]^+BF_4^-$

.....

_chemical_name_common	azaphenyldioxatriangulenium tetrafluoroborate
_chemical_formula_moiety	$C_{25}\ H_{14}\ N\ O_2$, $B\ F_4$
_symmetry_cell_setting	monoclinic
_symmetry_space_group_name_H-M	'P 21/n'

loop_

_symmetry_equiv_pos_as_xyz
'x, y, z'
'-x+1/2, y+1/2, -z+1/2'
'-x, -y, -z'
'x-1/2, -y-1/2, z-1/2'

_cell_length_a	8.8122(6)
_cell_length_b	14.8725(9)
_cell_length_c	14.6406(9)
_cell_angle_alpha	90.00
_cell_angle_beta	104.212(3)
_cell_angle_gamma	90.00
_cell_formula_units_Z	4

loop_
_atom_site_label
_atom_site_type_symbol
_atom_site_fract_x
_atom_site_fract_y
_atom_site_fract_z
_atom_site_U_iso_or_equiv
_atom_site_adp_type
_atom_site_occupancy
_atom_site_symmetry_multiplicity
_atom_site_calc_flag
_atom_site_refinement_flags
_atom_site_disorder_assembly
_atom_site_disorder_group
B1 B 0.06294(19) 0.20150(11) 0.30623(11) 0.0207(3) Uani 1 1 d . . .
F1 F 0.19048(10) 0.19466(6) 0.38265(6) 0.0277(2) Uani 1 1 d . . .
F2 F 0.08779(10) 0.14960(6) 0.23240(6) 0.0305(2) Uani 1 1 d . . .
F3 F -0.07195(10) 0.17433(6) 0.33026(6) 0.0297(2) Uani 1 1 d . . .
F4 F 0.04642(10) 0.29134(6) 0.27765(6) 0.0280(2) Uani 1 1 d . . .
N1 N 0.30487(13) 0.26068(7) 0.99506(8) 0.0184(3) Uani 1 1 d . . .
O1 O 0.21927(11) 0.00358(6) 0.78940(7) 0.0215(2) Uani 1 1 d . . .
C1 C 0.78142(17) 0.19302(10) 1.07830(10) 0.0228(3) Uani 1 1 d . . .
H1 H 0.8893 0.1778 1.0974 0.027 Uiso 1 1 calc R . .
O2 O 0.73493(11) 0.06983(6) 0.97409(7) 0.0211(2) Uani 1 1 d . . .
C2 C 0.72197(18) 0.26713(10) 1.11652(10) 0.0238(3) Uani 1 1 d . . .
H2 H 0.7922 0.3019 1.1627 0.029 Uiso 1 1 calc R . .
C3 C 0.56742(17) 0.29251(9) 1.09105(9) 0.0214(3) Uani 1 1 d . . .
H3 H 0.5327 0.3441 1.1184 0.026 Uiso 1 1 calc R . .
C4 C 0.04031(16) 0.22447(9) 0.90308(10) 0.0207(3) Uani 1 1 d . . .
H4 H -0.0037 0.2752 0.9265 0.025 Uiso 1 1 calc R . .
C5 C -0.05332(17) 0.16620(10) 0.84041(10) 0.0229(3) Uani 1 1 d . . .
H5 H -0.1626 0.1778 0.8224 0.027 Uiso 1 1 calc R . .

C6 C 0.00331(17) 0.09124(10) 0.80191(10) 0.0226(3) Uani 1 1 d . . .
H6 H -0.0651 0.0526 0.7590 0.027 Uiso 1 1 calc R . .
C7 C 0.43124(17) -0.08821(9) 0.77515(9) 0.0219(3) Uani 1 1 d . . .
H7 H 0.3629 -0.1253 0.7304 0.026 Uiso 1 1 calc R . .
C8 C 0.59054(17) -0.10537(9) 0.80259(10) 0.0234(3) Uani 1 1 d . . .
H8 H 0.6305 -0.1552 0.7753 0.028 Uiso 1 1 calc R . .
C9 C 0.69470(17) -0.05333(10) 0.86803(10) 0.0225(3) Uani 1 1 d . . .
H9 H 0.8034 -0.0669 0.8849 0.027 Uiso 1 1 calc R . .
C10 C 0.67954(16) 0.14334(9) 1.01283(9) 0.0194(3) Uani 1 1 d . . .
C11 C 0.52004(16) 0.16578(9) 0.98563(9) 0.0184(3) Uani 1 1 d . . .
C12 C 0.46255(16) 0.24146(9) 1.02446(9) 0.0187(3) Uani 1 1 d . . .
C13 C 0.20071(16) 0.20765(9) 0.93156(9) 0.0186(3) Uani 1 1 d . . .
C14 C 0.26020(16) 0.13214(9) 0.89321(9) 0.0184(3) Uani 1 1 d . . .
C15 C 0.16039(17) 0.07551(9) 0.82817(9) 0.0198(3) Uani 1 1 d . . .
C16 C 0.37564(16) -0.01540(9) 0.81506(9) 0.0199(3) Uani 1 1 d . . .
C17 C 0.47684(16) 0.03799(9) 0.88110(9) 0.0190(3) Uani 1 1 d . . .
C18 C 0.63590(16) 0.01820(9) 0.90753(9) 0.0196(3) Uani 1 1 d . . .
C19 C 0.41860(16) 0.11273(9) 0.92040(9) 0.0180(3) Uani 1 1 d . . .
C20 C 0.25070(16) 0.34356(9) 1.02811(9) 0.0200(3) Uani 1 1 d . . .
C21 C 0.28691(17) 0.42358(9) 0.99020(10) 0.0233(3) Uani 1 1 d . . .
H21 H 0.3405 0.4236 0.9413 0.028 Uiso 1 1 calc R . .
C22 C 0.24364(18) 0.50358(10) 1.02479(10) 0.0258(3) Uani 1 1 d . . .
H22 H 0.2692 0.5592 1.0004 0.031 Uiso 1 1 calc R . .
C23 C 0.16327(17) 0.50263(10) 1.09481(10) 0.0252(3) Uani 1 1 d . . .
H23 H 0.1333 0.5577 1.1182 0.030 Uiso 1 1 calc R . .
C24 C 0.12631(17) 0.42186(10) 1.13096(10) 0.0233(3) Uani 1 1 d . . .
H24 H 0.0699 0.4217 1.1786 0.028 Uiso 1 1 calc R . .
C25 C 0.17100(16) 0.34139(9) 1.09819(9) 0.0208(3) Uani 1 1 d . . .
H25 H 0.1473 0.2858 1.1234 0.025 Uiso 1 1 calc R . .

A-12: Crystallographic Information File (CIF) for $[1(O)_3(OH)_3]^+BF_4^-$

.....

_chemical_name_common	trihydroxytrioxatriangulenium tetrafluoroborate
_chemical_formula_moiety	C_{19} H_9 O_6, 3(C_2 H_6 O S), B F_4
_symmetry_cell_setting	triclinic
_symmetry_space_group_name_H-M	'P -1'

loop_
 _symmetry_equiv_pos_as_xyz
 'x, y, z'
 '-x, -y, -z'

_cell_length_a 12.1733(4)
_cell_length_b 13.3503(4)
_cell_length_c 19.8027(6)
_cell_angle_alpha 74.3610(10)
_cell_angle_beta 77.7980(10)
_cell_angle_gamma 68.3240(10)
_cell_formula_units_Z 4

loop_
 _atom_site_label
 _atom_site_type_symbol
 _atom_site_fract_x
 _atom_site_fract_y
 _atom_site_fract_z
 _atom_site_U_iso_or_equiv
 _atom_site_adp_type
 _atom_site_occupancy
 _atom_site_symmetry_multiplicity
 _atom_site_calc_flag
 _atom_site_refinement_flags
 _atom_site_disorder_assembly
 _atom_site_disorder_group
O1A O 0.36148(9) -0.39929(9) 0.51464(6) 0.0152(2) Uani 1 1 d . . .
O2A O 0.61232(9) -0.22955(9) 0.56687(5) 0.0149(2) Uani 1 1 d . . .
O3A O 0.44769(9) -0.09423(8) 0.34594(5) 0.0145(2) Uani 1 1 d . . .
O4A O 0.52213(11) -0.53149(10) 0.73027(6) 0.0223(3) Uani 1 1 d . . .
H4OA H 0.5693 -0.5234 0.7521 0.034 Uiso 1 1 calc R . .
O5A O 0.69058(10) 0.07256(9) 0.40259(6) 0.0193(2) Uani 1 1 d . . .
H5A H 0.6772 0.1112 0.3621 0.029 Uiso 1 1 calc R . .
O6A O 0.21877(10) -0.27910(9) 0.29383(6) 0.0208(2) Uani 1 1 d . . .
H6OA H 0.2261 -0.2379 0.2540 0.031 Uiso 1 1 calc R . .
C1A C 0.43945(14) -0.46552(13) 0.62466(8) 0.0162(3) Uani 1 1 d . . .
H1A H 0.3990 -0.5180 0.6387 0.019 Uiso 1 1 calc R . .
C2A C 0.51275(14) -0.45969(13) 0.66887(8) 0.0169(3) Uani 1 1 d . . .
C3A C 0.57305(14) -0.38188(13) 0.64983(8) 0.0162(3) Uani 1 1 d . . .
H3A H 0.6232 -0.3805 0.6801 0.019 Uiso 1 1 calc R . .
C4A C 0.65352(13) -0.07744(13) 0.48452(8) 0.0149(3) Uani 1 1 d . . .
H4A H 0.7013 -0.0733 0.5152 0.018 Uiso 1 1 calc R . .
C5A C 0.63715(13) -0.00367(12) 0.41867(8) 0.0152(3) Uani 1 1 d . . .
C6A C 0.56829(13) -0.00794(12) 0.37130(8) 0.0146(3) Uani 1 1 d . . .
H6A H 0.5594 0.0422 0.3269 0.018 Uiso 1 1 calc R . .
C7A C 0.33423(13) -0.18362(12) 0.31650(8) 0.0150(3) Uani 1 1 d . . .
H7A H 0.3279 -0.1354 0.2713 0.018 Uiso 1 1 calc R . .
C8A C 0.28068(14) -0.26629(13) 0.33684(8) 0.0159(3) Uani 1 1 d . . .
C9A C 0.28815(13) -0.33900(12) 0.40354(8) 0.0155(3) Uani 1 1 d . . .
H9A H 0.2505 -0.3935 0.4163 0.019 Uiso 1 1 calc R . .

C10A C 0.42851(13) -0.39299(12) 0.56078(8) 0.0139(3) Uani 1 1 d . . .
C11A C 0.48544(13) -0.31346(12) 0.54125(8) 0.0135(3) Uani 1 1 d . . .
C12A C 0.55695(13) -0.30867(12) 0.58650(8) 0.0145(3) Uani 1 1 d . . .
C13A C 0.59824(13) -0.15530(12) 0.50284(8) 0.0137(3) Uani 1 1 d . . .
C14A C 0.52763(13) -0.16048(12) 0.45723(8) 0.0130(3) Uani 1 1 d . . .
C15A C 0.51462(13) -0.08715(12) 0.39166(8) 0.0135(3) Uani 1 1 d . . .
C16A C 0.39559(13) -0.17523(12) 0.36393(8) 0.0140(3) Uani 1 1 d . . .
C17A C 0.40583(13) -0.24743(12) 0.43021(8) 0.0132(3) Uani 1 1 d . . .
C18A C 0.35117(13) -0.32853(12) 0.44912(8) 0.0137(3) Uani 1 1 d . . .
C19A C 0.47205(13) -0.23985(12) 0.47647(8) 0.0135(3) Uani 1 1 d . . .
O1B O -0.15208(9) -0.46420(8) 0.55152(5) 0.0141(2) Uani 1 1 d . . .
O2B O 0.09647(9) -0.29152(9) 0.60263(6) 0.0166(2) Uani 1 1 d . . .
O3B O -0.06738(9) -0.15979(8) 0.38110(6) 0.0154(2) Uani 1 1 d . . .
O4B O 0.01856(11) -0.60162(10) 0.76344(6) 0.0224(3) Uani 1 1 d . . .
H4OB H 0.0612 -0.5903 0.7869 0.034 Uiso 1 1 calc R . .
O5B O 0.17731(10) 0.00690(9) 0.43629(6) 0.0211(2) Uani 1 1 d . . .
H5B H 0.1604 0.0480 0.3969 0.032 Uiso 1 1 calc R . .
O6B O -0.31742(10) -0.33245(9) 0.33780(6) 0.0178(2) Uani 1 1 d . . .
H6OB H -0.3211 -0.2839 0.3003 0.027 Uiso 1 1 calc R . .
C1B C -0.07107(13) -0.53137(13) 0.66034(8) 0.0157(3) Uani 1 1 d . . .
H1B H -0.1099 -0.5851 0.6741 0.019 Uiso 1 1 calc R . .
C2B C 0.00282(14) -0.52526(13) 0.70436(8) 0.0171(3) Uani 1 1 d . . .
C3B C 0.05824(14) -0.44353(13) 0.68610(8) 0.0172(3) Uani 1 1 d . . .
H3B H 0.1061 -0.4399 0.7169 0.021 Uiso 1 1 calc R . .
C4B C 0.13687(14) -0.13966(13) 0.51965(9) 0.0174(3) Uani 1 1 d . . .
H4B H 0.1838 -0.1344 0.5504 0.021 Uiso 1 1 calc R . .
C5B C 0.12170(14) -0.06754(13) 0.45321(9) 0.0179(3) Uani 1 1 d . . .
C6B C 0.05290(14) -0.07222(13) 0.40600(9) 0.0170(3) Uani 1 1 d . . .
H6B H 0.0440 -0.0222 0.3615 0.020 Uiso 1 1 calc R . .
C7B C -0.18859(13) -0.24468(12) 0.35478(8) 0.0141(3) Uani 1 1 d . . .
H7B H -0.1957 -0.1966 0.3096 0.017 Uiso 1 1 calc R . .
C8B C -0.24647(13) -0.32433(12) 0.37733(8) 0.0137(3) Uani 1 1 d . . .
C9B C -0.23415(13) -0.39953(12) 0.44302(8) 0.0138(3) Uani 1 1 d . . .
H9B H -0.2724 -0.4537 0.4565 0.017 Uiso 1 1 calc R . .
C10B C -0.08468(13) -0.45721(12) 0.59722(8) 0.0137(3) Uani 1 1 d . . .
C11B C -0.02974(13) -0.37609(12) 0.57754(8) 0.0140(3) Uani 1 1 d . . .
C12B C 0.04103(13) -0.37008(13) 0.62295(8) 0.0154(3) Uani 1 1 d . . .
C13B C 0.08185(13) -0.21757(13) 0.53846(8) 0.0160(3) Uani 1 1 d . . .
C14B C 0.01279(13) -0.22431(12) 0.49235(8) 0.0142(3) Uani 1 1 d . . .
C15B C -0.00074(13) -0.15141(12) 0.42646(8) 0.0151(3) Uani 1 1 d . . .
C16B C -0.12177(13) -0.23909(12) 0.40038(8) 0.0136(3) Uani 1 1 d . . .
C17B C -0.10921(13) -0.31179(12) 0.46618(8) 0.0132(3) Uani 1 1 d . . .
C18B C -0.16543(13) -0.39200(12) 0.48660(8) 0.0130(3) Uani 1 1 d . . .
C19B C -0.04225(13) -0.30410(12) 0.51232(8) 0.0137(3) Uani 1 1 d . . .
B1C B 0.92048(19) 0.22974(17) 0.04066(11) 0.0275(4) Uani 1 1 d . . .
F1C F 1.00096(12) 0.22791(11) -0.01965(7) 0.0457(3) Uani 1 1 d . . .

F2C F 0.84455(11) 0.17458(11) 0.03992(7) 0.0441(3) Uani 1 1 d . . .
F3C F 0.85318(11) 0.33894(9) 0.04473(7) 0.0412(3) Uani 1 1 d . . .
F4C F 0.97859(11) 0.18010(11) 0.10034(6) 0.0434(3) Uani 1 1 d . . .
B1D B 0.55747(18) 0.78981(17) -0.05620(11) 0.0258(4) Uani 1 1 d . . .
F1D F 0.64715(11) 0.81595(11) -0.03929(7) 0.0423(3) Uani 1 1 d . . .
F2D F 0.58555(11) 0.67633(9) -0.04304(7) 0.0425(3) Uani 1 1 d . . .
F3D F 0.54585(11) 0.83383(10) -0.12780(6) 0.0375(3) Uani 1 1 d . . .
F4D F 0.45237(10) 0.83490(10) -0.01597(6) 0.0390(3) Uani 1 1 d . . .
S1E S 0.25823(4) 0.59021(3) 0.15141(2) 0.02456(11) Uani 1 1 d . . .
O1E O 0.33987(13) 0.50147(11) 0.20199(7) 0.0350(3) Uani 1 1 d . . .
C1E C 0.20013(17) 0.51585(16) 0.11483(10) 0.0291(4) Uani 1 1 d . . .
H1E1 H 0.2659 0.4590 0.0944 0.044 Uiso 1 1 calc R . .
H1E2 H 0.1519 0.5665 0.0778 0.044 Uiso 1 1 calc R . .
H1E3 H 0.1504 0.4810 0.1520 0.044 Uiso 1 1 calc R . .
C2E C 0.3531(2) 0.6300(2) 0.07664(11) 0.0436(5) Uani 1 1 d . . .
H2E1 H 0.3985 0.6677 0.0895 0.065 Uiso 1 1 calc R . .
H2E2 H 0.3052 0.6799 0.0393 0.065 Uiso 1 1 calc R . .
H2E3 H 0.4082 0.5644 0.0596 0.065 Uiso 1 1 calc R . .
S1F S 0.79977(4) 0.64157(3) 0.10518(2) 0.02192(10) Uani 1 1 d . . .
O1F O 0.87515(12) 0.55470(11) 0.15963(7) 0.0310(3) Uani 1 1 d . . .
C1F C 0.85954(17) 0.59607(16) 0.02476(10) 0.0291(4) Uani 1 1 d . . .
H1F1 H 0.9381 0.6045 0.0088 0.044 Uiso 1 1 calc R . .
H1F2 H 0.8063 0.6402 -0.0112 0.044 Uiso 1 1 calc R . .
H1F3 H 0.8673 0.5183 0.0321 0.044 Uiso 1 1 calc R . .
C2F C 0.66508(17) 0.61114(17) 0.12141(10) 0.0326(4) Uani 1 1 d . . .
H2F1 H 0.6832 0.5337 0.1203 0.049 Uiso 1 1 calc R . .
H2F2 H 0.6141 0.6586 0.0849 0.049 Uiso 1 1 calc R . .
H2F3 H 0.6236 0.6244 0.1679 0.049 Uiso 1 1 calc R . .
S1G S 0.72070(4) 0.21276(3) 0.21530(2) 0.02589(11) Uani 1 1 d . . .
O1G O 0.63867(12) 0.19577(11) 0.28339(7) 0.0332(3) Uani 1 1 d . . .
C1G C 0.78991(18) 0.30220(17) 0.22700(11) 0.0327(4) Uani 1 1 d . . .
H1G1 H 0.7288 0.3664 0.2427 0.049 Uiso 1 1 calc R . .
H1G2 H 0.8343 0.3267 0.1821 0.049 Uiso 1 1 calc R . .
H1G3 H 0.8448 0.2628 0.2626 0.049 Uiso 1 1 calc R . .
C2G C 0.62215(18) 0.30732(18) 0.15465(10) 0.0353(4) Uani 1 1 d . . .
H2G1 H 0.5729 0.2708 0.1443 0.053 Uiso 1 1 calc R . .
H2G2 H 0.6684 0.3328 0.1108 0.053 Uiso 1 1 calc R . .
H2G3 H 0.5707 0.3706 0.1753 0.053 Uiso 1 1 calc R . .
S1H S 0.60458(4) 0.91130(4) 0.18680(2) 0.02411(10) Uani 1 1 d . . .
O1H O 0.67265(12) 0.79188(11) 0.21688(6) 0.0307(3) Uani 1 1 d . . .
C1H C 0.53400(19) 0.90661(16) 0.11855(11) 0.0351(4) Uani 1 1 d . . .
H1H1 H 0.5941 0.8682 0.0842 0.053 Uiso 1 1 calc R . .
H1H2 H 0.4919 0.9819 0.0948 0.053 Uiso 1 1 calc R . .
H1H3 H 0.4770 0.8671 0.1389 0.053 Uiso 1 1 calc R . .
C2H C 0.71579(18) 0.96468(17) 0.13414(11) 0.0356(4) Uani 1 1 d . . .
H2H1 H 0.7620 0.9757 0.1648 0.053 Uiso 1 1 calc R . .

H2H2 H 0.6780 1.0354 0.1034 0.053 Uiso 1 1 calc R . .
H2H3 H 0.7689 0.9125 0.1051 0.053 Uiso 1 1 calc R . .
S1I S 0.77412(4) 0.85444(3) -0.25565(2) 0.02458(10) Uani 1 1 d . . .
O1I O 0.86975(12) 0.86076(11) -0.31840(7) 0.0347(3) Uani 1 1 d . . .
C1I C 0.85427(17) 0.76409(17) -0.18514(10) 0.0315(4) Uani 1 1 d . . .
H1I1 H 0.9073 0.6961 -0.2001 0.047 Uiso 1 1 calc R . .
H1I2 H 0.7981 0.7465 -0.1443 0.047 Uiso 1 1 calc R . .
H1I3 H 0.9017 0.7999 -0.1722 0.047 Uiso 1 1 calc R . .
C2I C 0.70772(17) 0.76495(16) -0.27023(10) 0.0295(4) Uani 1 1 d . . .
H2I1 H 0.6637 0.8010 -0.3112 0.044 Uiso 1 1 calc R . .
H2I2 H 0.6529 0.7481 -0.2284 0.044 Uiso 1 1 calc R . .
H2I3 H 0.7700 0.6965 -0.2792 0.044 Uiso 1 1 calc R . .
S1J S 0.15863(4) 0.94773(4) 0.14510(2) 0.02441(15) Uani 0.9043(17) 1 d PD A 1
O1J O 0.2508(3) 0.8395(5) 0.17121(17) 0.0308(5) Uani 0.9043(17) 1 d PD A 1
C1J C 0.0386(2) 0.9107(3) 0.12979(19) 0.0477(8) Uani 0.9043(17) 1 d PD A 1
H1J1 H 0.0676 0.8668 0.0932 0.072 Uiso 0.9043(17) 1 calc PR A 1
H1J2 H -0.0268 0.9779 0.1142 0.072 Uiso 0.9043(17) 1 calc PR A 1
H1J3 H 0.0100 0.8675 0.1737 0.072 Uiso 0.9043(17) 1 calc PR A 1
C2J C 0.2109(4) 0.9909(2) 0.0558(2) 0.0380(8) Uani 0.9043(17) 1 d PD A 1
H2J1 H 0.2819 1.0107 0.0531 0.057 Uiso 0.9043(17) 1 calc PR A 1
H2J2 H 0.1487 1.0552 0.0336 0.057 Uiso 0.9043(17) 1 calc PR A 1
H2J3 H 0.2312 0.9309 0.0309 0.057 Uiso 0.9043(17) 1 calc PR A 1
S1J' S 0.1994(4) 0.8579(3) 0.1096(2) 0.0218(13) Uiso 0.0957(17) 1 d PD A 2
O1J' O 0.267(3) 0.835(5) 0.1707(16) 0.0308(5) Uani 0.0957(17) 1 d PD A 2
C1J' C 0.0474(13) 0.928(3) 0.143(2) 0.0477(8) Uani 0.0957(17) 1 d PD A 2
H1J4 H 0.0136 0.8741 0.1756 0.072 Uiso 0.0957(17) 1 calc PR A 2
H1J5 H 0.0001 0.9650 0.1034 0.072 Uiso 0.0957(17) 1 calc PR A 2
H1J6 H 0.0462 0.9827 0.1678 0.072 Uiso 0.0957(17) 1 calc PR A 2
C2J' C 0.228(4) 0.974(3) 0.051(3) 0.0380(8) Uani 0.0957(17) 1 d PD A 2
H2J4 H 0.3113 0.9526 0.0297 0.057 Uiso 0.0957(17) 1 calc PR A 2
H2J5 H 0.2111 1.0321 0.0763 0.057 Uiso 0.0957(17) 1 calc PR A 2
H2J6 H 0.1761 1.0008 0.0130 0.057 Uiso 0.0957(17) 1 calc PR A 2

A-13: Crystallographic Information File (CIF) for $2[1(O)_3(OH)_3]^+SiF_6^{2-}$

.....

_chemical_name_common	trihydroxytrioxatriangulenium hexafluorosilicate
_chemical_formula_moiety	$2(C_{19}\ H_9\ O_6)$, $F_6\ Si$, $2(H_2\ O)$
_symmetry_cell_setting	triclinic
_symmetry_space_group_name_H-M	'P -1'

_
loop_

_symmetry_equiv_pos_as_xyz
'x, y, z'
'-x, -y, -z'

_cell_length_a	7.2001(2)
_cell_length_b	15.0922(3)
_cell_length_c	15.1793(3)
_cell_angle_alpha	71.767(1)
_cell_angle_beta	78.869(1)
_cell_angle_gamma	86.646(1)
_cell_formula_units_Z	2

loop_
_atom_site_label
_atom_site_type_symbol
_atom_site_fract_x
_atom_site_fract_y
_atom_site_fract_z
_atom_site_U_iso_or_equiv
_atom_site_adp_type
_atom_site_occupancy
_atom_site_symmetry_multiplicity
_atom_site_calc_flag
_atom_site_refinement_flags
_atom_site_disorder_assembly
_atom_site_disorder_group
O1A O 0.4993(2) 0.77515(12) 0.66572(12) 0.0144(4) Uani 1 1 d . . .
O2A O 0.6089(2) 0.63687(12) 0.98423(12) 0.0149(4) Uani 1 1 d . . .
O3A O 0.3776(2) 0.95272(12) 0.88587(12) 0.0137(4) Uani 1 1 d . . .
O4A O 0.7198(3) 0.46237(12) 0.77137(13) 0.0192(4) Uani 1 1 d . . .
H4A H 0.7125 0.4647 0.7161 0.029 Uiso 1 1 calc R . .
O5A O 0.4764(3) 0.81828(13) 1.19692(13) 0.0211(4) Uani 1 1 d . . .
H5A H 0.5296 0.7731 1.2311 0.032 Uiso 1 1 calc R . .
O6A O 0.2836(3) 1.08385(12) 0.56783(12) 0.0180(4) Uani 1 1 d . . .
H6A H 0.2578 1.1310 0.5861 0.027 Uiso 1 1 calc R . .
C1A C 0.6105(4) 0.61955(18) 0.71260(18) 0.0156(5) Uani 1 1 d . . .
H1A H 0.6131 0.6153 0.6512 0.019 Uiso 1 1 calc R . .
C2A C 0.6643(4) 0.54319(18) 0.78519(19) 0.0155(5) Uani 1 1 d . . .
C3A C 0.6625(4) 0.54804(17) 0.87694(18) 0.0153(5) Uani 1 1 d . . .
H3A H 0.6981 0.4957 0.9246 0.018 Uiso 1 1 calc R . .
C4A C 0.5456(4) 0.72258(18) 1.09459(18) 0.0159(5) Uani 1 1 d . . .
H4A1 H 0.5841 0.6712 1.1423 0.019 Uiso 1 1 calc R . .
C5A C 0.4833(4) 0.80632(18) 1.11260(17) 0.0158(5) Uani 1 1 d . . .
C6A C 0.4240(4) 0.88410(17) 1.04389(18) 0.0150(5) Uani 1 1 d . . .
H6A1 H 0.3801 0.9394 1.0585 0.018 Uiso 1 1 calc R . .

C7A C 0.3272(3) 1.02301(17) 0.72852(18) 0.0145(5) Uani 1 1 d . . .
H7A H 0.2884 1.0795 0.7417 0.017 Uiso 1 1 calc R . .
C8A C 0.3317(3) 1.01318(18) 0.63841(18) 0.0148(5) Uani 1 1 d . . .
C9A C 0.3860(4) 0.93045(18) 0.61630(17) 0.0145(5) Uani 1 1 d . . .
H9A H 0.3842 0.9259 0.5555 0.017 Uiso 1 1 calc R . .
C10A C 0.5546(3) 0.69962(17) 0.73436(18) 0.0140(5) Uani 1 1 d . . .
C11A C 0.5533(3) 0.70634(17) 0.82509(18) 0.0135(5) Uani 1 1 d . . .
C12A C 0.6086(3) 0.62942(18) 0.89540(18) 0.0139(5) Uani 1 1 d . . .
C13A C 0.5487(3) 0.71778(17) 1.00543(18) 0.0139(5) Uani 1 1 d . . .
C14A C 0.4936(3) 0.79469(17) 0.93518(17) 0.0129(5) Uani 1 1 d . . .
C15A C 0.4319(3) 0.87700(18) 0.95542(18) 0.0141(5) Uani 1 1 d . . .
C16A C 0.3818(3) 0.94670(18) 0.79621(17) 0.0132(5) Uani 1 1 d . . .
C17A C 0.4402(3) 0.86422(17) 0.77582(17) 0.0124(5) Uani 1 1 d . . .
C18A C 0.4418(3) 0.85647(17) 0.68554(17) 0.0130(5) Uani 1 1 d . . .
C19A C 0.4965(3) 0.78832(17) 0.84516(18) 0.0133(5) Uani 1 1 d . . .
O1B O -0.0049(3) 0.77711(12) 0.66231(12) 0.0150(4) Uani 1 1 d . . .
O2B O 0.1039(2) 0.63870(12) 0.98085(12) 0.0143(4) Uani 1 1 d . . .
O3B O -0.1215(2) 0.95558(12) 0.88169(12) 0.0141(4) Uani 1 1 d . . .
O4B O 0.2257(3) 0.46534(13) 0.76784(13) 0.0217(4) Uani 1 1 d . . .
H4B H 0.2223 0.4678 0.7121 0.033 Uiso 1 1 calc R . .
O5B O -0.0206(3) 0.82079(13) 1.19211(12) 0.0196(4) Uani 1 1 d . . .
H5B H -0.0040 0.7692 1.2317 0.029 Uiso 1 1 calc R . .
O6B O -0.2161(3) 1.08700(13) 0.56436(12) 0.0201(4) Uani 1 1 d . . .
H6B H -0.2350 1.1350 0.5817 0.030 Uiso 1 1 calc R . .
C1B C 0.1086(4) 0.62153(18) 0.70930(18) 0.0168(5) Uani 1 1 d . . .
H1B H 0.1104 0.6168 0.6482 0.020 Uiso 1 1 calc R . .
C2B C 0.1648(4) 0.54576(18) 0.78166(19) 0.0166(5) Uani 1 1 d . . .
C3B C 0.1620(4) 0.55041(17) 0.87330(18) 0.0151(5) Uani 1 1 d . . .
H3B H 0.1985 0.4983 0.9209 0.018 Uiso 1 1 calc R . .
C4B C 0.0414(4) 0.72447(18) 1.09093(18) 0.0155(5) Uani 1 1 d . . .
H4B1 H 0.0770 0.6727 1.1391 0.019 Uiso 1 1 calc R . .
C5B C -0.0173(4) 0.80887(18) 1.10829(18) 0.0155(5) Uani 1 1 d . . .
C6B C -0.0740(3) 0.88669(17) 1.03933(17) 0.0141(5) Uani 1 1 d . . .
H6B1 H -0.1152 0.9424 1.0536 0.017 Uiso 1 1 calc R . .
C7B C -0.1710(4) 1.02633(18) 0.72438(18) 0.0154(5) Uani 1 1 d . . .
H7B H -0.2073 1.0831 0.7375 0.018 Uiso 1 1 calc R . .
C8B C -0.1689(4) 1.01664(18) 0.63422(18) 0.0166(5) Uani 1 1 d . . .
C9B C -0.1172(4) 0.93313(18) 0.61285(18) 0.0152(5) Uani 1 1 d . . .
H9B H -0.1208 0.9282 0.5523 0.018 Uiso 1 1 calc R . .
C10B C 0.0517(3) 0.70194(18) 0.73050(18) 0.0141(5) Uani 1 1 d . . .
C11B C 0.0507(3) 0.70843(18) 0.82122(18) 0.0141(5) Uani 1 1 d . . .
C12B C 0.1056(3) 0.63146(18) 0.89174(18) 0.0141(5) Uani 1 1 d . . .
C13B C 0.0453(3) 0.71969(17) 1.00188(18) 0.0132(5) Uani 1 1 d . . .
C14B C -0.0083(3) 0.79716(17) 0.93099(17) 0.0129(5) Uani 1 1 d . . .
C15B C -0.0679(3) 0.87971(17) 0.95101(18) 0.0137(5) Uani 1 1 d . . .
C16B C -0.1179(3) 0.94971(18) 0.79196(17) 0.0139(5) Uani 1 1 d . . .

C17B C -0.0613(3) 0.86674(18) 0.77206(17) 0.0130(5) Uani 1 1 d . . .
C18B C -0.0614(3) 0.85896(18) 0.68199(18) 0.0141(5) Uani 1 1 d . . .
C19B C -0.0055(3) 0.79064(17) 0.84115(18) 0.0130(5) Uani 1 1 d . . .
Si1 Si 0.22762(12) 0.34621(5) 0.59821(5) 0.0241(2) Uani 1 1 d . . .
F2 F 0.1027(3) 0.38536(13) 0.51237(12) 0.0373(5) Uani 1 1 d . . .
F3 F 0.4274(3) 0.35106(14) 0.52041(13) 0.0421(5) Uani 1 1 d . . .
F5 F 0.0283(3) 0.33977(12) 0.68025(12) 0.0320(4) Uani 1 1 d . . .
F1 F 0.3519(3) 0.30888(13) 0.68790(12) 0.0346(4) Uani 1 1 d . . .
F4 F 0.1886(3) 0.23466(13) 0.60609(13) 0.0436(5) Uani 1 1 d . . .
F6 F 0.2629(3) 0.45737(12) 0.59602(12) 0.0367(5) Uani 1 1 d . . .
O1W O 0.6919(3) 0.44903(15) 0.61049(15) 0.0296(5) Uani 1 1 d D . .
H1W1 H 0.770(4) 0.480(2) 0.568(2) 0.036 Uiso 1 1 d D . .
H2W1 H 0.594(4) 0.464(2) 0.590(2) 0.036 Uiso 1 1 d D . .
O2W O -0.2546(4) 1.24980(16) 0.5835(2) 0.0406(6) Uani 1 1 d D . .
H1W2 H -0.177(5) 1.288(2) 0.570(3) 0.049 Uiso 1 1 d D . .
H2W2 H -0.350(4) 1.273(3) 0.567(3) 0.049 Uiso 1 1 d D . .

A-14: Crystallographic Information File (CIF) for (2)$^-$Bu$_4$N$^+$

.....

_chemical_name_common	tetra-*n*-butylammonium trioxytriangulenate
_chemical_formula_moiety	C_{38} H_{43} N O_3
_symmetry_cell_setting	monoclinic
_symmetry_space_group_name_H-M	P 21/n

loop_
 _symmetry_equiv_pos_as_xyz
 'x, y, z'
 '-x+1/2, y+1/2, -z+1/2'
 '-x, -y, -z'
 'x-1/2, -y-1/2, z-1/2'

_cell_length_a	9.5406(2)
_cell_length_b	18.4914(4)
_cell_length_c	17.7186(4)
_cell_angle_alpha	90.00
_cell_angle_beta	96.9689(7)
_cell_angle_gamma	90.00
_cell_formula_units_Z	4

loop_
 _atom_site_label
 _atom_site_type_symbol
 _atom_site_fract_x

_atom_site_fract_y
_atom_site_fract_z
_atom_site_U_iso_or_equiv
_atom_site_adp_type
_atom_site_occupancy
_atom_site_symmetry_multiplicity
_atom_site_calc_flag
_atom_site_refinement_flags
_atom_site_disorder_assembly
_atom_site_disorder_group
O1 O 0.5668(2) -0.33762(12) -0.28538(11) 0.0477(6) Uani 1 1 d . . .
O2 O 0.1975(2) -0.30892(18) 0.04273(12) 0.0766(9) Uani 1 1 d . . .
O3 O 0.2297(2) -0.00356(16) -0.20517(12) 0.0649(7) Uani 1 1 d . . .
C1 C 0.4664(3) -0.4056(2) -0.16112(17) 0.0492(9) Uani 1 1 d . . .
H1 H 0.5179 -0.4339 -0.1930 0.059 Uiso 1 1 calc R . .
C2 C 0.4193(3) -0.4374(2) -0.09730(17) 0.0565(10) Uani 1 1 d . . .
H2 H 0.4383 -0.4868 -0.0858 0.068 Uiso 1 1 calc R . .
C3 C 0.3448(3) -0.3958(3) -0.05119(17) 0.0605(11) Uani 1 1 d . . .
H3 H 0.3144 -0.4171 -0.0071 0.073 Uiso 1 1 calc R . .
C4 C 0.0941(3) -0.1701(3) -0.00208(19) 0.0727(14) Uani 1 1 d . . .
H4 H 0.0595 -0.1917 0.0407 0.087 Uiso 1 1 calc R . .
C5 C 0.0513(3) -0.1014(3) -0.0239(2) 0.0783(15) Uani 1 1 d . . .
H5 H -0.0154 -0.0765 0.0022 0.094 Uiso 1 1 calc R . .
C6 C 0.1058(3) -0.0688(2) -0.08404(18) 0.0636(11) Uani 1 1 d . . .
H6 H 0.0788 -0.0206 -0.0975 0.076 Uiso 1 1 calc R . .
C7 C 0.3894(3) -0.08252(18) -0.29954(16) 0.0424(8) Uani 1 1 d . . .
H7 H 0.3642 -0.0342 -0.3135 0.051 Uiso 1 1 calc R . .
C8 C 0.4742(3) -0.12150(17) -0.34320(16) 0.0409(8) Uani 1 1 d . . .
H8 H 0.5081 -0.0998 -0.3860 0.049 Uiso 1 1 calc R . .
C9 C 0.5088(3) -0.19213(18) -0.32389(15) 0.0384(7) Uani 1 1 d . . .
H9 H 0.5673 -0.2186 -0.3537 0.046 Uiso 1 1 calc R . .
C10 C 0.4393(3) -0.33336(19) -0.17875(15) 0.0411(8) Uani 1 1 d . . .
C11 C 0.3595(3) -0.2902(2) -0.13249(15) 0.0451(9) Uani 1 1 d . . .
C12 C 0.3129(3) -0.3240(2) -0.06739(15) 0.0517(10) Uani 1 1 d . . .
C13 C 0.1878(3) -0.2087(2) -0.04178(16) 0.0570(10) Uani 1 1 d . . .
C14 C 0.2397(3) -0.1771(2) -0.10608(15) 0.0492(9) Uani 1 1 d . . .
C15 C 0.1999(3) -0.1049(2) -0.12552(16) 0.0504(9) Uani 1 1 d . . .
C16 C 0.3405(3) -0.11272(18) -0.23584(15) 0.0402(8) Uani 1 1 d . . .
C17 C 0.3748(2) -0.18523(18) -0.21531(14) 0.0377(7) Uani 1 1 d . . .
C18 C 0.4599(3) -0.22531(17) -0.26167(14) 0.0358(7) Uani 1 1 d . . .
C19 C 0.3261(3) -0.2176(2) -0.15040(15) 0.0416(8) Uani 1 1 d . . .
C20 C 0.4938(3) -0.30114(19) -0.24462(15) 0.0411(8) Uani 1 1 d . . .
C21 C 0.2304(3) -0.2822(3) -0.01717(17) 0.0628(12) Uani 1 1 d . . .
C22 C 0.2543(3) -0.0688(2) -0.18994(17) 0.0525(10) Uani 1 1 d . . .
N1A N 0.5332(2) 0.16973(11) -0.20023(13) 0.0344(6) Uani 1 1 d . . .
C1A C 0.4006(3) 0.18901(18) -0.16469(17) 0.0472(8) Uani 1 1 d . . .

H1A1 H 0.3449 0.2240 -0.1984 0.057 Uiso 1 1 calc R . .
H1A2 H 0.3427 0.1448 -0.1628 0.057 Uiso 1 1 calc R . .
C2A C 0.4251(3) 0.22113(18) -0.08510(17) 0.0477(8) Uani 1 1 d . . .
H2A1 H 0.4838 0.2653 -0.0854 0.057 Uiso 1 1 calc R . .
H2A2 H 0.4758 0.1859 -0.0496 0.057 Uiso 1 1 calc R . .
C3A C 0.2822(3) 0.2398(3) -0.0590(2) 0.0802(14) Uani 1 1 d . . .
C4A C 0.2997(4) 0.2678(2) 0.0231(2) 0.0716(11) Uani 1 1 d . . .
H4A1 H 0.3364 0.2289 0.0575 0.107 Uiso 1 1 calc R . .
H4A2 H 0.2080 0.2838 0.0364 0.107 Uiso 1 1 calc R . .
H4A3 H 0.3660 0.3085 0.0277 0.107 Uiso 1 1 calc R . .
C5A C 0.6224(3) 0.23660(14) -0.21026(18) 0.0411(8) Uani 1 1 d . . .
H5A1 H 0.7154 0.2205 -0.2234 0.049 Uiso 1 1 calc R . .
H5A2 H 0.6390 0.2620 -0.1608 0.049 Uiso 1 1 calc R . .
C6A C 0.5606(4) 0.29085(18) -0.2705(2) 0.0621(10) Uani 1 1 d . . .
H6A1 H 0.5572 0.2686 -0.3215 0.075 Uiso 1 1 calc R . .
H6A2 H 0.4628 0.3030 -0.2618 0.075 Uiso 1 1 calc R . .
C7A C 0.6474(4) 0.3592(2) -0.2682(3) 0.0897(16) Uani 1 1 d . . .
H7A1 H 0.7485 0.3461 -0.2656 0.108 Uiso 1 1 calc R . .
H7A2 H 0.6214 0.3866 -0.3158 0.108 Uiso 1 1 calc R . .
C8A C 0.6272(5) 0.4055(2) -0.2032(3) 0.1051(17) Uani 1 1 d . . .
H8A1 H 0.5260 0.4133 -0.2016 0.158 Uiso 1 1 calc R . .
H8A2 H 0.6738 0.4521 -0.2086 0.158 Uiso 1 1 calc R . .
H8A3 H 0.6682 0.3820 -0.1561 0.158 Uiso 1 1 calc R . .
C9A C 0.4841(3) 0.13516(16) -0.27645(15) 0.0373(7) Uani 1 1 d . . .
H9A1 H 0.4180 0.0954 -0.2684 0.045 Uiso 1 1 calc R . .
H9A2 H 0.4311 0.1717 -0.3094 0.045 Uiso 1 1 calc R . .
C10A C 0.6010(3) 0.10514(15) -0.31800(15) 0.0381(7) Uani 1 1 d . . .
H10A H 0.6418 0.0617 -0.2910 0.046 Uiso 1 1 calc R . .
H10B H 0.6769 0.1416 -0.3181 0.046 Uiso 1 1 calc R . .
C11A C 0.5455(3) 0.08521(16) -0.39966(15) 0.0402(7) Uani 1 1 d . . .
H11A H 0.4609 0.0542 -0.3996 0.048 Uiso 1 1 calc R . .
H11B H 0.5165 0.1298 -0.4283 0.048 Uiso 1 1 calc R . .
C12A C 0.6546(3) 0.04569(17) -0.43960(16) 0.0419(8) Uani 1 1 d . . .
H12A H 0.7421 0.0739 -0.4352 0.063 Uiso 1 1 calc R . .
H12B H 0.6187 0.0394 -0.4934 0.063 Uiso 1 1 calc R . .
H12C H 0.6734 -0.0018 -0.4160 0.063 Uiso 1 1 calc R . .
C13A C 0.6267(3) 0.11811(14) -0.14914(15) 0.0346(7) Uani 1 1 d . . .
H13A H 0.7136 0.1089 -0.1730 0.042 Uiso 1 1 calc R . .
H13B H 0.6552 0.1426 -0.1000 0.042 Uiso 1 1 calc R . .
C14A C 0.5611(3) 0.04631(16) -0.13337(17) 0.0463(8) Uani 1 1 d . . .
H14A H 0.5345 0.0203 -0.1818 0.056 Uiso 1 1 calc R . .
H14B H 0.4744 0.0544 -0.1090 0.056 Uiso 1 1 calc R . .
C15A C 0.6648(4) 0.00064(18) -0.08130(19) 0.0619(10) Uani 1 1 d . . .
H15A H 0.7536 -0.0040 -0.1046 0.074 Uiso 1 1 calc R . .
H15B H 0.6873 0.0264 -0.0323 0.074 Uiso 1 1 calc R . .
C16A C 0.6130(4) -0.0728(2) -0.0658(2) 0.0820(13) Uani 1 1 d . . .

H16A H 0.5230 -0.0691 -0.0448 0.123 Uiso 1 1 calc R . .
H16B H 0.6824 -0.0974 -0.0292 0.123 Uiso 1 1 calc R . .
H16C H 0.5995 -0.1006 -0.1133 0.123 Uiso 1 1 calc R . .
O1W O 0.1314(5) 0.0929(3) -0.1196(3) 0.038(2) Uiso 0.375(7) 1 d P . .
H1WO H 0.1388 0.0573 -0.1493 0.13(5) Uiso 0.375(7) 1 d PR . .
H2WO H 0.0513 0.1001 -0.1452 0.04(2) Uiso 0.375(7) 1 d PR . .

A-15: Crystallographic Information File (CIF) for (2)$^-$Hex$_4$N$^+$

.....

_chemical_name_common	tetra-n-hexylammonium trioxytriangulenetae
_chemical_formula_moiety	C_{24} H_{52} N, C_{22} H_9 O_3
_symmetry_cell_setting	monoclinic
_symmetry_space_group_name_H-M	P 21/n

loop_
_symmetry_equiv_pos_as_xyz
'x, y, z'
'-x+1/2, y+1/2, -z+1/2'
'-x, -y, -z'
'x-1/2, -y-1/2, z-1/2'

_cell_length_a	11.7395(2)
_cell_length_b	21.6818(4)
_cell_length_c	14.8784(3)
_cell_angle_alpha	90.00
_cell_angle_beta	91.0030(10)
_cell_angle_gamma	90.00
_cell_formula_units_Z	4

loop_
_atom_site_label
_atom_site_type_symbol
_atom_site_fract_x
_atom_site_fract_y
_atom_site_fract_z
_atom_site_U_iso_or_equiv
_atom_site_adp_type
_atom_site_occupancy
_atom_site_symmetry_multiplicity
_atom_site_calc_flag
_atom_site_refinement_flags
_atom_site_disorder_assembly

_atom_site_disorder_group
O1 O 0.45636(9) 0.52907(4) 0.39387(7) 0.0299(2) Uani 1 1 d . . .
O2 O 0.80582(8) 0.25757(5) 0.40590(6) 0.0265(2) Uani 1 1 d . . .
O3 O 0.19570(8) 0.22942(5) 0.38877(6) 0.0264(2) Uani 1 1 d . . .
C1 C 0.16943(12) 0.35793(7) 0.40567(8) 0.0245(3) Uani 1 1 d . . .
H1 H 0.1028 0.3331 0.4077 0.029 Uiso 1 1 calc R . .
C2 C 0.15931(12) 0.42160(7) 0.40884(9) 0.0271(3) Uani 1 1 d . . .
H2 H 0.0865 0.4402 0.4139 0.033 Uiso 1 1 calc R . .
C3 C 0.25650(12) 0.45789(7) 0.40458(9) 0.0254(3) Uani 1 1 d . . .
H3 H 0.2491 0.5015 0.4052 0.030 Uiso 1 1 calc R . .
C4 C 0.36460(12) 0.43180(6) 0.39942(8) 0.0216(3) Uani 1 1 d . . .
C5 C 0.46540(12) 0.47213(6) 0.39497(8) 0.0231(3) Uani 1 1 d . . .
C6 C 0.57738(12) 0.44145(6) 0.39151(8) 0.0222(3) Uani 1 1 d . . .
C7 C 0.67570(12) 0.47695(7) 0.38849(9) 0.0260(3) Uani 1 1 d . . .
H7 H 0.6696 0.5206 0.3875 0.031 Uiso 1 1 calc R . .
C8 C 0.78304(12) 0.44977(7) 0.38683(9) 0.0279(3) Uani 1 1 d . . .
H8 H 0.8494 0.4747 0.3844 0.033 Uiso 1 1 calc R . .
C9 C 0.79254(12) 0.38616(7) 0.38867(9) 0.0252(3) Uani 1 1 d . . .
H9 H 0.8659 0.3677 0.3876 0.030 Uiso 1 1 calc R . .
C10 C 0.69568(11) 0.34871(6) 0.39207(8) 0.0207(3) Uani 1 1 d . . .
C11 C 0.70974(11) 0.28169(6) 0.39872(8) 0.0215(3) Uani 1 1 d . . .
C12 C 0.60529(11) 0.24451(6) 0.39698(8) 0.0209(3) Uani 1 1 d . . .
C13 C 0.61335(12) 0.18029(6) 0.39556(8) 0.0245(3) Uani 1 1 d . . .
H13 H 0.6864 0.1615 0.3961 0.029 Uiso 1 1 calc R . .
C14 C 0.51690(13) 0.14340(6) 0.39345(9) 0.0262(3) Uani 1 1 d . . .
H14 H 0.5239 0.0998 0.3917 0.031 Uiso 1 1 calc R . .
C15 C 0.40977(13) 0.17079(6) 0.39389(9) 0.0251(3) Uani 1 1 d . . .
H15 H 0.3437 0.1455 0.3934 0.030 Uiso 1 1 calc R . .
C16 C 0.39756(11) 0.23483(6) 0.39498(8) 0.0209(3) Uani 1 1 d . . .
C17 C 0.28280(11) 0.26190(6) 0.39400(8) 0.0215(3) Uani 1 1 d . . .
C18 C 0.27595(11) 0.32969(6) 0.39950(8) 0.0210(3) Uani 1 1 d . . .
C19 C 0.37676(11) 0.36632(6) 0.39809(8) 0.0192(3) Uani 1 1 d . . .
C20 C 0.49616(11) 0.27340(6) 0.39569(8) 0.0190(3) Uani 1 1 d . . .
C21 C 0.58539(11) 0.37578(6) 0.39269(8) 0.0195(3) Uani 1 1 d . . .
C22 C 0.48610(11) 0.33855(6) 0.39548(8) 0.0187(3) Uani 1 1 d . . .
N1 N 0.48304(9) 0.28875(5) 0.69253(7) 0.0167(2) Uani 1 1 d . . .
C23 C 0.37366(11) 0.28634(6) 0.63709(8) 0.0190(3) Uani 1 1 d . . .
H23A H 0.3895 0.2652 0.5797 0.023 Uiso 1 1 calc R . .
H23B H 0.3504 0.3291 0.6225 0.023 Uiso 1 1 calc R . .
C24 C 0.27414(11) 0.25404(6) 0.68098(8) 0.0208(3) Uani 1 1 d . . .
H24A H 0.2446 0.2801 0.7300 0.025 Uiso 1 1 calc R . .
H24B H 0.3002 0.2145 0.7074 0.025 Uiso 1 1 calc R . .
C25 C 0.17943(11) 0.24197(6) 0.61167(8) 0.0220(3) Uani 1 1 d . . .
H25A H 0.1632 0.2805 0.5782 0.026 Uiso 1 1 calc R . .
H25B H 0.2059 0.2109 0.5680 0.026 Uiso 1 1 calc R . .
C26 C 0.06986(11) 0.21907(6) 0.65405(9) 0.0228(3) Uani 1 1 d . . .

H26A H 0.0875 0.1826 0.6918 0.027 Uiso 1 1 calc R . .
H26B H 0.0398 0.2517 0.6937 0.027 Uiso 1 1 calc R . .
C27 C -0.02159(12) 0.20175(7) 0.58488(10) 0.0300(3) Uani 1 1 d . . .
H27A H -0.0369 0.2377 0.5454 0.036 Uiso 1 1 calc R . .
H27B H 0.0071 0.1678 0.5469 0.036 Uiso 1 1 calc R . .
C28 C -0.13218(13) 0.18163(8) 0.62760(12) 0.0381(4) Uani 1 1 d . . .
H28A H -0.1180 0.1454 0.6656 0.057 Uiso 1 1 calc R . .
H28B H -0.1881 0.1712 0.5804 0.057 Uiso 1 1 calc R . .
H28C H -0.1618 0.2153 0.6644 0.057 Uiso 1 1 calc R . .
C29 C 0.46611(11) 0.32148(6) 0.78195(8) 0.0180(3) Uani 1 1 d . . .
H29A H 0.4106 0.2975 0.8171 0.022 Uiso 1 1 calc R . .
H29B H 0.5394 0.3210 0.8158 0.022 Uiso 1 1 calc R . .
C30 C 0.42461(11) 0.38782(6) 0.77596(8) 0.0206(3) Uani 1 1 d . . .
H30A H 0.3440 0.3888 0.7553 0.025 Uiso 1 1 calc R . .
H30B H 0.4706 0.4110 0.7323 0.025 Uiso 1 1 calc R . .
C31 C 0.43619(12) 0.41737(6) 0.86935(9) 0.0243(3) Uani 1 1 d . . .
H31A H 0.3884 0.3940 0.9117 0.029 Uiso 1 1 calc R . .
H31B H 0.5164 0.4137 0.8904 0.029 Uiso 1 1 calc R . .
C32 C 0.40164(12) 0.48524(6) 0.87222(9) 0.0262(3) Uani 1 1 d . . .
H32A H 0.4277 0.5029 0.9304 0.031 Uiso 1 1 calc R . .
H32B H 0.4418 0.5075 0.8240 0.031 Uiso 1 1 calc R . .
C33 C 0.27485(12) 0.49698(7) 0.86107(10) 0.0295(3) Uani 1 1 d . . .
H33A H 0.2339 0.4746 0.9087 0.035 Uiso 1 1 calc R . .
H33B H 0.2484 0.4805 0.8023 0.035 Uiso 1 1 calc R . .
C34 C 0.24556(15) 0.56543(7) 0.86611(12) 0.0406(4) Uani 1 1 d . . .
H34A H 0.2700 0.5818 0.9247 0.061 Uiso 1 1 calc R . .
H34B H 0.1631 0.5708 0.8585 0.061 Uiso 1 1 calc R . .
H34C H 0.2848 0.5876 0.8184 0.061 Uiso 1 1 calc R . .
C35 C 0.57027(10) 0.32224(6) 0.63582(8) 0.0180(3) Uani 1 1 d . . .
H35A H 0.5887 0.2959 0.5837 0.022 Uiso 1 1 calc R . .
H35B H 0.5351 0.3606 0.6122 0.022 Uiso 1 1 calc R . .
C36 C 0.68057(11) 0.33894(6) 0.68475(8) 0.0209(3) Uani 1 1 d . . .
H36A H 0.7075 0.3032 0.7207 0.025 Uiso 1 1 calc R . .
H36B H 0.6669 0.3737 0.7264 0.025 Uiso 1 1 calc R . .
C37 C 0.77164(11) 0.35717(6) 0.61779(8) 0.0199(3) Uani 1 1 d . . .
H37A H 0.7868 0.3219 0.5774 0.024 Uiso 1 1 calc R . .
H37B H 0.7434 0.3919 0.5804 0.024 Uiso 1 1 calc R . .
C38 C 0.88167(11) 0.37606(6) 0.66566(8) 0.0226(3) Uani 1 1 d . . .
H38A H 0.9060 0.3422 0.7063 0.027 Uiso 1 1 calc R . .
H38B H 0.8663 0.4126 0.7034 0.027 Uiso 1 1 calc R . .
C39 C 0.97933(11) 0.39121(6) 0.60340(9) 0.0239(3) Uani 1 1 d . . .
H39A H 0.9895 0.3567 0.5606 0.029 Uiso 1 1 calc R . .
H39B H 0.9598 0.4286 0.5682 0.029 Uiso 1 1 calc R . .
C40 C 1.09057(12) 0.40208(7) 0.65491(10) 0.0279(3) Uani 1 1 d . . .
H40A H 1.0819 0.4373 0.6955 0.042 Uiso 1 1 calc R . .
H40B H 1.1514 0.4107 0.6124 0.042 Uiso 1 1 calc R . .

H40C H 1.1101 0.3652 0.6901 0.042 Uiso 1 1 calc R . .
C41 C 0.52448(11) 0.22396(6) 0.71645(8) 0.0181(3) Uani 1 1 d . . .
H41A H 0.5996 0.2276 0.7472 0.022 Uiso 1 1 calc R . .
H41B H 0.4710 0.2059 0.7600 0.022 Uiso 1 1 calc R . .
C42 C 0.53603(11) 0.17921(6) 0.63861(8) 0.0210(3) Uani 1 1 d . . .
H42A H 0.5878 0.1968 0.5934 0.025 Uiso 1 1 calc R . .
H42B H 0.4606 0.1726 0.6094 0.025 Uiso 1 1 calc R . .
C43 C 0.58342(11) 0.11748(6) 0.67249(9) 0.0219(3) Uani 1 1 d . . .
H43A H 0.6582 0.1245 0.7026 0.026 Uiso 1 1 calc R . .
H43B H 0.5312 0.1002 0.7175 0.026 Uiso 1 1 calc R . .
C44 C 0.59775(12) 0.07094(6) 0.59635(9) 0.0244(3) Uani 1 1 d . . .
H44A H 0.6499 0.0887 0.5516 0.029 Uiso 1 1 calc R . .
H44B H 0.5229 0.0647 0.5661 0.029 Uiso 1 1 calc R . .
C45 C 0.64423(13) 0.00809(7) 0.62618(10) 0.0304(3) Uani 1 1 d . . .
H45A H 0.5983 -0.0071 0.6767 0.036 Uiso 1 1 calc R . .
H45B H 0.6347 -0.0214 0.5758 0.036 Uiso 1 1 calc R . .
C46 C 0.76861(14) 0.00898(8) 0.65545(11) 0.0375(4) Uani 1 1 d . . .
H46A H 0.8150 0.0240 0.6059 0.056 Uiso 1 1 calc R . .
H46B H 0.7928 -0.0328 0.6720 0.056 Uiso 1 1 calc R . .
H46C H 0.7784 0.0364 0.7074 0.056 Uiso 1 1 calc R . .

A-16: Crystallographic Information File (CIF) for $(3)^{2-}2Bu_4N^+$

.....

_chemical_name_common	tetra-*n*-butylammonium trioxaditriangulentae
_chemical_formula_moiety	$2(C_{16}H_{36}N), C_{19}H_6O_6, C_2H_3N, 4(H_2O)$
_symmetry_cell_setting	triclinic
_symmetry_space_group_name_H-M	'P -1'

loop_
_symmetry_equiv_pos_as_xyz
'x, y, z'
'-x, -y, -z'

_cell_length_a	10.4469(1)
_cell_length_b	13.4585(1)
_cell_length_c	20.3609(3)
_cell_angle_alpha	107.9449(5)
_cell_angle_beta	98.1921(5)
_cell_angle_gamma	98.4178(5)
_cell_formula_units_Z	2

loop_

_atom_site_label
_atom_site_type_symbol
_atom_site_fract_x
_atom_site_fract_y
_atom_site_fract_z
_atom_site_U_iso_or_equiv
_atom_site_adp_type
_atom_site_occupancy
_atom_site_symmetry_multiplicity
_atom_site_calc_flag
_atom_site_refinement_flags
_atom_site_disorder_assembly
_atom_site_disorder_group
O1 O 0.60099(11) 0.10226(9) 0.71003(6) 0.0230(3) Uani 1 1 d . . .
O2 O 0.36834(11) 0.38043(8) 0.71430(6) 0.0189(3) Uani 1 1 d . . .
O3 O 0.13214(11) 0.65586(9) 0.71375(6) 0.0233(3) Uani 1 1 d . . .
O4 O 0.12198(11) 0.38757(8) 0.49669(6) 0.0182(2) Uani 1 1 d . . .
O5 O 0.10760(11) 0.11130(9) 0.28340(6) 0.0218(3) Uani 1 1 d . . .
O6 O 0.37902(11) 0.11556(8) 0.49339(6) 0.0186(3) Uani 1 1 d . . .
C1 C 0.41747(15) 0.15695(12) 0.56637(8) 0.0165(3) Uani 1 1 d . . .
C2 C 0.49720(16) 0.10898(13) 0.60075(9) 0.0184(3) Uani 1 1 d . . .
H2A H 0.5298 0.0498 0.5747 0.022 Uiso 1 1 calc R . .
C3 C 0.53145(15) 0.14845(13) 0.67635(9) 0.0180(3) Uani 1 1 d . . .
C4 C 0.48491(15) 0.24096(13) 0.71395(9) 0.0181(3) Uani 1 1 d . . .
H4A H 0.5064 0.2685 0.7640 0.022 Uiso 1 1 calc R . .
C5 C 0.40946(15) 0.28920(12) 0.67743(8) 0.0165(3) Uani 1 1 d . . .
C6 C 0.28906(15) 0.43024(12) 0.67873(8) 0.0170(3) Uani 1 1 d . . .
C7 C 0.25254(16) 0.52109(12) 0.71600(9) 0.0186(3) Uani 1 1 d . . .
H7A H 0.2826 0.5511 0.7656 0.022 Uiso 1 1 calc R . .
C8 C 0.16821(16) 0.57118(12) 0.67966(9) 0.0188(3) Uani 1 1 d . . .
C9 C 0.12466(16) 0.52352(13) 0.60442(9) 0.0194(4) Uani 1 1 d . . .
H9A H 0.0683 0.5548 0.5794 0.023 Uiso 1 1 calc R . .
C10 C 0.16472(15) 0.43329(12) 0.56929(8) 0.0169(3) Uani 1 1 d . . .
C11 C 0.16292(15) 0.29651(12) 0.45940(8) 0.0167(3) Uani 1 1 d . . .
C12 C 0.11558(15) 0.25151(12) 0.38839(8) 0.0176(3) Uani 1 1 d . . .
H12A H 0.0575 0.2833 0.3647 0.021 Uiso 1 1 calc R . .
C13 C 0.15453(15) 0.15599(13) 0.35008(8) 0.0183(3) Uani 1 1 d . . .
C14 C 0.24557(15) 0.11089(12) 0.38668(8) 0.0179(3) Uani 1 1 d . . .
H14A H 0.2739 0.0485 0.3618 0.021 Uiso 1 1 calc R . .
C15 C 0.29067(15) 0.15909(12) 0.45761(8) 0.0168(3) Uani 1 1 d . . .
C16 C 0.37328(15) 0.24801(12) 0.60349(8) 0.0159(3) Uani 1 1 d . . .
C18 C 0.24994(15) 0.25138(12) 0.49537(8) 0.0158(3) Uani 1 1 d . . .
C17 C 0.24782(15) 0.38532(12) 0.60506(8) 0.0164(3) Uani 1 1 d . . .
C19 C 0.29088(15) 0.29543(12) 0.56796(8) 0.0161(3) Uani 1 1 d . . .
N1A N 0.69004(13) 0.05640(11) 0.23069(7) 0.0185(3) Uani 1 1 d . . .
C1A C 0.75416(16) 0.10479(13) 0.18182(9) 0.0203(4) Uani 1 1 d . . .

H1AA H 0.7738 0.1834 0.2040 0.024 Uiso 1 1 calc R . .
H1AB H 0.8395 0.0820 0.1780 0.024 Uiso 1 1 calc R . .
C2A C 0.67406(17) 0.07642(14) 0.10821(9) 0.0243(4) Uani 1 1 d . . .
H2AA H 0.5937 0.1072 0.1104 0.029 Uiso 1 1 calc R . .
H2AB H 0.6463 -0.0020 0.0867 0.029 Uiso 1 1 calc R . .
C3A C 0.75660(19) 0.11975(16) 0.06320(10) 0.0312(4) Uani 1 1 d . . .
H3AA H 0.7990 0.1951 0.0897 0.037 Uiso 1 1 calc R . .
H3AB H 0.8275 0.0790 0.0541 0.037 Uiso 1 1 calc R . .
C4A C 0.6754(2) 0.11296(19) -0.00669(10) 0.0415(5) Uani 1 1 d . . .
H4AA H 0.7328 0.1418 -0.0334 0.062 Uiso 1 1 calc R . .
H4AB H 0.6061 0.1544 0.0020 0.062 Uiso 1 1 calc R . .
H4AC H 0.6349 0.0383 -0.0338 0.062 Uiso 1 1 calc R . .
C5A C 0.66712(16) -0.06448(13) 0.20299(9) 0.0212(4) Uani 1 1 d . . .
H5AA H 0.5928 -0.0912 0.1619 0.025 Uiso 1 1 calc R . .
H5AB H 0.6396 -0.0915 0.2399 0.025 Uiso 1 1 calc R . .
C6A C 0.78448(17) -0.11164(13) 0.18098(9) 0.0241(4) Uani 1 1 d . . .
H6AA H 0.8630 -0.0788 0.2195 0.029 Uiso 1 1 calc R . .
H6AB H 0.8043 -0.0949 0.1390 0.029 Uiso 1 1 calc R . .
C7A C 0.75672(18) -0.23261(14) 0.16394(10) 0.0283(4) Uani 1 1 d . . .
H7AA H 0.8390 -0.2587 0.1563 0.034 Uiso 1 1 calc R . .
H7AB H 0.7313 -0.2488 0.2051 0.034 Uiso 1 1 calc R . .
C8A C 0.6483(2) -0.29280(16) 0.09942(11) 0.0416(5) Uani 1 1 d . . .
H8AA H 0.6382 -0.3696 0.0906 0.062 Uiso 1 1 calc R . .
H8AB H 0.6721 -0.2767 0.0584 0.062 Uiso 1 1 calc R . .
H8AC H 0.5650 -0.2708 0.1077 0.062 Uiso 1 1 calc R . .
C9A C 0.78458(16) 0.10260(13) 0.30211(8) 0.0200(4) Uani 1 1 d . . .
H9AA H 0.8678 0.0766 0.2972 0.024 Uiso 1 1 calc R . .
H9AB H 0.8059 0.1812 0.3149 0.024 Uiso 1 1 calc R . .
C10A C 0.73406(17) 0.07588(14) 0.36227(9) 0.0239(4) Uani 1 1 d . . .
H10A H 0.7370 0.0008 0.3574 0.029 Uiso 1 1 calc R . .
H10B H 0.6412 0.0843 0.3606 0.029 Uiso 1 1 calc R . .
C11A C 0.81939(18) 0.14995(15) 0.43270(9) 0.0294(4) Uani 1 1 d . . .
H11A H 0.9113 0.1389 0.4346 0.035 Uiso 1 1 calc R . .
H11B H 0.8201 0.2249 0.4357 0.035 Uiso 1 1 calc R . .
C12A C 0.7706(2) 0.13145(17) 0.49550(10) 0.0379(5) Uani 1 1 d . . .
H12B H 0.8241 0.1844 0.5391 0.057 Uiso 1 1 calc R . .
H12C H 0.7781 0.0597 0.4955 0.057 Uiso 1 1 calc R . .
H12D H 0.6780 0.1383 0.4925 0.057 Uiso 1 1 calc R . .
C13A C 0.55627(16) 0.08581(13) 0.23683(9) 0.0211(4) Uani 1 1 d . . .
H13A H 0.5130 0.0462 0.2641 0.025 Uiso 1 1 calc R . .
H13B H 0.5007 0.0619 0.1890 0.025 Uiso 1 1 calc R . .
C14A C 0.56059(16) 0.20405(13) 0.27168(10) 0.0243(4) Uani 1 1 d . . .
H14B H 0.6132 0.2287 0.3203 0.029 Uiso 1 1 calc R . .
H14C H 0.6039 0.2449 0.2451 0.029 Uiso 1 1 calc R . .
C15A C 0.42169(17) 0.22449(14) 0.27370(10) 0.0269(4) Uani 1 1 d . . .
H15A H 0.3737 0.2087 0.2249 0.032 Uiso 1 1 calc R . .

H15B H 0.3745 0.1751 0.2937 0.032 Uiso 1 1 calc R . .
C16A C 0.41918(19) 0.33770(15) 0.31668(11) 0.0337(5) Uani 1 1 d . . .
H16A H 0.3275 0.3468 0.3144 0.051 Uiso 1 1 calc R . .
H16B H 0.4670 0.3873 0.2977 0.051 Uiso 1 1 calc R . .
H16C H 0.4614 0.3524 0.3658 0.051 Uiso 1 1 calc R . .
N1B N 0.13856(13) 0.55686(10) 0.23106(7) 0.0191(3) Uani 1 1 d . . .
C1B C 0.13227(17) 0.67434(12) 0.25098(9) 0.0209(4) Uani 1 1 d . . .
H1BA H 0.1129 0.6914 0.2071 0.025 Uiso 1 1 calc R . .
H1BB H 0.2206 0.7168 0.2771 0.025 Uiso 1 1 calc R . .
C2B C 0.03120(17) 0.71014(13) 0.29527(9) 0.0235(4) Uani 1 1 d . . .
H2BA H 0.0424 0.6869 0.3370 0.028 Uiso 1 1 calc R . .
H2BB H -0.0591 0.6772 0.2673 0.028 Uiso 1 1 calc R . .
C3B C 0.04998(18) 0.83167(14) 0.31891(10) 0.0266(4) Uani 1 1 d . . .
H3BA H 0.1405 0.8637 0.3468 0.032 Uiso 1 1 calc R . .
H3BB H 0.0407 0.8541 0.2768 0.032 Uiso 1 1 calc R . .
C4B C -0.04866(19) 0.87343(15) 0.36282(11) 0.0343(5) Uani 1 1 d . . .
H4BA H -0.0312 0.9515 0.3776 0.051 Uiso 1 1 calc R . .
H4BB H -0.0402 0.8512 0.4045 0.051 Uiso 1 1 calc R . .
H4BC H -0.1384 0.8446 0.3347 0.051 Uiso 1 1 calc R . .
C5B C 0.00881(16) 0.48719(13) 0.18490(9) 0.0206(4) Uani 1 1 d . . .
H5BA H 0.0146 0.4116 0.1763 0.025 Uiso 1 1 calc R . .
H5BB H -0.0625 0.5016 0.2116 0.025 Uiso 1 1 calc R . .
C6B C -0.03102(17) 0.50134(14) 0.11416(9) 0.0234(4) Uani 1 1 d . . .
H6BA H 0.0267 0.4706 0.0821 0.028 Uiso 1 1 calc R . .
H6BB H -0.0206 0.5782 0.1205 0.028 Uiso 1 1 calc R . .
C7B C -0.17442(18) 0.44549(16) 0.08229(10) 0.0303(4) Uani 1 1 d . . .
H7BA H -0.2318 0.4803 0.1131 0.036 Uiso 1 1 calc R . .
H7BB H -0.1855 0.3703 0.0805 0.036 Uiso 1 1 calc R . .
C8B C -0.2183(2) 0.44830(17) 0.00828(10) 0.0344(5) Uani 1 1 d . . .
H8BA H -0.3118 0.4139 -0.0092 0.052 Uiso 1 1 calc R . .
H8BB H -0.1653 0.4103 -0.0231 0.052 Uiso 1 1 calc R . .
H8BC H -0.2063 0.5225 0.0096 0.052 Uiso 1 1 calc R . .
C9B C 0.25215(16) 0.54220(13) 0.19251(9) 0.0210(4) Uani 1 1 d . . .
H9BA H 0.2379 0.5709 0.1534 0.025 Uiso 1 1 calc R . .
H9BB H 0.3343 0.5863 0.2254 0.025 Uiso 1 1 calc R . .
C10B C 0.27425(17) 0.42959(13) 0.16242(9) 0.0240(4) Uani 1 1 d . . .
H10C H 0.1981 0.3858 0.1247 0.029 Uiso 1 1 calc R . .
H10D H 0.2824 0.3969 0.1998 0.029 Uiso 1 1 calc R . .
C11B C 0.40053(17) 0.43288(15) 0.13260(10) 0.0276(4) Uani 1 1 d . . .
H11C H 0.3883 0.4611 0.0931 0.033 Uiso 1 1 calc R . .
H11D H 0.4737 0.4831 0.1696 0.033 Uiso 1 1 calc R . .
C12B C 0.4398(2) 0.32556(16) 0.10653(11) 0.0352(5) Uani 1 1 d . . .
H12E H 0.5194 0.3335 0.0868 0.053 Uiso 1 1 calc R . .
H12F H 0.3678 0.2749 0.0701 0.053 Uiso 1 1 calc R . .
H12G H 0.4577 0.2989 0.1459 0.053 Uiso 1 1 calc R . .
C13B C 0.15911(16) 0.52335(13) 0.29606(8) 0.0196(4) Uani 1 1 d . . .

H13C H 0.1648 0.4471 0.2806 0.024 Uiso 1 1 calc R . .
H13D H 0.0798 0.5295 0.3173 0.024 Uiso 1 1 calc R . .
C14B C 0.27996(16) 0.58526(13) 0.35335(9) 0.0217(4) Uani 1 1 d . . .
H14D H 0.2865 0.6628 0.3632 0.026 Uiso 1 1 calc R . .
H14E H 0.3610 0.5658 0.3376 0.026 Uiso 1 1 calc R . .
C15B C 0.26646(17) 0.55819(14) 0.41976(9) 0.0251(4) Uani 1 1 d . . .
H15C H 0.2478 0.4797 0.4076 0.030 Uiso 1 1 calc R . .
H15D H 0.1903 0.5849 0.4376 0.030 Uiso 1 1 calc R . .
C16B C 0.38978(19) 0.60587(17) 0.47796(10) 0.0354(5) Uani 1 1 d . . .
H16D H 0.3741 0.5888 0.5199 0.053 Uiso 1 1 calc R . .
H16E H 0.4101 0.6835 0.4895 0.053 Uiso 1 1 calc R . .
H16F H 0.4643 0.5760 0.4618 0.053 Uiso 1 1 calc R . .
O1W O 0.05990(12) 0.26016(10) 0.22046(6) 0.0248(3) Uani 1 1 d D . .
H1W1 H -0.0001(16) 0.2854(14) 0.2401(10) 0.037 Uiso 1 1 d D . .
H2W1 H 0.0774(18) 0.2143(13) 0.2397(10) 0.037 Uiso 1 1 d D . .
O2W O 0.07107(14) -0.23343(11) 0.10734(8) 0.0352(3) Uani 1 1 d D . .
H1W2 H 0.0158(19) -0.2206(16) 0.0769(8) 0.053 Uiso 1 1 d D . .
H2W2 H 0.100(2) -0.1713(11) 0.1390(8) 0.053 Uiso 1 1 d D . .
O3W O 0.20925(15) -0.04506(11) 0.20411(7) 0.0360(3) Uani 1 1 d D . .
H1W3 H 0.2703(17) -0.0597(17) 0.2291(10) 0.054 Uiso 1 1 d D . .
H2W3 H 0.186(2) 0.0072(14) 0.2312(10) 0.054 Uiso 1 1 d D . .
O4W O 0.64517(18) 0.23194(15) 0.85802(10) 0.0598(5) Uani 1 1 d D . .
H1W4 H 0.643(3) 0.1797(18) 0.8155(8) 0.090 Uiso 1 1 d D . .
H2W4 H 0.7288(15) 0.230(2) 0.8781(12) 0.090 Uiso 1 1 d D . .
C1S C 1.1127(2) 0.12819(17) 0.04389(11) 0.0383(5) Uani 1 1 d . . .
C2S C 1.1402(2) 0.08207(17) 0.09827(10) 0.0396(5) Uani 1 1 d . . .
H2S1 H 1.0899 0.0086 0.0824 0.059 Uiso 1 1 calc R . .
H2S2 H 1.1145 0.1241 0.1411 0.059 Uiso 1 1 calc R . .
H2S3 H 1.2348 0.0821 0.1082 0.059 Uiso 1 1 calc R . .
N1S N 1.0902(2) 0.16420(18) 0.00072(11) 0.0613(6) Uani 1 1 d . . .

A-17: Crystallographic Information File (CIF) for 1(NPr)$_3$•2

.....

_chemical_name_common	triazatripropyltriangulenium trioxotriangulenate
_chemical_formula_moiety	C_{28} H_{30} N_3, C_{22} H_9 O_3
_symmetry_cell_setting	triclinic
_symmetry_space_group_name_H-M	'P -1'

loop_
_symmetry_equiv_pos_as_xyz
'x, y, z'
'-x, -y, -z'

_cell_length_a 8.0919(4)
_cell_length_b 10.5549(5)
_cell_length_c 20.7536(10)
_cell_angle_alpha 85.528(2)
_cell_angle_beta 81.889(2)
_cell_angle_gamma 74.393(2)
_cell_formula_units_Z 2

loop_
 _atom_site_label
 _atom_site_type_symbol
 _atom_site_fract_x
 _atom_site_fract_y
 _atom_site_fract_z
 _atom_site_U_iso_or_equiv
 _atom_site_adp_type
 _atom_site_occupancy
 _atom_site_symmetry_multiplicity
 _atom_site_calc_flag
 _atom_site_refinement_flags
 _atom_site_disorder_assembly
 _atom_site_disorder_group
N1C N 0.65048(14) 0.68285(11) 0.64602(5) 0.0152(2) Uani 1 1 d . . .
N2C N 0.48861(14) 0.41220(11) 0.82892(5) 0.0158(2) Uani 1 1 d . . .
N3C N 0.19665(14) 0.87481(11) 0.81406(5) 0.0162(2) Uani 1 1 d . . .
C1C C 0.26497(17) 1.00887(13) 0.71837(7) 0.0186(3) Uani 1 1 d . . .
H1C H 0.1855 1.0857 0.7359 0.022 Uiso 1 1 calc R . .
C2C C 0.35748(17) 1.01414(13) 0.65745(7) 0.0189(3) Uani 1 1 d . . .
H2C H 0.3348 1.0951 0.6327 0.023 Uiso 1 1 calc R . .
C3C C 0.48084(17) 0.90825(13) 0.63077(6) 0.0173(3) Uani 1 1 d . . .
H3C H 0.5403 0.9161 0.5884 0.021 Uiso 1 1 calc R . .
C4C C 0.81242(17) 0.45493(13) 0.65724(6) 0.0178(3) Uani 1 1 d . . .
H4C H 0.8850 0.4625 0.6177 0.021 Uiso 1 1 calc R . .
C5C C 0.83740(17) 0.33739(13) 0.69313(7) 0.0184(3) Uani 1 1 d . . .
H5C H 0.9304 0.2656 0.6780 0.022 Uiso 1 1 calc R . .
C6C C 0.73361(17) 0.31899(13) 0.75003(7) 0.0179(3) Uani 1 1 d . . .
H6C H 0.7538 0.2359 0.7730 0.021 Uiso 1 1 calc R . .
C7C C 0.27392(18) 0.50953(14) 0.91740(7) 0.0198(3) Uani 1 1 d . . .
H7C H 0.2903 0.4276 0.9414 0.024 Uiso 1 1 calc R . .
C8C C 0.15568(18) 0.61999(14) 0.94198(7) 0.0219(3) Uani 1 1 d . . .
H8C H 0.0911 0.6123 0.9834 0.026 Uiso 1 1 calc R . .
C9C C 0.12631(18) 0.74150(14) 0.90945(7) 0.0209(3) Uani 1 1 d . . .
H9C H 0.0430 0.8152 0.9282 0.025 Uiso 1 1 calc R . .
C10C C 0.29001(16) 0.88931(13) 0.75362(6) 0.0154(3) Uani 1 1 d . . .
C11C C 0.41597(16) 0.77807(13) 0.72764(6) 0.0141(3) Uani 1 1 d . . .
C12C C 0.51706(17) 0.78941(13) 0.66684(6) 0.0150(3) Uani 1 1 d . . .

C13C C 0.68034(16) 0.56212(13) 0.67934(6) 0.0152(3) Uani 1 1 d . . .
C14C C 0.57378(16) 0.54767(13) 0.73823(6) 0.0143(3) Uani 1 1 d . . .
C15C C 0.59949(17) 0.42403(13) 0.77303(6) 0.0155(3) Uani 1 1 d . . .
C16C C 0.36939(17) 0.51954(13) 0.85670(6) 0.0157(3) Uani 1 1 d . . .
C17C C 0.34382(17) 0.64351(13) 0.82256(6) 0.0148(3) Uani 1 1 d . . .
C18C C 0.21989(17) 0.75515(13) 0.84883(6) 0.0165(3) Uani 1 1 d . . .
C19C C 0.44400(16) 0.65612(13) 0.76256(6) 0.0143(3) Uani 1 1 d . . .
C20C C 0.77298(16) 0.70173(13) 0.58914(6) 0.0170(3) Uani 1 1 d . . .
H20A H 0.8899 0.6477 0.5965 0.020 Uiso 1 1 calc R . .
H20B H 0.7761 0.7951 0.5858 0.020 Uiso 1 1 calc R . .
C21C C 0.73202(17) 0.66624(13) 0.52481(6) 0.0190(3) Uani 1 1 d . . .
H21A H 0.6123 0.7144 0.5180 0.023 Uiso 1 1 calc R . .
H21B H 0.7419 0.5706 0.5251 0.023 Uiso 1 1 calc R . .
C22C C 0.85915(18) 0.70335(16) 0.47042(7) 0.0250(3) Uani 1 1 d . . .
H22A H 0.8426 0.7990 0.4684 0.037 Uiso 1 1 calc R . .
H22B H 0.8393 0.6756 0.4288 0.037 Uiso 1 1 calc R . .
H22C H 0.9776 0.6595 0.4790 0.037 Uiso 1 1 calc R . .
C23C C 0.49810(17) 0.28095(13) 0.85986(6) 0.0181(3) Uani 1 1 d . . .
H23A H 0.5346 0.2148 0.8259 0.022 Uiso 1 1 calc R . .
H23B H 0.3814 0.2780 0.8809 0.022 Uiso 1 1 calc R . .
C24C C 0.62309(18) 0.24452(14) 0.91054(7) 0.0225(3) Uani 1 1 d . . .
H24A H 0.7421 0.2387 0.8892 0.027 Uiso 1 1 calc R . .
H24B H 0.5931 0.3139 0.9429 0.027 Uiso 1 1 calc R . .
C25C C 0.6155(2) 0.11355(15) 0.94485(8) 0.0295(3) Uani 1 1 d . . .
H25A H 0.5004 0.1216 0.9691 0.044 Uiso 1 1 calc R . .
H25B H 0.7027 0.0884 0.9751 0.044 Uiso 1 1 calc R . .
H25C H 0.6384 0.0461 0.9125 0.044 Uiso 1 1 calc R . .
C26C C 0.09605(17) 0.99322(13) 0.84832(6) 0.0187(3) Uani 1 1 d . . .
H26A H -0.0068 0.9749 0.8752 0.022 Uiso 1 1 calc R . .
H26B H 0.0558 1.0656 0.8163 0.022 Uiso 1 1 calc R . .
C27C C 0.20750(18) 1.03437(13) 0.89159(6) 0.0201(3) Uani 1 1 d . . .
H27A H 0.2669 0.9562 0.9170 0.024 Uiso 1 1 calc R . .
H27B H 0.2973 1.0686 0.8638 0.024 Uiso 1 1 calc R . .
C28C C 0.10337(19) 1.13900(13) 0.93815(7) 0.0223(3) Uani 1 1 d . . .
H28A H 0.0529 1.2195 0.9133 0.033 Uiso 1 1 calc R . .
H28B H 0.1792 1.1577 0.9669 0.033 Uiso 1 1 calc R . .
H28C H 0.0107 1.1073 0.9643 0.033 Uiso 1 1 calc R . .
O1A O 0.30333(12) 0.72149(10) 0.52871(5) 0.0231(2) Uani 1 1 d . . .
O2A O 0.12331(13) 0.31228(9) 0.80643(5) 0.0220(2) Uani 1 1 d . . .
O3A O -0.33805(13) 0.99411(10) 0.79090(5) 0.0268(2) Uani 1 1 d . . .
C1A C -0.17575(17) 1.02626(13) 0.66435(7) 0.0193(3) Uani 1 1 d . . .
H1A H -0.2684 1.0968 0.6810 0.023 Uiso 1 1 calc R . .
C2A C -0.08685(18) 1.04150(13) 0.60345(7) 0.0207(3) Uani 1 1 d . . .
H2A H -0.1188 1.1214 0.5783 0.025 Uiso 1 1 calc R . .
C3A C 0.04903(17) 0.93904(14) 0.57958(7) 0.0190(3) Uani 1 1 d . . .
H3A H 0.1128 0.9506 0.5385 0.023 Uiso 1 1 calc R . .

C4A C 0.09417(17) 0.81968(13) 0.61443(6) 0.0169(3) Uani 1 1 d . . .
C5A C 0.22891(17) 0.71040(14) 0.58437(6) 0.0171(3) Uani 1 1 d . . .
C6A C 0.26752(17) 0.58532(13) 0.62292(6) 0.0162(3) Uani 1 1 d . . .
C7A C 0.39869(17) 0.47934(13) 0.59854(6) 0.0181(3) Uani 1 1 d . . .
H7A H 0.4641 0.4897 0.5576 0.022 Uiso 1 1 calc R . .
C8A C 0.43597(17) 0.35930(13) 0.63254(7) 0.0190(3) Uani 1 1 d . . .
H8A H 0.5280 0.2886 0.6157 0.023 Uiso 1 1 calc R . .
C9A C 0.33810(17) 0.34288(13) 0.69136(7) 0.0183(3) Uani 1 1 d . . .
H9A H 0.3625 0.2599 0.7144 0.022 Uiso 1 1 calc R . .
C10A C 0.20461(17) 0.44590(13) 0.71735(6) 0.0163(3) Uani 1 1 d . . .
C11A C 0.09951(17) 0.42259(13) 0.77851(6) 0.0168(3) Uani 1 1 d . . .
C12A C -0.03542(17) 0.53613(13) 0.80467(6) 0.0166(3) Uani 1 1 d . . .
C13A C -0.13885(18) 0.52077(14) 0.86261(7) 0.0194(3) Uani 1 1 d . . .
H13A H -0.1201 0.4368 0.8847 0.023 Uiso 1 1 calc R . .
C14A C -0.26817(18) 0.62463(14) 0.88880(7) 0.0206(3) Uani 1 1 d . . .
H14A H -0.3379 0.6120 0.9284 0.025 Uiso 1 1 calc R . .
C15A C -0.29535(17) 0.74742(14) 0.85685(7) 0.0194(3) Uani 1 1 d . . .
H15A H -0.3838 0.8190 0.8750 0.023 Uiso 1 1 calc R . .
C16A C -0.19531(17) 0.76744(13) 0.79878(6) 0.0169(3) Uani 1 1 d . . .
C17A C -0.23061(17) 0.89853(13) 0.76587(7) 0.0180(3) Uani 1 1 d . . .
C18A C -0.13191(17) 0.90966(13) 0.70160(7) 0.0168(3) Uani 1 1 d . . .
C19A C 0.00228(17) 0.80190(13) 0.67657(6) 0.0153(3) Uani 1 1 d . . .
C20A C 0.16879(17) 0.57118(13) 0.68426(6) 0.0152(3) Uani 1 1 d . . .
C21A C -0.06279(17) 0.66112(13) 0.77093(6) 0.0153(3) Uani 1 1 d . . .
C22A C 0.03774(17) 0.67837(13) 0.71102(6) 0.0151(3) Uani 1 1 d . . .

A-18: Crystallographic Information File (CIF) for 1(NOct)$_3$•2

.....

_chemical_name_common	triazatrioctyltriangulenium trioxotriangulenate
_chemical_formula_moiety	C_{60} H_{40} N_3 O_3
_symmetry_cell_setting	monoclinic
_symmetry_space_group_name_H-M	P 21/n

loop_
 _symmetry_equiv_pos_as_xyz
 'x, y, z'
 '-x+1/2, y+1/2, -z+1/2'
 '-x, -y, -z'
 'x-1/2, -y-1/2, z-1/2'

_cell_length_a 8.5228(9)
_cell_length_b 16.448(2)
_cell_length_c 38.007(4)
_cell_angle_alpha 90.00
_cell_angle_beta 93.667(6)
_cell_angle_gamma 90.00
_cell_formula_units_Z 5

loop_
 _atom_site_label
 _atom_site_type_symbol
 _atom_site_fract_x
 _atom_site_fract_y
 _atom_site_fract_z
 _atom_site_U_iso_or_equiv
 _atom_site_adp_type
 _atom_site_occupancy
 _atom_site_symmetry_multiplicity
 _atom_site_calc_flag
 _atom_site_refinement_flags
 _atom_site_disorder_assembly
 _atom_site_disorder_group
N1 N -0.0825(9) 0.2164(5) -0.26885(18) 0.0335(18) Uani 1 1 d . . .
N2 N -0.2789(8) 0.1767(5) -0.15424(19) 0.0364(19) Uani 1 1 d . . .
O3 O 0.3476(8) 0.5364(4) 0.18405(16) 0.0467(17) Uani 1 1 d . . .
N4 N 0.0589(9) 0.4043(5) -0.17558(19) 0.0337(18) Uani 1 1 d . . .
C5 C 0.6625(11) 0.7210(6) 0.1213(2) 0.036(2) Uani 1 1 d . . .
C6 C -0.1046(10) 0.2672(6) -0.1993(2) 0.031(2) Uani 1 1 d . . .
C7 C 0.7601(11) 0.8547(6) 0.2153(2) 0.037(2) Uani 1 1 d . . .
O8 O 0.7176(7) 0.8721(4) 0.27584(16) 0.0425(17) Uani 1 1 d . . .
O9 O 0.8117(9) 0.8172(5) 0.09158(18) 0.057(2) Uani 1 1 d . . .
C10 C 0.0591(10) 0.3840(6) -0.2099(2) 0.032(2) Uani 1 1 d . . .
C11 C -0.1959(10) 0.2430(6) -0.1406(2) 0.035(2) Uani 1 1 d . . .
C12 C 0.6304(11) 0.7414(6) 0.1842(2) 0.032(2) Uani 1 1 d . . .
C13 C 0.4678(10) 0.6449(6) 0.2164(2) 0.032(2) Uani 1 1 d . . .
C14 C -0.1880(10) 0.1975(5) -0.2120(2) 0.0273(19) Uani 1 1 d . . .
C15 C 0.7282(10) 0.8097(6) 0.1843(2) 0.033(2) Uani 1 1 d . . .
C16 C -0.0202(10) 0.3147(5) -0.2227(2) 0.029(2) Uani 1 1 d . . .
C17 C -0.2521(11) 0.1022(6) -0.2592(3) 0.040(2) Uani 1 1 d . . .
C18 C 0.5284(11) 0.7334(6) 0.2779(2) 0.036(2) Uani 1 1 d . . .
C19 C 0.5936(10) 0.7594(6) 0.2468(2) 0.031(2) Uani 1 1 d . . .
C20 C -0.0137(10) 0.2884(6) -0.2577(2) 0.034(2) Uani 1 1 d . . .
C22 C 0.5654(10) 0.7156(6) 0.2158(2) 0.033(2) Uani 1 1 d . . .
C23 C 0.5015(11) 0.6255(6) 0.1529(2) 0.037(2) Uani 1 1 d . . .
C24 C 0.6005(10) 0.6960(6) 0.1533(2) 0.033(2) Uani 1 1 d . . .
C25 C 0.4066(11) 0.6205(6) 0.2478(3) 0.039(2) Uani 1 1 d . . .

C26 C -0.1101(10) 0.2900(5) -0.1641(2) 0.028(2) Uani 1 1 d . . .
C27 C -0.0235(10) 0.3592(6) -0.1517(2) 0.036(2) Uani 1 1 d . . .
C28 C -0.2745(10) 0.1531(6) -0.1891(2) 0.031(2) Uani 1 1 d . . .
C29 C 0.1470(11) 0.4760(6) -0.1611(2) 0.037(2) Uani 1 1 d . . .
C30 C 0.8624(10) 0.9219(6) 0.2162(3) 0.039(2) Uani 1 1 d . . .
C31 C 0.1420(11) 0.4072(6) -0.2685(2) 0.038(2) Uani 1 1 d . . .
C32 C 0.7930(10) 0.8361(6) 0.1531(2) 0.038(2) Uani 1 1 d . . .
C33 C 0.8905(11) 0.9041(6) 0.1534(3) 0.043(2) Uani 1 1 d . . .
C34 C 0.7620(11) 0.7934(6) 0.1205(3) 0.041(2) Uani 1 1 d . . .
C35 C -0.3503(11) 0.0819(6) -0.2010(3) 0.040(2) Uani 1 1 d . . .
C36 C 0.6921(10) 0.8312(6) 0.2486(2) 0.036(2) Uani 1 1 d . . .
C37 C -0.0250(11) 0.3809(6) -0.1164(2) 0.038(2) Uani 1 1 d . . .
C38 C 0.0651(11) 0.3380(6) -0.2816(2) 0.035(2) Uani 1 1 d . . .
C39 C -0.0465(12) 0.1811(6) -0.3032(2) 0.043(3) Uani 1 1 d . . .
C40 C -0.1771(10) 0.1726(6) -0.2473(2) 0.034(2) Uani 1 1 d . . .
C41 C -0.1919(12) 0.2631(6) -0.1054(2) 0.042(2) Uani 1 1 d . . .
C42 C 0.4363(10) 0.5977(6) 0.1846(2) 0.033(2) Uani 1 1 d . . .
C43 C -0.3786(13) 0.1321(6) -0.1316(3) 0.049(3) Uani 1 1 d . . .
C44 C 0.4704(12) 0.5834(7) 0.1219(3) 0.050(3) Uani 1 1 d . . .
C45 C 0.1405(10) 0.4318(6) -0.2338(2) 0.034(2) Uani 1 1 d . . .
C46 C 0.1727(12) 0.6012(6) -0.1009(2) 0.041(2) Uani 1 1 d . . .
C47 C -0.2827(14) 0.1223(8) -0.4607(3) 0.060(3) Uani 1 1 d . . .
C48 C 0.5322(12) 0.6079(7) 0.0895(3) 0.048(3) Uani 1 1 d . . .
C49 C -0.1085(12) 0.3310(7) -0.0942(2) 0.046(3) Uani 1 1 d . . .
C50 C 0.6298(11) 0.6761(6) 0.0903(3) 0.042(2) Uani 1 1 d . . .
C51 C -0.3419(11) 0.0596(6) -0.2357(3) 0.041(2) Uani 1 1 d . . .
C52 C 0.4339(11) 0.6654(6) 0.2781(2) 0.038(2) Uani 1 1 d . . .
C53 C 0.1330(11) 0.6208(6) -0.1395(2) 0.040(2) Uani 1 1 d . . .
C54 C 0.9279(12) 0.9467(6) 0.1847(2) 0.043(3) Uani 1 1 d . . .
C55 C -0.2221(13) 0.1691(8) -0.3984(3) 0.059(3) Uani 1 1 d . . .
C56 C 0.2317(14) 0.6793(6) -0.0814(2) 0.051(3) Uani 1 1 d . . .
C57 C -0.1632(11) 0.2040(6) -0.3329(2) 0.039(2) Uani 1 1 d . . .
C58 C 0.0427(11) 0.5503(6) -0.1593(2) 0.038(2) Uani 1 1 d . . .
C60 C -0.1279(12) 0.1481(7) -0.3638(2) 0.048(3) Uani 1 1 d . . .
C61 C 0.2764(13) 0.6656(7) -0.0424(2) 0.049(3) Uani 1 1 d . . .
C62 C 0.3503(18) 0.7433(8) -0.0250(3) 0.082(4) Uani 1 1 d . . .
C63 C -0.2885(13) 0.0601(7) -0.1126(3) 0.055(3) Uani 1 1 d . . .
C64 C -0.3481(15) 0.0687(8) -0.5222(3) 0.068(3) Uani 1 1 d . . .
C66 C 0.392(2) 0.7306(9) 0.0142(3) 0.099(5) Uani 1 1 d . . .
C67 C -0.1976(13) 0.1032(8) -0.4266(3) 0.062(3) Uani 1 1 d . . .
C68 C -0.2504(15) 0.0561(8) -0.4889(3) 0.066(3) Uani 1 1 d . . .
C903 C -1.033(3) -0.1357(14) -0.1222(5) 0.135(7) Uiso 1 1 d . . .
C904 C -0.786(3) -0.1072(15) -0.1199(6) 0.149(8) Uiso 1 1 d . . .
C906 C -0.520(3) -0.0378(14) -0.1060(6) 0.185(10) Uiso 1 1 d D . .
C908 C -0.680(4) -0.0621(18) -0.0951(7) 0.187(10) Uiso 1 1 d . . .
C909 C -0.918(5) -0.098(2) -0.0991(10) 0.277(18) Uiso 1 1 d . . .

C914 C -0.4013(17) 0.0204(9) -0.0856(4) 0.085(4) Uiso 1 1 d D . .
O1W O 1.0474(9) 0.8894(4) 0.02629(18) 0.056(2) Uiso 1 1 d . . .
O2W O 0.8941(11) 0.8330(6) 0.0004(2) 0.086(3) Uiso 1 1 d . . .

A-19: Crystallographic Information File (CIF) for 1(NDec)$_3$•2

.....

_chemical_name_common	triazatridecyltriangulenium trioxotriangulenate
_chemical_formula_moiety	C_{49} H_{72} N_3, C_{22} H_9 O_3
_symmetry_cell_setting	monoclinic
_symmetry_space_group_name_H-M	P 2/n

loop_
 _symmetry_equiv_pos_as_xyz
 'x, y, z'
 'x+1/2, -y, z+1/2'
 '-x, -y, -z'
 '-x-1/2, y, -z-1/2'

_cell_length_a	14.2627(6)
_cell_length_b	18.3892(10)
_cell_length_c	20.8803(11)
_cell_angle_alpha	90.00
_cell_angle_beta	90.893(3)
_cell_angle_gamma	90.00
_cell_formula_units_Z	4

loop_
 _atom_site_label
 _atom_site_type_symbol
 _atom_site_fract_x
 _atom_site_fract_y
 _atom_site_fract_z
 _atom_site_U_iso_or_equiv
 _atom_site_adp_type
 _atom_site_occupancy
 _atom_site_symmetry_multiplicity
 _atom_site_calc_flag
 _atom_site_refinement_flags
 _atom_site_disorder_assembly
 _atom_site_disorder_group
N1 N 0.5413(3) -0.1295(4) -0.3544(2) 0.0657(17) Uani 1 1 d . . .

N2 N 0.4694(3) -0.1095(4) -0.1305(2) 0.0638(17) Uani 1 1 d . . .
N3 N 0.5036(4) 0.1050(4) -0.2573(3) 0.0752(18) Uani 1 1 d . . .
C1 C 0.5487(4) 0.0972(5) -0.3681(4) 0.077(2) Uani 1 1 d . . .
H1 H 0.5543 0.1485 -0.3719 0.092 Uiso 1 1 calc R A .
C2 C 0.5643(4) 0.0536(5) -0.4202(4) 0.074(2) Uani 1 1 d . A .
H2 H 0.5790 0.0763 -0.4597 0.089 Uiso 1 1 calc R . .
C3 C 0.5599(4) -0.0205(5) -0.4188(3) 0.071(2) Uani 1 1 d . . .
H3 H 0.5692 -0.0485 -0.4564 0.085 Uiso 1 1 calc R A .
C4 C 0.5121(4) -0.2397(5) -0.2924(3) 0.070(2) Uani 1 1 d . . .
H4 H 0.5213 -0.2694 -0.3290 0.084 Uiso 1 1 calc R . .
C5 C 0.4921(4) -0.2707(4) -0.2340(4) 0.073(2) Uani 1 1 d . . .
H5 H 0.4879 -0.3221 -0.2310 0.087 Uiso 1 1 calc R . .
C6 C 0.4781(4) -0.2291(5) -0.1797(3) 0.067(2) Uani 1 1 d . . .
H6 H 0.4653 -0.2522 -0.1401 0.080 Uiso 1 1 calc R . .
C7 C 0.4418(4) 0.0071(5) -0.0831(3) 0.068(2) Uani 1 1 d . . .
H7 H 0.4263 -0.0146 -0.0433 0.082 Uiso 1 1 calc R . .
C8 C 0.4419(4) 0.0809(5) -0.0903(4) 0.071(2) Uani 1 1 d . A .
H8 H 0.4259 0.1103 -0.0547 0.085 Uiso 1 1 calc R . .
C9 C 0.4640(4) 0.1142(5) -0.1463(4) 0.074(2) Uani 1 1 d . . .
H9 H 0.4648 0.1658 -0.1484 0.089 Uiso 1 1 calc R A .
C10 C 0.5245(4) 0.0660(5) -0.3095(4) 0.064(2) Uani 1 1 d . A .
C11 C 0.5231(3) -0.0097(5) -0.3062(3) 0.061(2) Uani 1 1 d . . .
C12 C 0.5412(4) -0.0542(4) -0.3598(3) 0.0613(19) Uani 1 1 d . A .
C13 C 0.5184(4) -0.1644(4) -0.2970(3) 0.0601(19) Uani 1 1 d . A .
C14 C 0.5012(3) -0.1191(4) -0.2428(3) 0.0571(19) Uani 1 1 d . . .
C15 C 0.4827(4) -0.1537(4) -0.1828(3) 0.0579(18) Uani 1 1 d . A .
C16 C 0.4647(4) -0.0346(4) -0.1346(3) 0.0610(19) Uani 1 1 d . A .
C17 C 0.4856(3) -0.0009(4) -0.1940(3) 0.0558(19) Uani 1 1 d . . .
C18 C 0.4850(4) 0.0747(4) -0.1989(4) 0.0613(19) Uani 1 1 d . A .
C19 C 0.5039(3) -0.0440(4) -0.2469(3) 0.0529(17) Uani 1 1 d . A .
C20 C 0.5636(4) -0.1757(4) -0.4088(3) 0.073(2) Uani 1 1 d D . .
H20A H 0.5960 -0.2200 -0.3931 0.088 Uiso 1 1 calc R . .
H20B H 0.6071 -0.1494 -0.4371 0.088 Uiso 1 1 calc R . .
C21 C 0.4770(4) -0.1976(4) -0.4470(3) 0.078(2) Uani 1 1 d D . .
H21A H 0.4409 -0.1534 -0.4587 0.093 Uiso 1 1 calc R . .
H21B H 0.4367 -0.2285 -0.4201 0.093 Uiso 1 1 calc R . .
C22 C 0.5015(4) -0.2387(4) -0.5075(3) 0.078(2) Uani 1 1 d D . .
H22A H 0.4434 -0.2463 -0.5332 0.094 Uiso 1 1 calc R . .
H22B H 0.5441 -0.2083 -0.5331 0.094 Uiso 1 1 calc R . .
C23 C 0.5473(5) -0.3114(5) -0.4958(4) 0.091(3) Uani 1 1 d D . .
H23A H 0.6062 -0.3039 -0.4710 0.109 Uiso 1 1 calc R . .
H23B H 0.5053 -0.3417 -0.4696 0.109 Uiso 1 1 calc R . .
C24 C 0.5691(6) -0.3518(5) -0.5564(4) 0.103(3) Uani 1 1 d D . .
H24A H 0.5101 -0.3590 -0.5813 0.123 Uiso 1 1 calc R . .
H24B H 0.6112 -0.3215 -0.5826 0.123 Uiso 1 1 calc R . .
C25 C 0.6138(6) -0.4234(5) -0.5454(4) 0.112(3) Uani 1 1 d D . .

H25A H 0.5691 -0.4556 -0.5233 0.135 Uiso 1 1 calc R . .
H25B H 0.6693 -0.4170 -0.5169 0.135 Uiso 1 1 calc R . .
C26 C 0.6447(8) -0.4605(6) -0.6087(5) 0.134(4) Uani 1 1 d D . .
H26A H 0.5894 -0.4655 -0.6376 0.161 Uiso 1 1 calc R . .
H26B H 0.6906 -0.4287 -0.6302 0.161 Uiso 1 1 calc R . .
C27 C 0.6875(9) -0.5334(7) -0.5987(6) 0.160(5) Uani 1 1 d D . .
H27A H 0.7392 -0.5281 -0.5669 0.192 Uiso 1 1 calc R . .
H27B H 0.6396 -0.5652 -0.5793 0.192 Uiso 1 1 calc R . .
C28 C 0.7233(11) -0.5697(8) -0.6528(6) 0.191(6) Uani 1 1 d D . .
H28A H 0.7725 -0.5386 -0.6715 0.229 Uiso 1 1 calc R . .
H28B H 0.6721 -0.5738 -0.6851 0.229 Uiso 1 1 calc R . .
C29 C 0.7618(10) -0.6400(7) -0.6433(6) 0.182(6) Uani 1 1 d D . .
H29A H 0.7819 -0.6598 -0.6844 0.273 Uiso 1 1 calc R . .
H29B H 0.7143 -0.6720 -0.6250 0.273 Uiso 1 1 calc R . .
H29C H 0.8159 -0.6369 -0.6139 0.273 Uiso 1 1 calc R . .
C30 C 0.4641(4) -0.1468(4) -0.0677(3) 0.070(2) Uani 1 1 d D . .
H30A H 0.4877 -0.1136 -0.0338 0.084 Uiso 1 1 calc R . .
H30B H 0.5054 -0.1900 -0.0681 0.084 Uiso 1 1 calc R . .
C31 C 0.3672(4) -0.1701(4) -0.0517(3) 0.072(2) Uani 1 1 d D . .
H31A H 0.3427 -0.2024 -0.0860 0.087 Uiso 1 1 calc R . .
H31B H 0.3261 -0.1268 -0.0499 0.087 Uiso 1 1 calc R . .
C32 C 0.3642(4) -0.2102(4) 0.0123(3) 0.074(2) Uani 1 1 d D . .
H32A H 0.4003 -0.2561 0.0092 0.089 Uiso 1 1 calc R . .
H32B H 0.3939 -0.1798 0.0461 0.089 Uiso 1 1 calc R . .
C33 C 0.2648(5) -0.2271(5) 0.0303(4) 0.103(3) Uani 1 1 d D . .
H33A H 0.2298 -0.1808 0.0333 0.123 Uiso 1 1 calc R . .
H33B H 0.2354 -0.2560 -0.0046 0.123 Uiso 1 1 calc R . .
C34 C 0.2536(8) -0.2674(7) 0.0912(5) 0.145(4) Uani 1 1 d D . .
H34A H 0.3110 -0.2623 0.1181 0.174 Uiso 1 1 calc R . .
H34B H 0.2003 -0.2472 0.1152 0.174 Uiso 1 1 calc R . .
C35 C 0.2372(14) -0.3414(7) 0.0773(6) 0.219(8) Uani 1 1 d D . .
H35A H 0.2929 -0.3588 0.0541 0.263 Uiso 1 1 calc R . .
H35B H 0.1842 -0.3427 0.0461 0.263 Uiso 1 1 calc R . .
C36 C 0.2157(10) -0.4000(10) 0.1286(7) 0.210(7) Uani 1 1 d D . .
H36A H 0.2773 -0.4206 0.1415 0.252 Uiso 1 1 calc R . .
H36B H 0.1929 -0.3729 0.1662 0.252 Uiso 1 1 calc R . .
C37 C 0.1533(14) -0.4618(8) 0.1213(8) 0.227(9) Uani 1 1 d D . .
H37A H 0.0901 -0.4421 0.1117 0.272 Uiso 1 1 calc R . .
H37B H 0.1732 -0.4883 0.0825 0.272 Uiso 1 1 calc R . .
C38 C 0.1433(11) -0.5113(9) 0.1673(7) 0.191(6) Uani 1 1 d D . .
H38A H 0.1244 -0.4856 0.2067 0.229 Uiso 1 1 calc R . .
H38B H 0.2055 -0.5332 0.1761 0.229 Uiso 1 1 calc R . .
C39 C 0.0798(12) -0.5677(8) 0.1566(8) 0.219(8) Uani 1 1 d D . .
H39A H 0.0770 -0.5985 0.1948 0.328 Uiso 1 1 calc R . .
H39B H 0.1003 -0.5970 0.1201 0.328 Uiso 1 1 calc R . .
H39C H 0.0176 -0.5475 0.1472 0.328 Uiso 1 1 calc R . .

C40 C 0.4863(15) 0.1915(11) -0.2654(16) 0.103(3) Uani 0.659(10) 1 d PDU A 1
H40A H 0.4728 0.2030 -0.3110 0.123 Uiso 0.659(10) 1 calc PR A 1
H40B H 0.4314 0.2064 -0.2401 0.123 Uiso 0.659(10) 1 calc PR A 1
C41 C 0.5689(12) 0.2316(8) -0.2438(10) 0.115(3) Uani 0.659(10) 1 d PDU A 1
H41A H 0.6200 0.2271 -0.2750 0.139 Uiso 0.659(10) 1 calc PR A 1
H41B H 0.5914 0.2133 -0.2017 0.139 Uiso 0.659(10) 1 calc PR A 1
C42 C 0.5354(13) 0.3140(9) -0.2382(8) 0.134(3) Uani 0.659(10) 1 d PDU A 1
H42A H 0.5919 0.3452 -0.2361 0.161 Uiso 0.659(10) 1 calc PR A 1
H42B H 0.5007 0.3267 -0.2781 0.161 Uiso 0.659(10) 1 calc PR A 1
C43 C 0.4749(12) 0.3329(8) -0.1826(9) 0.146(4) Uani 0.659(10) 1 d PDU A 1
H43A H 0.5057 0.3117 -0.1441 0.175 Uiso 0.659(10) 1 calc PR A 1
H43B H 0.4153 0.3061 -0.1890 0.175 Uiso 0.659(10) 1 calc PR A 1
C44 C 0.4485(13) 0.4098(9) -0.1652(11) 0.179(4) Uani 0.659(10) 1 d PDU A 1
H44A H 0.3934 0.4088 -0.1370 0.214 Uiso 0.659(10) 1 calc PR A 1
H44B H 0.4306 0.4366 -0.2047 0.214 Uiso 0.659(10) 1 calc PR A 1
C45 C 0.5279(15) 0.4498(10) -0.1315(11) 0.190(4) Uani 0.659(10) 1 d PDU A 1
H45A H 0.5859 0.4354 -0.1538 0.228 Uiso 0.659(10) 1 calc PR A 1
H45B H 0.5327 0.4285 -0.0880 0.228 Uiso 0.659(10) 1 calc PR A 1
C46 C 0.5343(18) 0.5374(11) -0.1220(11) 0.199(5) Uani 0.659(10) 1 d PDU A 1
H46A H 0.5696 0.5577 -0.1583 0.239 Uiso 0.659(10) 1 calc PR A 1
H46B H 0.4698 0.5573 -0.1249 0.239 Uiso 0.659(10) 1 calc PR A 1
C47 C 0.5771(17) 0.5640(11) -0.0633(11) 0.193(5) Uani 0.659(10) 1 d PDU A 1
H47A H 0.5496 0.5337 -0.0293 0.232 Uiso 0.659(10) 1 calc PR A 1
H47B H 0.6435 0.5488 -0.0659 0.232 Uiso 0.659(10) 1 calc PR A 1
C48 C 0.5806(18) 0.6296(12) -0.0389(10) 0.191(5) Uani 0.659(10) 1 d PDU A 1
H48A H 0.5141 0.6446 -0.0362 0.229 Uiso 0.659(10) 1 calc PR A 1
H48B H 0.6076 0.6599 -0.0731 0.229 Uiso 0.659(10) 1 calc PR A 1
C49 C 0.6222(15) 0.6563(13) 0.0179(10) 0.204(7) Uani 0.659(10) 1 d PDU A 1
H49A H 0.6091 0.7084 0.0219 0.307 Uiso 0.659(10) 1 calc PR A 1
H49B H 0.6902 0.6487 0.0167 0.307 Uiso 0.659(10) 1 calc PR A 1
H49C H 0.5965 0.6305 0.0547 0.307 Uiso 0.659(10) 1 calc PR A 1
C40' C 0.480(3) 0.175(2) -0.269(3) 0.103(3) Uani 0.341(10) 1 d PDU A 2
H40C H 0.4295 0.1919 -0.2409 0.123 Uiso 0.341(10) 1 calc PR A 2
H40D H 0.4593 0.1818 -0.3146 0.123 Uiso 0.341(10) 1 calc PR A 2
C41' C 0.568(2) 0.2130(13) -0.2560(18) 0.107(4) Uiso 0.341(10) 1 d PDU A 2
H41C H 0.6175 0.1951 -0.2848 0.128 Uiso 0.341(10) 1 calc PR A 2
H41D H 0.5886 0.2039 -0.2112 0.128 Uiso 0.341(10) 1 calc PR A 2
C42' C 0.551(2) 0.2975(13) -0.2670(15) 0.126(4) Uiso 0.341(10) 1 d PDU A 2
H42C H 0.6129 0.3224 -0.2642 0.151 Uiso 0.341(10) 1 calc PR A 2
H42D H 0.5266 0.3046 -0.3111 0.151 Uiso 0.341(10) 1 calc PR A 2
C43' C 0.486(2) 0.3342(14) -0.2213(17) 0.143(5) Uiso 0.341(10) 1 d PDU A 2
H43C H 0.4236 0.3113 -0.2275 0.171 Uiso 0.341(10) 1 calc PR A 2
H43D H 0.5076 0.3215 -0.1775 0.171 Uiso 0.341(10) 1 calc PR A 2
C44' C 0.471(3) 0.4138(15) -0.2223(17) 0.181(6) Uiso 0.341(10) 1 d PDU A 2
H44C H 0.4836 0.4299 -0.2665 0.217 Uiso 0.341(10) 1 calc PR A 2
H44D H 0.4028 0.4214 -0.2158 0.217 Uiso 0.341(10) 1 calc PR A 2

C45' C 0.519(3) 0.4646(18) -0.180(2) 0.192(5) Uiso 0.341(10) 1 d PDU A 2
H45C H 0.5468 0.5007 -0.2095 0.231 Uiso 0.341(10) 1 calc PR A 2
H45D H 0.5717 0.4367 -0.1617 0.231 Uiso 0.341(10) 1 calc PR A 2
C46' C 0.479(3) 0.512(2) -0.1215(18) 0.198(5) Uiso 0.341(10) 1 d PDU A 2
H46C H 0.4156 0.5296 -0.1345 0.237 Uiso 0.341(10) 1 calc PR A 2
H46D H 0.4698 0.4783 -0.0851 0.237 Uiso 0.341(10) 1 calc PR A 2
C47' C 0.531(3) 0.575(2) -0.0967(17) 0.196(5) Uiso 0.341(10) 1 d PDU A 2
H47C H 0.5975 0.5610 -0.1018 0.235 Uiso 0.341(10) 1 calc PR A 2
H47D H 0.5190 0.6134 -0.1290 0.235 Uiso 0.341(10) 1 calc PR A 2
C48' C 0.530(3) 0.610(2) -0.0418(17) 0.194(6) Uiso 0.341(10) 1 d PDU A 2
H48C H 0.4634 0.6241 -0.0394 0.233 Uiso 0.341(10) 1 calc PR A 2
H48D H 0.5634 0.6552 -0.0530 0.233 Uiso 0.341(10) 1 calc PR A 2
C49' C 0.554(3) 0.603(3) 0.0239(16) 0.202(8) Uiso 0.341(10) 1 d PDU A 2
H49D H 0.5248 0.6416 0.0482 0.303 Uiso 0.341(10) 1 calc PR A 2
H49E H 0.6227 0.6057 0.0293 0.303 Uiso 0.341(10) 1 calc PR A 2
H49F H 0.5326 0.5554 0.0396 0.303 Uiso 0.341(10) 1 calc PR A 2
O3 O 0.3087(3) 0.2068(3) 0.0840(2) 0.0840(17) Uani 1 1 d . . .
O4 O 0.2500 -0.1305(4) 0.2500 0.0717(19) Uani 1 2 d S . .
C63 C 0.2500 0.3226(6) 0.2500 0.091(4) Uani 1 2 d S . .
H63 H 0.2500 0.3743 0.2500 0.110 Uiso 1 2 calc SR . .
C64 C 0.2690(4) 0.2834(5) 0.1938(4) 0.079(2) Uani 1 1 d . . .
H64 H 0.2814 0.3091 0.1554 0.094 Uiso 1 1 calc R . .
C65 C 0.2701(4) 0.2092(4) 0.1932(3) 0.0560(17) Uani 1 1 d . . .
C66 C 0.2909(4) 0.1713(5) 0.1338(3) 0.066(2) Uani 1 1 d . . .
C67 C 0.2902(3) 0.0929(4) 0.1360(3) 0.0493(16) Uani 1 1 d . . .
C68 C 0.3085(3) 0.0534(5) 0.0806(3) 0.063(2) Uani 1 1 d . . .
H68 H 0.3217 0.0786 0.0421 0.076 Uiso 1 1 calc R . .
C69 C 0.3078(4) -0.0208(5) 0.0804(3) 0.065(2) Uani 1 1 d . . .
H69 H 0.3200 -0.0471 0.0423 0.078 Uiso 1 1 calc R . .
C70 C 0.2892(4) -0.0566(4) 0.1362(3) 0.0618(19) Uani 1 1 d . . .
H70 H 0.2897 -0.1083 0.1360 0.074 Uiso 1 1 calc R . .
C71 C 0.2698(3) -0.0210(3) 0.1931(3) 0.0445(15) Uani 1 1 d . . .
C72 C 0.2698(3) 0.0546(4) 0.1936(2) 0.0431(16) Uani 1 1 d . . .
C73 C 0.2500 0.0941(5) 0.2500 0.0378(18) Uani 1 2 d S . .
C74 C 0.2500 0.1699(5) 0.2500 0.049(2) Uani 1 2 d S . .
C75 C 0.2500 -0.0629(6) 0.2500 0.052(2) Uani 1 2 d S . .
O1 O 0.1849(3) -0.0625(3) -0.0845(3) 0.098(2) Uani 1 1 d . . .
O2 O 0.2500 0.2725(5) -0.2500 0.094(2) Uani 1 2 d S . .
C50 C 0.2500 -0.1805(7) -0.2500 0.099(4) Uani 1 2 d S . .
H50 H 0.2500 -0.2321 -0.2500 0.119 Uiso 1 2 calc SR . .
C51 C 0.2270(5) -0.1413(5) -0.1950(4) 0.091(3) Uani 1 1 d . . .
H51 H 0.2102 -0.1671 -0.1575 0.109 Uiso 1 1 calc R . .
C52 C 0.2277(4) -0.0668(5) -0.1935(4) 0.071(2) Uani 1 1 d . . .
C53 C 0.2075(4) -0.0279(6) -0.1339(4) 0.077(2) Uani 1 1 d . . .
C54 C 0.2141(4) 0.0494(5) -0.1349(3) 0.063(2) Uani 1 1 d . . .
C55 C 0.2072(4) 0.0881(6) -0.0784(3) 0.075(2) Uani 1 1 d . . .

H55 H 0.1949 0.0627 -0.0398 0.090 Uiso 1 1 calc R . .
C56 C 0.2175(5) 0.1622(6) -0.0766(4) 0.089(3) Uani 1 1 d . . .
H56 H 0.2148 0.1878 -0.0371 0.107 Uiso 1 1 calc R . .
C57 C 0.2320(4) 0.1990(5) -0.1330(4) 0.083(2) Uani 1 1 d . . .
H57 H 0.2376 0.2504 -0.1315 0.099 Uiso 1 1 calc R . .
C58 C 0.2387(4) 0.1645(4) -0.1921(4) 0.067(2) Uani 1 1 d . . .
C59 C 0.2339(3) 0.0865(4) -0.1929(3) 0.062(2) Uani 1 1 d . . .
C60 C 0.2500 0.0484(5) -0.2500 0.049(2) Uani 1 2 d S . .
C61 C 0.2500 -0.0250(6) -0.2500 0.059(3) Uani 1 2 d S . .
C62 C 0.2500 0.2056(8) -0.2500 0.074(3) Uani 1 2 d S . .

A-20: Crystallographic Information File (CIF) for 1(NPh)$_3$•2

.....

_chemical_name_common	triazatriphenyltriangulenium trioxotriangulenate
_chemical_formula_moiety	C_{37} H_{24} N_3, C_{22} H_9 O_3
_symmetry_cell_setting	monoclinic
_symmetry_space_group_name_H-M	'P 21/c'

loop_
_symmetry_equiv_pos_as_xyz
'x, y, z'
'-x, y+1/2, -z+1/2'
'-x, -y, -z'
'x, -y-1/2, z-1/2'

_cell_length_a	8.0649(1)
_cell_length_b	23.1195(2)
_cell_length_c	20.5942(2)
_cell_angle_alpha	90.00
_cell_angle_beta	90.6445(4)
_cell_angle_gamma	90.00
_cell_formula_units_Z	4

loop_
_atom_site_label
_atom_site_type_symbol
_atom_site_fract_x
_atom_site_fract_y
_atom_site_fract_z
_atom_site_U_iso_or_equiv
_atom_site_adp_type

_atom_site_occupancy
_atom_site_symmetry_multiplicity
_atom_site_calc_flag
_atom_site_refinement_flags
_atom_site_disorder_assembly
_atom_site_disorder_group
O1A O 0.08699(15) 0.67234(5) 0.75927(6) 0.0393(3) Uani 1 1 d . . .
O2A O 0.36825(16) 0.91269(5) 0.57028(6) 0.0397(3) Uani 1 1 d . . .
O3A O 0.29515(14) 0.63112(5) 0.42455(6) 0.0352(3) Uani 1 1 d . . .
C1A C 0.1979(2) 0.78765(8) 0.75607(8) 0.0319(4) Uani 1 1 d . . .
H1A H 0.1600 0.7728 0.7963 0.038 Uiso 1 1 calc R . .
C2A C 0.2560(2) 0.84402(8) 0.75331(8) 0.0346(4) Uani 1 1 d . . .
H2A H 0.2626 0.8669 0.7916 0.042 Uiso 1 1 calc R . .
C3A C 0.3045(2) 0.86666(8) 0.69423(8) 0.0337(4) Uani 1 1 d . . .
H3A H 0.3412 0.9056 0.6921 0.040 Uiso 1 1 calc R . .
C4A C 0.3884(2) 0.84303(8) 0.45805(8) 0.0337(4) Uani 1 1 d . . .
H4A H 0.4054 0.8835 0.4534 0.040 Uiso 1 1 calc R . .
C5A C 0.4053(2) 0.80742(8) 0.40420(9) 0.0358(4) Uani 1 1 d . . .
H5A H 0.4363 0.8232 0.3635 0.043 Uiso 1 1 calc R . .
C6A C 0.3766(2) 0.74897(8) 0.41056(8) 0.0327(4) Uani 1 1 d . . .
H6A H 0.3928 0.7243 0.3743 0.039 Uiso 1 1 calc R . .
C7A C 0.1465(2) 0.58745(8) 0.53705(8) 0.0323(4) Uani 1 1 d . . .
H7A H 0.1485 0.5634 0.4997 0.039 Uiso 1 1 calc R . .
C8A C 0.0828(2) 0.56592(8) 0.59395(9) 0.0360(4) Uani 1 1 d . . .
H8A H 0.0408 0.5276 0.5955 0.043 Uiso 1 1 calc R . .
C9A C 0.0802(2) 0.60043(8) 0.64875(9) 0.0333(4) Uani 1 1 d . . .
H9A H 0.0388 0.5850 0.6881 0.040 Uiso 1 1 calc R . .
C10A C 0.1936(2) 0.75229(7) 0.70150(8) 0.0271(4) Uani 1 1 d . . .
C11A C 0.24933(19) 0.77452(7) 0.64081(8) 0.0254(4) Uani 1 1 d . . .
C12A C 0.3003(2) 0.83327(7) 0.63782(8) 0.0282(4) Uani 1 1 d . . .
C13A C 0.3474(2) 0.82111(7) 0.51854(8) 0.0282(4) Uani 1 1 d . . .
C14A C 0.30922(19) 0.76158(7) 0.52478(8) 0.0250(4) Uani 1 1 d . . .
C15A C 0.3242(2) 0.72545(7) 0.46912(8) 0.0264(4) Uani 1 1 d . . .
C16A C 0.2079(2) 0.64361(7) 0.53294(8) 0.0270(4) Uani 1 1 d . . .
C17A C 0.20066(19) 0.68038(7) 0.58854(8) 0.0246(4) Uani 1 1 d . . .
C18A C 0.1371(2) 0.65729(7) 0.64742(8) 0.0276(4) Uani 1 1 d . . .
C19A C 0.25411(19) 0.73856(7) 0.58472(8) 0.0249(4) Uani 1 1 d . . .
C20A C 0.1347(2) 0.69271(8) 0.70658(8) 0.0301(4) Uani 1 1 d . . .
C21A C 0.3407(2) 0.86004(8) 0.57504(8) 0.0300(4) Uani 1 1 d . . .
C22A C 0.2780(2) 0.66418(8) 0.47230(8) 0.0284(4) Uani 1 1 d . . .
N1C N 0.77069(17) 0.63940(6) 0.45081(6) 0.0253(3) Uani 1 1 d . . .
N2C N 0.64208(17) 0.64416(6) 0.67950(6) 0.0263(3) Uani 1 1 d . . .
N3C N 0.79423(17) 0.82057(5) 0.56799(6) 0.0248(3) Uani 1 1 d . . .
C1C C 0.6925(2) 0.55064(7) 0.50576(8) 0.0296(4) Uani 1 1 d . . .
H1C H 0.7027 0.5291 0.4668 0.035 Uiso 1 1 calc R . .
C2C C 0.6495(2) 0.52338(7) 0.56321(8) 0.0310(4) Uani 1 1 d . . .

H2C H 0.6314 0.4828 0.5628 0.037 Uiso 1 1 calc R . .
C3C C 0.6320(2) 0.55293(7) 0.62103(8) 0.0303(4) Uani 1 1 d . . .
H3C H 0.6034 0.5327 0.6595 0.036 Uiso 1 1 calc R . .
C4C C 0.6421(2) 0.73547(7) 0.73807(8) 0.0285(4) Uani 1 1 d . . .
H4C H 0.6119 0.7167 0.7772 0.034 Uiso 1 1 calc R . .
C5C C 0.6632(2) 0.79440(7) 0.73648(8) 0.0292(4) Uani 1 1 d . . .
H5C H 0.6441 0.8157 0.7751 0.035 Uiso 1 1 calc R . .
C6C C 0.7108(2) 0.82425(7) 0.68158(8) 0.0279(4) Uani 1 1 d . . .
H6C H 0.7234 0.8651 0.6827 0.033 Uiso 1 1 calc R . .
C7C C 0.8928(2) 0.81606(7) 0.45654(8) 0.0287(4) Uani 1 1 d . . .
H7C H 0.9241 0.8557 0.4578 0.034 Uiso 1 1 calc R . .
C8C C 0.9143(2) 0.78402(7) 0.40070(8) 0.0295(4) Uani 1 1 d . . .
H8C H 0.9605 0.8023 0.3637 0.035 Uiso 1 1 calc R . .
C9C C 0.8709(2) 0.72595(7) 0.39669(8) 0.0276(4) Uani 1 1 d . . .
H9C H 0.8826 0.7055 0.3570 0.033 Uiso 1 1 calc R . .
C10C C 0.7204(2) 0.60996(7) 0.50610(8) 0.0255(4) Uani 1 1 d . . .
C11C C 0.70202(19) 0.64155(7) 0.56488(7) 0.0239(4) Uani 1 1 d . . .
C12C C 0.6566(2) 0.61241(7) 0.62259(8) 0.0267(4) Uani 1 1 d . . .
C13C C 0.6656(2) 0.70369(7) 0.68147(8) 0.0250(4) Uani 1 1 d . . .
C14C C 0.7136(2) 0.73293(7) 0.62404(8) 0.0234(4) Uani 1 1 d . . .
C15C C 0.7400(2) 0.79346(7) 0.62460(8) 0.0245(4) Uani 1 1 d . . .
C16C C 0.8248(2) 0.78987(7) 0.51116(8) 0.0243(4) Uani 1 1 d . . .
C17C C 0.78781(19) 0.72968(7) 0.50944(8) 0.0233(4) Uani 1 1 d . . .
C18C C 0.81012(19) 0.69806(7) 0.45124(8) 0.0237(4) Uani 1 1 d . . .
C19C C 0.73379(19) 0.70141(7) 0.56593(7) 0.0232(4) Uani 1 1 d . . .
C20C C 0.7836(2) 0.60726(7) 0.39074(8) 0.0261(4) Uani 1 1 d . . .
C21C C 0.9375(2) 0.59205(7) 0.36769(8) 0.0310(4) Uani 1 1 d . . .
H21C H 1.0353 0.6026 0.3909 0.037 Uiso 1 1 calc R . .
C22C C 0.9475(2) 0.56111(7) 0.31007(9) 0.0351(4) Uani 1 1 d . . .
H22C H 1.0528 0.5508 0.2934 0.042 Uiso 1 1 calc R . .
C23C C 0.8051(2) 0.54528(7) 0.27693(8) 0.0345(5) Uani 1 1 d . . .
H23C H 0.8126 0.5240 0.2376 0.041 Uiso 1 1 calc R . .
C24C C 0.6510(2) 0.56038(7) 0.30080(8) 0.0328(4) Uani 1 1 d . . .
H24C H 0.5533 0.5491 0.2780 0.039 Uiso 1 1 calc R . .
C25C C 0.6390(2) 0.59199(7) 0.35791(8) 0.0281(4) Uani 1 1 d . . .
H25C H 0.5338 0.6029 0.3742 0.034 Uiso 1 1 calc R . .
C26C C 0.6125(2) 0.61328(7) 0.73966(8) 0.0248(4) Uani 1 1 d . . .
C27C C 0.4561(2) 0.59352(7) 0.75349(8) 0.0300(4) Uani 1 1 d . . .
H27C H 0.3658 0.6015 0.7249 0.036 Uiso 1 1 calc R . .
C28C C 0.4314(2) 0.56169(8) 0.80987(9) 0.0373(5) Uani 1 1 d . . .
H28C H 0.3240 0.5475 0.8195 0.045 Uiso 1 1 calc R . .
C29C C 0.5618(3) 0.55065(7) 0.85175(8) 0.0362(5) Uani 1 1 d . . .
H29C H 0.5453 0.5281 0.8897 0.043 Uiso 1 1 calc R . .
C30C C 0.7167(2) 0.57264(7) 0.83804(9) 0.0343(4) Uani 1 1 d . . .
H30C H 0.8061 0.5660 0.8675 0.041 Uiso 1 1 calc R . .
C31C C 0.7440(2) 0.60414(7) 0.78227(8) 0.0304(4) Uani 1 1 d . . .

H31C H 0.8509 0.6192 0.7733 0.037 Uiso 1 1 calc R . .
C32C C 0.8244(2) 0.88230(7) 0.56928(8) 0.0260(4) Uani 1 1 d . . .
C33C C 0.9499(2) 0.90373(7) 0.60840(9) 0.0352(4) Uani 1 1 d . . .
H33C H 1.0148 0.8782 0.6344 0.042 Uiso 1 1 calc R . .
C34C C 0.9809(2) 0.96255(8) 0.60966(9) 0.0411(5) Uani 1 1 d . . .
H34C H 1.0672 0.9774 0.6366 0.049 Uiso 1 1 calc R . .
C35C C 0.8877(2) 0.99949(8) 0.57213(9) 0.0396(5) Uani 1 1 d . . .
H35C H 0.9098 1.0398 0.5731 0.047 Uiso 1 1 calc R . .
C36C C 0.7617(2) 0.97827(7) 0.53283(9) 0.0350(4) Uani 1 1 d . . .
H36C H 0.6974 1.0039 0.5068 0.042 Uiso 1 1 calc R . .
C37C C 0.7294(2) 0.91926(7) 0.53158(8) 0.0319(4) Uani 1 1 d . . .
H37C H 0.6424 0.9044 0.5049 0.038 Uiso 1 1 calc R . .

A-21: ^{1}H NMR of $[1(NEt)_3]^{+}BF_4^{-}$ in d_6-DMSO

.....

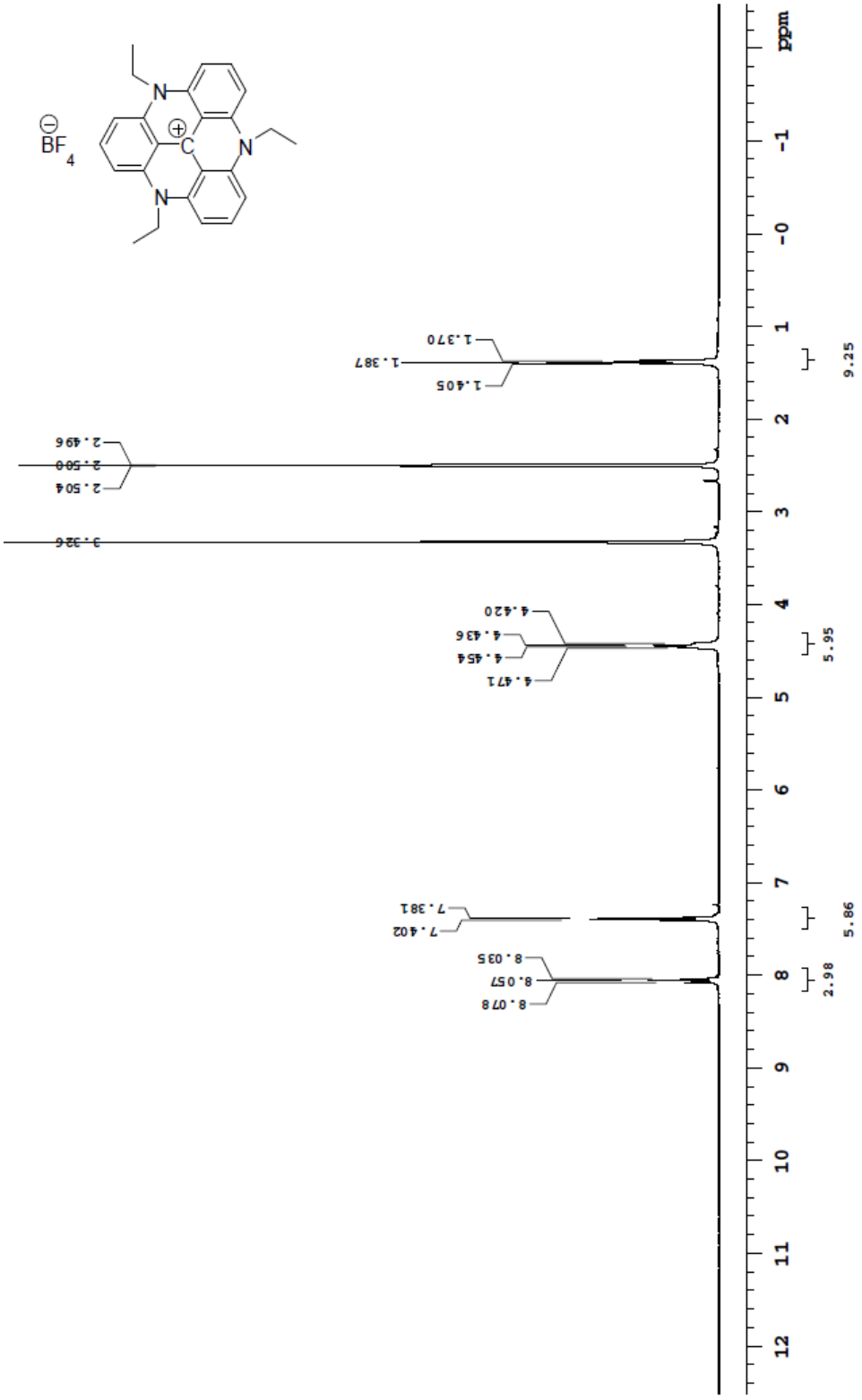

A-22: ^{13}C NMR of $[1(NEt)_3]^+BF_4^-$ in d_6-DMSO

.....

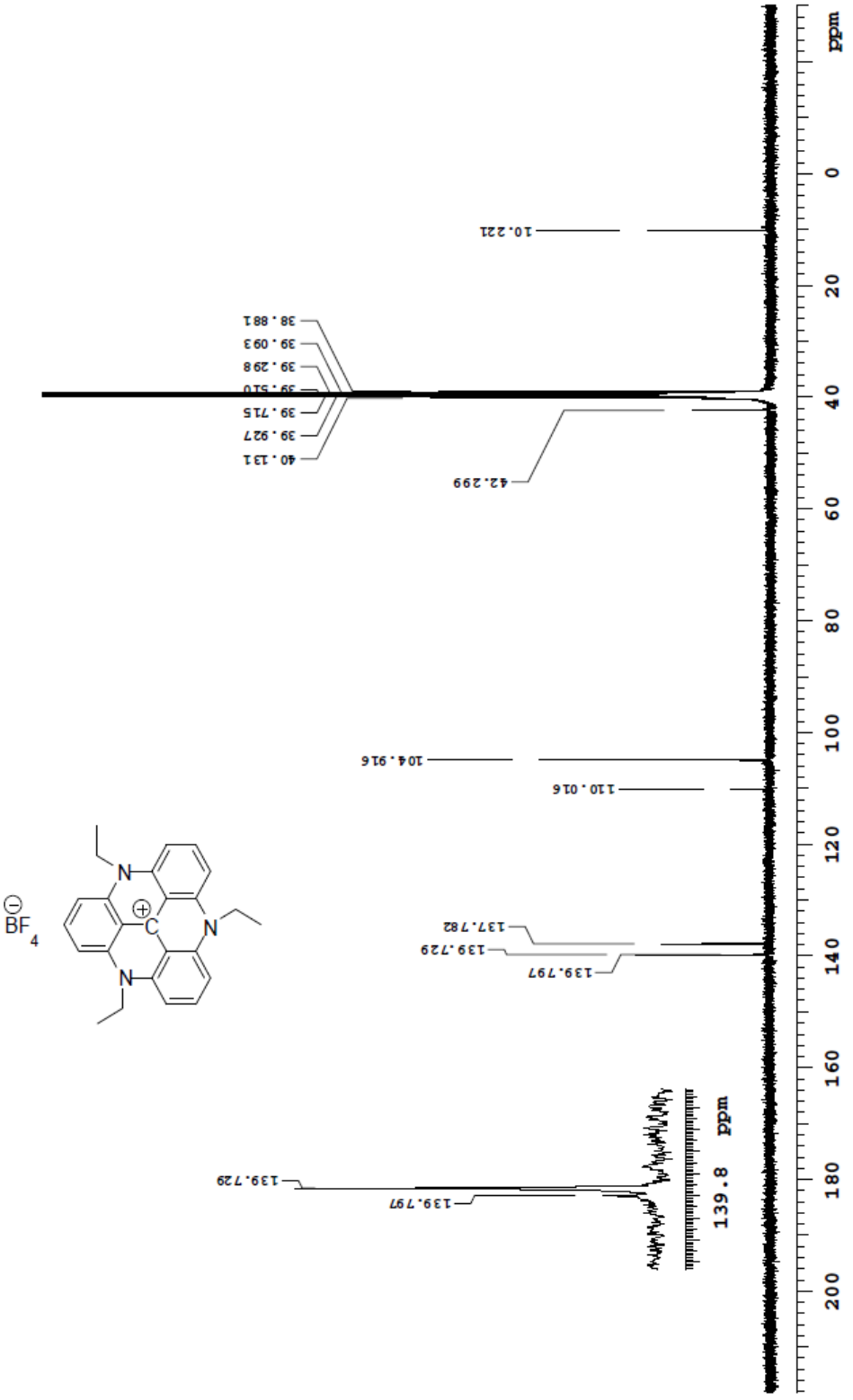

A-23: ^{1}H NMR of $[1(NPh)_3]^{+}BF_4^{-}$ in $CDCl_3$

.....

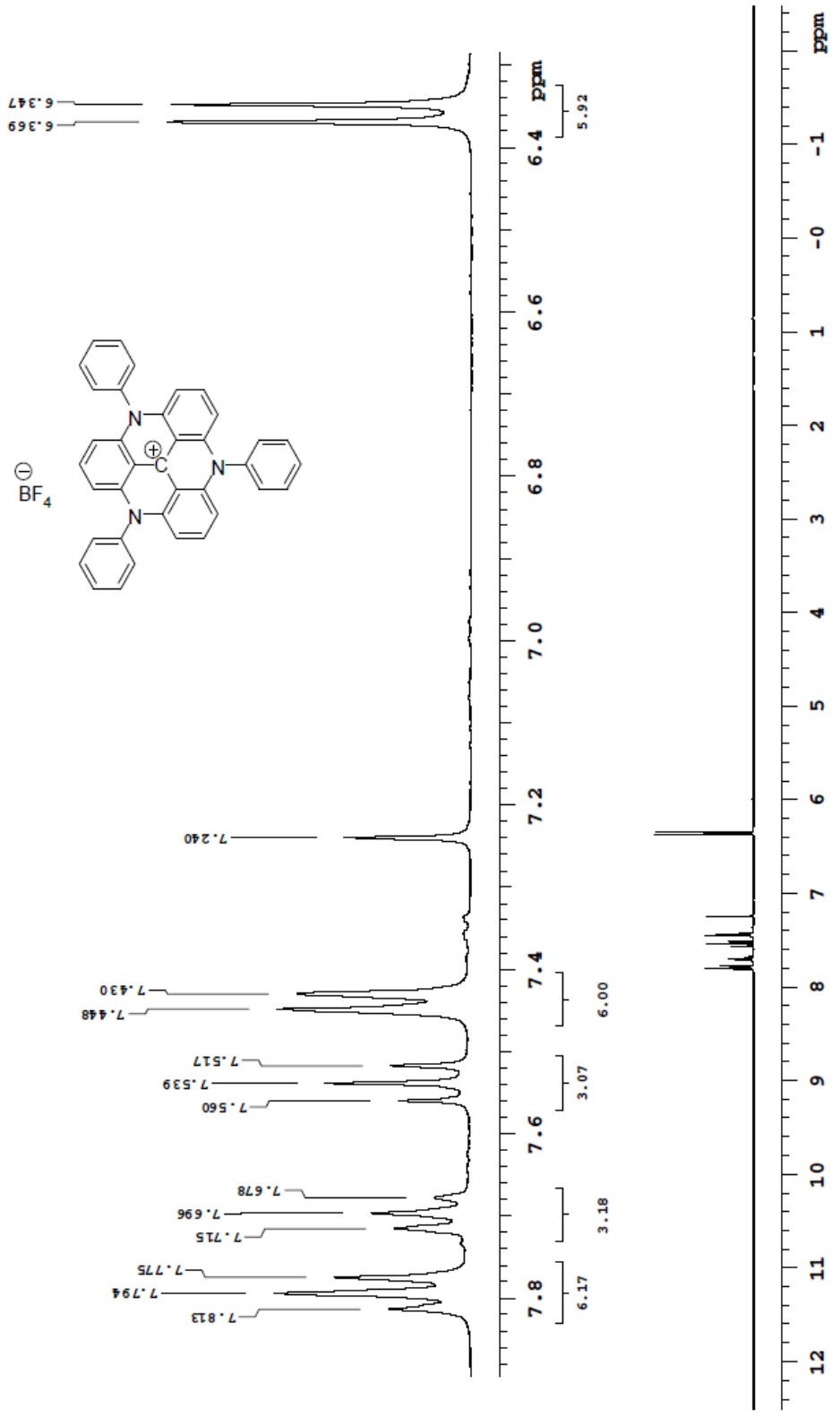

A-24: ^{13}C NMR of $[1(NPh)_3]^+BF_4^-$ in d_6-DMSO

.....

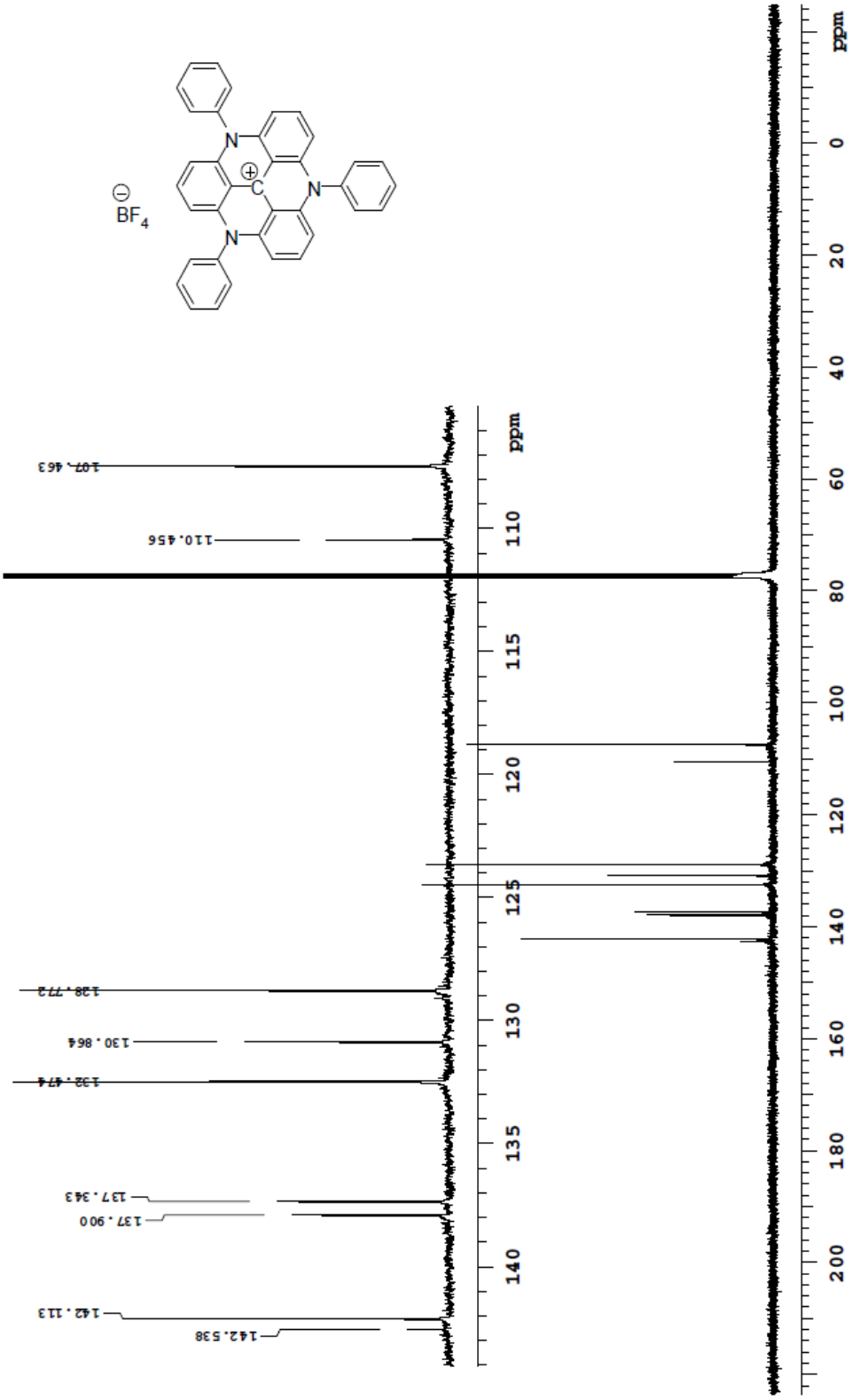

A-25: ^{13}C NMR of $[1(NDec)_3]^+BF_4^-$ in d_6-DMSO

.....

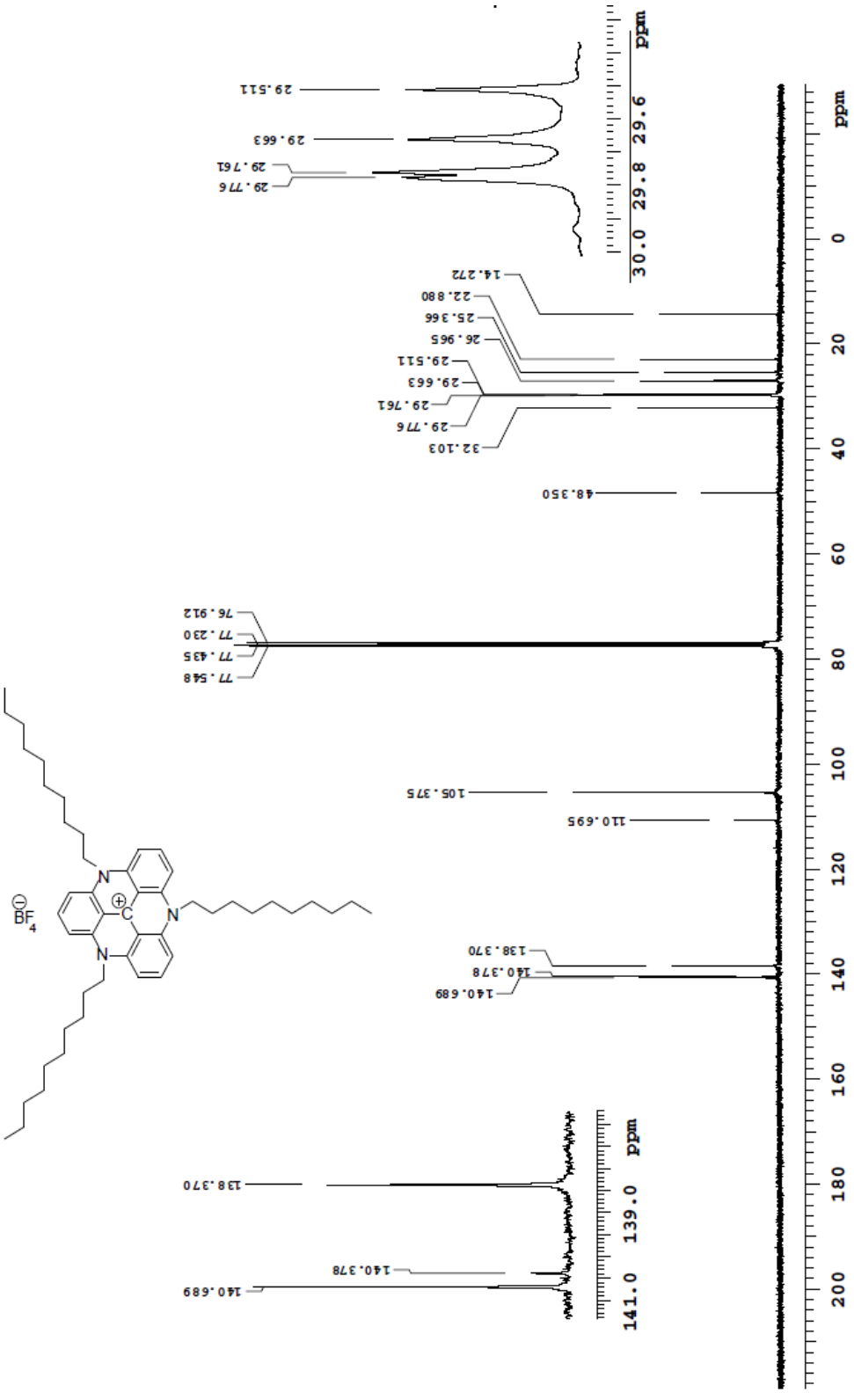

A-26: ^{13}C NMR of $[1(NDodec)_3]^+BF_4^-$ in $CDCl_3$

.....

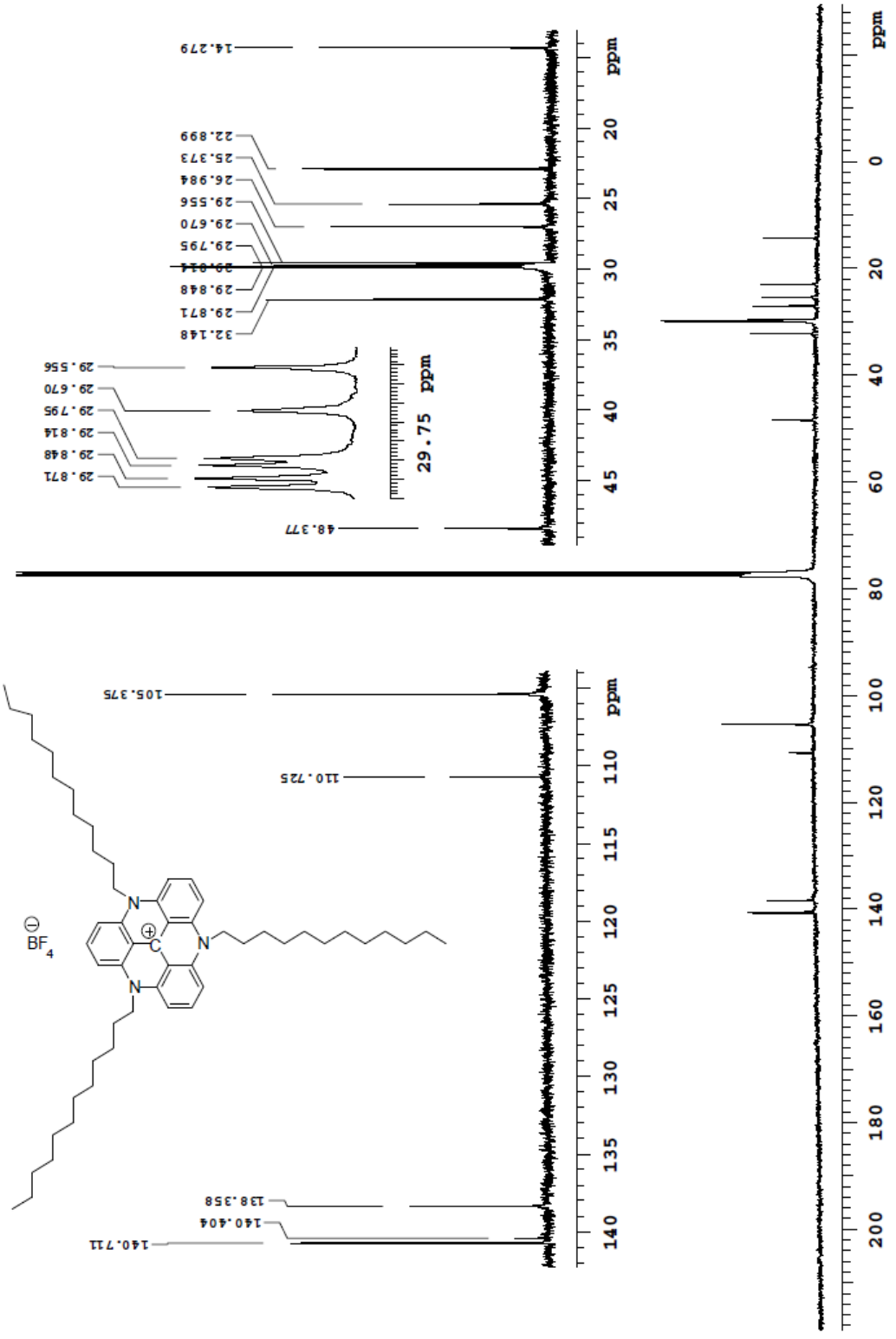

A-27: ^{1}H NMR of $[1(NHexadec)_3]^{+}BF_4^{-}$ in $CDCl_3$

.....

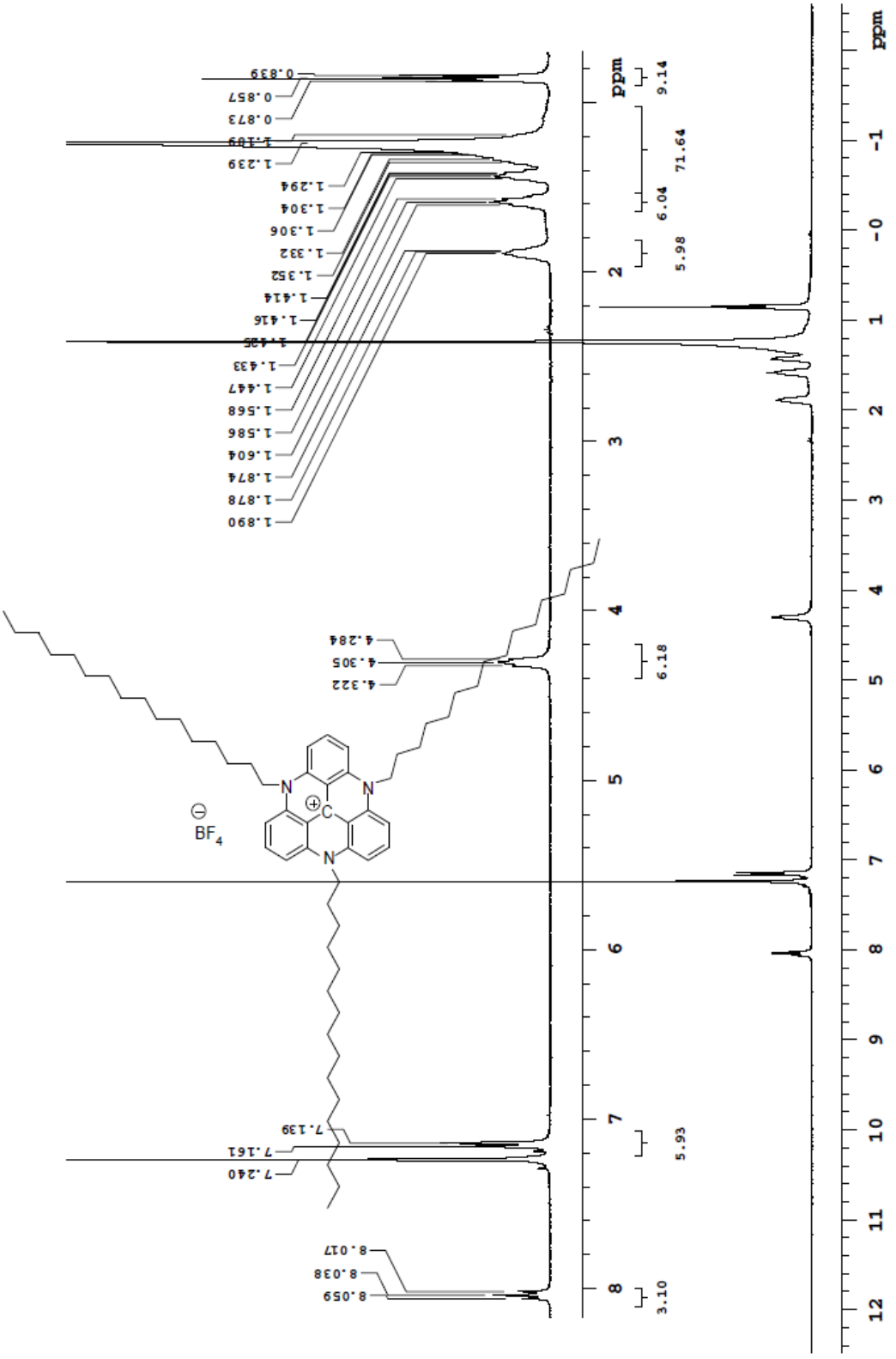

A-28: ^{13}C NMR of (2)$^{-}$Hex$_4$N^{+} in d$_6$-DMSO

.....

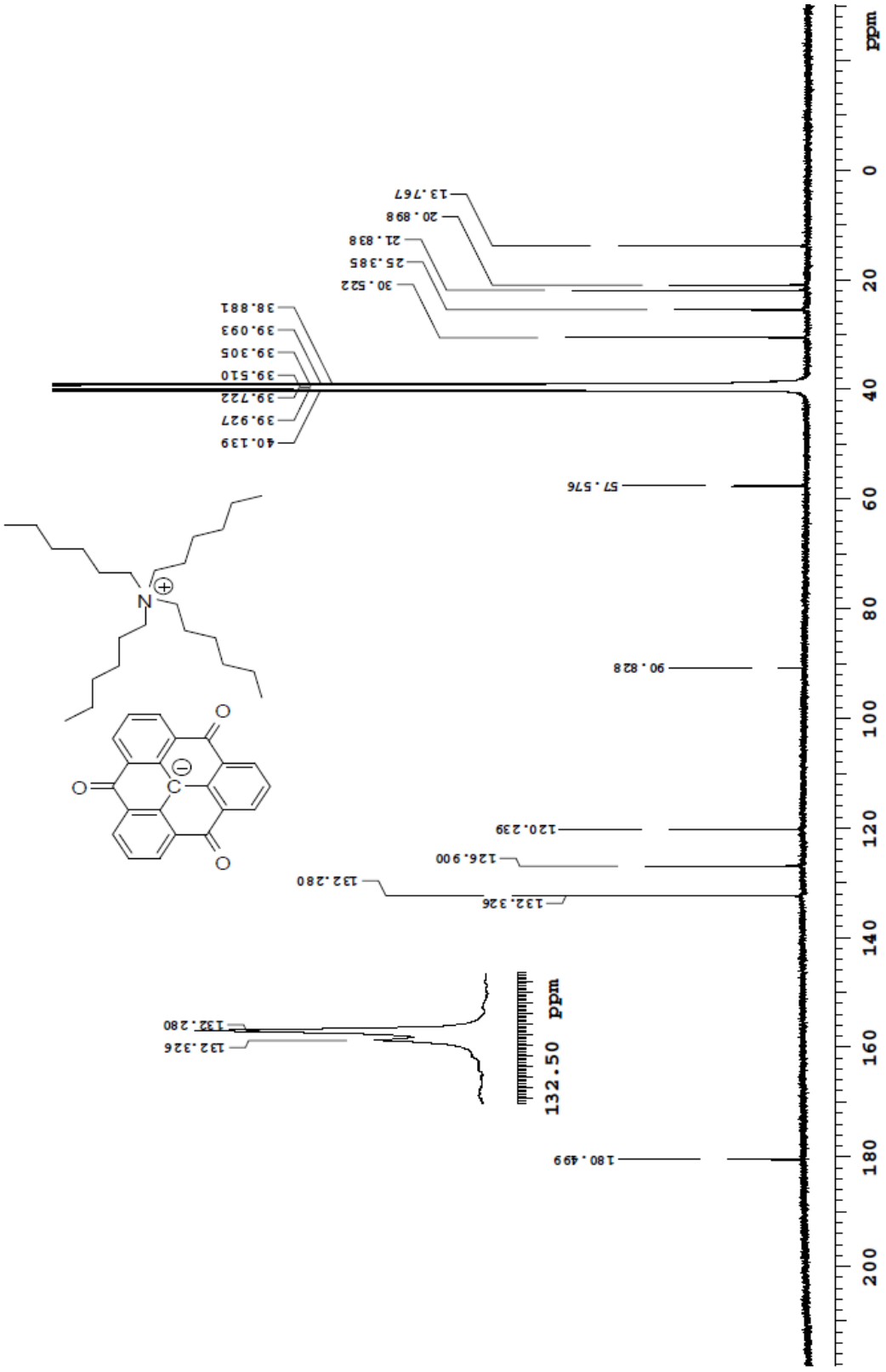

A-29: ^{1}H NMR of [(3)$^{2-}$ 2Bu$_4$N^{+}] in d$_6$-DMSO

.....

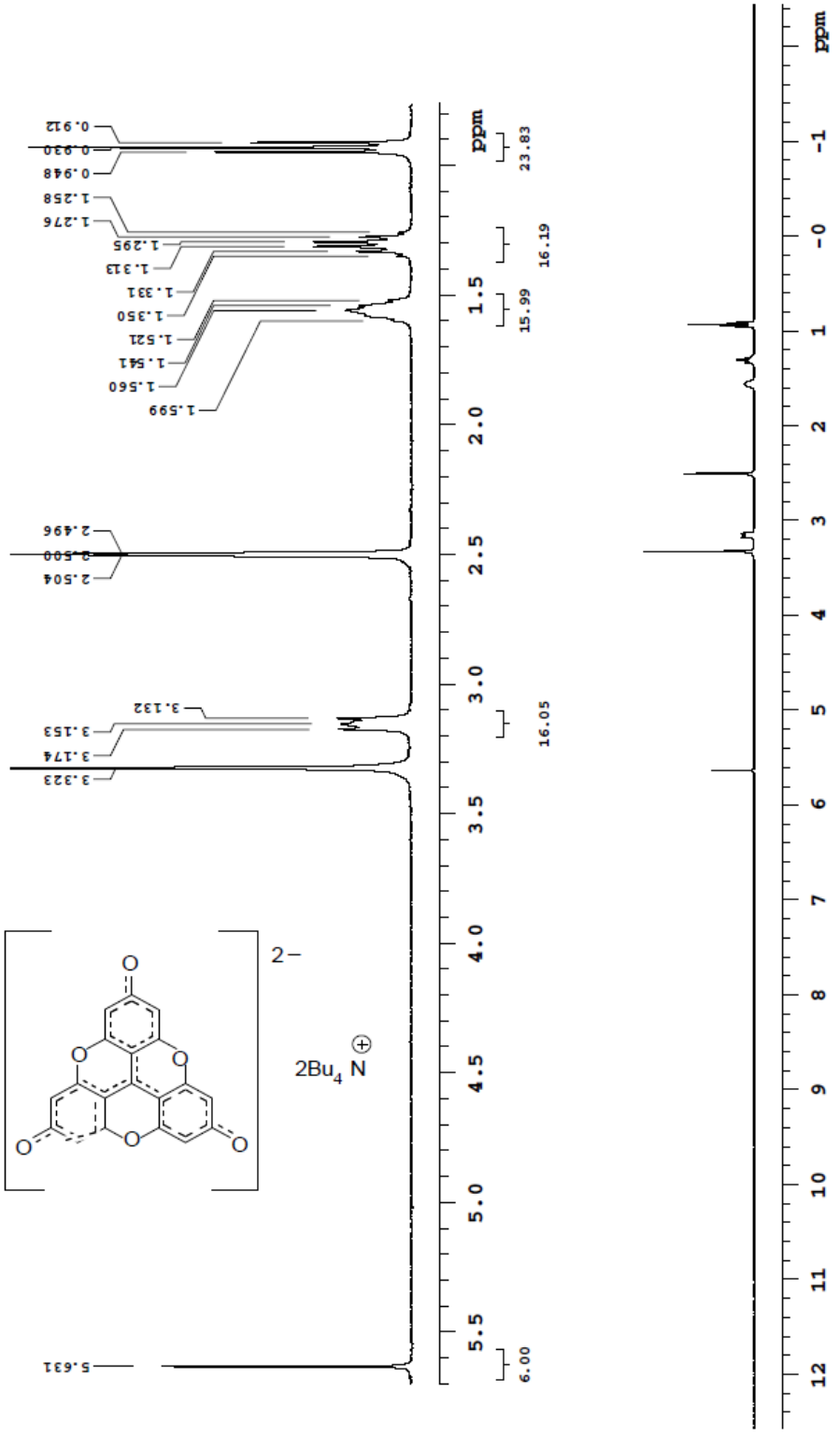

A-30: ^{13}C NMR of $[(3)^{2-}\ 2Bu_4N^+]$ in d_6-DMSO

.....

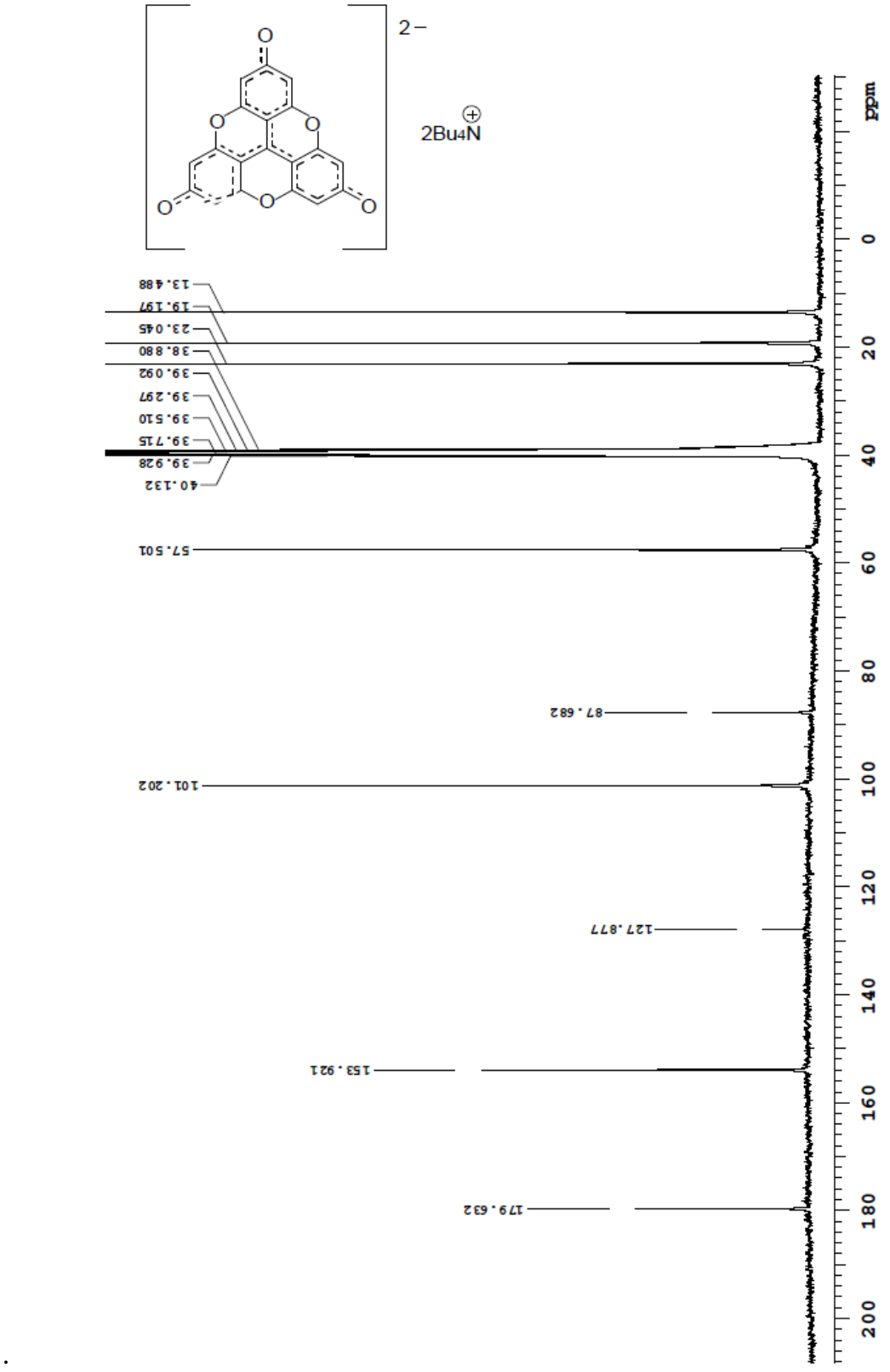

.

A-31: ^{1}H NMR of 1(NMe)$_3$•2 in d$_6$-DMSO

.....

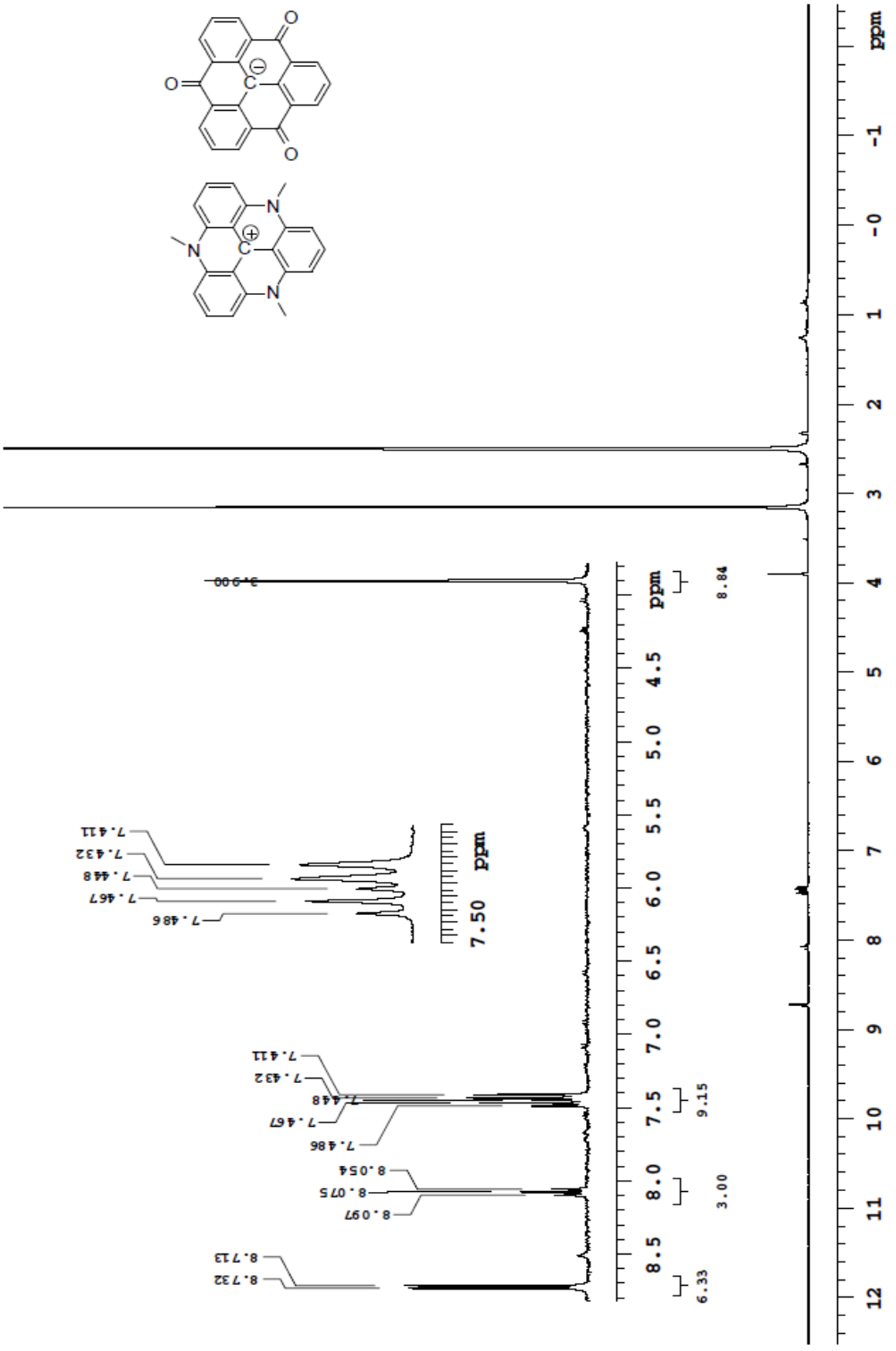

A-32: ^{1}H NMR of 1(NEt)$_3$•2 in d$_6$-DMSO

.....

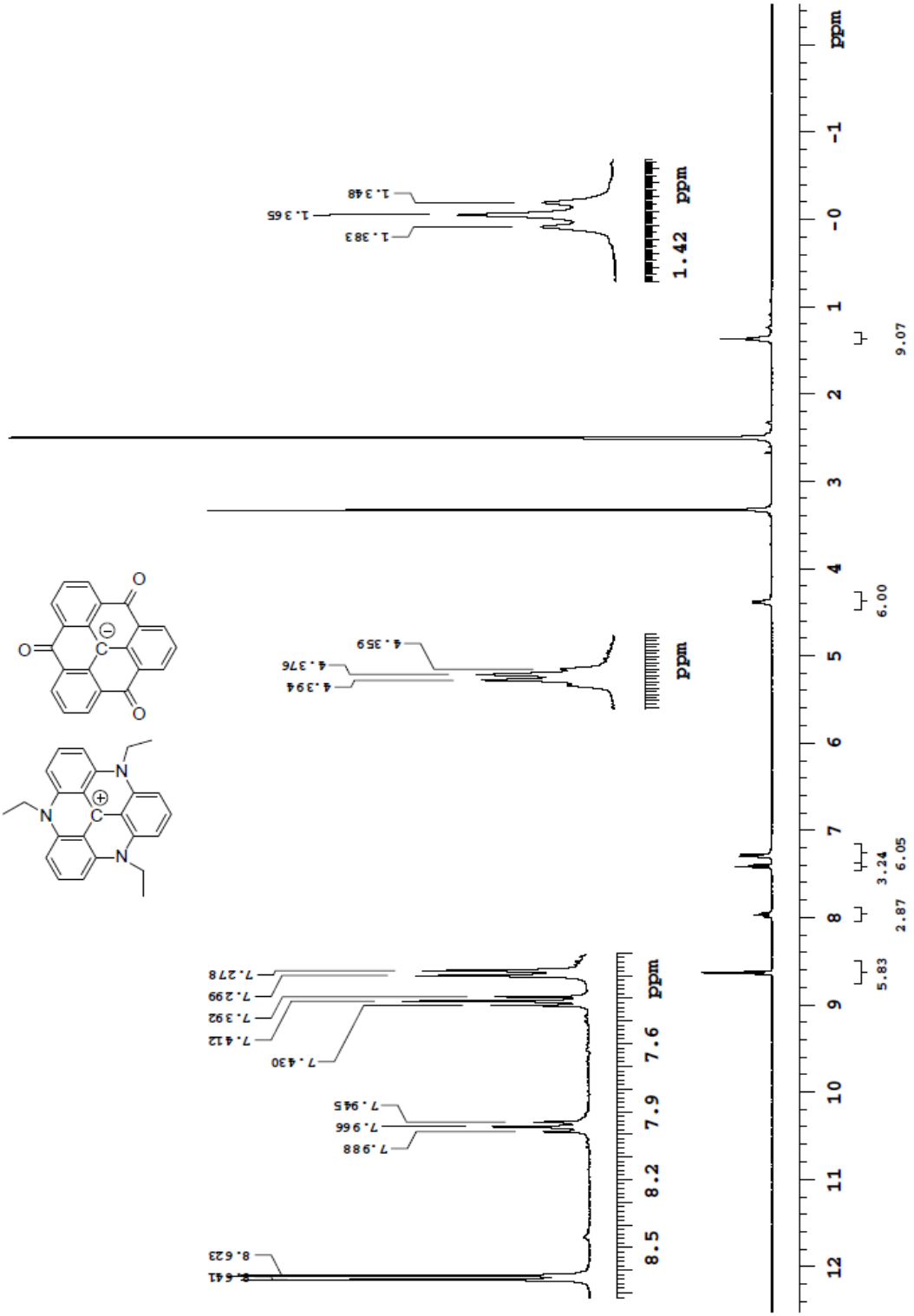

A-33: ^{13}C NMR of 1(NEt)$_3$•2 in d$_6$-DMSO

.....

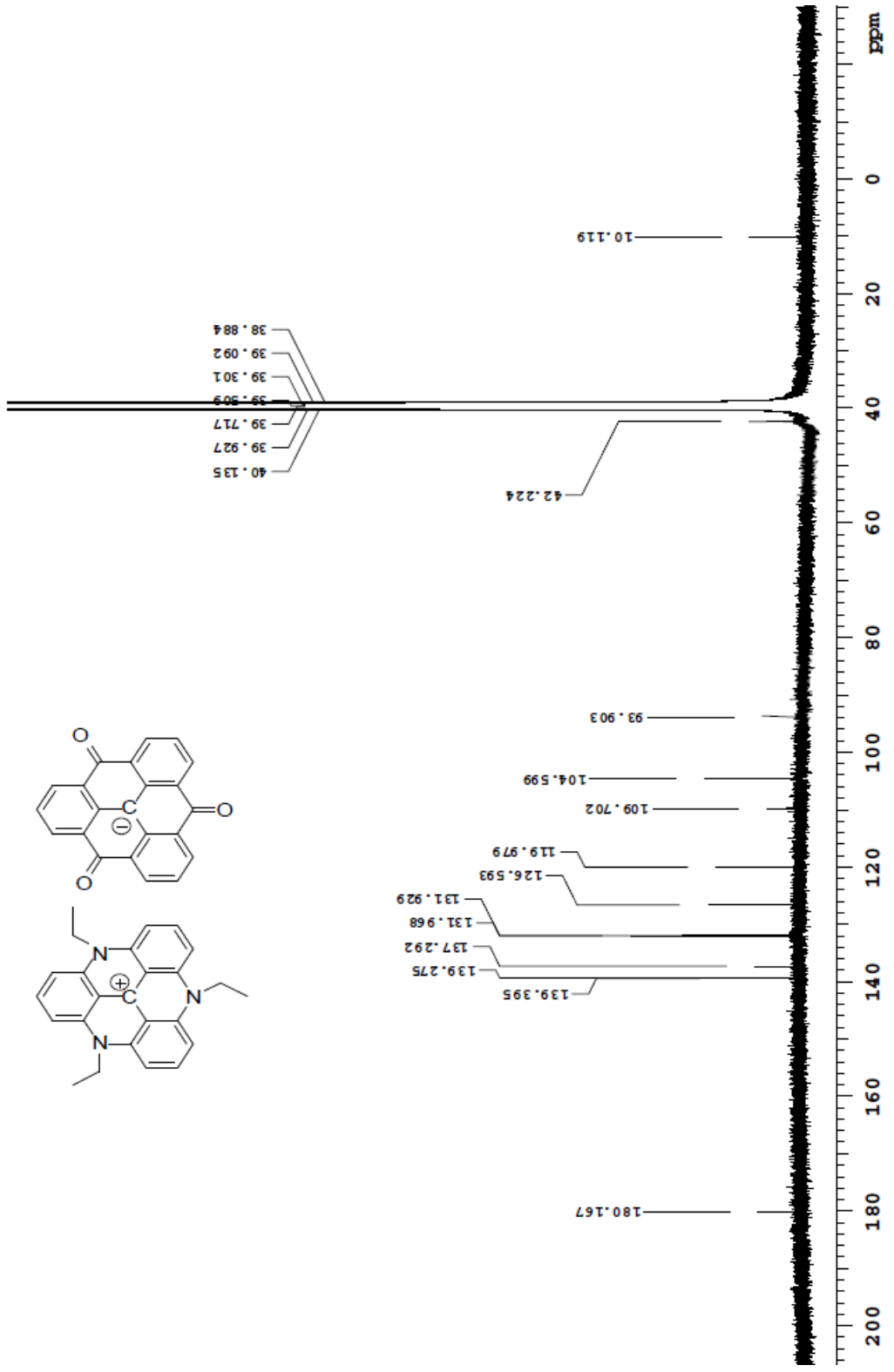

A-34: ^{1}H NMR of 1(NPr)$_3$•2 in d$_6$-DMSO

.....

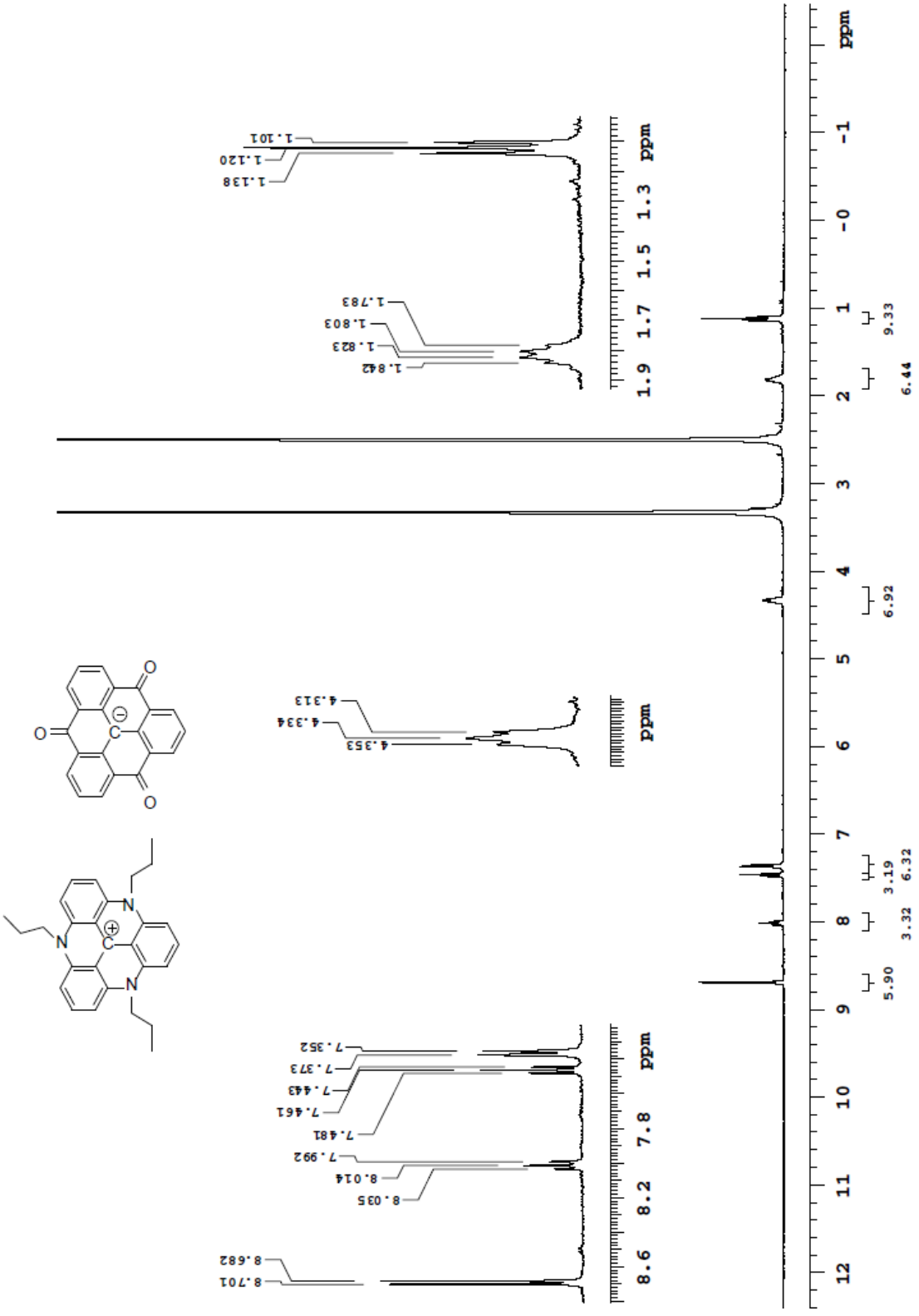

A-35: ^{13}C NMR of 1(NPr)$_3$•2 in d$_6$-DMSO

.....

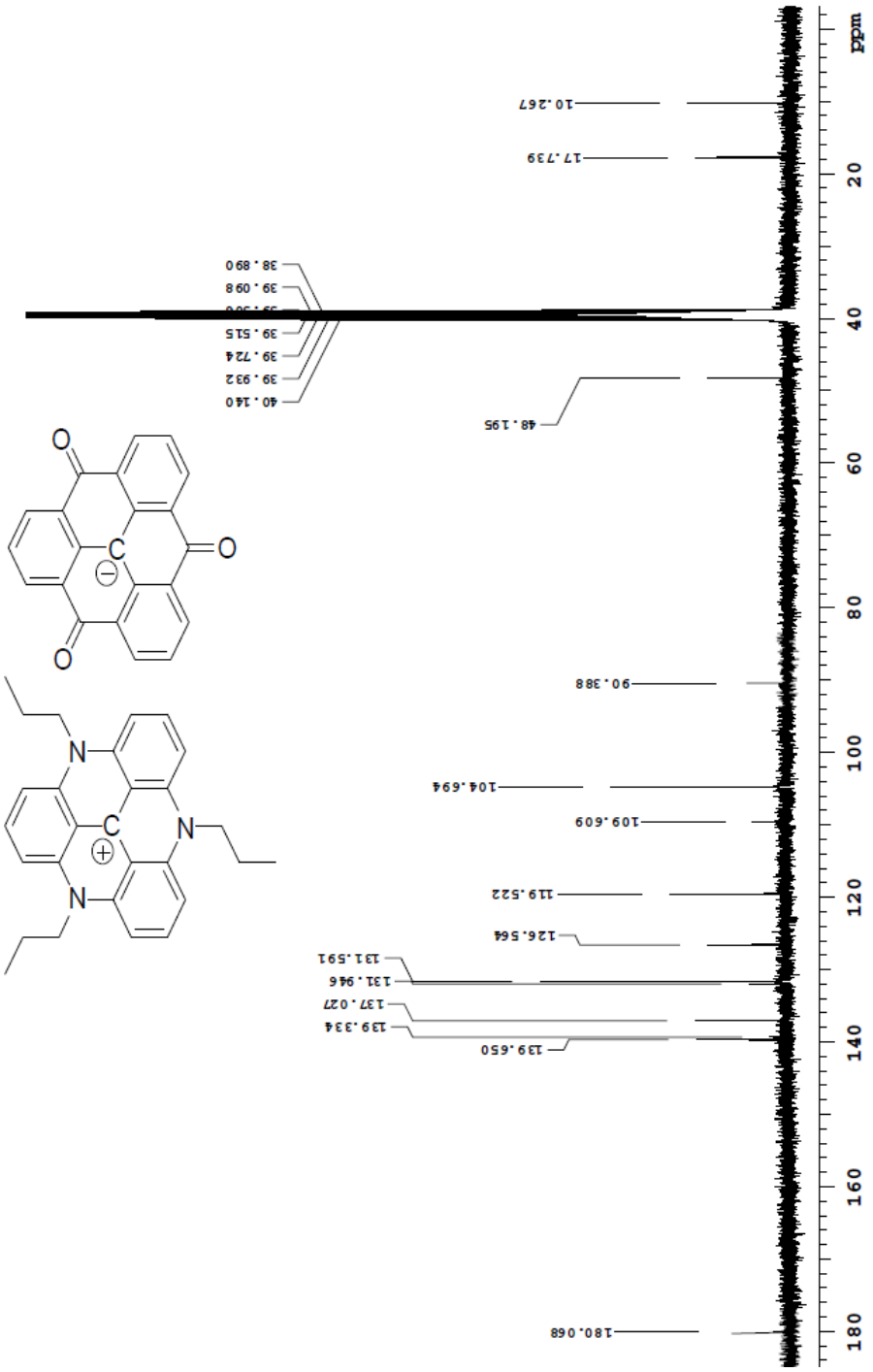

A-36: ^{1}H NMR of 1(NBu)$_3$•2 in d$_6$-DMSO

.....

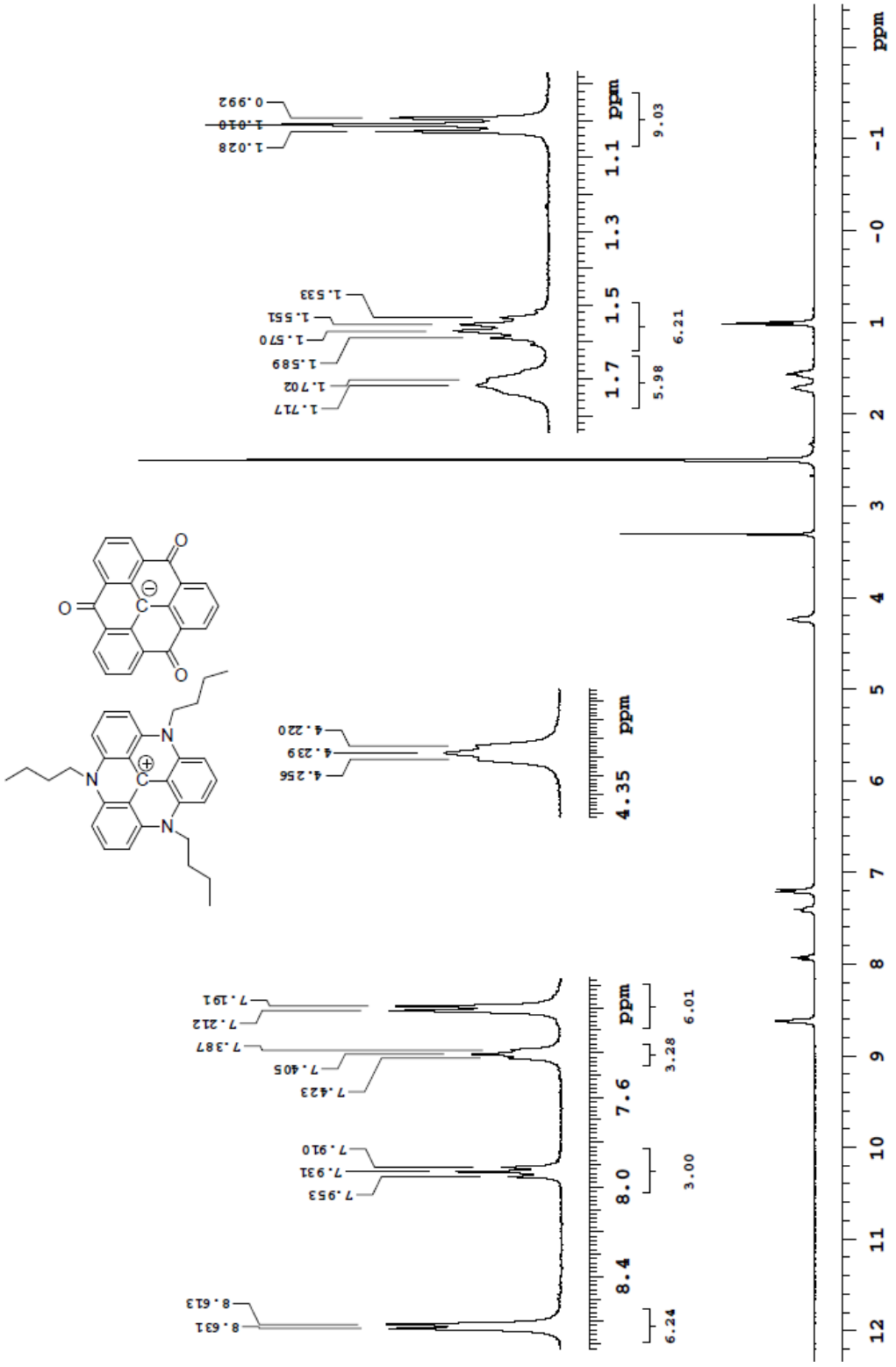

A-37: ^{13}C NMR of 1(NBu)$_3$•2 in d$_6$-DMSO

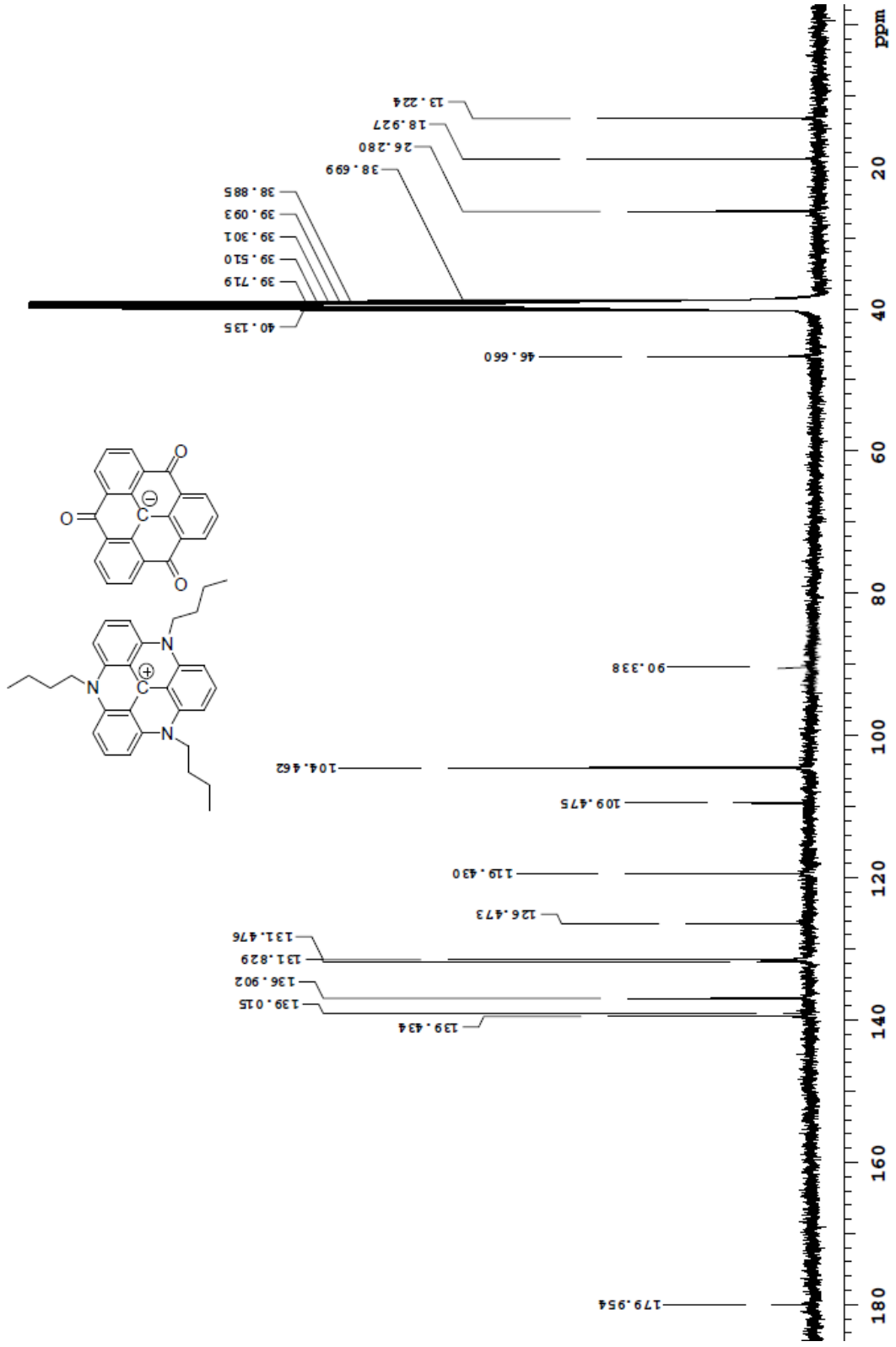

A-38: ^{1}H NMR of 1(NPh)$_3$•2 in d$_6$-DMSO

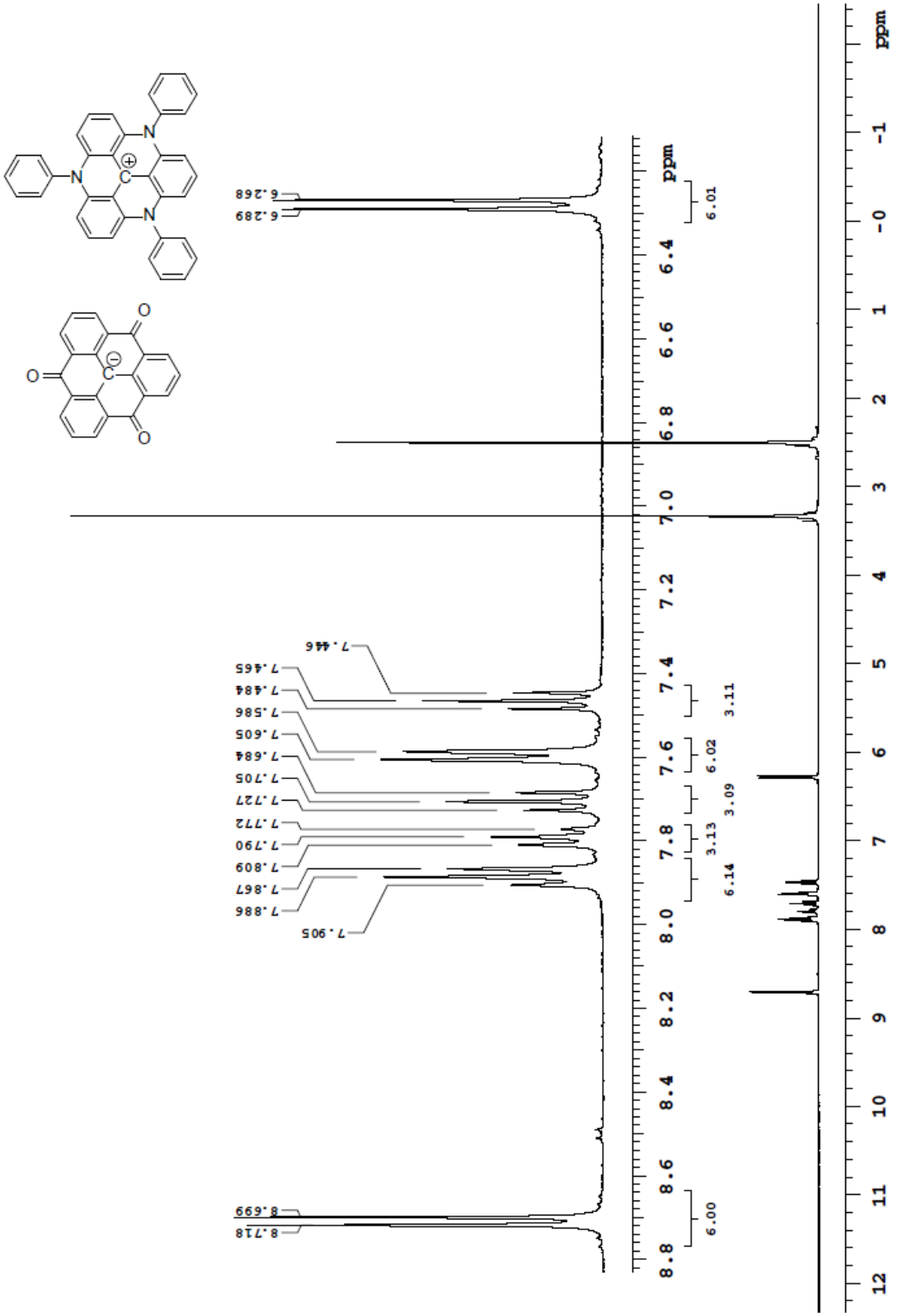

A-39: ^{13}C NMR of 1(NPh)$_3$•2 in d$_6$-DMSO

.....

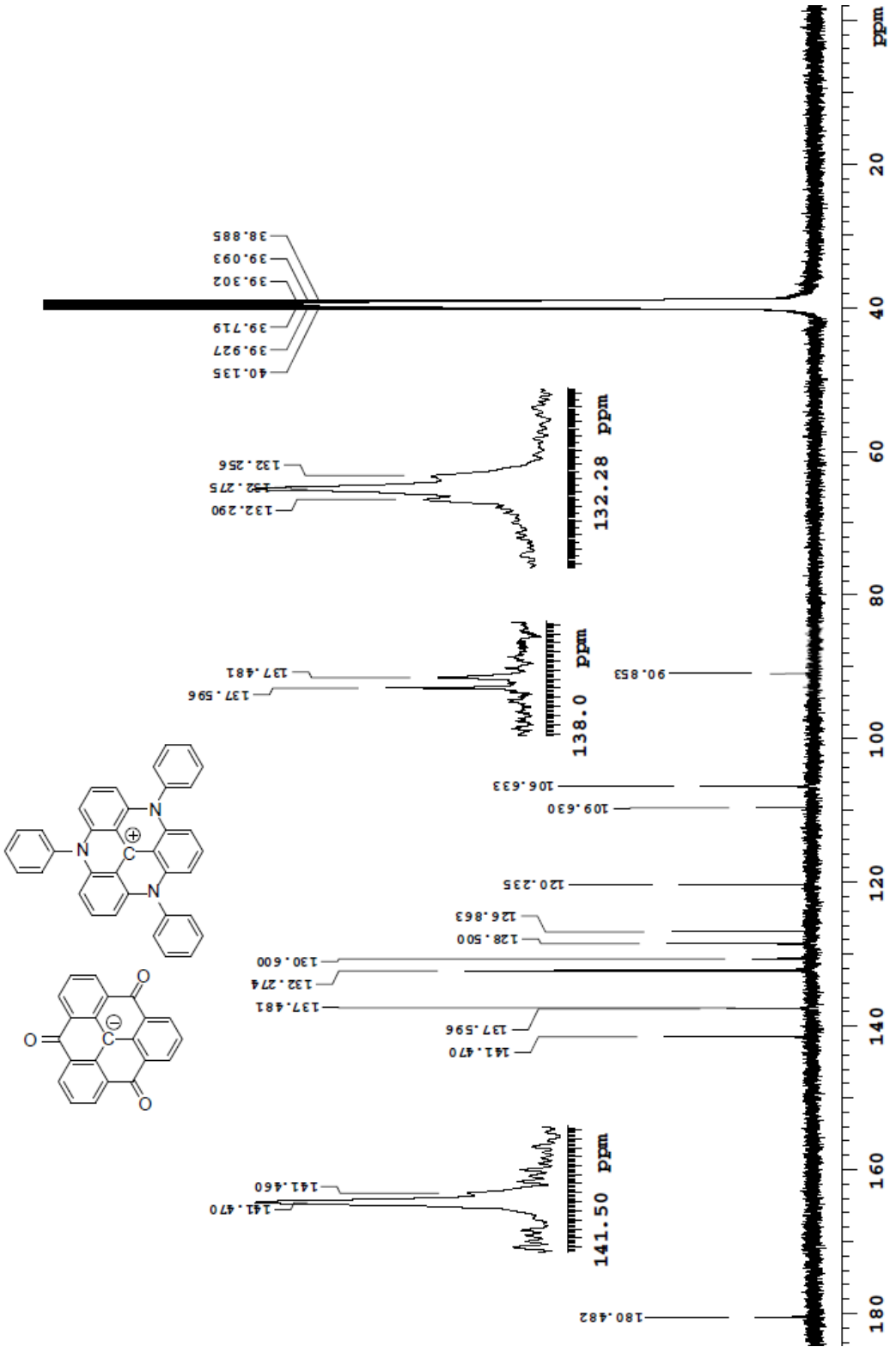

A-40: ^{1}H NMR of 1(NOct)$_3$•2 in d$_6$-DMSO

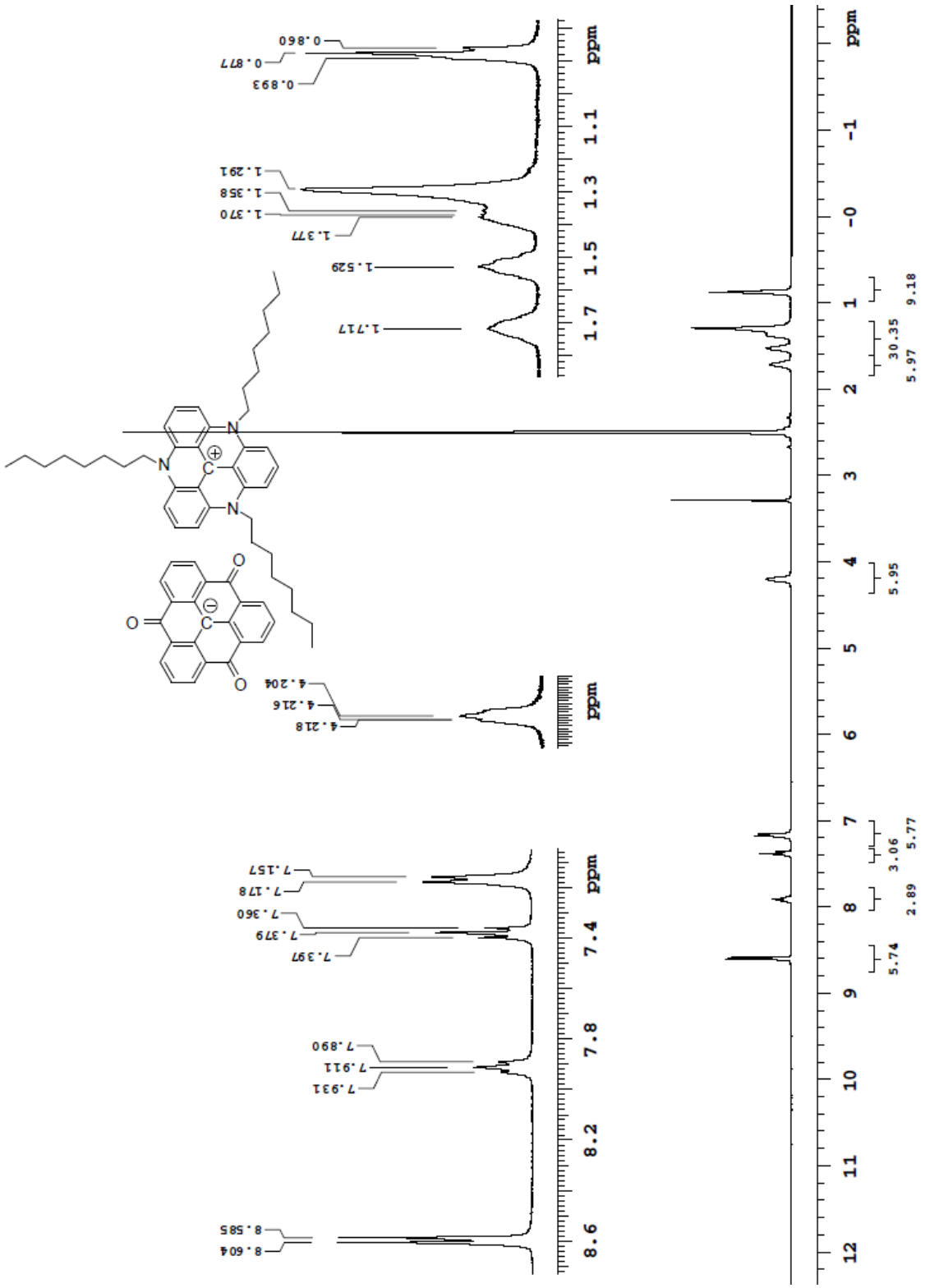

A-41: ^{1}H NMR of 1(NDec)$_3$•2 in d$_6$-DMSO

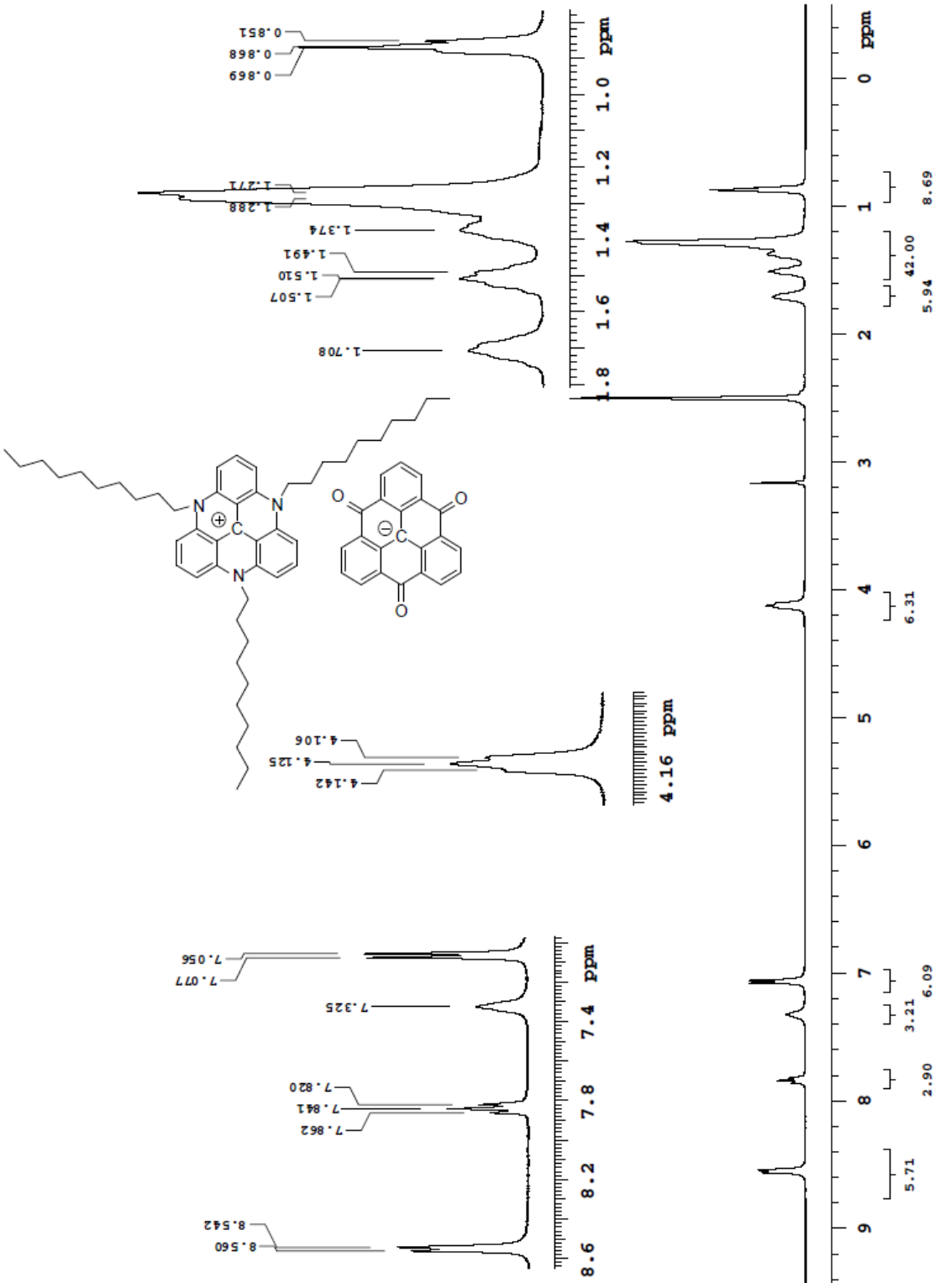

A-42: ^{13}C NMR of 1(NDec)$_3$•2 in d$_6$-DMSO

.....

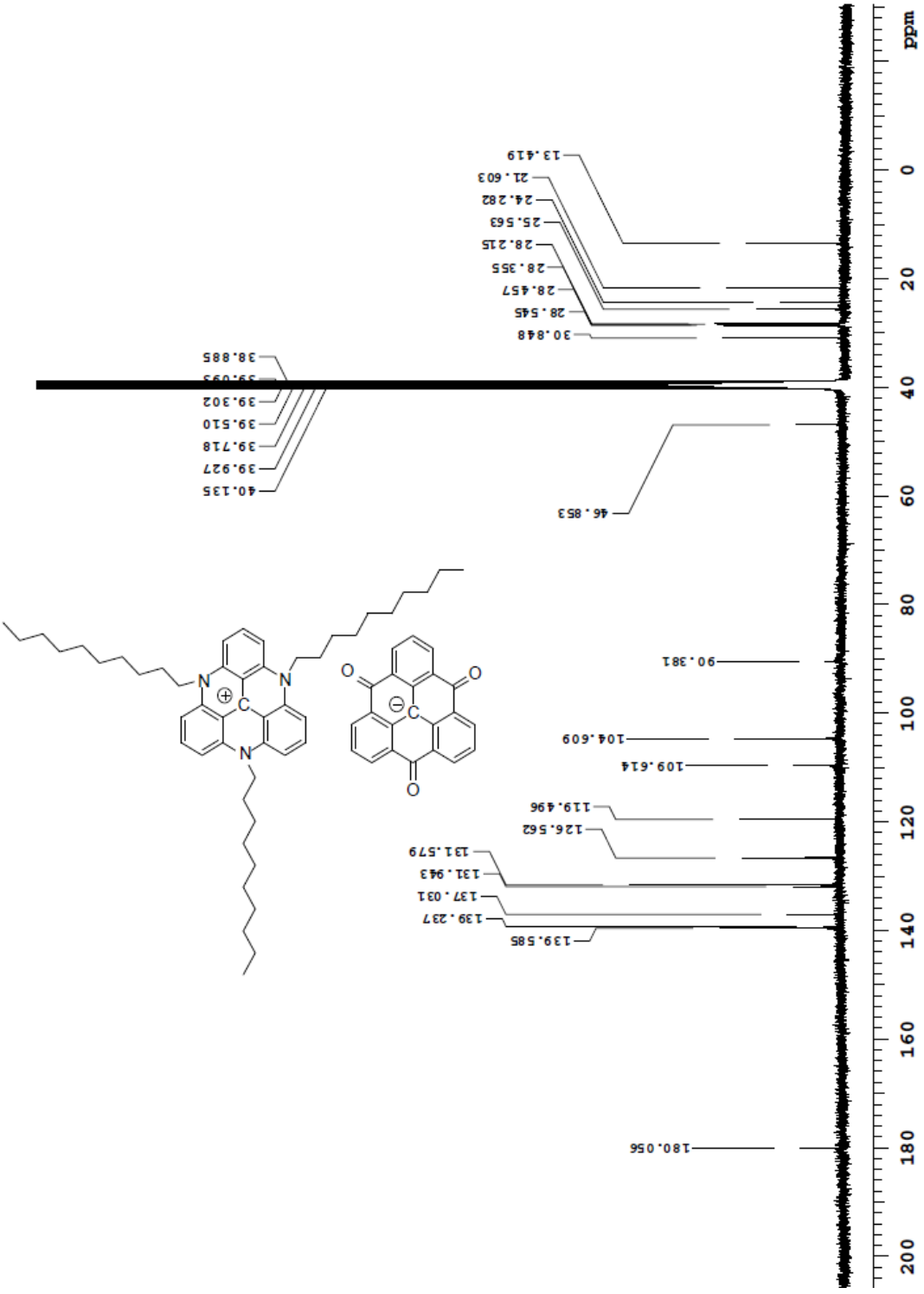

A-43: ^{1}H NMR of $[1(NBu)_3]^{+}BF_4^{-}$ in d_6-DMSO

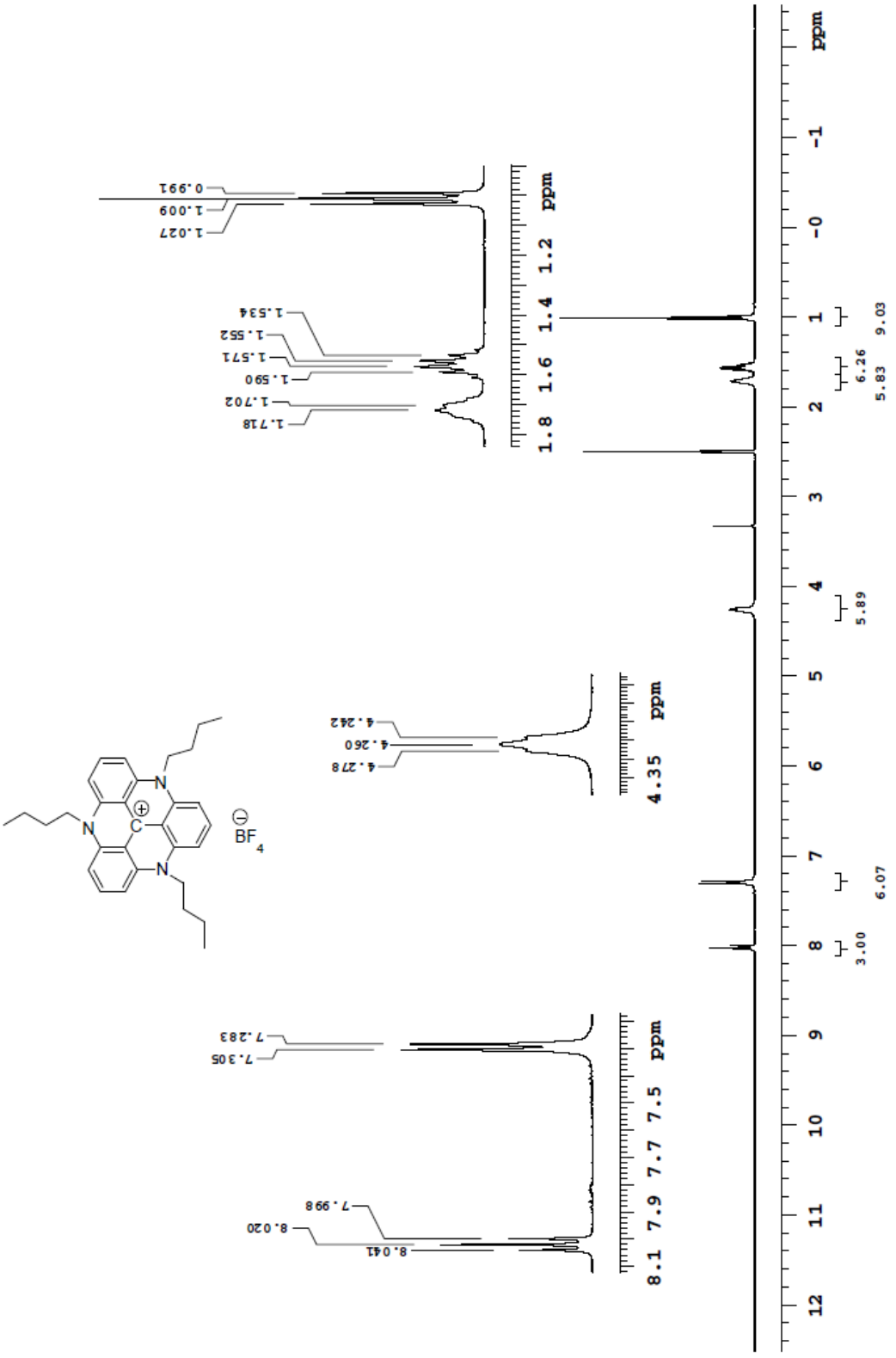

A-44: ^{13}C NMR of $[1(NBu)_3]^+BF_4^-$ in d_6-DMSO

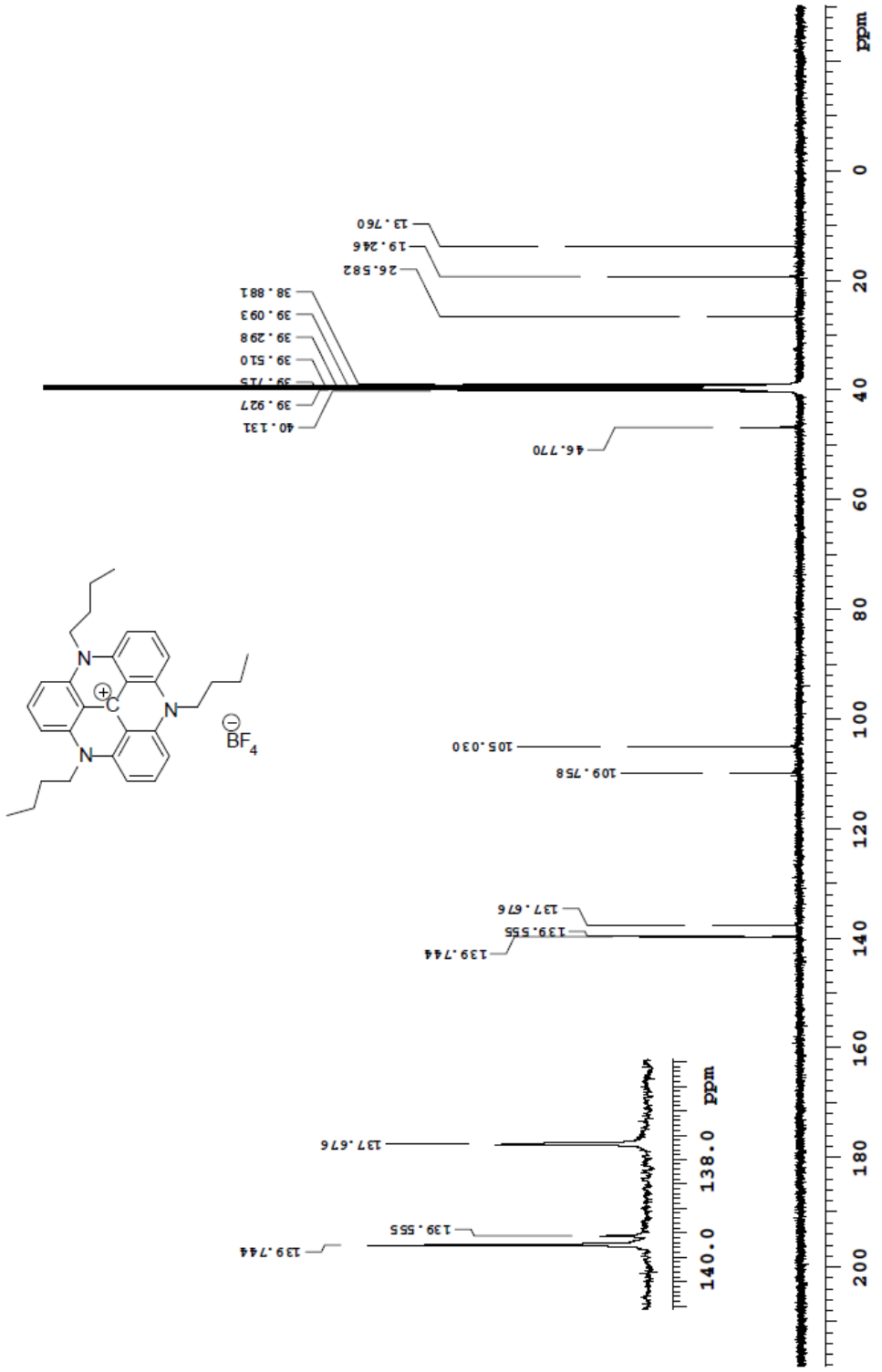

A-45: ESI-MS (+ mode) of [1(NMe)$_3$•2] in CH_3CN / H_2O

…….

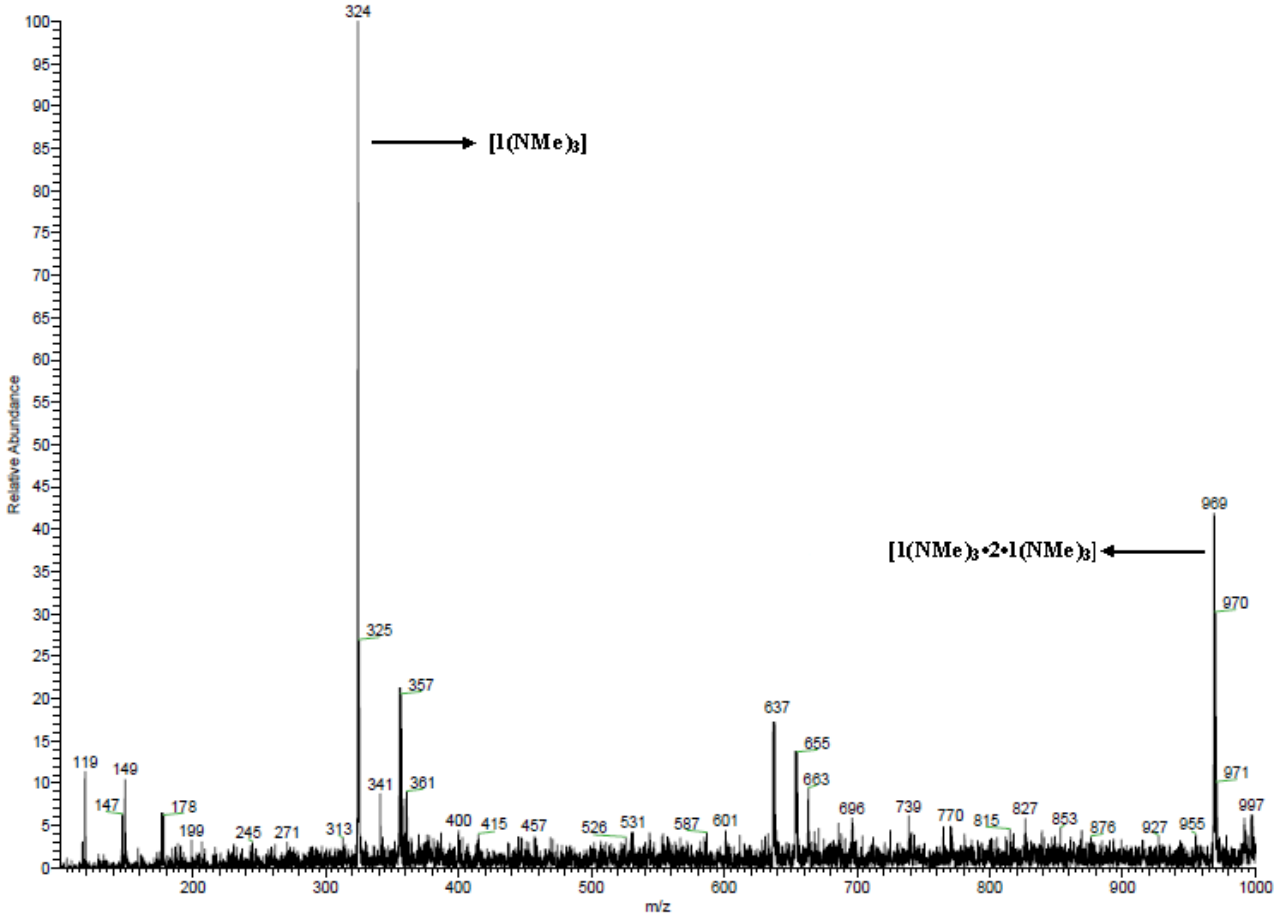

A-46: ESI-MS (+ mode) of [1(NEt)$_3$•2] in CH_3CN / H_2O

……

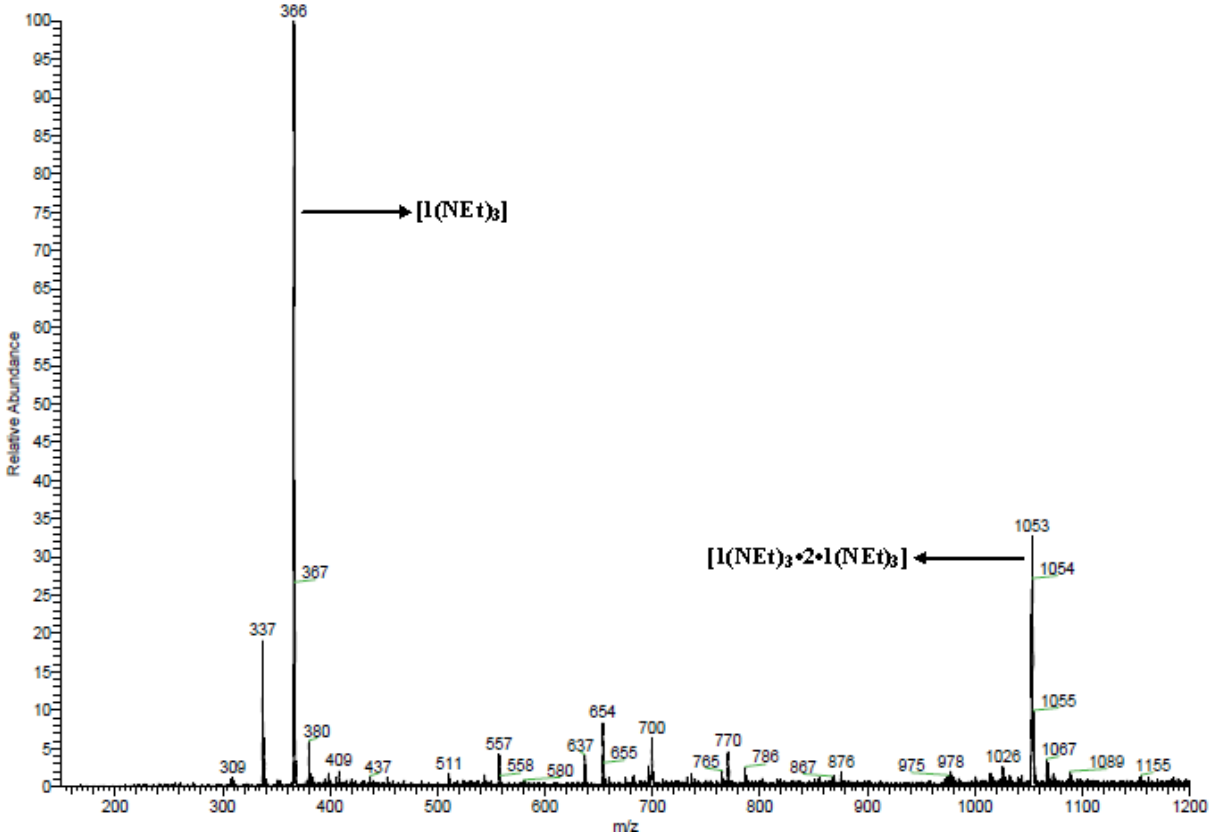

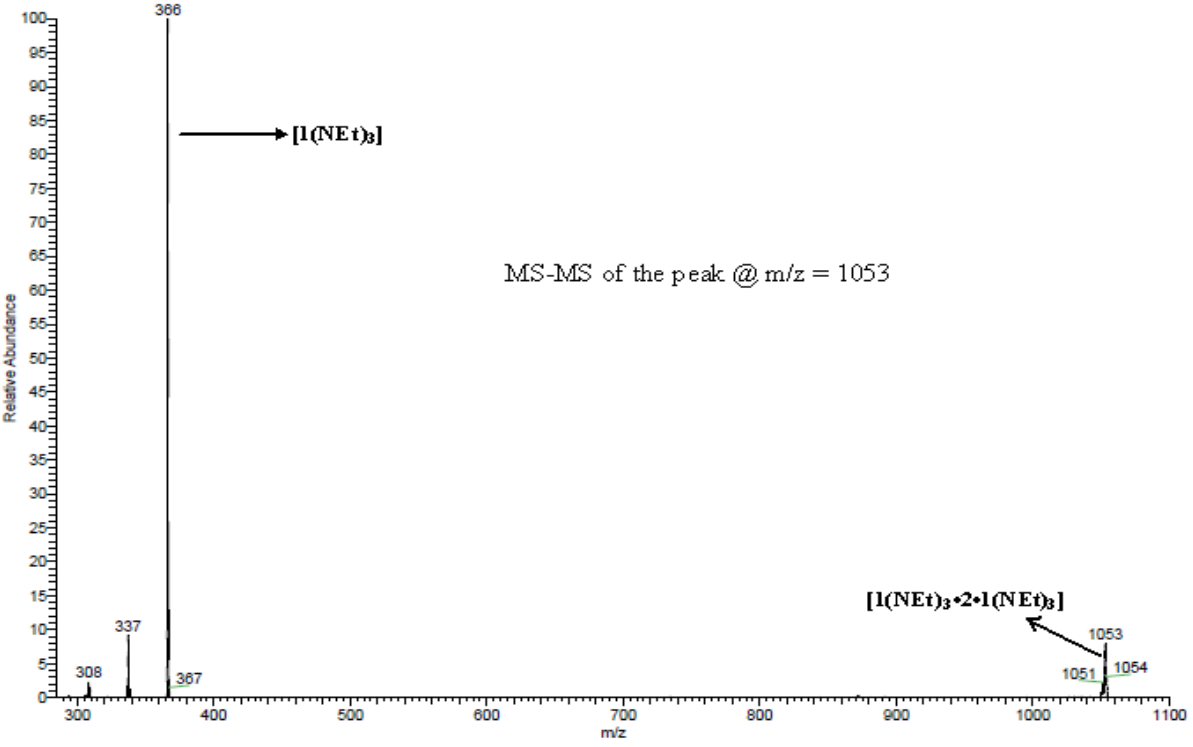

References

(1) Martin, C. B.; Mulla, H. R.; Willis, P. G.; Cammers-Goodwin, A. *Journal of Organic Chemistry* **1999**, *64*, 7802-7806.

(2) Mulla, H. R.; Cammers-Goodwin, A. *Journal of the American Chemical Society* **2000**, *122*, 738-739.

(3) Sindkhedkar, M. D.; Mulla, H. R.; Cammers-Goodwin, A. *Journal of the American Chemical Society* **2000**, *122*, 9271-9277.

(4) Chen, J.; Cammers-Goodwin, A. *European Journal of Organic Chemistry* **2003**, 3861-3867.

(5) Poudel, P. P.; Chen, J.; Cammers, A. *European Journal of Organic Chemistry* **2008**, 5511-5517.

(6) Guckian, K. M.; Schweitzer, B. A.; Ren, R. X. F.; Sheils, C. J.; Paris, P. L.; Kool, E. T. *Journal of the American Chemical Society* **1996**, *118*, 8182-8183.

(7) Selsing, E.; Wells, R. D.; Alden, C. J.; Arnott, S. *Journal of Biological Chemistry* **1979**, *254*, 5417-5422.

(8) Saenger, W. *Principles of Nucleic Acid Structure*, 1984.

(9) Wang, L.; Sun, N.; Terzyan, S.; Zhang, X.; Benson, D. R. *Biochemistry* **2006**, *45*, 13750-13759.

(10) Bullock, J. E.; Carmieli, R.; Mickley, S. M.; Vura-Weis, J.; Wasielewski, M. R. *Journal of the American Chemical Society* **2009**, *131*, 11919-11929.

(11) Ihm, H.; Ahn, J.-S.; Lah, M. S.; Ko, Y. H.; Paek, K. *Organic Letters* **2004**, *6*, 3893-3896.

(12) Liu, Z. H.; He, C.; Duan, C. Y.; You, X. Z. *Inorganic Chemistry Communications* **1999**, *2*, 279-282.

(13) Ranganathan, D.; Haridas, V.; Gilardi, R.; Karle, I. L. *Journal of the American Chemical Society* **1998**, *120*, 10793-10800.

(14) Claessens, C. G.; Stoddart, J. F. *Journal of Physical Organic Chemistry* **1997**, *10*, 254-272.

(15) Kitamura, N.; Suzuki, Y.; Ishizaka, S. *Photochemical & Photobiological Sciences* **2005**, *4*, 135-142.

(16) Cozzi, F.; Ponzini, F.; Annunziata, R.; Cinquini, M.; Siegel, J. S. *Angewandte Chemie, International Edition in English* **1995**, *34*, 1019-1020.

(17) Hunter, C. A.; Sanders, J. K. M.; *J. Am. Chem. Soc* **1990**, *112*, 5525-5534.

(18) Nichols, P. J.; Raston, C. L.; Steed, J. W. *Chem. Commun.* **2001**, *12*, 1062-1063.

(19) Caradoc-Davies, P. L.; Hanton, L. R. *Chem. Commun.* **2001**, *12*, 1098-1099.

(20) Allan, G. G.; Chopra, C. S. *Phytochemistry (Elsevier)* **1971**, *10*, 1363-1366.

(21) Figgemeier, E.; Hiltrop, K. *Langmuir* **2002**, *18*, 1949-1951.

(22) Sakajiri, K.; Saeki, S.; Kawauchi, S.; Watanabe, J. *Polymer Journal (Tokyo)* **2000**, *32*, 803-806.

(23) Nashed, Y. E.; Guirgis, G. A.; Durig, J. R. *Vibrational Spectroscopy* **2001**, *25*, 151-161.

(24) Babkov, L. M.; Vedyaeva, E. S.; Puchkovskaya, G. A. *Journal of Structural Chemistry (Translation of Zhurnal Strukturnoi Khimii)* **2002**, *43*, 1027-1032.

(25) Lightner, D. A.; Gurst, J. E. *Organic Conformational Analysis and Stereochemistry from Circular Dichroism Spectroscopy*, 2000.

(26) Kirin, S. I.; Schatzschneider, U.; De Hatten, X.; Weyhermueller, T.; Metzler-Nolte, N. *Journal of Organometallic Chemistry* **2006**, *691*, 3451-3457.

(27) Kover, K. E.; Kerekes, P. *Magnetic Resonance in Chemistry* **1986**, *24*, 113-122.

(28) Gambino, J.; Yang, T.-F.; Wright, G. E. *Tetrahedron* **1994**, *50*, 11363-11368.

(29) Werner, M. H.; Bianchi, M. E.; Gronenborn, A. M.; Clore, G. M. *Biochemistry* **1995**, *34*, 11998-2004.

(30) Brukwicki, T.; Przybyl, A.; Wysocka, W.; Sosnicki, J. *Tetrahedron* **1999**, *55*, 14501-14512.

(31) Haruyama, H.; Sato, S.; Kawazoe, K.; Kondo, M. *Chemical & Pharmaceutical Bulletin* **1987**, *35*, 957-969.

(32) Tanswell, P.; Thornton, J. M.; Korda, V.; Williams, R. J. P. *European Journal of Biochemistry* **1975**, *57*, 135-145.

(33) Dirinck, P.; Anteunis, M. *Canadian Journal of Chemistry* **1972**, *50*, 412-422.

(34) Barry, C. D.; North, A. C. T.; Glasel, J. A.; Williams, R. J. P.; Xavier, A. V. *Nature (London, United Kingdom)* **1971**, *232*, 236-245.

(35) Reisse, J.; Celotti, J. C.; Ottinger, R. *Tetrahedron Letters* **1966**, 2167-2172.

(36) Karabatsos, G. J.; Fenoglio, D. J. *Topics in Stereochemistry* **1970**, *5*, 167-203.

(37) Bagno, A. *Chemistry--A European Journal* **2001**, *7*, 1652-1661.

(38) Cheeseman, J. R.; Trucks, G. W.; Keith, T. A.; Frisch, M. J. *Journal of Chemical Physics* **1996**, *104*, 5497-5509.

(39) Helgaker, T.; Jaszunski, M.; Ruud, K. *Chemical Reviews* **1999**, *99*, 293-352.

(40) Zvilichovsky, G. *Journal of the Chemical Society, Perkin Transactions 2: Physical Organic Chemistry (1972-1999)* **1988**, 2015-2019.

(41) Chang, F. C.; Swenson, R. P. *Biochemistry* **1999**, *38*, 7168-7176.

(42) Baxter, N. J.; Williamson, M. P. *J Biomol NMR* **1997**, *9*, 359-369.

(43) Cross, B. P.; Schleich, T. *Organic Magnetic Resonance* **1977**, *10*, 82-85.

(44) Marciacq-Rousselot, M. M.; De Trobriand, A.; Lucas, M. *Journal of Physical Chemistry* **1972**, *76*, 1455-1459.

(45) Burdett, J. L.; Rogers, M. T. *Journal of Physical Chemistry* **1966**, *70*, 939-941.

(46) Pardi, A.; Wagner, G.; Wuethrich, K. *European Journal of Biochemistry* **1983**, *137*, 445-454.

(47) Cheung, H. T. A. *Journal of Chemical Research, Synopses* **1980**, 342-343.

(48) Abraham, R. J.; Cooper, M. A.; Salmon, J. R.; Whittaker, D. *Org. Magn. Resonance* **1972**, *4*, 489-507.

(49) Montaudo, G.; Caccamese, S.; Finocchiaro, P.; Bottino, F. *Bulletin of the Chemical Society of Japan* **1971**, *44*, 1439.

(50) Fukazawa, Y.; Usui, S.; Tanimoto, K.; Hirai, Y. *Journal of the American Chemical Society* **1994**, *116*, 8169-8175.

(51) Martin, C. B.; Patrick, B. O.; Cammers-Goodwin, A. *Journal of Organic Chemistry* **1999**, *64*, 7807-7812.

(52) Chen, J. *Ph. D. Dissertation* **2006**, *Department of Chemistry, University of Kentucky*.

(53) Gardner, R. R.; McKay, S. L.; Gellman, S. H. *Org Lett* **2000**, *2*, 2335-2338.

(54) Perrin, C. L.; Fabian, M. A.; Rivero, I. A. *Journal of the American Chemical Society* **1998**, *120*, 1044-1047.

(55) Hunter, C. A.; Lawson, K. R.; Perkins, J.; Urch, C. J. *Journal of the Chemical Society, Perkin Transactions 2: Physical Organic Chemistry (1972-1999)* **2001**, 651-669.

(56) Yamada, S. *Organic & Biomolecular Chemistry* **2007**, *5*, 2903-2912.

(57) Richter, I.; Minari, J.; Axe, P.; Lowe John, P.; James Tony, D.; Sakurai, K.; Bull Steven, D.; Fossey John, S. *Chemical communications (Cambridge, England)* **2008**, 1082-4.

(58) Yamada, S.; Morita, C.; Yamamoto, J. *Tetrahedron Letters* **2004**, *45*, 7475-7478.

(59) Rashkin, M. J.; Hughes, R. M.; Calloway, N. T.; Waters, M. L. *Journal of the American Chemical Society* **2004**, *126*, 13320-13325.

(60) Yamada, S.; Morita, C. *Journal of the American Chemical Society* **2002**, *124*, 8184-8185.

(61) Vaden, T. D.; de Boer, T. S. J. A.; Simons, J. P.; Snoek, L. C. *Physical Chemistry Chemical Physics* **2008**, *10*, 1443-1447.

(62) Ishihara, K.; Fushimi, M. *Organic Letters* **2006**, *8*, 1921-1924.

(63) Milcic, M.; Zaric, S. D. *European Journal of Inorganic Chemistry* **2001**, 2143-2150.

(64) Heaton, N. J.; Bello, P.; Herradon, B.; Del Campo, A.; Jimenez-Barbero, J. *Journal of the American Chemical Society* **1998**, *120*, 12371-12384.

(65) Gung, B. W.; Xue, X.; Reich, H. J. *Journal of Organic Chemistry* **2005**, *70*, 3641-3644.

(66) Gung, B. W.; Xue, X.; Zou, Y. *Journal of Organic Chemistry* **2007**, *72*, 2469-2475.

(67) Heaton, N. J.; Bello, P.; Herradon, B.; del Campo, A.; Jimenez-Barbero, J. *Journal of the American Chemical Society* **1998**, *120*, 12371-12384.

(68) Kim, E.-i.; Paliwal, S.; Wilcox, C. S. *Journal of the American Chemical Society* **1998**, *120*, 11192-11193.

(69) Cockroft, S. L.; Hunter, C. A. *Chemical Communications (Cambridge, United Kingdom)* **2006**, 3806-3808.

(70) Hof, F.; Scofield Denise, M.; Schweizer, W. B.; Diederich, F. *Angewandte Chemie (International ed. in English)* **2004**, *43*, 5056-5059.

(71) Shetty, A. S.; Zhang, J.; Moore, J. S. *Journal of the American Chemical Society* **1996**, *118*, 1019-1027.

(72) Cockroft Scott, L.; Perkins, J.; Zonta, C.; Adams, H.; Spey Sharon, E.; Low Caroline, M. R.; Vinter Jeremy, G.; Lawson Kevin, R.; Urch Christopher, J.; Hunter Christopher, A. *Organic & biomolecular chemistry* **2007**, *5*, 1062-1080.

(73) Cockroft, S. L.; Hunter, C. A.; Lawson, K. R.; Perkins, J.; Urch, C. J. *Journal of the American Chemical Society* **2005**, *127*, 8594-8595.

(74) Laursen, B. W.; Krebs, F. C.; *Chem. Eur. J.* **2001**, *7*, 1773-1783.

(75) Krebs, F. C.; Laursen, B. W.; Johannsen, I.; Faldt, A.; Bechgaard, K.; Jacobsen, C. S.; Thorup, N.; Boubekeur, K. *Acta Crystallogr., Sect. B: Struct. Sci.* **1999**, *B55*, 410-423.

(76) Allison, G.; Brushby, R. J.; Paillaud, J.-L.; Thornton-Pett, M. *Journal of the Chemical Society, Perkin Transactions 1: Organic and Bio-Organic Chemistry* **1995**, 385-90.

(77) McNaught, A. D.; Wilkinson, A. *IUPAC. Compendium of Chemical Terminology* **1997**, *2nd ed. (the "Gold Book")*

(78) Latimer, W. M.; Rodebush, W. H. *Journal of the American Chemical Society* **1920**, *42*, 1419-33.

(79) Lassettre, E. N. *Chem. Rev.* **1937**, *20*, 259-303.

(80) London, F. *Zeitschrift fuer Physik* **1930**, *63*, 245-79.

(81) MacDougall, F. H. *Journal of the American Chemical Society* **1941**, *63*, 3420-4.

(82) Reynisson, J.; McDonald, E. *Journal of computer-aided molecular design* **2004**, *18*, 421-31.

(83) Stokes, R. H. *Journal of the American Chemical Society* **1964**, *86*, 982-6.

(84) Oki, M.; Iwamura, H. *Bull. Chem. Soc. Jpn.* **1959**, *32*, 567-70.

(85) Oki, M.; Iwamura, H. *Bull. Chem. Soc. Jpn.* **1959**, *32*, 1135-43.

(86) Oki, M.; Iwamura, H. *Bull. Chem. Soc. Jpn.* **1959**, *32*, 950-5.

(87) Oki, M.; Iwamura, H. *Bull. Chem. Soc. Jpn.* **1959**, *32*, 955-9.

(88) Traetteberg, M.; Bakken, P.; Hopf, H.; Mlynek, C.; Mahle, A. H. *Journal of Molecular Structure* **2000**, *554*, 191-202.

(89) Traetteberg, M.; Bakken, P.; Seip, R.; Luettke, W.; Knieriem, B. *Journal of Molecular Structure* **1985**, *128*, 191-206.

(90) Krueger, P. J.; Mettee, H. D. *Tetrahedron Letters* **1966**, 1587-90.

(91) Plevin Michael, J.; Hayashi, I.; Ikura, M. *J Am Chem Soc* **2008**, *130*, 14918-9.

(92) Schweizer, W. B.; Dunitz, J. D.; Pfund, R. A.; Tombo, G. M. R.; Ganter, C. *Helv. Chim. Acta* **1981**, *64*, 2738-40.

(93) Singelenberg, F. A. J.; Van Eijck, B. P. *Acta Crystallographica, Section C: Crystal Structure Communications* **1987**, *C43*, 309-11.

(94) Perutz, M. F.; Fermi, G.; Abraham, D. J.; Poyart, C.; Bursaux, E. *Journal of the American Chemical Society* **1986**, *108*, 1064-78.

(95) Levitt, M.; Perutz, M. F. *J Mol Biol* **1988**, *201*, 751-4.

(96) Chakrabarti, P.; Samanta, U. *J Mol Biol* **1995**, *251*, 9-14.

(97) Umezawa, Y.; Nishio, M. *Bioorganic & medicinal chemistry* **2000**, *8*, 2643-50.

(98) Umezawa, Y.; Nishio, M. *Bioorganic & medicinal chemistry* **1998**, *6*, 493-504.

(99) Umezawa, Y.; Nishio, M. *Bioorganic & medicinal chemistry* **1998**, *6*, 2507-15.

(100) Maeda, I.; Shimohigashi, Y.; Ikesue, K.; Nose, T.; Ide, Y.; Kawano, K.; Ohno, M. *Journal of biochemistry* **1996**, *119*, 870-7.

(101) Tewari, A. K.; Dubey, R. *ARKIVOC (Gainesville, FL, United States)* **2009**, 283-291.

(102) Kobayashi, Y.; Maeda, J.; Morisawa, F.; Saigo, K. *Tetrahedron: Asymmetry* **2006**, *17*, 967-974.

(103) Tsue, H.; Ishibashi, K.; Takahashi, H.; Tamura, R. *Organic Letters* **2005**, *7*, 2165-2168.

(104) Iwamoto, H.; Takahashi, N.; Maeda, T.; Hidaka, Y.; Fukazawa, Y. *Tetrahedron Letters* **2005**, *46*, 6839-6842.

(105) Bazzicalupi, C.; Dapporto, P. *Structural Chemistry* **2004**, *15*, 259-268.

(106) Takahashi, O.; Kohno, Y.; Saito, K.; Nishio, M. *Chemistry--A European Journal* **2003**, *9*, 756-762.

(107) Takahashi, O.; Yasunaga, K.; Gondoh, Y.; Kohno, Y.; Saito, K.; Nishio, M. *Bull. Chem. Soc. Jpn.* **2002**, *75*, 1777-1783.

(108) Tsuzuki, S.; Houjou, H.; Nagawa, Y.; Hiratani, K. *Journal of the Chemical Society, Perkin Transactions 2: Physical Organic Chemistry (1972-1999)* **2001**, 1951-1955.

(109) Ramirez-Gualito, K.; Alonso-Rios, R.; Quiroz-Garcia, B.; Rojas-Aguilar, A.; Diaz, D.; Jimenez-Barbero, J.; Cuevas, G. *Journal of the American Chemical Society* **2009**, *131*, 18129-18138.

(110) Le Barbu-Debus, K.; Broquier, M.; Mahjoub, A.; Zehnacker-Rentien, A. *Physical Chemistry Chemical Physics* **2009**, *11*, 7589-7598.

(111) Bautista-Ibanez, L.; Ramirez-Gualito, K.; Quiroz-Garcia, B.; Rojas-Aguilar, A.; Cuevas, G. *Journal of Organic Chemistry* **2008**, *73*, 849-857.

(112) Re, S.; Nagase, S. *Chemical Communications (Cambridge, United Kingdom)* **2004**, 658-659.

(113) Nishio, M.; Umezawa, Y.; Hirota, M. *Yuki Gosei Kagaku Kyokaishi* **1997**, *55*, 18-28.

(114) Carrillo, R.; Lopez-Rodriguez, M.; Martin, V. S.; Martin, T. *Angewandte Chemie, International Edition* **2009**, *48*, 7803-7808, S7803/1-S7803/40.

(115) Tsuzuki, S.; Honda, K.; Uchimaru, T.; Mikami, M.; Tanabe, K. *Journal of the American Chemical Society* **2000**, *122*, 11450-11458.

(116) Gross, J.; Harder, G.; Siepen, A.; Harren, J.; Voegtle, F.; Stephan, H.; Gloe, K.; Ahlers, B.; Cammann, K.; Rissanen, K. *Chemistry--A European Journal* **1996**, *2*, 1585-1595.

(117) Gross, J.; Harder, G.; Voegtle, F.; Stephan, H.; Gloe, K. *Angewandte Chemie, International Edition in English* **1995**, *34*, 481-4.

(118) Sunner, J.; Nishizawa, K.; Kebarle, P. *Journal of Physical Chemistry* **1981**, *85*, 1814-20.

(119) Mason, R. S.; Williams, C. M.; Anderson, P. D. J. *Journal of the Chemical Society, Chemical Communications* **1995**, 1027-8.

(120) Meot-Ner, M.; Deakyne, C. A. *Journal of the American Chemical Society* **1985**, *107*, 474-9.

(121) Meot-Ner, M.; Deakyne, C. A. *Journal of the American Chemical Society* **1985**, *107*, 469-74.

(122) Taft, R. W.; Anvia, F.; Gal, J. F.; Walsh, S.; Capon, M.; Holmes, M. C.; Hosn, K.; Oloumi, G.; Vasanwala, R.; Yazdani, S. *Pure and Applied Chemistry* **1990**, *62*, 17-23.

(123) Guo, B. C.; Purnell, J. W.; Castleman, A. W., Jr. *Chemical Physics Letters* **1990**, *168*, 155-60.

(124) Caldwell, J. W.; Kollman, P. A. *Journal of the American Chemical Society* **1995**, *117*, 4177-8.

(125) Schneider, H. J.; Werner, F.; Blatter, T. *Journal of Physical Organic Chemistry* **1993**, *6*, 590-4.

(126) Alkorta, I.; Rozas, I.; Elguero, J. *J Am Chem Soc* **2002**, *124*, 8593-8.

(127) Quinonero, D.; Garau, C.; Rotger, C.; Frontera, A.; Ballester, P.; Costa, A.; Deya, P. M. *Angewandte Chemie, International Edition* **2002**, *41*, 3389-3392.

(128) Mascal, M.; Armstrong, A.; Bartberger, M. D. *Journal of the American Chemical Society* **2002**, *124*, 6274-6276.

(129) Garau, C.; Frontera, A.; Quinonero, D.; Ballester, P.; Costa, A.; Deya, P. M. *ChemPhysChem* **2003**, *4*, 1344-1348.

(130) Cox, E. G.; Smith, J. A. S. *Nature* **1954**, *173*, 75.

(131) Gavezzotti, A. *Acc. Chem. Res.* **1994**, *27*, 309.

(132) Janiak, C. *J. Chem. Soc., Dalton Trans* **2000**, 3885-3896.

(133) Hobza, P.; Selzle, H. L.; Schlag, E. W. *J. Phys. Chem* **1996**, *100*, 18790-18794.

(134) Jaffe, R. L.; Smith, G. D. *J. Chem. Phys* **1996**, *105*.

(135) Tran, F.; Weber, J.; Wesolowski, T. A. *Helv. Chim. Acta* **2001**, *84*, 1489-1503.

(136) Tsuzuki, S.; Honda, K.; Uchimaru, T.; Mikami, M.; Tanabe, K. *J. Am. Chem. Soc.* **2002**, *124*, 104-112.

(137) Desiraju, G. R.; Gavezzotti, A. *J. Chem. Soc. Chem. Commun.* **1989**, 621-623.

(138) Williams, J. H. *Acc. Chem. Res.* **1993**, 593-598.

(139) Patrick, C. R.; Prosser, G. S. *Nature* **1960**, 1021.

(140) Vrbancich, J.; Ritchie, G. L. D. *J. Chem. Soc., Faraday Tran.* **1980**, *2* 649-659.

(141) Meyer, E. A.; Castellano, R. K.; Diederich, F. *Angew. Chem. Int. Ed* **2003**, *42*, 1210-1250.

(142) Chen, J. *Ph. D. Dissertation* **2006**, *Department of Chemistry, University of Kentucky*.

(143) Muehldorf, A. V.; Engen, D. V.; Warner, J. C.; Hamilton, A. D. *J. Am. Chem. Soc.* **1988**, *110*,, 6561-6562.

(144) Garcia, F.; Aparicio, F.; Fernandez, G.; Sanchez, L. *Organic Letters* **2009**, *11*, 2748-2751.

(145) Garcia-Frutos, E. M.; Hennrich, G.; Gutierrez, E.; Monge, A.; Gomez-Lor, B. *Journal of Organic Chemistry*, *75*, 1070-1076.

(146) Lahiri, S.; Thompson, J. L.; Moore, J. S. *Journal of the American Chemical Society* **2000**, *122*, 11315-11319.

(147) Smithrud, D. B.; Diederich, F. *Journal of the American Chemical Society* **1990**, *112*, 339-43.

(148) Garcia-Frutos Eva, M.; Hennrich, G.; Gutierrez, E.; Monge, A.; Gomez-Lor, B. *The Journal of organic chemistry*, *75*, 1070-6.

(149) Krishnamoorthi, R.; La Mar, G. N. *European journal of biochemistry / FEBS* **1984**, *138*, 135-40.

(150) Burattini, S.; Colquhoun, H. M.; Fox, J. D.; Friedmann, D.; Greenland, B. W.; Harris, P. J. F.; Hayes, W.; Mackay, M. E.; Rowan, S. J. *Chemical Communications (Cambridge, United Kingdom)* **2009**, 6717-6719.

(151) Colquhoun, H. M.; Zhu, Z.; Williams, D. J.; Drew, M. G. B.; Cardin, C. J.; Gan, Y.; Crawford, A. G.; Marder, T. B. *Chemistry--A European Journal*, *16*, 907-918.

(152) Jaggi, M.; Blum, C.; Dupont, N.; Grilj, J.; Liu, S.-X.; Hauser, J.; Hauser, A.; Decurtins, S. *Organic Letters* **2009**, *11*, 3096-3099.

(153) Novoa, J. J.; Lafuente, P.; Del Sesto, R. E.; Miller, J. S. *Angewandte Chemie, International Edition* **2001**, *40*, 2540-2545.

(154) Del Sesto, R. E.; Miller, J. S.; Lafuente, P.; Novoa, J. J. *Chemistry--A European Journal* **2002**, *8*, 4894-4908.

(155) Garcia-Yoldi, I.; Miller, J. S.; Novoa, J. J. *J. Phys. Chem. A* **2007**, *111*, 8020-8027.

(156) Garcia-Yoldi, I.; Miller, J. S.; Novoa, J. J. *Physical Chemistry Chemical Physics* **2008**, *10*, 4106-4109.

(157) Garcia-Yoldi, I.; Miller, J. S.; Novoa, J. J. *J. Phys. Chem. A* **2009**, *113*, 7124-7132.

(158) Garcia-Yoldi, I.; Miller, J. S.; Novoa, J. J. *J. Phys. Chem. A* **2009**, *113*, 484-492.

(159) Garcia-Yoldi, I.; Mota, F.; Novoa, J. J. *J. Comput. Chem.* **2007**, *28*, 326-334.

(160) Mota, F.; Miller, J. S.; Novoa, J. J. *Journal of the American Chemical Society* **2009**, *131*, 7699-7707.

(161) Novoa, J. J.; Lafuente, P.; Del Sesto, R. E.; Miller, J. S. *CrystEngComm* **2002**, *4*, 373-377.

(162) Novoa Juan, J.; Novoa Juan, N.; Ribas-Arino, J.; Shum William, W.; Miller Joel, S. *Inorg Chem* **2007**, *46*, 103-7.

(163) Cho, D. M.; Parkin, S. R.; Watson, M. D. *Organic Letters* **2005**, *7*, 1067-1068.

(164) Wheeler, S. E. *Journal of the American Chemical Society* **2011**, *133*, 10262-10274.

(165) Maly, K. E. *Cryst. Growth Des.* **2011**, ACS ASAP.

(166) Hunter, C. A.; Sanders, J. K. M.; *J. Am. Chem. Soc* **1990**, 5525-5534.

(167) Nichols, P. J.; Raston, C. L.; Steed, J. W. *Chem. Commun.* **2001**, 1062.

(168) Caradoc-Davies, P. L.; Hanton, L. R. *Chem. Commun.* **2001**, 1098.

(169) Kato, R. *Chem. Rev* **2004**, *104*, 5319.

(170) Shivaeva, R. P.; Yagubskii, E. B. *Chem. Rev* **2004**, *104*, 5347.

(171) Inabe, T.; Tajima, H. *Chem. Rev* **2004**, *104*, 5503.

(172) Tseng, H.; Vignon, S. A.; Stoddart, J. F. *Angew. Chem. Int. Ed.* **2003**, *42*, 1491.

(173) Jeon, W. S.; Ziganshina, A. Y.; Lee, J. W.; Ko, Y. H.; Kang, J.; Lee, C.; Kim, K. *Angew. Chem. Int. Ed* **2003**, *42*, 4097.

(174) Collier, C. P.; Wong, E. W.; Belohradsky, M.; Raymo, F. M.; Stoddart, J. F.; Kuekes, P. J.; Williams, R. S.; Heath, J. R. *Science* **1999**, *285*, 391.

(175) Fu, L.; Cao, L.; Liu, Y.; Zhu, D. *Adv. Colloid Interface Sci.* **2004**, *111*, 133.

(176) Chandrasekar, S.; Sadashiva, B. K.; Suresh, K. A. *Pramana* **1977**, *9*, 471-480.

(177) Chandrasekhar, S. *Handb. Liq. Cryst. Res.* **1998**, *2B*, 749-780.

(178) Schmidt-Mendle, L.; Fechtenkotter, A.; Mullen, K.; Moons, E.; Friend, R. H.; MacKeinzie, J. D. *Science* **2001**, *293*, 1119-1122.

(179) Adam, D.; Schuhmacher, P.; Simmerer, J.; Hanssling, L.; Siemensmeyer, K.; Etzbach, K. H.; Ringsdorf, H.; Haarer, D. *Nature* **1994**, *371*, 141-143.

(180) Curis, M. D.; J, C.; Kampf, J. W. *J. Am. Chem. Soc.* **2004**, *126*, 4318.

(181) Bredas, J. L.; Beljonne, D.; Coropceanu, V.; Cornil, J. *J. Chem. Rev.* **2004**, *104*, 4971.

(182) Cornil, J.; Beljonne, D.; Calbert, J. P.; Bredas, J. L. *Adv. Mater* **2001**, *13*, 1054.

(183) Naraso, N.; Nishida, J.; Ando, S.; Yamaguchi, J.; Itika, K.; Koinuma, H.; Tada, H.; Tokito, S.; Yamashita, Y. *J. Am. Che. Soc.* **2005**, *127*, 10142.

(184) Li, X.-C.; Sirringhaus, H.; Garnier, F.; Holmes, A. B.; Moratti, S. C.; Feeder, N.; Clegg, W.; Teat, S. J.; Friend, R. H. *J. Am. Che. Soc.* **1998**, *120*, 2206.

(185) Pappenfus, T. M.; Chesterfield, R. J.; Frisbie, C. D.; Mann, K. R.; Casado, J.; Raff, J. D.; Miller, L. L. *J. Am. Che. Soc.* **2002**, *124*, 4184.

(186) Clar, E.; Stewart, D. G. *Journal of the American Chemical Society* **1953**, *75*, 2667-2672.

(187) Clar, E.; Kemp, W.; Stewart, D. G. *Tetrahedron* **1958**, *3*, 325-33.

(188) Martin, J. C.; Smith, R. G. *Journal of the American Chemical Society* **1964**, *86*, 2252-6.

(189) Laursen, B. W.; Krebs, F. C.; *Angew. Chem. Int. Ed.* **2000**, *39*, 3432-3434.

(190) Bellott, E. M.; Bu, D.; Childs, J. J.; Lambert, C. R.; Nienaber, H. A.; Shi, S. J.; Wang, Z.; Workman, J. J., Jr.; Zelenchuk, A. R.; (Argose, Inc., USA). Application: WO WO, 2005; Vol. WO 2005065241, p 196 pp.

(191) Wada, M.; Konishi, H.; Kirishima, K.; Takeuchi, H.; Natsume, S.; Erabi, T. *Bulletin of the Chemical Society of Japan* **1997**, *70*, 2737-2741.

(192) Westerlund, F.; Hildebrandt, C. B.; Soerensen, T. J.; Laursen, B. W. *Chemistry--A European Journal*, *16*, 2992-2996, S2992/1-S2992/18.

(193) Weisstein, E. W. *"Circle-Circle Intersection." From MathWorld--A Wolfram Web Resource.* *http://mathworld.wolfram.com/Circle-CircleIntersection.html*

(194) Rauk, A. *Orbital Interaction Theory of Organic Chemistry*, 1994.

(195) Desiraju, G. R.; Gavezzotti, A. *J. Chem. Soc. Chem. Commun.* **1989**, 621-623.

(196) Patrick, C. R.; Prosser, G. S. *Nature* **1960**, 1021.

(197) Booth, H.; Everett, J. R. *Journal of the Chemical Society, Perkin Transactions 2 Physical Organic Chemistry (1972-1999)* **1980**, 255-9.

(198) Taft, R. W. *John Wiley & Sons, Inc., New York, N.Y.* **1956**, *M. S. Newman, Ed.*, 710 pp.

(199) Lu, J.-M.; Rosokha Sergiy, V.; Kochi Jay, K. *Journal of the American Chemical Society* **2003**, *125*, 12161-71.

(200) Shimomura, M.; Karthaus, O.; Ijiro, K. *Synth. Met.* **1996**, *81*, 251-257.

(201) Grimme, S. *Angewandte Chemie, International Edition* **2008**, *47*, 3430-3434.

(202) Sinnokrot Mutasem, O.; Sherrill, C. D. *J Phys Chem A* **2006**, *110*, 10656-68.

(203) Tsuzuki, S.; Honda, K.; Uchimaru, T.; Mikami, M. *Journal of Chemical Physics* **2006**, *124*, 114304/1-114304/7.

(204) Rosokha, S. V.; Zhang, J.; Lu, J.; Kochi, J. K. *Journal of Physical Organic Chemistry* **2010**, *23*, 395-399.

(205) Konno, M.; Saito, Y. *Acta Crystallogr., Sect. B* **1974**, *30*, 1294-9.

(206) Zanotti, G.; Del Pra, A.; Bozio, R. *Acta Crystallogr., Sect. B* **1982**, *B38*, 1225-9.

(207) Vazquez, C.; Calabrese, J. C.; Dixon, D. A.; Miller, J. S. *Journal of Organic Chemistry* **1993**, *58*, 65-81.

(208) Yan, Y.-K.; Mingos, D. M. P.; Mueller, T. E.; Williams, D. J.; Kurmoo, M. *J. Chem. Soc., Dalton Trans.* **1995**, 2509-14.

(209) Pasimeni, L.; Brustolon, M.; Zanonato, P. L.; Corvaja, C. *Chem. Phys.* **1980**, *51*, 381-7.

(210) Marzotto, A.; Clemente, D. A.; Pasimeni, L. *J. Crystallogr. Spectrosc. Res.* **1988**, *18*, 545-54.

(211) Goto, K.; Kubo, T.; Yamamoto, K.; Nakasuji, K.; Sato, K.; Shiomi, D.; Takui, T.; Kubota, M.; Kobayashi, T.; Yakusi, K.; Ouyang, J. *Journal of the American Chemical Society* **1999**, *121*, 1619-1620.

(212) Fukui, K.; Sato, K.; Shiomi, D.; Takui, T.; Itoh, K.; Gotoh, K.; Kubo, T.; Yamamoto, K.; Nakasuji, K.; Naito, A. *Synth. Met.* **1999**, *103*, 2257-2258.

(213) Kochi, J. K.; Rathore, R.; Le Magueres, P. *Journal of Organic Chemistry* **2000**, *65*, 6826-6836.

(214) Eckhardt, C. J.; Merski, J. *Surface Sci.* **1973**, *37*, 937-46.

(215) Hasegawa, T.; Mochida, T.; Kondo, R.; Kagoshima, S.; Iwasa, Y.; Akutagawa, T.; Nakamura, T.; Saito, G. *Phys. Rev. B: Condens. Matter Mater. Phys.* **2000**, *62*, 10059-10066.

(216) Deibel, C.; Strobel, T.; Dyakonov, V. *Adv. Mater. (Weinheim, Ger.)*, *22*, 4097-4111.

(217) Mayoh, B.; Prout, C. K. *J. Chem. Soc., Faraday Trans. 2* **1972**, *68*, 1072-82.

(218) Kochi, J. K. *Pure and Applied Chemistry* **1991**, *63*, 255-64.

(219) Yamashita, Y.; Tomura, M. *J. Mater. Chem.* **1998**, *8*, 1933-1944.

(220) Fyfe, C. A.; Harold-Smith, D. *J. Chem. Soc., Faraday Trans. 2* **1976**, *72*, 2269-82.

(221) Soos, Z. G. *Annu. Rev. Phys. Chem.* **1974**, *25*, 121-53.

(222) Rosokha, S. V.; Kochi, J. K. *Accounts of Chemical Research* **2008**, *41*, 641-653.

(223) Foster, R. *Organic Charge-Transfer Complexes (Organic Chemistry: a Series of Monographs, Vol. 15)*, 1969.

(224) Pandey, R.; Ghosh, S.; Mukhopadhyay, S.; Ramasesha, S.; Das, P. K. *Journal of Chemical Physics*, *134*, 044533/1-044533/8.

(225) Colquhoun, H. M.; Zhu, Z.; Williams, D. J. *Organic Letters* **2003**, *5*, 4353-4356.

(226) Greenland, B. W.; Burattini, S.; Hayes, W.; Colquhoun, H. M. *Tetrahedron* **2008**, *64*, 8346-8354.

(227) Hardacre, C.; Holbrey, J. D.; Mullan, C. L.; Nieuwenhuyzen, M.; Youngs, T. G. A.; Bowron, D. T.; Teat, S. J. *Physical Chemistry Chemical Physics*, *12*, 1842-1853.

(228) Tahara, K.; Fujita, T.; Sonoda, M.; Shiro, M.; Tobe, Y. *Journal of the American Chemical Society* **2008**, *130*, 14339-14345.

(229) Rosokha, S. V.; Newton, M. D.; Jalilov, A. S.; Kochi, J. K. *Journal of the American Chemical Society* **2008**, *130*, 1944-1952.

(230) Kumar, N. S. S.; Gujrati Maneesh, D.; Wilson James, N. *Chemical communications (Cambridge, England)*, *46*, 5464-6.

(231) Job, P. *Ann. Chim. Appl.* **1928**, *9*, 113-203.

(232) Huang, C. Y. *Methods in Enzymology* **1982**, *87*, 509-25.

(233) Yamashita, M.; Fenn, J. B. *Journal of Physical Chemistry* **1984**, *88*, 4451-9.

(234) Ramos Catarina, I. V.; Barros Cristina, M.; Fernandes Ana, M.; Santana-Marques, M. G.; Correia, A. J. F.; Tome Joao, P. C.; Carrilho Maria do Carmo, T.; Faustino Maria Amparo, F.; Tome Augusto, C.; Neves, M. G. P. M. S.; Cavaleiro, J. A. S. *J Mass Spectrom* **2005**, *40*, 1439-47.

(235) Sarni-Manchado, P.; Cheynier, V. *J. Mass Spectrom.* **2002**, *37*, 609-616.

(236) De Vriendt, K.; Sandra, K.; Desmet, T.; Nerinckx, W.; Van Beeumen, J.; Devreese, B. *Rapid Commun. Mass Spectrom.* **2004**, *18*, 3061-3067.

(237) Urathamakul, T.; Waller, D. J.; Beck, J. L.; Aldrich-Wright, J. R.; Ralph, S. F. *Inorg. Chem. (Washington, DC, U. S.)* **2008**, *47*, 6621-6632.

(238) Plet, B.; Schmitter, J.-M. *Pract. Aspects Trapped Ion Mass Spectrom.* **2009**, 153-167.

(239) He, X.-W.; Long, H.-T.; Yuan, G.; Xu, X.-J.; Zhou, Y.-W. *Wuli Huaxue Xuebao*, *26*, 1082-1086.

(240) Henrotte, V.; Laurent, S.; Gabelica, V.; Vander Elst, L.; Depauw, E.; Muller, R. N. *Rapid Commun. Mass Spectrom.* **2004**, *18*, 1919-1924.

(241) Li, J.; Xu, H.-W.; Wang, S.-M.; Li, H.-Y.; Han, D.; Liu, H.-M. *Fenxi Huaxue* **2008**, *36*, 1212-1216.

(242) Liu, J.; Cao, S.; Jia, B.; Lu, J.; Liao, X.; Zhao, Y. *Fenxi Ceshi Xuebao* **2009**, *28*, 757-763.

(243) Liu, X.-x.; Fang, H.; Liu, Y.; Zhao, Y.-f. *Phosphorus, Sulfur Silicon Relat. Elem.* **2008**, *183*, 791-796.

(244) Qiang, L.; Dong, X.; Lu, M.; Cao, S.; Lu, K.; Zhao, Y. *Huaxue Xuebao* **2009**, *67*, 2607-2612.

(245) Qiang, L.; Yang, L.; Cao, S.; Lu, K.; Zhao, Y. *Fenxi Ceshi Xuebao* **2009**, *28*, 1304-1307.

(246) Kang, J.-K.; Hwang, I.; Ko, Y. H.; Jeon, W. S.; Kim, H.-J.; Kim, K. *Supramol. Chem.* **2008**, *20*, 149-155.

(247) Kampars, V.; Kokars, V.; Kaimin'sh, A. *Chem. Heterocycl. Compd. (N. Y.)* **2000**, *36*, 18-21.

(248) Li, Y.-L.; Xie, Q.-J.; Yao, S.-Z. *Yingyong Huaxue* **2007**, *24*, 628-631.

(249) Liu, L.; Wang, S.; Zhu, Z.; Li, M.; Sun, B. *J. Phys. Chem. C* **2011**, *115*, 5966-5973.

(250) Balandier, J.-Y.; Quist, F.; Sebaihi, N.; Niebel, C.; Tylleman, B.; Boudard, P.; Bouzakraoui, S.; Lemaur, V.; Cornil, J.; Lazzaroni, R.; Geerts, Y. H.; Stas, S. *Tetrahedron* **2011**, *67*, 7156-7161.

(251) Fry, A. J. *Synthetic Organic Electrochemistry (2nd edition)* Wiley-Interscience Publication, 1989.

(252) Dileesh, S.; Gopidas, K. R. *Chemical Physics Letters* **2000**, *330*, 397-402.

(253) Dileesh, S.; Gopidas, K. R. *J. Photochem. Photobiol., A* **2004**, *162*, 115-120.

(254) Shetty, A. S.; Zhang, J.; Moore, J. S. *Journal of the American Chemical Society* **1996**, *118*, 1019-27.

(255) Zhang, J.; Moore, J. S. *Journal of the American Chemical Society* **1992**, *114*, 9701-2.

(256) Mukhopadhyay, S.; Pandey, R.; Das, P. K.; Ramasesha, S. *Journal of Chemical Physics*, *134*, 044534/1-044534/8.

(257) Gott, J. R.; Maisch, W. G. *Journal of Chemical Physics* **1963**, *39*, 2229-35.

(258) Frag, E. Y.; Mohamed, G. G. *Journal of Molecular Structure*, *979*, 46-55.

(259) Bergman, S. D.; Reshef, D.; Groysman, S.; Goldberg, I.; Kol, M. *Chemical Communications (Cambridge, United Kingdom)* **2002**, 2374-2375.

(260) *Bruker Nokius* **2004**, *APEX2. Bruker Nonius AXS Inc., Madison, Wisconsin, USA.*

(261) Otwinowski, Z.; Minor, W. *Methods in Enzymology* **1997**, *276*, 307-326.

(262) Sheldrick, G. M. *Acta Crystallogr., Sect. A: Found. Crystallogr.* **2008**, *A64*, 112-122.

(263) Wilson, A. J. C.; Editor *International Tables for Crystallography, Vol. C; Mathematical, Physical and Chemical Tables*, 1992.

Vita

Pramod Prasad Poudel was born in December 23, 1975 at Katuwachaupari VDC of Parbat district in Nepal. He did his schooling at Syangja (Secondary School), Pokhara (B.Sc.), and Kathmandu (M.Sc. in Chemistry) all in Nepal. After receiving his M.Sc. degree in 2000, he joined Budhanilkantha Higher Secondary School as a Chemistry teacher where he taught for 7 months before joining Kanthmandu University in late 2000. He worked as a faculty in Chemistry department of Kathmandu University until he joined Chemistry department of the University of Kentucky as a PhD student in 2004. In addition to being engaged in performing research work at Dr. Cammers lab, he spent a large portion of his time as a TA (teaching assistant) and '*Super-TA*' to develop undergraduate studies within the Chemistry department. He was recognized not only with a '***Departmental Best TA Award***', but also with a highly prestious '***College of Arts & Sciences's outstanding TA award***'. He was also a receipient of '***100 % plus award***' (a research award) for his outstanding achievemens in Chemistry. Currently, he is working at Escent Technologies as a senior research scientist.

List of Publications/presentations

1. **Pramod Prasad Poudel**, Jing Chen and Arthur Cammers "Intramolecular Pi-Stacking in Isostructural Conformational Probes Depends Strongly on Charge Separation, a Proton NMR Study" E*ur. J. Org. Chem.* **2008**, 33, 5511- 5517 http://onlinelibrary.wiley.com/doi/10.1002/ejoc.200800663/pdf

2. **Pramod Prasad Poudel** and Arthur Cammers "Novel Aromatic Salts: Synergy between Electrostatic and Aromatic Interactions**"** *Naff Symposium* **2010**, Department of Chemistry, University of Kentucky, Lexington, KY 40506

3. **Pramod Prasad Poudel** and Arthur Cammers "Interesting Structural Aspects of Triangulenium Cation and Triangulene Anion Salt Pairs" *Naff Symposium*, **2008**, Department of Chemistry, University of Kentucky, Lexington, KY 40506

4. **Pramod Prasad Poudel**, Jing Chen, Subrahmanyam Modekruti and Arthur Cammers “Cohesion between Triangulene Aromatic Salts (I): Synergy between Point Charge Electrostatics and pi-Stacking Molecular Interactions”, *Manuscript to be submitted to JACS.*

5. **Pramod Prasad Poudel**, Jing Chen, Sean Parkin and Arthur Cammers “Cationic Discotics in Crystalline-State Tectonic Construction of Coaxial Aromatic Stacks in Triangulenes (II)”, *Manuscript to be submitted to Crystal Growth & Design*